2000

FROM RIVERS TO OCEANS: A COMPARISON OF CONTRASTING AQUATIC ECOSYSTEMS USING BENTHIC SIZE SPECTRA

ABADA, AHMED EL-SAYED AHMED

FROM RIVERS TO OCEANS: A COMPARISON OF CONTRASTING AQUATIC ECOSYSTEMS USING BENTHIC SIZE SPECTRA

By

AHMED EL-SAYED AHMED ABADA

A thesis submitted to the University of Plymouth
in partial fulfilment for the degree of

DOCTOR OF PHILOSOPHY

Department of Biological Sciences
Faculty of Science
In Collaboration with
Plymouth Marine Laboratory

February 2000

From Rivers To Oceans: A Comparison of Contrasting Aquatic Ecosystems Using Benthic Size Spectra

AHMED EL-SAYED AHMED ABADA

Abstract

This thesis uses a range of different size spectra to compare contrasting benthic habitats in the aquatic realm. Temporal and spatial variation in benthic size spectra were investigated across a full salinity gradient (i.e. from freshwater, through estuarine to marine) in the River Yealm, south Devon, in order to gauge the influence of large differences in taxonomy and evolutionary history. Abundance and biomass size spectra showed a similar pattern among sites in all seasons but winter, suggesting that the size structure of benthic communities may be similar in sites with very different community compositions. A subsequent study comparing size spectra across salinity by employing artificial substrata suggested that substratum type also had little effect on the size structure of these benthic communities. A technique was developed for obtaining microbial size distributions for benthic communities and showed that microbial size structures were also similar between the marine and freshwater sites within the Yealm system. A final study demonstrated that the shape of size spectra was clearly affected by metal contamination. Size spectra across a salinity gradient (i.e. from freshwater to lower estuary) in the highly contaminated Fal system were very different to those in the uncontaminated Yealm, due mostly to the low macrofaunal abundance in the former.

This thesis is the first to assess patterns in benthic size spectra across a full salinity range in the same system. It is hoped that it will provide a base line for further studies in this exciting research area in macroecology and that biomass spectra might also prove useful as metrics for biomonitoring.

LIST OF CONTENTS

LIST OF FIGURES

LIST OF TABLES

ACKNOWLEDGEMENTS

I would like to take the opportunity to thank my supervisor Dr. Simon Rundle for all the continuous encouragement, guidance and support given to me throughout my studies. It has been a great privilege to have him as a supervisor and also to be able to share his vast knowledge and experience. Deepest appreciation is also extended to my second supervisor, Dr. Martin Attrill for his constructive comments and guidance. I would like to thank Prof. Richard Warwick for his encouragement and assistance. Many thanks to Dr. Paul Ramsay for his invaluable assistance in biomass calculation and data representation.

I would also like to acknowledge the assistance granted to me by Dr. Graham Bradley of the University of Plymouth in helping me processing the microbial samples as well as his cordial support. Many thanks to Dr. John Moody for his personal generosity in allowing me to use his advanced laboratory and helping me in ATP estimation for the sub-micron microbial community.

I am most indebted to the technicians of the Department of Biological Sciences for their logistic support and special thanks to Mrs. Anne torr who occasionally accompanied me to the field and Miss. Alex Fraser for helping with the trace metal analysis. Special thanks to Mr. Roger Haslam, Richard Ticehurst and for the diving staff in the University Diving & Sailing Centre, Jerry Barker, Pete Brown, Peter Ede, Pete Rustage, Sue Syson and Jon Yorke who were the diving team for collecting the samples from the Lower estuary and the marine sites. My thanks to Mr. Pett for providing me with the laboratory equipments. Many thanks to Mr. Paul Russell for his assistance in processing the microbial samples using the image analyser unit. I would also like to thank the staff of the Department of Geography for their assistance with the total organic carbon. The assistance and companionship of Dr. Aziz Arshad throughout the studies are also appreciated and I thank him for his continuos assistance during the field sampling. Many thanks to Mr Sean Nicholson in Plymouth marine Laboratory for providing me with the software used for measuring the organisms. The friendship of the past and present PhD colleagues in the department is gratefully acknowledged.

The thesis would not have been possible without the scholarship awarded by the Egyptian Government. This scholarship allowed me to fulfill a life long ambition and to gain an invaluable training in a forigen research istituation.

Finally, I would like to thank my wife for her endless share of loves, utmost understanding and incessant inspiration throughout the studies; to my lovely children, Ghada and Mohammed for cheering me up over the difficult periods, and to my parents for their loving care and support.

AUTHOR'S DECLARATION

At no time during the registration for the degree of Doctor of Philosophy has the author been registered for any other award.

This study was financed by the Egyptian Government.

A programme of advanced study was undertaken, which included instruction in macro-; meiofaunal & microbial sample processing; and instructions for using the STATGRAPHICSPLUS programme for statistical analysis. Practical training has been achieved in Image analysis; Epifluorescence; Bioluminescence and X-ray microanalysis.

Relevant scientific seminars and conferences were attended, at some of which work was presented:

- Poster presentation at the 10th International Meiofauna Conference (XIMCO), Plymouth, July, 1998, entitled: "Is the benthos really bimodal? An assessment of biomass size spectra across the freshwater-marine sites".

- Oral presentation to the Department of Biological Sciences, University of Plymouth, April, 1998, entitled: "Biomass size spectra: a metric of aquatic communities".

- Attendance at The Biology of Crustacea Conference, University of Plymouth, April, 1996.

- Assisting in publishing a paper entitled "A rapid method for estimating biomass size spectra of benthic metazoan communities" with Ramsay, P. M.; Rundle, S. D.; Attrill, M. J.; Uttley, M. G.; Williams, P. R.; Elsmere, P. S. and A. Abada. In Canadian Journal of Fishies and Aquatic Sciences 54: 1716-1724 (1997).

- An accepted abstract to be presented orally in Germany (SETAC) 1999, entitled "Benthic biomass size spectra as a monitor of aquatic ecosystems".

Signed .....

Date 1/3/2000.....

CHAPTER 1

General Introduction

1. INTRODUCTION

1.1 The concept of body size in ecology

Body size plays an important role in the determination of the niche size of species. The tendency of adjacent species to exhibit regular differences in body size is considered as a common feature for animal guilds that are strongly segregated along a single-resource dimension (Begon *et al.* 1996). Hutchinson (1959) reported that sequences of potential competitors had a weight ratio of approximately 2 or length ratio of approximately 1.3, which was likened to the body length of a conventional musical ensemble of recorders. Accordingly, some authors have used the log biomass or $\log_2$ Equivalent Spherical Diameter (ESD) as a fractionating unit for the biomass of organisms in biomass size spectra (Warwick *et al.* 1986; Warwick and Joint, 1987; Ramsay *et al.* 1997 and Duplisea and Drgas, 1999; as examples) arguing that this scale corresponds to Hutchinson's size ratio for explaining niche differentiation among coexisting species. However, some authors have used a $\log_{10}$ scale (Schwinghamer, 1985; Strayer, 1986; Poff *et al.* 1993) probably due to its simplicity as a standard log.

The relationship between abundance and body size has received much recent attention from ecologists (Blackburn *et al.* 1990; Griffiths, 1992; Blackburn *et al.* 1993; Strayer, 1994; and Warwick and Clarke, 1996). Blackburn *et al.* (1990) reported that, for a large range of species drawn from different communities, population densities generally decreased with increasing body size, although, for some groups (birds and beetles) highest densities tended to be in the intermediate size categories. They argued that this was probably due to the presence of more intermediate-sized species in the communities, and that the lower densities at large and small body sizes was due to there being so few species in these size classes. Justification for the density decline among very small species was suggested to be due to increased energy needs per unit body size. From the aquatic realm, Warwick and Clarke (1996) showed that for European macrobenthic assemblages, plots of

species abundance against body size show more species of intermediate size compared with larger or smaller sizes.

Some workers have also tried to relate abundance/body size relationships to energetics. Damuth, (1981, 1987), Peters and Wassenberg, (1983) and Peters and Raelson, (1984), came to the conclusion that there was a linear relationship (on logarithmically transformed scales) between population density and body size, with an approximate slope of -0.75. Damuth, (1981, 1987, 1991) combined this abundance body size relationship with the metabolic rate body weight relationship (i.e. the chemical food energy obtained by organisms of different size classes (Schmidt-Nielsen, 1984) which scales to the 0.75 power with the body weight (Kleiber, 1961)) to generate the "energetic equivalence rule". This rule states that equal amounts of energy are available to each species in a community regardless of its size. This was criticized by Blackburn *et al.* (1993) and Strayer (1994) who argued that the slope of abundance body size relationship differs significantly from -0.75 within many individual assemblages. Moreover, Marquet *et al.* (1995) proposed that the positive slope characterizing the allometry of maximum densities for small organisms violates the Energy Equivalence Rule (i.e. that maximum energy use is dependent on body size). This may be due to the different slope, which will result in this case. In other words, the presence of a positive slope in small organisms will alter the overall slope from -0.75, which will consequently affect the validity of the energy equivalence rule. Moreover, Schmidt-Nielsen (1984) demonstrated that slopes of the metabolic rate/body size relationship for invertebrates could vary from less than 0.67 to over 1.0.

Blackburn *et al.* (1993) concluded that ecological assemblages are characterized by weak negative relationships between body size and abundance and that size is a poor predictor of population abundance. Depending on the statistics used (e.g. OLS, Ordinary Least Squares or RMA, Reduced Major Axis) the largest proportion of available energy is controlled by either large species or small species respectively. They concluded that no evidence for a general energetic equivalence rule exists.

Marquet *et al.* (1995) showed that medium sized organisms attain highest population densities, which subsequently decrease towards both larger and smaller organisms. They added that for measurements of the metabolic rates for mammalian primary consumers, the energy use fluctuates widely among species and its upper limit is dependent on the organism's body size, peaking at a body size of 100 g then decreasing towards smaller or larger body sizes. It has been proposed that this value is the optimum mammalian body size in both evolutionary and ecological time scales. This is the result of physiological constraints related to the rate at which resources are obtained from the environment and transformed into energy to do reproductive work. Moreover, the relationship between population energy use and body size is strongly affected by diet. For example, omnivores showed a positive relationship while carnivores and insectivores species showed a negative relationship.

Marquet *et al.* (1995) reported that variability in population energy use, even for species of similar size, is likely to be the result of different amounts of energy being available to them. Under this concept, energy is not equally available to species of all sizes. The way in which individuals are distributed among species within communities (i.e., relative abundance pattern) should parallel the way energy is distributed. They added that the detection of an optimal body size, in the multiphyletic intertidal communities studied, could reflect more the effect of an ecosystem/habitat-related evolutionary constraint.

1.2 Size spectra in aquatic habitats

1.2.1 Pelagic size spectra

The study of size spectra began in pelagic habitats, where Sheldon *et al.* (1972) suggested that the biomass of organisms, grouped in logarithmically increasing size classes, was roughly constant, i.e. biomass in each size class is roughly the same. By adaptation of automatic particle counters (Sheldon *et al.* 1972), it was possible to describe quickly the size structure of entire pelagic communities. The resulting size spectra were used to

compare pelagic communities from different environments and to develop models of the energetics of planktonic food webs by combining these size spectra with physiological rate laws (e.g., Sheldon *et al.* 1972; Kerr, 1974).

Body size approaches have been used widely and successfully in the pelagic zone (Silvert and Platt, 1978; Platt and Denman, 1978; Garcia *et al.* 1995; Wen, 1995; Cyr and Peters, 1996; Tittel *et al.* 1998 and Havens, 1998). Biomass size spectra may have important applications; for example, as a quick, inexpensive method for assessment of fish communities for management purposes (Mills and Schiavone, 1982 and Mills *et al.* 1987). Moreover, Sheldon size spectra have been used both to compare aquatic systems (e.g. Sprules and Munawar, 1986) and to develop models of food web energetics leading ultimately to predictions of fish yield (e.g. Borgmann, 1987).

1.2.2 Benthic size spectra

Benthic communities have their own characteristics that promote using a size-based approach. They are often species rich and difficult to describe taxonomically. They may also contain organisms spanning a wide size range (perhaps 10 orders of magnitude within the metazoan community). Moreover, much of benthic ecology is implicitly size-based because benthic ecologists usually use sieves to separate organisms from sediment (Strayer, 1991).

Schwinghamer (1981) was the first to use biomass fractionation to compare the benthic biomass size spectra of several marine sites in Nova Scotia. He described the size structure of an entire benthic community as a trimodal spectrum. The three peaks represent microbiota (bacteria and algae), meiofauna (small benthic animals such as copepods and nematodes), and macrofauna (large benthic organisms such as clams and large worms). Few organisms fell into the intervening size ranges resulting in the appearance of troughs. Schwinghamer hypothesized that the largest (i.e., much larger than the grain size of the sediment) macrofaunal organisms perceive the sediment as a solid volume, on which they settle, or in which they can burrow. Meiofaunal-sized organisms live in the interstices of

the sediment, and the microbiota attach to sediment grains. It follows that the size structure of the zoobenthos should differ between two sites with different sediment grain sizes. However, Warwick (1984) showed that the species size structure of the marine zoobenthos was relatively unresponsive to sediment characteristics and confirmed that zoobenthic metazoan size spectra are bimodal in marine sediments with a trough at an adult body size of about 45 μg dry mass. Warwick suggested that this bimodal spectrum had an evolutionary basis: large organisms and small organisms have different suites of important biological attributes with intermediate forms being maladapted.

Despite the speculative discussion of Warwick *et al.* (1986) in terms of a benthic/pelagic interaction, they gave important explanations for the bimodality of the biomass size spectra in marine sites. They argued that many macrobenthic species have planktotrophic larvae within the size range of adult meiobenthic species. These larvae grow to the maximum size, which corresponds with the benthic trough or the pelagic peak. If these larvae remained on the bottom, they would find niches according to their size, comprising a highly efficient consumer unit (as well as the settled larvae on the bottom after they began competing with the holoplankton) due to their high diversity and variety of narrowly specialized feeding mechanisms. They added that competition for food with the meiobenthos is not the only factor which may render the benthos inhospitable to the young larvae of macrofauna. Predation by meiobenthos on such larvae is another factor, which may be potentially intense. They gave another possible explanation for the benthic trough between macrobenthos and meiobenthos, in that feeding and safety conditions for these macrobenthic larvae are more favorable in the water column than on the bottom. This suggests that the interaction of these larvae with the meiofauna over an evolutionary time-scale may have a significant role in shaping macrobenthic life-history patterns.

Warwick *et al.* (1986) examined the effect of the absence of pelagic interaction pressure (i.e. the possibility that the pelagic community might preferentially graze parts of the phytoplankton size spectrum before arriving on the bottom) in a community with non-

phytoplankton particulate material (highly organically enriched). They concluded that this community has a size distribution occupying the trough in normal benthic communities. Therefore, the absence of pelagic interaction with the benthic realms may be a reason for this convergence of macrofauna and meiofauna.

The bimodality pattern previously suggested has not been found universally in marine systems. For example Ramsay *et al.* (1997) recorded a biomass increase with the body size for brackish water sites in South West Britain and the same pattern of biomass size spectra was recorded in the Baltic Sea (Duplisea, 1998; Drgas *et al.* 1998; Duplisea and Drgas, 1999).

Benthic biomass spectra in freshwater sites also show different patterns. Strayer (1991) suggested that the presence or absence of a biomass trough between macrobenthos and meiobenthos for marine and freshwater benthic biomass size spectra respectively, could be as a result of the presence of chironomid midges and Oligochaeta in freshwater sites which have body weights in the range representing the marine biomass trough. Moreover, Giere (1993) reported that, in freshwater systems, macrofauna have predominantly holobenthic larvae with rare planktonic stages resulting in a predictable unimodal benthic biomass size spectra without troughs. In addition, the lack of adult insects, which leave the aquatic biota after metamorphosis, and thus do not compete with the other macrobenthos, forms another principal difference from the marine realm. The majority of freshwater size spectra conform to this pattern of unimodality of benthic biomass size spectra, for example: Strayer (1986) for a lacustrine zoobenthic community; Morin and Nadon (1991) for 12 streams of the Ottawa-Hull region; Bourassa and Morin (1995) for 9 stream sites in Eastern Ontario and Western Quebec; Cattaneo (1993) for 3 Laurentian streams (Quebec); and Ramsay *et al.* (1997) for 2 freshwater sites in the River Yealm UK. However, some other freshwater studies have shown bimodal patterns similar to those observed in marine sites; for example: Poff *et al.* (1993) for the sandy bottom of the Piedmont stream; Rasmussen (1993) for the macrobenthic community in 11 lakes of the Quebec Eastern Townships;

Rodriguez and Magnan (1993) for the Lacustrine macrobenthos of 3 Laurentian Shield lakes and Hanson *et al.* (1989) for macrobenthos in 3 depth zones in a deep lake in Alberta. This variability in benthic biomass size spectra could be the result of the different methodologies used; there still a lot to know about the forces forming biomass size spectra in terms of temporal and spatial scales. Recently, Ramsay *et al.* (1997) developed a more rapid method for estimating metazoan benthic biomass size spectra using a geometric series of nested sieves. The advantage of this method is that it enables the investigator to be consistent over the whole size range being examined which could at the end eliminate the possible artifacts resulting from using inconsistent methodology. Ramsay *et al*'s method has an important application in terms of reliable comparison of a wide variety of aquatic systems.

1.3 Importance of bacterial size spectra

Despite the very important role of microorganisms in the aquatic habitats, most size-based studies have focused on metazoan components. To date the only previous work on benthic microbial size spectra is for marine systems (Schwinghamer, 1981, 1985; Warwick and Joint, 1987). However, there are some studies dealing with the microbial size fractionation in the water column in separate systems i.e., either freshwater or marine systems, for example, Weinbauer and Hofle (1998) studied the size-specific mortality by natural virus communities for bacterioplankton in Lake Plußsee, Germany; Gasol (1991) investigated a planktonic community in Lake Cisó in North East Spain; Cole *et al.* (1993) examined bacterial biomass and cell size distributions in 20 Lakes in U.S.A.; and Azam and Hodson (1977) investigated size distribution and activity of marine microheterotrophs in a variety of water masses. Therefore, the application of a size-based approach to the microbial components of benthic communities in both freshwater and marine systems in one study will promote direct comparison of the size-specific activities and biomasses in these two contrasting habitats. Microbial spectra might help to explain some of the variation in the

total biomass among sites as microbes are one of the most important sources of food in both benthic and pelagic communities (primary producers). For example, Linley and Koop (1986) reported that pelagic bacteria may be an important food source for benthic consumers exclusively dependent on these smaller size ranges. Danovaro *et al.* (1998) pointed out the importance of benthic nanoflagellates in the food web as a significant contributor for the direct transfer of bacterial biomass to the metazoan component in the Cretan Sea.

Moreover, size fractionation of bacterial activity may provide valuable information about which bacterial size classes are active (Delgiorgio and Scarborough, 1995; Berman *et al.* 1990). These active size classes could then be studied separately to evaluate their importance in many biological processes (e.g. biodegradation etc. Gilmour and Henry, 1991).

One of the most important challenges in size spectra construction over the whole benthic size range from microbes to metazoans is the usage of a consistent methodology which may eliminate any artifacts that could result from using different methodology and allow better understanding of benthic ecology. Therefore, the recently developed technique (Ramsay *et al.* 1997) was adopted for microbes (bacteria) to achieve consistent methodology for both metazoans and microbes. Accordingly, one of the thesis' aims is to develop such technique to be used for the whole microbial category as well as metazoans.

1.4 Size spectra as a contamination biomonitor

Benthic organisms have been widely used for contamination monitoring in aquatic systems (e.g., Hendricks *et al.* 1974; Brown, 1977; Aston and Milner, 1980; Martin and Castle, 1984; Lambshead, 1984; Shiells and Anderson, 1985; Warwick, 1986; Hodda and Nicholas, 1986; Raffaelli, 1987; Warwick *et al.* 1987; Mair *et al.* 1987; Moore and Bett, 1989; Gower *et al.* 1994; Somerfield *et al.* 1995; Ahn and Choi, 1998). The benthic mode of life and the close association of benthic organisms with the sediment mean that such organisms may be the most sensitive to contamination. Moreover, sediment contaminant

concentrations (e.g. heavy metals) usually exceed those of the overlying water by between three and four orders of magnitude (Bryan and Langston, 1992).

Warwick (1993) suggested that small organisms have a large surface area relative to the body size, indicating more sensitivity. He pointed out that methods employing lower levels of organization than the community level (such as biochemistry and physiology) reflect the condition of the organisms just at the time of sampling, whereas the structure of an assemblage of organisms reflects the integrated conditions over a period of time.

Schwinghamer (1988) suggested body size as a sensitive indicator of contamination and an accessible community level to investigate contamination effects. Moreover, the characteristic patterns of benthic biomass size spectra, despite the large differences in the taxonomic structure, have encouraged ecologists to use them as a contamination biomonitor (Schwinghamer, 1988; Duplisea and Hargrave, 1996). In terms of the differential response of macrobenthos and meiobenthos to contamination, Warwick (1993) suggested that, in organically enriched habitats, macrofaunal and meiofaunal sizes converge in the species size distribution leading to the formation of one peak. This would correspond to the biomass trough between macrofauna and meiofauna peaks in unperturbed communities. He argued, however, that this is unlikely due to the insensitivity of species size distribution to the increased number of individuals which occur in such contaminated habitats (species size distribution do not take number of individuals into account). Moreover, species size distribution is not an easy task for routine purposes due to demanding a high level of expertise in taxonomy.

1.5 Aims

It is clear that we still have much to learn about benthic size spectra and that there is a need for a consistent methodology if they are to be useful in understanding fundamental ecology and for monitoring. The main research objectives of the current study were:

1. To refine the method for benthic biomass size spectra construction developed by Ramsay *et al.* (1997). This was to be achieved by constructing BBSS using three

different site-specific biomass conversion factors mainly mean sieve, mean shape and predicted mean major taxon biomasses. The latter was to be generated from the measured values by regression analysis.

2. To assess the seasonal variation in benthic size spectra (abundance and biomass) across a full salinity gradient (i.e. from freshwater to marine) within the same river/coastal system.
3. To develop a standard methodology for microbenthos in terms of constructing biomass size spectra and to compare microbial (bacterial abundance, biomass and ATP activity) size classes between the freshwater and the marine sites within the same system (the River Yealm).
4. To standardise the sediment grain size effect on the BBSS by comparing these size spectra in artificial substrata with those in the natural sediments at the sites representing a range of salinities and heavy metal contamination.
5. To assess the impact of heavy metal contamination on the shape of benthic biomass size spectra across a salinity gradient within a polluted estuary in comparison with an uncontaminated system.

CHAPTER 2

Site Description, Physico-Chemistry and Sampling Methodology

2. Site description and physico-chemistry.

2.1. Introduction

The systems studied, the Yealm and Fal estuaries, lie within the counties of Devon and Cornwall, respectively, Southwest Britain. These two estuarine systems were chosen to compare benthic size spectra across a full salinity gradient (Yealm) and to assess the effect of metal contamination impacts on these spectra (Fal).

2.2. Aims

This chapter aims to describe the study sites, to document their physico–chemistry and to describe the sampling methodology used for benthic fauna.

2.3. Study areas and sampling sites

2.3.1. Study areas

Two river systems were chosen for the current study. The first (River Yealm) represented a putative clean system and the second (Carnon river/Restronguet Creek in the Fal) a system heavily contaminated with trace metals.

The Yealm system (Figure 2.1a) is situated on the south coast of Devon to the east of Plymouth Sound. The Yealm estuary extends from the Bar at its mouth for 6.5 km to its maximum tidal extent. Newton Creek is an arm of the Yealm, which is 1.5 km long. There are no major industries or docks bordering the Yealm and the shores are mainly unaltered by the activities of man, except for a small walled area built in the mid-estuary to make ponds, and some further flood defenses bordering Newton Ferrers, particularly in Newton Creek, which extend into the main Yealm estuary. Extensive Yacht moorings are present in the lower estuary but the river bed above this is privately owned and only a few moorings exist beyond this point (Hiscock and Moore, 1986).

Figure 2.1Study sites in: A) the Yealm and B) the Fal. Key: FW-freshwater, UE-upper estuary, ME-middle estuary, LE-lower estuary and MA-marine sites.

A)

B)

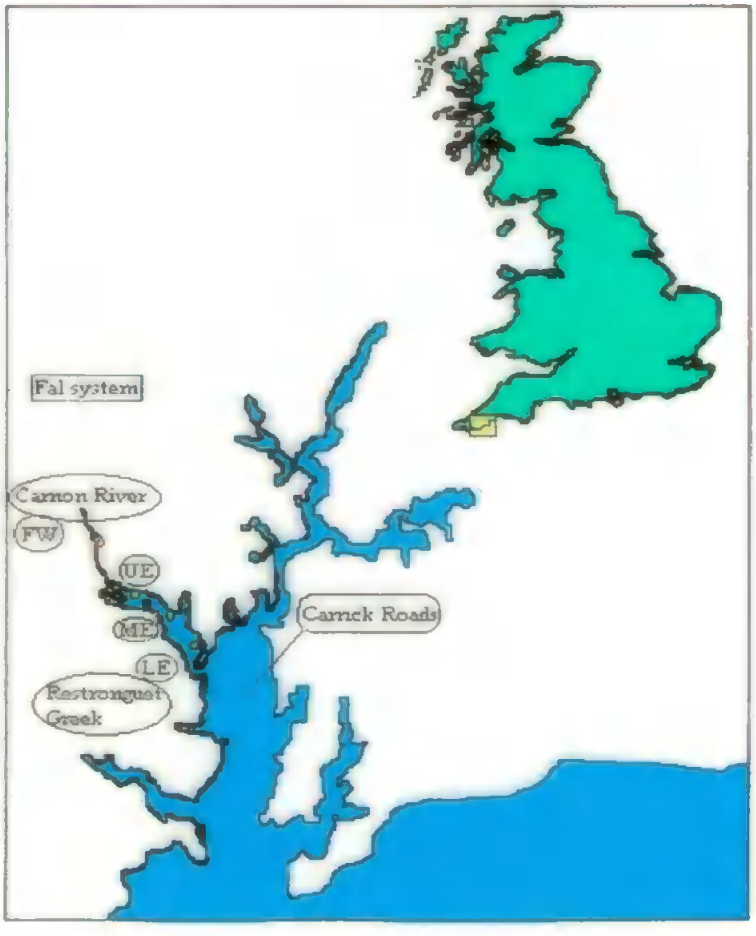

The second study site was part of the Fal estuary system, which is situated in southern Cornwall. The Fal estuary contains tidal creeks, which open into Carrick Roads at the mouth of the system. Each of these creeks has a small central stream and extensive areas of mudflats (Figure 2.1b).

Mining of metals in this part of Cornwall probably started following the recovery of alluvial tin. Up to 50% of the world's supply of copper, tin and arsenic was produced during the 19th century from mining activity in Cornwall. A considerable number of such mines was located in the Carnon Valley to the west of the main Fal system. After the closure of the last tin mine in the Carnon Valley in March 1991, and the removal of the pumps that had been de-watering the mine, water in the mine which was acidic and contained significant levels of heavy metals (Cd, Zn, Ni, As, Cu, and Fe) began to rise and started discharging to the Carnon River in November 1991. Approximately 45 million litres of acidic (pH 3.1), metal laden (Cd concentration > 600 $\mu l\ l^{-1}$) water discharged via the Carnon River into Restronguet Creek, where it mixed with neutral seawater.

In 1992 treatment of waters resumed and metal concentrations in the river water entering Restronguet creek quickly returned to pre-November (1991) levels. However, over time, due to the mining activities, a marked gradient of sediment metal concentrations was produced in creeks leading into Carrick Roads. In the 1970s, the levels of heavy metals in otherwise similar creeks in the different parts of the Fal estuary system differed by orders of magnitude (Bryan and Gibbs, 1983) and sediment Cu concentrations in Restronguet creek are the highest in the UK, (Bryan and Langston, 1992). The persistence of this contamination gradient has been confirmed by recent studies (e.g. Williams *et al* 1998). Therefore, Restronguet creek presents an ideal site for a natural experiment on the effects of heavy metal contamination on benthic communities (Somerfield *et al* 1994).

2.3.2. Sampling sites

2.3.2.1. Yealm sites

Five sites covering the full salinity gradient from freshwater through estuarine to marine conditions were located in the Yealm system. These sites are referred to as freshwater (FW) (NGR: SX 570 510), upper estuary (UE) (NGR: SX 562 508), middle estuary (ME) (NGR: SX 549 503), lower estuary (LE) (NGR: SX 539 474), and marine (MA) (NGR: SX 515 472) (Figure 2.1a).

2.3.2.2. Fal sites

Four sites in the most contaminated Creek (Restronguet) of the Fal estuary were used to investigate biomass size spectra across a similar salinity gradient in a metal polluted system (Figure 2.1b). The four chosen sites are referred to as freshwater (FW) (Carnon River) (NGR: SW 783 408), upper estuary (UE) (NGR: SW 796 389), middle estuary (ME) (NGR: SW 814 381), and lower estuary (LE) (NGR: SW 818 378) (Figure 2.1b).

2.4. Materials and methods

2.4.1. Biotic sampling

2.4.1.1. Standard core samples

Five replicate cylindrical core samples (diameter 5.3 cm, depth 10.0 cm) were collected seasonally in 1996 from soft sediment at each site in Yealm system (Table 2.1) and in the summer and autumn of 1996 in the Fal system. Samples from Freshwater (river channel), upper and middle estuarine sites (extreme low water mark) in both systems, and the lower estuary (subtidal) in the Fal system were taken from land, whereas, in the lower estuarine and marine sites (subtidal) in the Yealm system, core samples were collected by divers; sediment samples were placed in polythene bags underwater. All samples (whether

collected by standard corer, box corer or artificial substrata) were fixed with 10% buffered formalin.

2.4.1.2.Box corer (30 x 30 x 10 cm)

This sampler was used in one season (autumn) in both systems (Yealm and Fal) (Table 2.1) to examine whether any size bias occurred when using the cylindrical corer (i.e. the under-sampling of large macrofauna). In freshwater, upper estuary, middle estuary in both systems and the lower estuary in the Fal system, the corer was pressed into the sediment to 10 cm depth. The sediment was collected from inside the corer and washed in the field through a 500 μm mesh sieve. In the lower estuary and marine sites in the Yealm system, sieving was performed on the boat.

2.4.1.3. Artificial substrata (Pan scourers)

Five replicate nylon pan scourers were fixed to bricks (see Gee and Warwick, 1996) and placed, during spring 1997, on the river/sea bed at all sites (Fal and Yealm, Table 2.1) to be collected after a three month colonization period. These replicates were placed and collected by SCUBA divers in the lower estuary and marine sites. For the other sites in the Yealm and Fal they were placed and collected by accessing the sites as for corer sampling. Pan scourers were collected by detaching them from the brick, placing them in plastic pots and fixing with 10% formalin. These artificial substrata were used in attempt to eliminate any effect of sediment grain size on the shape of benthic biomass size spectra (see chapter 6).

2.4.1.4. Faunal processing

Macrofauna were initially separated from meiofauna by passing the sample through 500 μm and 45 μm sieves; organisms trapped by 45 μm sieve size were kept for further processing. Macrofauna were further separated into different size classes using 5 sieves

(2000, 1400, 1000, 710 and 500 μm) then each size category was preserved in 70% alcohol (IMS). Macrofauna were enumerated and identified to the major groups.

Meiofauna were separated from sediment particles using Ludox-TM with a specific gravity of 1.15 (Gee and Warwick, 1996). Any residuals of formalin were firstly removed by washing organisms, then rinsing them into a tall 125 ml beaker where Ludox-TM was added. The sample was stirred and left to settle for 1 hour. The supernatant comprising the floating meiofauna was poured over a 45 μm sieve size and preserved in 70% alcohol (IMS). Extraction was repeated three times to ensure complete separation of organisms.

For artificial substrata samples, the fauna was extracted by unravelling the pan scourers and then processed as the other samplers (see above).

Details of macrofaunal and meiofaunal measurements are given in chapter 3.

Table 2.1 Sampling dates for the Yealm and Fal systems, using different samplers. *- sample unavailable due to detachment of pan scourers.

Season	Site	Yealm System			Fal system		
		Cylindrical corer	Box corer	Artificial substrata	Cylindrical corer	Box corer	Artificial substrata
Winter	Freshwater	19-01-1996					
	Upper estuary	19-01-1996					
	Middle estuary	19-01-1996					
	Lower estuary	25-01-1996					
	Marine site	25-01-1996					
Spring	Freshwater	18-04-1996		(Placing) 23-04-1997			(Placing) 24-04-1997
	Upper estuary	18-04-1996		(Placing) 23-04-1997			(Placing) 24-04-1997
	Middle estuary	18-04-1996		(Placing) 23-04-1997			(Placing) 24-04-1997
	Lower estuary	19-04-1996		(Placing) 22-04-1997			(Placing) 24-04-1997
	Marine site	19-04-1996		(Placing) 22-04-1997			
Summer	Freshwater	29-07-1996		(Collecting) 25-07-1997	29-08-1996		*
	Upper estuary	29-07-1996		(Collecting) 25-07-1997	29-08-1996		(Collecting) 22-07-1997
	Middle estuary	29-07-1996		(Collecting) 25-07-1997	29-08-1996		(Collecting) 22-07-1997
	Lower estuary	28-08-1996		(Collecting) 23-08-1997	29-08-1996		(Collecting) 22-07-1997
	Marine site	28-08-1996		*			
Autumn	Freshwater	25-10-1996	25-10-1996		12-11-1996	12-11-1996	
	Upper estuary	25-10-1996	25-10-1996		12-11-1996	12-11-1996	
	Middle estuary	25-10-1996	25-10-1996		12-11-1996	12-11-1996	
	Lower estuary	11-11-1996	11-11-1996		12-11-1996	12-11-1996	
	Marine site	11-11-1996	11-11-1996				

2.4.2. Measurement of physico–chemical variables

Sediment samples were taken using a 2.2 cm in diameter corer from each site in both systems at the time of sampling for measuring organic carbon content, sediment grain size and heavy metal concentrations. Samples were collected in acid washed bottles and immediately frozen on return to the laboratory (below –20 °C).

2.4.2.1. Salinity, temperature, conductivity and pH

Field measurements of sediment salinity, temperature, conductivity and pH were made at the same time as biotic sampling. A Phox 2E meter was used to measure pH, and a YSI Model 30 meter for measuring salinity, temperature and conductivity. The probes were inserted *in situ* into the sediments at freshwater, upper and middle estuary sites. In case of lower estuary and marine sites, sediment samples were brought from the seabed and analysed at the surface.

2.4.2.2. Total organic carbon analysis

Sediment samples were first acidified with 10% hydrochloric acid to remove inorganic carbon, then washed thoroughly by distilled water to remove any traces of hydrochloric acid. The washed samples were dried and analyzed using a SHIMADZU Total Organic Carbon Analyzer 5000.

2.4.2.3. Heavy metal analysis

The sediment samples were freeze dried after being wet sieved through 63 μm sieve size for collecting the fine fraction. One gram of the dried sediments (or 0.5 g if the organic levels were high) was transferred into a 120 ml Teflon tube to be digested in 10 ml aqua regia (concentrated Nitric acid HNO_3 (18%), and Hydrochloric acid HCl (82%)). A microwave oven was used for heating the tubes at 100% power (80 psi) for 5 minutes and then at 100% power (160 psi) for 20 minutes. After this, samples were centrifuged and the extracts were decanted and made up to 25 ml using concentrated HNO_3 and kept at 4 °C

throughout the analysis. Concentrations of eleven trace elements were measured, namely (Cu, Pb, Cd, Zn, Cr, Mn, Fe, Ni, Mg, Co and Al) (Appendix (2.1)) in the two systems, using the Spectr AA600 Series Varian Atomic Absorption Spectrophotometer.

2.4.2.4. Sediment granulometry

Sediment granulometry was investigated by washing sediment samples through a series of stacked sieves (500, 250, 125 and 63 μm being in the bottom) on top of a bucket for collecting the smaller median grain sizes. The percentage weight contribution of each sediment portion was then calculated. For the smaller size fractions (16 & 31 μm) a known portion of the suspension was collected in the bucket (using a method based on sedimentation rates in graduated cylinders), dried, then weighed. Its percentage relative to the original sediment sample was calculated. This method is modified from Buchanan (1984), as suggested by Palmer and Strayer (1996).

2.5. Results

2.5.1. Environmental variables

In summer, temperatures in the Fal were slightly higher than in the Yealm, whilst in autumn, they were higher in the Yealm (Table 2.2). Temperature showed the expected seasonal pattern decreasing from summer to winter in both systems (Figure 2.2). The other environmental variables showed no clear seasonal variation. pH ranged from 6.7 to 8.0 in the Yealm system, whilst in Fal system it was less variable, ranging from 7.1 to 7.4 (Table 2.3). Conductivity showed the expected increase from freshwater to marine sites in both systems (Table 2.4) (Figures 2.3), although no consistent seasonal pattern was evident for this variable.

Table 2.2. Annual values of temperature (°C) in Yealm and Fal systems.

System	Yealm system					Fal. System			
Site	Freshwater	Upper estuary	Middle estuary	Lower estuary	Marine site	Freshwater	Estuary		
Season	Freshwater	Upper	Middle	Lower	Marine site	Freshwater	Upper	Middle	Lower
Winter	9.1	8.7	9.9	9.3	9.4				
Spring	11.6	11.7	12.7	10.7	11.0				
Summer	14.4	15.8	17.7	14.5	15.7	14.8	17.9	18.1	17.8
Autumn	9.5	9.1	10.7	11.2	11.0	8	8.7	8.9	8.9
Mean	11.2	11.3	12.8	11.4	11.8	11.4	13.3	13.5	13.4
SD	2.4	3.3	3.5	2.2	2.7	4.8	6.5	6.5	6.3

Table 2.3. Annual values of pH values in Yealm and Fal systems.

System	Yealm system					Fal. System			
Site	Freshwater	Upper estuary	Middle estuary	Lower estuary	Marine site	Freshwater	Upper estuary	Middle estuary	Lower estuary
Season	Freshwater	Upper	Middle	Lower	Marine site	Freshwater	Upper	Middle	Lower
Winter	7.8	7.8	7.6	7.7	7.7				
Spring	7.1	7.3	7.5	8.0	8.0				
Summer	6.7	7.1	7.1	7.2	7.2	7.1	7.2	7.1	7.4
Autumn	7.3	7.3	7.4	7.5	7.5	7.2	7.21	7.3	7.3
Mean	7.2	7.4	7.4	7.6	7.6	7.2	7.2	7.2	7.4
SD	0.5	0.3	0.2	0.3	0.3	0.1	0.0	0.1	0.1

Table 2.4. Annual values of Conductivity values (ms) and salinity (‰) in A) Yealm and B) Fal systems.

A)

System	Yealm system									
Site	Freshwater		Upper estuary		Middle estuary		Lower estuary		Marine site	
Season	Conductivity	Salinity	Conductivity	Salinity	Conductivity	Salinity	Conductivity	Salinity	Conductivity	Salinity
Winter	0.18	0	1.05	0.6	20	2.5	38.2	14.6	46.4	34.1
Spring	0.14	0	5.0	1.2	20.1	15	47	31	53	34.2
Summer	0.1	0	5.7	3.45	29.8	17.3	50.1	38	52	39
Autumn	0.12	0	3.1	0.2	19.3	8.7	40.3	32.3	47.2	34.2
Mean	0.1	0.0	3.7	1.4	22.3	10.9	43.9	29.0	49.7	35.4
SD	0.03	0.00	2.09	1.45	5.01	6.66	5.58	10.05	3.33	2.42

B)

System	Fal system							
Site	Freshwater		Upper estuary		Middle estuary		Lower estuary	
Season	Conductivity	Salinity	Conductivity	Salinity	Conductivity	Salinity	Conductivity	Salinity
Winter								
Spring								
Summer	0.23	0	25.3	16.5	30	20	32.3	29
Autumn	0.18	0	20.8	3	27.6	6	28	15.7
Mean	0.2	0.0	23.1	9.8	28.8	13.0	30.2	22.4
SD	0.04	0.00	3.18	9.55	1.70	9.90	3.04	9.40

Figure 2.2. Seasonal variation of temperature in the Yealm system. FW-freshwater, UE-upper estuary, ME-middle estuary, LE-lower estuary and MA-marine sites.

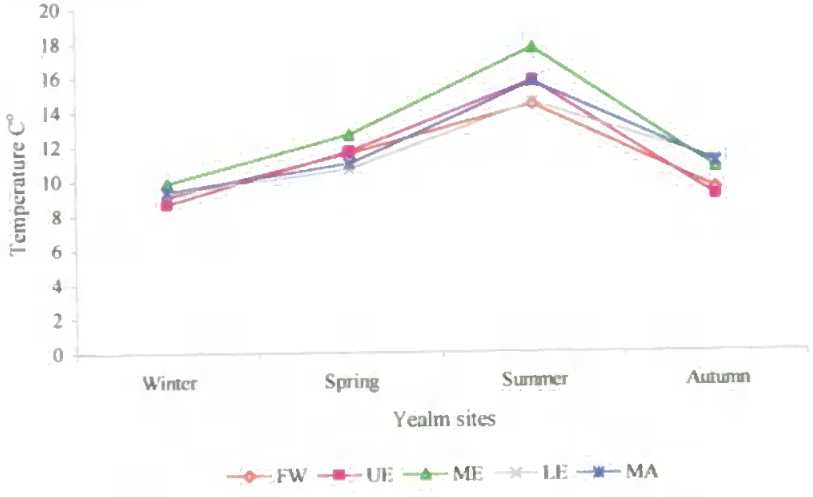

Figure 2.3. Seasonal variation of conductivity (ms) values in the Yealm system. FW-freshwater UE-upper estuary, ME-middle estuary, LE-lower estuary and MA-marine site.

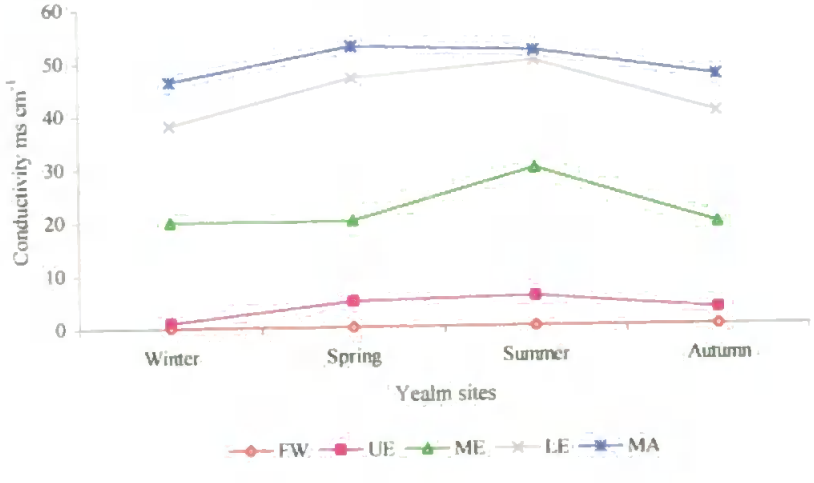

Salinity showed a gradual increase from freshwater (0.0 ‰) to marine (39 ‰) sites (Table 2.4) (Figure 2.4).

Mean seasonal organic carbon values in both systems showed an increase from freshwater to the middle estuary and then decreased towards the marine site (Table 2.5) (Figures 2.5).

Sediments from freshwater and upper estuary sites were coarser than any other site in Yealm, followed by marine, lower estuary and the middle estuary, where median grain size (Φ) was the finest. Sediment grain size in the Fal system was generally finer than that of the Yealm especially at freshwater and upper estuary sites. Whereas, the median grain size of the lower estuary site in the Fal was coarser than that of the lower estuary site in the Yealm. Middle estuary sites in the two systems had similar median grain sizes (Table 2.6) (Figures 2.6)

2.5.2. Heavy metals

Concentrations of Cu, Zn and Pb showed the most obvious differences in their concentration between systems. These metals are known to have important influences on benthic communities (Bryan and Langston 1992).

Heavy metal concentrations in the Yealm were orders of magnitude lower than that for the Fal (Table 2.7). the relative proportion of these metals was similar throughout the year in the Yealm (Zn > Pb > Cu) at all sites (Figures 2.7). In the Fal, metal concentrations peaked in summer and autumn (relative to the Yealm metal concentrations) and Cu and Zn concentrations were higher than Pb. The spatial distribution of these heavy metals in the Yealm system showed a consistent pattern, freshwater, upper estuary and middle estuary sites were consistently higher in their metal concentrations compared with the lower estuary and marine site in all seasons (Figures 2.7). In the Fal, however, the upper estuary site was the most contaminated, particularly for Cu and Zn.

Table 2.5 Annual values of % organic carbon in: A) the Yealm and B) the Fal systems.

A)

System / Site / Season	Yealm system				
	Freshwater	Estuary			Marine site
		Upper	Middle	Lower	
Winter	0.26	0.57	3.50	1.80	0.68
Spring	0.61	0.55	1.40	0.60	0.43
Summer	0.59	4.60	3.60	0.95	0.45
Autumn	0.64	0.50	4.50	0.92	1.20
Mean	0.53	1.56	3.25	1.07	0.69
SD	0.18	2.03	1.31	0.51	0.36

B)

System / Site / Season	Fal. System			
	Freshwater	Estuary		
		Upper	Middle	Lower
Winter				
Spring				
Summer	0.39	5.37	4.00	0.61
Autumn	0.10	3.40	2.70	1.28
Mean	0.25	4.39	3.35	0.95
SD	0.21	1.39	0.92	0.47

Table 2.6. Pooled annual values of sediment grain size in the Yealm and Fal systems. * denotes that the sorting coefficient could not be calculated due to the fact that the Φ value of the first and the second Quartiles (Q1 and Q2) in the Yealm (freshwater and upper estuary sites) and the first Quartile (Q1) in the Fal (lower estuary site) were smaller than 1. This was due to the usage of 500 μm sieve mesh size as the biggest mesh size in the grain separation process. The first Quartile (Q1) i.e. the 25% value in the comulative graph, in the mentioned sites were coarser than 500 μm.

System	Site	(phi) (50%)	Q1 (25%)	Q3(75%)	classification of sediment (Giere 1993)	
Yealm system	Freshwater	<1	<1	1.97	*	
	Upper estuary	<1	<1	2.93	*	
	Middle estuary	4.55	3.95	5.14	0.60	Moderatly well sorted
	Lower estuary	2.76	1.34	4.42	1.54	Poorly sorted
	Marine site	2.5	2.04	2.97	0.47	well sorted
Fal system	Freshwater	1.62	1.099	2.46	0.68	Moderatly well sorted
	Upper estuary	4.57	4.01	5.20	0.60	Moderatly well sorted
	Middle estuary	4.78	4.23	5.36	0.56	Moderatly well sorted
	Lower estuary	1.927	<1	4.02	*	

Table 2.7. Mean heavy metal concentrations in the Yealm and Fal systems in four seasons.

System	Site	Metal $\mu g\ g^{-1}$	Winter	Spring	Summer	Autumn	Mean	SD
Yealm system	Freshwater	Cu	49.44	24.94	24.97	25.05	31.10	12.22
	Upper estuary		27.38	27.44	37.94	23.47	29.06	6.21
	Middle estuary		49.06	29.78	46.30	52.92	44.51	10.19
	Lower estuary		19.43	12.47	9.63	14.56	14.02	4.13
	Marine site		7.33	8.01	8.89	15.92	10.04	3.97
	Freshwater	Zn	148.66	108.92	118.37	119.83	123.95	17.17
	Upper estuary		118.06	116.94	146.82	92.76	118.65	22.11
	Middle estuary		157.84	263.56	151.23	154.97	181.90	54.50
	Lower estuary		71.34	59.31	77.95	73.53	70.53	7.97
	Marine site		39.58	34.95	57.72	80.82	53.27	20.83
	Freshwater	Pb	45.16	31.13	41.89	27.81	36.50	8.33
	Upper estuary		43.04	36.61	87.28	29.71	49.16	25.99
	Middle estuary		77.85	50.91	69.68	72.90	67.84	11.77
	Lower estuary		32.93	27.68	26.83	38.80	31.56	5.53
	Marine site		28.88	24.77	32.71	35.34	30.42	4.61
Fal system	Freshwater	Cu			1065.13	676.93	871.03	274.50
	Upper estuary				2526.75	2813.55	2670.15	202.80
	Middle estuary				1767.28	1924.70	1845.99	111.31
	Lower estuary				1485.10	559.26	1022.18	654.67
	Freshwater	Zn			824.73	205.01	514.87	438.21
	Upper estuary				3491.55	2965.57	3228.56	371.92
	Middle estuary				2269.95	2946.01	2607.98	478.05
	Lower estuary				1341.04	941.43	1141.23	282.56
	Freshwater	Pb			148.36	493.57	320.97	244.09
	Upper estuary				243.89	247.49	245.69	2.54
	Middle estuary				217.91	267.68	242.80	35.20
	Lower estuary				151.45	67.45	109.45	59.40

Figure 2.4 Seasonal variation of salinity values in the Yealm system: FW-freshwater, UE-upper estuary, ME-middle estuary, LE-lower estuary and MA-marine sites.

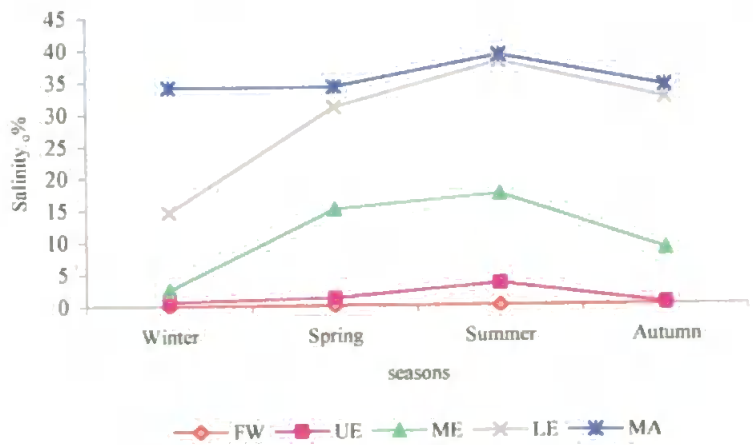

Figure 2.5. Seasonal variation of % of organic carbon in the Yealm system, FW-freshwater, UE-upper estuary, ME-middle estuary, LE-lower estuary and MA-marine sites.

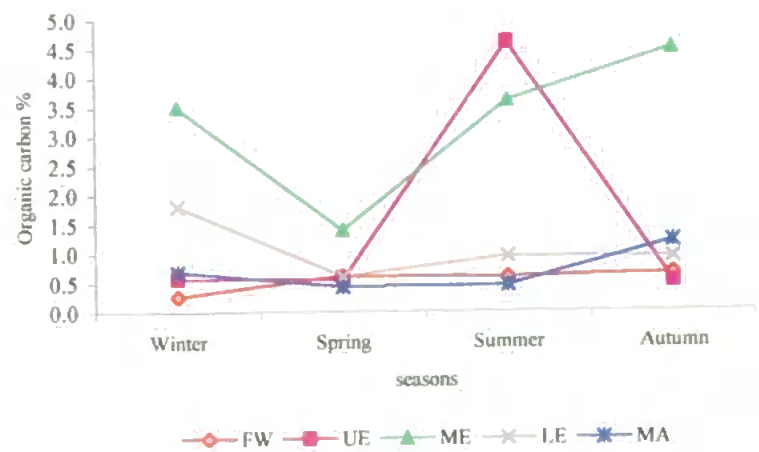

Figure 2.6 Diagram of grain size (phi) distribution illustrated as comulative curve in: A) the Yealm; and B) the Fal system: FW-freshwater, UE-upper estuary, ME-middle estuary, LE-lower estuary and MA-marine sites.

A)

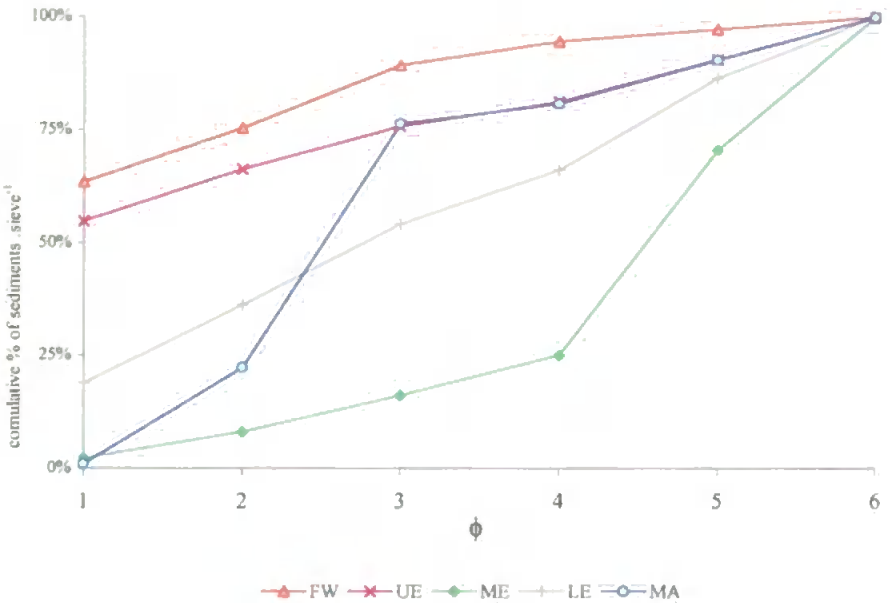

B)

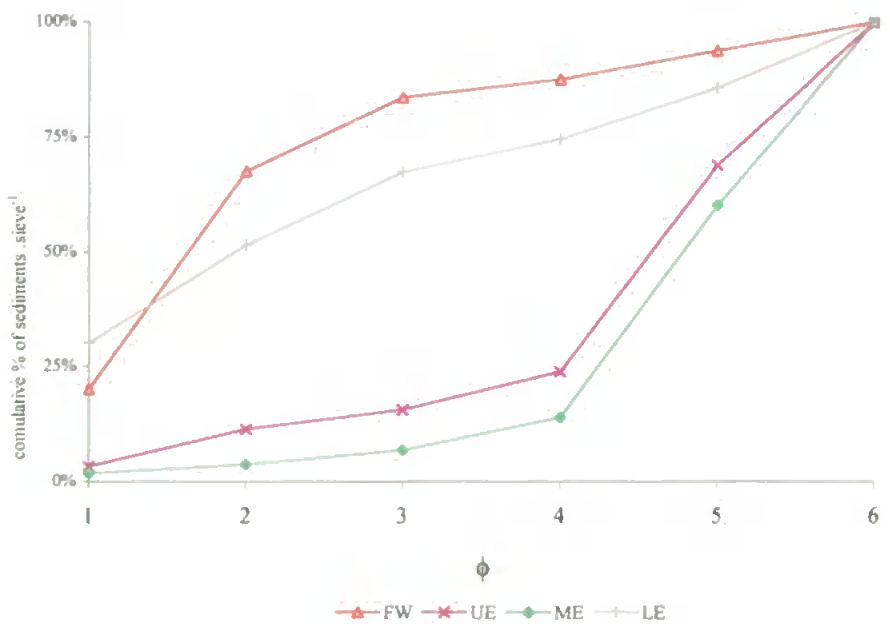

Figure 2.7. Seasonal concentrations (µg/g) of Cu, Zn and Pb in:
1) the Yealm and 2) the Fal: FW-freshwater, UE-upper estuary, ME-middle estuary, LE-lower estuary and MA-marine site. (note that the y axis scale varies among sites).

Yealm Cu

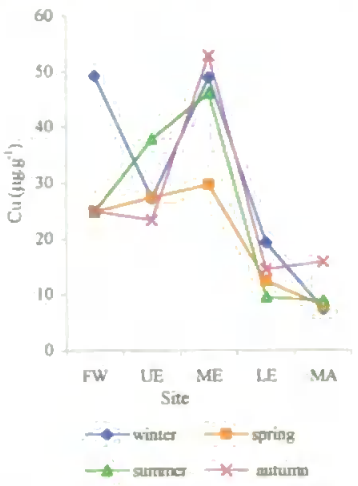

Fal Cu

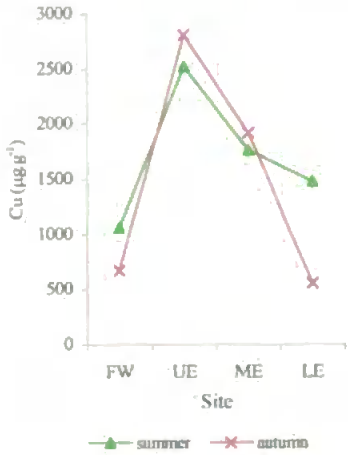

Yealm Zn

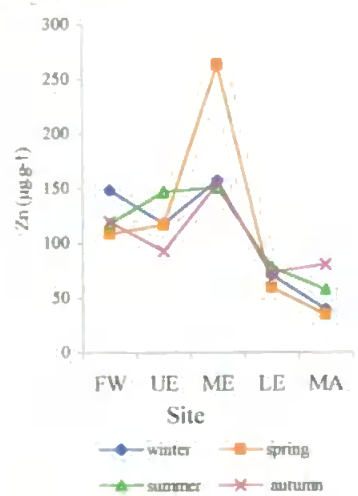

Fal Zn

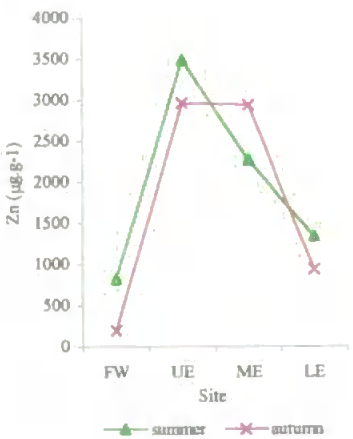

Yealm Pb

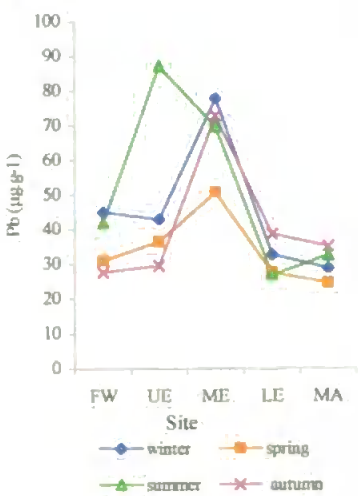

Fal Pb

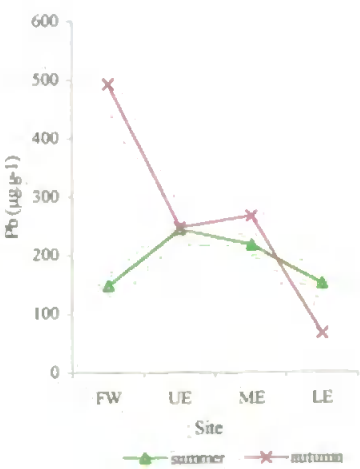

2.6. Discussion

The results of the current chapter demonstrate three main points. Firstly, a clear salinity gradient in both systems. Secondly, clear differences in metal concentrations between systems. Thirdly, differences within and among systems in sediment grain size. These results reflect the goodness of the chosen sites, which justifies for reasonable comparison of benthic size spectra.

CHAPTER 3

Benthic Biomass Size Spectra Construction

3. Benthic Biomass Size Spectra Construction

3.1. Introduction

Despite the recent increased utilisation of benthic size spectra in aquatic ecology, there is still much to learn about these community metrics, including the improvement of the techniques used in their construction (which currently are logistically demanding) and the evaluation of spatial and temporal variability in size spectra.

In essence, a size spectrum is a simple two-dimensional representation of a complex ecological community that is conceptually much simpler and more intuitive than alternatives such as ordination axes. Sheldon *et al* (1972) introduced to ecology a useful graphical representation of the community size composition since referred to as the Sheldon spectrum. Originally used to describe Coulter counter particle size distribution, this spectrum is a plot of particle concentration (by volume) against particle diameter. Since this pioneering study, there have been many approaches to the construction of size spectra, each technique relating body size to a different parameter such as abundance (number of individuals per size class), biomass (dry or wet weight of individuals per size class: Schwinghamer, 1981; Strayer, 1986; Hanson *et al* 1989) or species richness (number of species per size class: Warwick, 1984; Warwick *et al* 1986). The multitude of approaches used in construction of benthic biomass size spectra (BBSS) in aquatic environments has led to a lack of conformity in methodologies which in turn, may result in different shapes (i.e. underestimation or overestimation) of the BBSS within and between systems. Moreover, the construction of BBSS is a labour–intensive, time-consuming process. The various methodologies and approaches to BBSS construction are discussed below.

3.2. Measuring individual biomass

3.2.1. Direct weighing and volume displacement

Direct weighing can be used as a quick, inexpensive and direct estimation of biomass. The main disadvantage of this method is that it involves the destruction, through drying, of the organisms, preventing further studies. It is also not appropriate in the case of very small organisms, although some workers have attempted to weigh meiofauna. Wieser (1960), for example, determined the dry weight of nematodes by weighing batches on an analytical balance (Becker, 0.1 mg) or on a "Misco" quartz helix with a sensitivity of 1 mm per 10 mg. Dumont *et al* (1975) also reported that dry weight data were rare until the development of microbalances which made it possible to make routine weighing down to 10^{-7} g. Burns (1969) used a Cahn microbalance for obtaining accurate dry weight values in a number of *Daphnia* species, whilst Poff *et al.* (1993) dried and weighed most macrobenthic fauna to derive length–dry mass regressions. Similarly, Reise *et al.* (1994) dried the organisms to calculate the ash-free dry weight (AFDW). Direct weighing has also been used by Dugan *et al,* (1995) and Edgar (1990a), whilst Steimle (1990) specifically weighed each taxon.

Volume displacement has been used as an alternative approach to direct weighing that keeps organisms intact for further studies. This approach is straightforward only for organisms with simple geometry (Dumont *et al* 1975). Application of this approach to irregularly shaped species often involves an accumulation of errors, as the total taxon volume is assumed to be calculated by summing the volumes of the simple geometric shapes forming the final taxon shape. Despite this difficulty, Schwinghamer (1981) and Strayer (1994) used this approach for estimation of organism body volume.

3.2.2. Biomass estimation from body measurements

Another non-destructive technique for estimating the biomass of individual organisms is to relate an organism's body length to its weight through a regression equation. The main advantages of this approach are: 1) it is useful in routine sample analysis when insufficient

material may be available for weighing; 2) it does not damage the organisms; 3) in sampling programs at sea, this approach is more reliable that weighing which may be difficult; and 4) this approach is useful in determinations of biomass of ingested prey from partially digested remains in gut or faeces. The main disadvantage of this approach is that it is time consuming.

An example of this technique was that adopted by Burgis (1974) who described the relationship of formalin-preserved dry weight to total body length in two copepod species using the following equation:

$$LogW = 2.49LogL - 6.9039$$

Where (W) is the weight in μg and (L) is the body length in μm.

Rogers et al. (1977) concluded that taxon–specific regression equations provide a reliable method of estimating organism biomass from linear body measurements. Schoener (1980) also suggests that length–weight regressions help to provide a characterisation of ecological communities in terms of species–abundance and size distribution.

The availability of length–mass relationships for some organisms has greatly assisted in the estimation of organisms' body masses. Unfortunately, the main disadvantage of this approach is that not all organisms have published length–mass relationships. For these organisms, approximate simple geometric shapes close to the body shape (e.g. cylinders for vermiform organisms) have been used to obtain weights, using standard values of specific gravity and dry/wet weight ratios as conversion factors for dry weight estimation. This approach was adopted by Poff et al (1993).

3.2.3. Image analysis

The measurement of organism body dimensions using microscopy is a very time consuming process. Utilisation of image analysis enables more rapid and, often, more accurate estimations of organism body dimensions. Morin and Nadon (1991) and Morin *et al* (1995) measured body lengths of sorted organisms to the nearest 0.01 mm with an image analysis system connected to a dissecting microscope. Similarly, Rasmussen (1993)

measured organism lengths with an image analysis system, with fresh weights estimated from total body lengths using a series of length-weight regressions constructed from the organisms collected during the study. Garcia *et al.* (1995) used this approach differentially by tracing the contours of the organisms using a drawing tube which were then processed by an image – analysis program. The volume was estimated for each individual organism counted as the revolution volume of the organism according to its shape, either ellipsoidal or cylindrical, based on semi-automatic short and long axis measurements (Rodriguez *et al.*, 1987; Echevarria *et al.*, 1990; Garcia, 1991; Echevarria and Rodriguez, 1994). Soltwedel *et al* (1996) measured nematode lengths and widths by a semi–automated image analysis for size class discrimination. Likewise, Ramsay *et al* (1997) used an image analysis technique for estimating organism biomass.

3.3. Presentation of size spectra

Several different approaches have been used in the choice of the axes used to represent size spectra. The units used can markedly influence the shape of the biomass plot obtained. One of the most important considerations when constructing size spectra is that the scale along the body-size axis is ecologically meaningful with a resolution of data points fine enough to distinguish peaks and troughs in the data (Ramsay *et al.* 1997).

3.3.1. Scaling the X-axis

Hutchinson (1959) suggested that ecologically non-competing species tend to exhibit regular differences in body volume of approximately 2.0 or length ratios of approximately 1.3. Schwinghamer (1981) therefore used Log_2 size intervals (≡1.3 ratio) suggesting that they provide a much better resolution of the size spectrum than log_{10} intervals. Warwick (1984) also assigned species from a marine benthic community to body size classes on a x2 geometric scale. This scale gave a manageable number of classes, ranging from the largest organisms in class 30 (5-10 g) to the smallest in class 1 (0.0093-0.0186 μg), spanning nine orders of magnitude in body size. The choice of a logarithmic scale is useful in visualising

anticipated lognormal distributions, and a x2 geometric scale has been used extensively by those concerned with distributions of numbers of individuals among species, as advocated by Preston (1948). Although the weight of each species is usually determined as accurately as possible, precision is not of paramount importance when assigning species to a geometric class when those in the class above and below are either twice or half the size (in terms of volume). Misplacement of borderline species by one class would not alter the overall picture, so that the use of conversion factors from volume or wet weight to dry weight is not considered inappropriate.

To standardise for the variety of body shapes, size (in terms of volume) is often expressed as an equivalent spherical diameter (ESD), using the following equation (Schwinghamer 1981):

$$ESD = 2(3m/4\pi d)^{1/3}$$

Where m is the wet mass of the organism and d is its density (1.05 for freshwater organisms (Strayer 1986), 1.13 for marine organisms (Warwick 1984, Wieser 1960). For estuarine organisms densities were derived in the current study from those of the freshwater and marine organisms according to the mean annual values of salinity in the three estuarine sites.

3.3.2. Scaling the Y-axis

The Y–axis of size spectra can take several forms, depending on the goal of study. It may represent the abundance of organisms in each size category, (Strayer 1986,1994; Ramsay *et al* 1997, Warwick and Clarke 1996; Poff *et al* 1993, Dugan *et al* 1995, Morin *et al* 1995, Garcia et al. 1995 and Bourassa and Morin 1995), the biomass of different sized organisms, (Strayer, 1986; Ramsay *et al* 1997; Schwinghamer 1981; Hanson *et al* 1989; Cattaneo 1993; Duplisea and Hargrave 1996, Duplisea 1998, Hanson *et al* 1989, Rodriguez and Magnan 1993, Edgar 1990, Strayer 1991, Poff *et al* 1993, Rasmussen 1993, Morin *et al* 1995, Garcia *et al* 1995, and Cyr and Peters 1996), or the number of species in each size

category (Warwick, 1984 and Warwick *et al* 1986). The latter, species richness size spectra reflect how the species are distributed in terms of their body size (Strayer 1986, Warwick *et al* 1986, Warwick 1984, and Warwick and Clarke 1996). Assimilation size spectra have also been used to show how metabolic activity is spread through the size classes of the benthos, (Strayer 1986). Whilst respiration size spectra can indicate the amount of time needed for a community to consume available organic matter (Duplisea and Hargrave 1996, Poff *et al* 1993 and Bourassa and Morin 1995). Production size spectra reflect the interaction of the metabolic rate-body size relationship of individuals and the distribution of body sizes within the population (Edgar 1990 and Dickie *et al* 1987).

Normalised biomass size spectra have also been used to facilitate quantification of variation in shape and configuration of the biomass size spectra (Sprules and Munawar, 1986,Wen, 1995 and Tittel *et al.* 1998). Sprules and Munawar (1986) constructed normalised biomass size spectra by grouping organisms into adjacent categories of volume double the previous volume with size expressed as fresh weight on logarithmic scale. The vertical axis (Y-axis) is the total fresh biomass (per litre) of organisms in a particular weight category divided by the change in weight across the category, all on a logarithmic scale. Wen (1995) constructed normalised spectra by plotting on the ordinate the base 10 logarithm of the standardised biomass per interval (calculated as the dry mass (μg) in the size category divided by the change in model biomass between intervals) versus the base 10 logarithm of individual body weight on the abscissa. The intercept of the regression line provides an estimate of relative abundance at one mass unit along the size gradient. The slope reflects the overall trends in mass change from interval to interval. A slope of –1.0 indicates that biomass is approximately evenly distributed across size classes; steeper slopes (<-1.0) show that biomass declines with increasing size, and shallower slopes (>-1.0) the reverse.

3.3.3. The use of sieves in size spectra construction

Sieving has been used by several authors as a method for separating organisms into size categories. For example, Widbom (1984) used a series of sieves with different mesh sizes to divide meiofaunal taxa into different size fractions and to determine the average individual weight in each of these fractions. Edgar (1990a) also pointed out that the distribution of body sizes within benthic communities can be rapidly and easily determined by passing faunal samples through a series of nested sieves stacked in descending order of size. Ramsay *et al* (1997) sorted benthic samples by washing organisms through a series of 10 brass-frame laboratory test sieves with steel meshes graded on the $\sqrt{2}$ Wentworth scale (Buchanan 1984): 2000, 1500, 1000, 710, 500, 355, 250, 180, 90 and 63 μm. In this series, each step represents a halving in the area of the mesh aperture.

3.4. Aims

This chapter aims to introduce the approach used for the construction of BBSS in this thesis. The methods represent a refined version of those developed by Ramsay *et al* (1997). The main objectives were firstly for a range of aquatic systems, to obtain measures of: 1) mean total sieve biomass; 2) mean biomass of different organism shapes; and 3) mean major taxon biomass for 12 sieve sizes differing on a logarithmic scale. Biomass size spectra were then calculated using each of these measures as a conversion factor in order to establish which measure was to be used in biomass calculations. These exploratory analyses involved a comparison among sites within one season (summer) and among seasons for one site (marine).

3.5. Methods

3.5.1. Sample processing

Samples were collected as detailed in chapter 2 and were separated into macrofauna and meiofauna by washing them through 500 and 45μm sieves respectively. Macrofauna were

then separated from mineral particles by elutriation, prior to washing through 2000, 1400, 1000, 710 and 500μm sieves. Meiofauna were separated from fine sediments using the Ludox flotation method (McIntyre and Warwick 1984) and then washed through 355, 250, 180, 125, 90, 63 and 45 μm sieves.

Direct counts of all major groups (see below) of macrofauna and large meiofauna (355 and 250 μm sieve sizes) were made for each replicate sieve size in each sample. For smaller meiofauna, subsamples were taken by dividing the area of a petri dish into four sections, homogeneously distributing the sample across the dish and then extracting organisms from one quarter of the dish.

3.5.2. Measurement of organisms

Measurements were made on organisms from summer samples assuming that abundance and diversity were the highest.

Subsamples of organisms were chosen as in 3.5.1. from each replicate sieve sample from the freshwater, middle estuary and the marine sites in the Yealm. The acceptable minimum number of organisms in a subsample to be measured was determined by taking the first 150 organisms encountered from one sieve (the 125-μm sieve from a replicate sample of the middle estuary site). Biomass values were estimated for these organisms as described below. Simulated random subsampling of these data provided 150 estimations of mean individual biomass for a series of subsample sizes. In each case, an index of precision was calculated as the ratio of the standard error to the mean expressed as percentage (Ramsay *et al*, 1997; Elliott, 1977). The results of this analysis are summarized in Figure (3.1). Accepting a standard error at or below 20% of the mean ("a reasonable error in most bottom samples;" Elliott 1977), a minimum of ten organisms per sieve were measured giving a precision of about 12%, a higher precision than Ramsay *et al* (1997, 20%).

Organism body dimensions (length and width) were measured using a binocular microscope with a *camera lucida* attachment. Organism images (including body curvature

or the body waves) were projected onto a digitising tablet configured to act as a mouse under Microsoft Windows. Use of the digitising pad (Figure 3.2) allowed an absolute and repeatable co-ordinate system to be used, unlike the normal relative and unrepeatable co-ordinate system of a ball mouse. This allowed the operator to mark the required points to measure the body dimensions directly whilst looking at the organism. The computer then calculated the distance between the points automatically and subsequently allowed the operator to enter supporting sample identification details. The final file was saveable as an ASCII delimited file that could be read into MS Excel for analysis.

Methods differed for the calculation of individual biomass values. For those taxa with published length-mass relationships (Pearre (1980) for Copepoda; Smock (1980) for adult Coleoptera and Hemiptera; Meyer (1989) for Amphipoda, Coleoptera larvae, Chironomidae, Non-chironomid diptera, Ephemeroptera, Plecoptera, Trichoptera and Tricladida) biomass was calculated from the power equation:

$$m = al^b$$

Where (m) is the dry mass of the organism, (l) is the length and (a) and (b) are constants for each taxon. Other taxa were approximated to simple geometric shapes (Winberg and Duncan 1971): Collembola, Decapoda, dipteran pupae, Nematoda, Oligochaeta, Ostracoda, Rotifera and Tardigrada were approximated to cylinders; Cladocera, Hirudinea and Isopoda to half cylinders; and Hydracarina to spheres. Organism volumes were converted to dry weights using the appropriate conversion factors.

For the freshwater site a specific gravity of 1.05 and a dry- to wet-weight ratio of 0.15 were used (Strayer 1986, Kajak *et al* 1980). For marine site, a specific gravity of 1.13 and a dry- to wet-weight ratio of 0.25 were employed (Wieser, 1960; Warwick, 1984). Conversion factors for estuarine sites (Table 3.1) (upper, middle & lower estuary), were obtained from a simple regression analysis of the overall year salinity readings versus the published densities and dry- to wet-weight ratios of freshwater and marine sites.

Figure 3.1. The relationship between precision and subsample size.

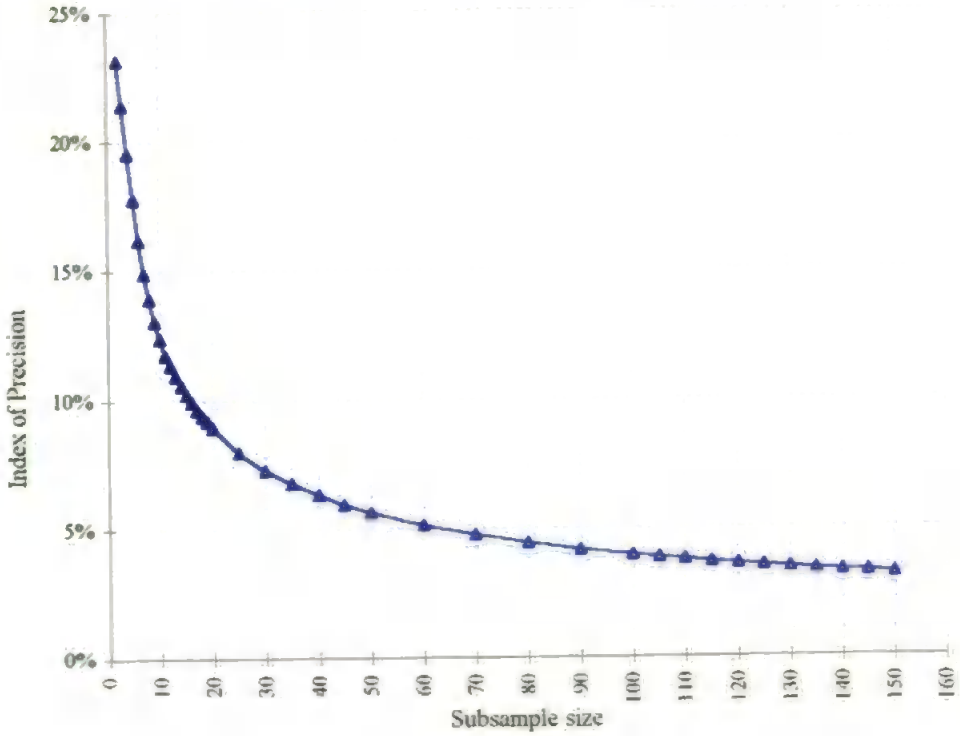

Figure 3.2. The digitising pad used for measuring organisms.

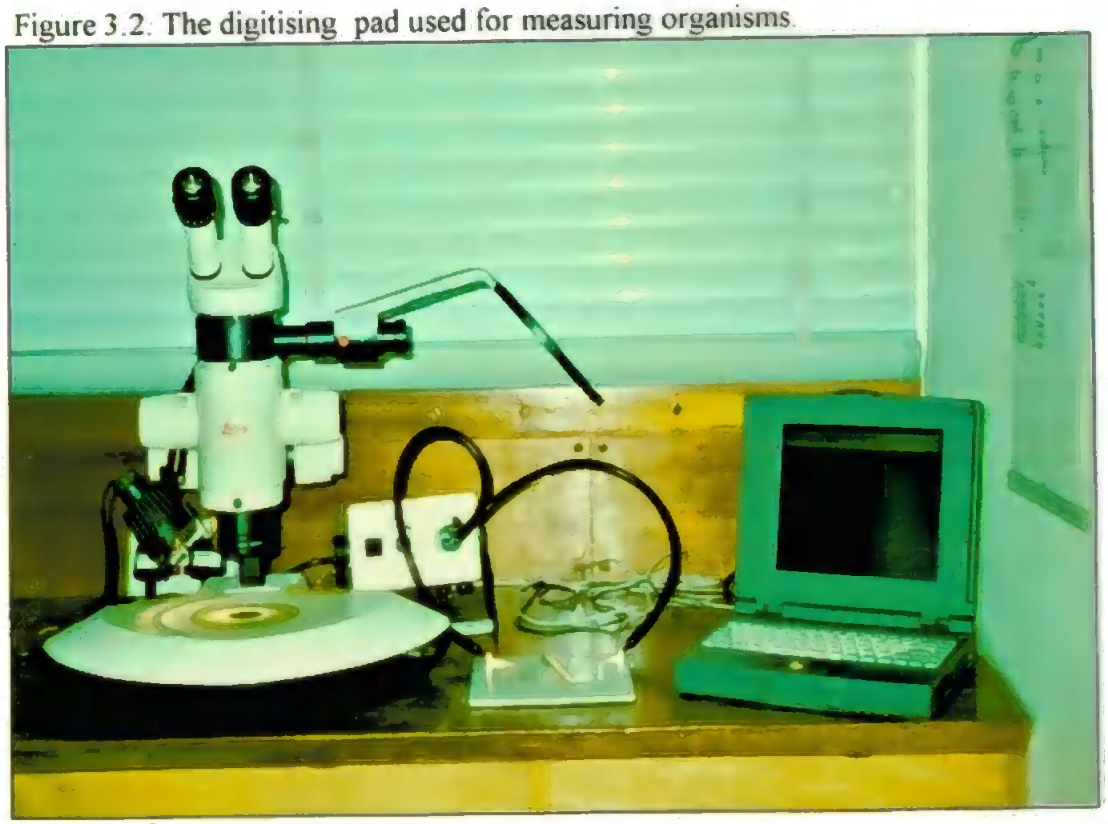

Size was expressed as an equivalent spherical diameter (ESD), to standardise for the variety of body shapes, calculated using the following equation (Schwinghamer 1981):

$$ESD = 2(3m / 4\pi d)^{1/3}$$

Table 3.1: Published and derived* values of density and dry/wt weight ratios for the different aquatic habitats.

Site	Mean salinity	Density	Dry/wet weight ratio
Freshwater	0	1.05	0.15
Upper estuary	0.9	1.052*	0.153*
Middle estuary	9.8	1.073*	0.179*
Lower estuary	33.8	1.129*	0.249*
Marine site	34.3	1.13	0.25

Where (m) is the wet mass of the organism and (d) is its density (from Table 3.1).

3.5.3. Statistical analysis

A multifactor analysis of Variance was used to compare log transformed values of ESD and biomass for: 1) all organisms (total sieve); 2) shape categories; 3) major taxa and 4) organisms' body lengths and widths, among sieves and sites to test for differences in these measures among sites and sieves, in order to assess which measure was suitable as a conversion factor and whether separate values were required for each site. Tests for normality were conducted visually using residuals plots to confirm homogeneity of variance. To achieve this goal a comparison between the total biomass size spectra resulting from each conversion factor was made firstly, in one season (e.g. summer) for all sites (freshwater, middle estuary and marine) and in all seasons for one site (e.g. marine).

For the mean major taxon biomass, there was considerable variation among sieves that masked the expected pattern; hence a multiple regression analysis was used to determine the best-fit line for these biomasses. Values for mean major taxon biomass for each site and each sieve were then derived from regression equations. The overall biomass value for each sieve in each study site was calculated using Edgar's formula (Edgar 1990).

$$B = \sum n_i * b_i$$

Where (B) is the overall biomass value for each sieve in each study site, (n_i) is the abundance of the major taxa $(_i)$ retained by that sieve size and (b_i) is the mean biomass of

the major taxon ($_i$) retained by that sieve size. This was to construct the total benthic biomass size spectra for the different sites separately in one season (summer) and for one site (marine) for all seasons as a test, which allowed a comparison of BBSS constructed using mean sieve, mean shape and mean major taxon biomasses.

3.5.3.1. Multiple regression analysis

Three models were possible in terms of regression line comparisons among sites. The first is that there is one model (one line) applicable for a major taxon in all sites. The second is that there are more than one model (i.e. a different line for each site), for each major taxon, but that these lines have the same slope (parallel lines). In the third model, each site again is represented by a different line, but in this case with different slopes. Figure (3.3) shows these different models. An example is given below for a hypothetical major taxon (nematodes) (Freshwater, middle estuary and marine sites will be referred as (FW), (ME) and (MA) respectively).

Dependent variable (Y): $\log_e$ nematode biomass in freshwater, middle estuary and marine sites. Independent variable (X): $\log_e$ sieve size.

From this point three subsequent models were calculated dependant on different assumptions, three important diagnostic parameters will be derived from each model, namely sum of squares (SS), degree of freedom (dF) and the mean square of the residuals (MS).

Assumption 1- the three sites are not significantly different in terms of nematode biomasses, (one line will represent all three sites, Figure 3.3 a) using the following model:

$$Y = a + bx \qquad \textbf{\{model 1\}}$$

Where (Y) is $\log_e$ nematode biomass, (a) is the intercept, (b) is the slope and (x) is $\log_e$ sieve size.

Assumption 2- the three sites are not equal in their nematode biomasses, three lines with three different intercepts and the same slope will represent the three sites, (three parallel lines Figure 3.3 b) using the following model:

$$Y = a_1 + bx + a_2(FW) + a_3(ME) \qquad \textbf{\{model 2\}}$$

Where (Y) is $\log_e$ nematode biomass, (a_1) is the intercept, (b) is the slope, (x) is $\log_e$ sieve size, $(a_2(FW))$ is the contribution of freshwater biomass in the intercept and $(a_3(ME))$ is the contribution of middle estuary biomass in the intercept. Neglecting $(a_2(FW) + a_3(ME))$ will enable the calculation of $\log_e$ nematode biomass in the marine site.

Assumption 3- the three sites are not equal in their nematode biomasses (three lines with three different intercepts and three different slopes will represent the three sites in terms of biomass, (three non-parallel lines Figure 3.3 c) using the following model:

$$Y = a_1 + b_1x(FW) + b_2x(ME) + b_3x(MA) + a_2(FW) + a_3(ME) \qquad \textbf{\{model 3\}}$$

Where (Y) is $\log_e$ nematode biomass, (a_1) is the intercept, (b_1) is the slope for freshwater site, $(x(FW))$ is $\log_e$ sieve size in case of freshwater site, (b_2) is the slope for middle estuary site, $(x(ME))$ is the $\log_e$ sieve size in case of middle estuary site. (b_3) is the slope for the marine site, $(x(MA))$ is the $\log_e$ sieve size of the marine site, $(a_2(FW))$ is the contribution of freshwater biomass in the intercept with (a_1) and $(a_3(ME))$ is the contribution of middle estuary biomass in the intercept with (a_1). If (FW) and (ME) are considered zeros this will result in calculating $\log_e$ nematode biomass for the marine site, (FW) and (MA) as zero will remove them from the model giving the value of $\log_e$ nematode biomass for the middle estuary site and finally, (ME) and (MA) as zero will result in calculating $\log_e$ nematode biomass for the freshwater site.

Figure 3.3. The three models of multiple regression analysis A) model 1, B) model 2 and C) model 3 (see text).

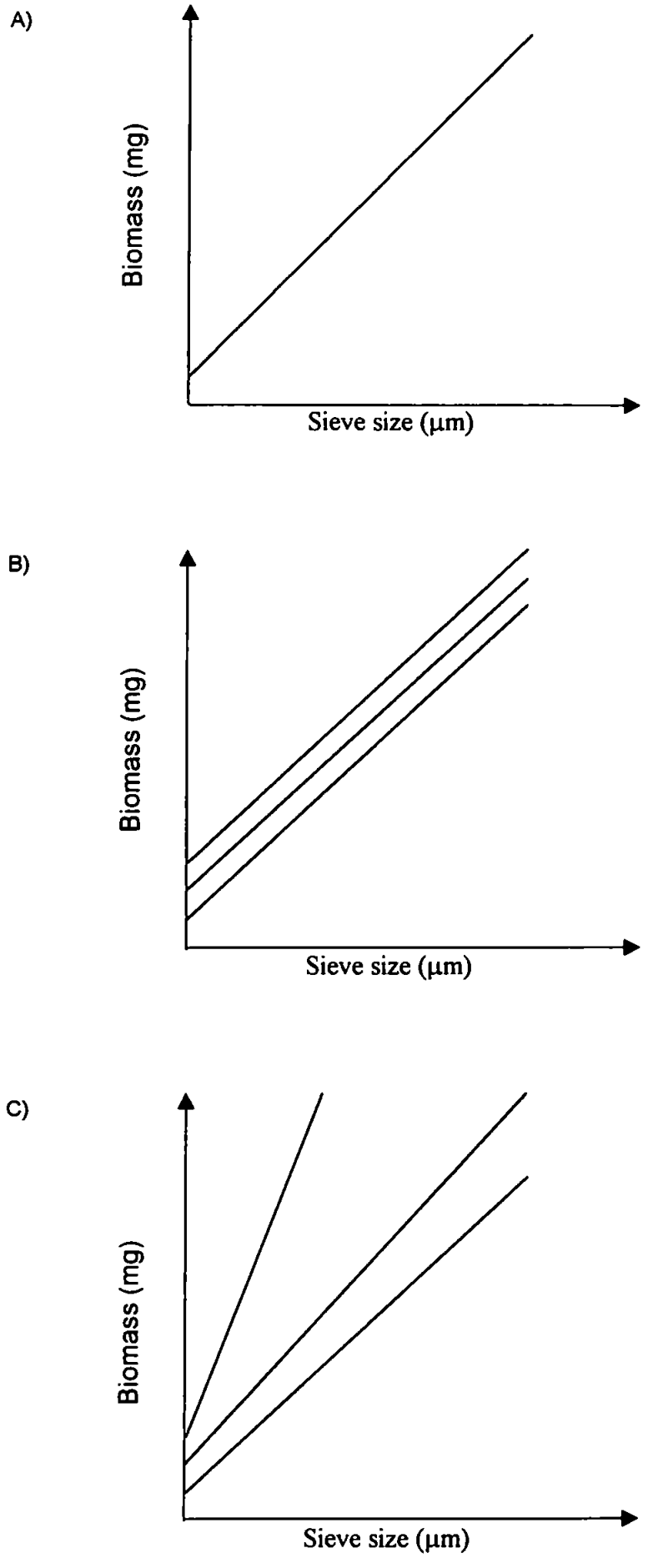

At this stage, the three previously mentioned parameters (sum of squares, degree of freedom and the mean square of the residuals) from each model will be used for calculating the F value, (see below):

1) To test if slopes are the same (model 2 is as good as model 3 so could replace model 3 for simplicity):

$$F = ((SS_2 - SS_3)/(df_2 - df_3))/MS_3$$

Where (SS_2) is the sum of squares of the residuals for model (2), (SS_3) is the sum of squares of the residuals for model (3), (df_2) is the degree of freedom of model (2), (df_3) is the degree of freedom of model (3) and (MS_3) is the mean square of model (3).

Here the decision should be taken, if the $F - calculated$ value is greater than the $F - tabulated$ value (column $(df_2 - df_3)$, row (df_3)), then there is a significant difference between the slopes (i.e. model 2 is not as good as model 3). If the $F - calculated$ value is smaller than the $F - tabulated$ value, then there is no significant difference between the slopes (i.e. model 2 is as good as model 3).

2) To test for a common line (same intercept) (model 1 is as good as model 2 so could replace model 2 for simplicity:

$$F = ((SS_1 - SS_2)/(df_1 - df_2))/MS_2$$

Where (SS_1) is the sum of squares of the residuals for model (1), (SS_2) is sum of squares of the residuals for model (2), (df_1) is the degree of freedom of model (1), (df_2) is the degree of freedom of model (2) and (MS_2) is the mean square of model (2). At this stage the $F - tabulated$ value is determined. Here the decision should be taken, if the $F - calculated$ value is greater than the $F - tabulated$ value, then there is a significant

Figure 3.4 Predicted and measured mean biomass values for A) Nematoda, B) Copepod and C) Oligochaeta in FW-freshwater, ME-middle estuary and MA-marine sites in Yealm system. (P, predicted; M. measured)

A)

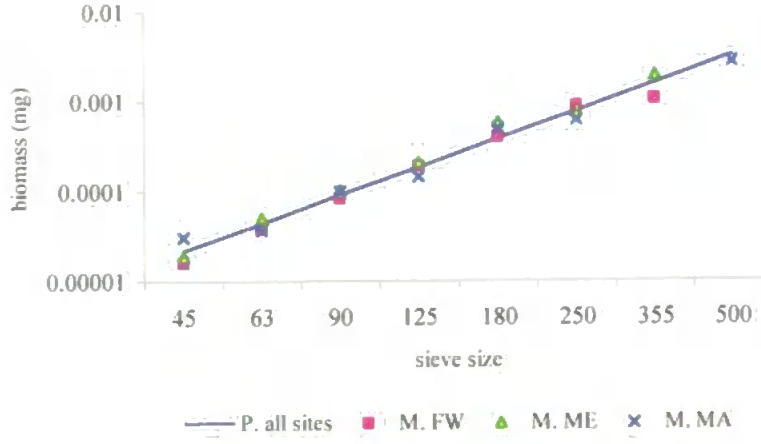

B)

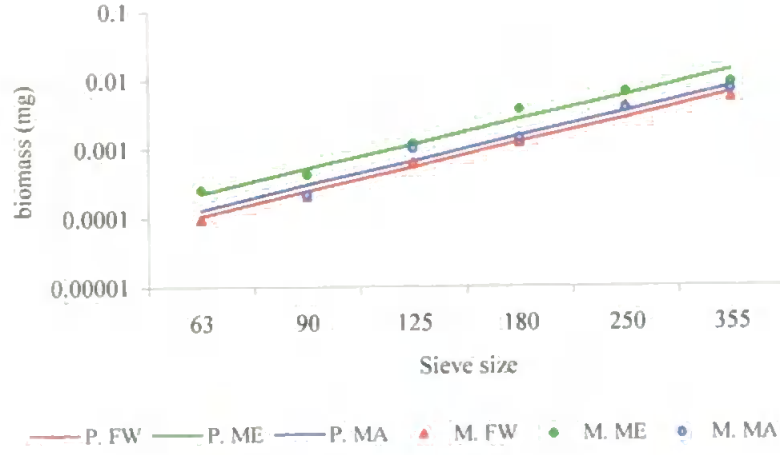

C)

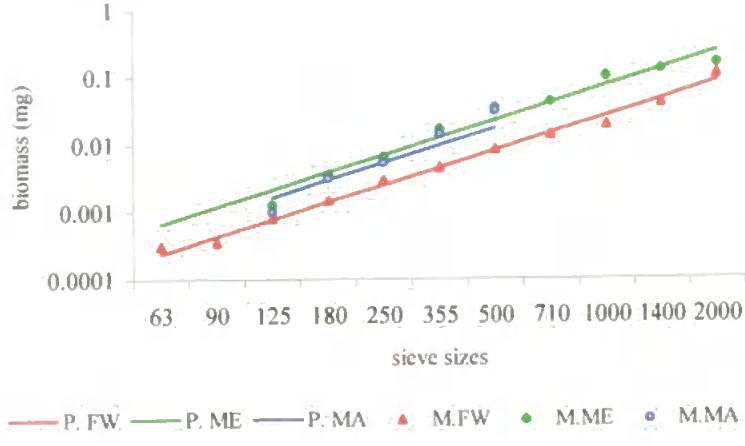

difference between the slopes (i.e. Model 1 is not as good as Model 2). If the $F-calculated$ value is smaller than the $F-tabulated$ value, then there is no significant difference between the slopes (i.e. Model 1 is as good as model 2).By these means, it could be possible to simplify from model 3 to model 1.

As an example of the detailed approach (see above) it was applied for different major taxa (Nematode, Copepoda and Oligochaeta) in three different sites namely (freshwater, middle estuary and marine) (Figure 3.4).

3.6. Results

Regression equations for the biomass of major taxa for each sieve derived using multiple regression analysis revealed that, in some cases, (e.g. nematodes) one regression equation could represent one major taxon in all sites, while in other cases (e.g. Copepoda and Oligochaeta) more than one regression equation was required to represent a single taxon (Table 3.2 and Figure 3.4). For taxa which were represented in only one or two sieve sizes, measured values were used. The most abundant organisms in samples from the Yealm system were those assumed to be cylinders (76.7%) followed by those for which power equations were available (20.8%). Only (2.5%) were classified as half cylinders and spheres (Table 3.3). Cylindrically shaped organisms were, on average, seven times longer than the mesh size they were retained by and organisms measured by power equation, about three times the length of the mesh.

Overall, mean individual ESD values (for the pooled average values in the three sites) increased with increasing mesh size and this pattern in the distribution of ESD values also existed among different shapes (Figure 3.5, Table 3.3). However, ESD values for the cylindrically shaped organisms were small relative to those for other shapes. Moreover, this difference in ESD between cylindrically-shaped and organisms of other shapes was greatest for macrofauna due to the dominance of long and thin macrofauna such as oligochaetes and polychaetes (Table 3.4 and Figure 3.6).

Although the shape of the plot of the log transformed mean sieve (total ESD) values of the study sites appeared consistent among sites (Figure 3.7), analysis of variance of log transformed mean sieve (total ESD, or total biomass) values revealed that there were significant differences ($p<0.0001$) among sites (freshwater, middle estuary and marine) and sieve sizes ($p<0.0001$). There was also a significant interaction between sites and sieve sizes resulting from between-site differences in the separation of data points along the body size axis (Table 3.5). Furthermore, these were also significant differences among sites, sieves and their interaction for the following levels: shape, taxonomy (major taxa) in terms of ESD and biomass and the biological level in terms of body dimensions (body lengths and widths) (Table 3.5), with the exception of mean ESD and mean biomass values of the nematode and polychaeta.

The influence of different levels of biomass (i.e. mean sieve, mean shape or mean major taxon biomass as conversion factors from total abundance to total biomass) on the final biomass size spectra among sites in one season (summer) is shown in Figure (3.8). Analysis of variance of log transformed total biomass size spectra values revealed that, within each site in summer there was no statistical difference among the BBSS constructed using different conversion factors (Figure 3.8). However, there was statistical difference between BBSS constructed from the same conversion factor among sites (Figure 3.9) (Table 3.6). For the analysis of one site (marine) in all seasons, there was a statistical difference between BBSS constructed from each of the biomass conversion factors within each season and among all seasons for BBSS constructed from the same conversion factor except in summer. Where there was no difference between BBSS constructed using any biomass conversion factor (Figure 3.10) (Table 3.7). These results highlight the influential role of abundance on BBSS (Figure 3.11).

Figures (3.9 to 3.12) illustrate two important points. Firstly, there was a significant difference in abundance size spectra between freshwater, middle estuarine and marine sites in one season (summer) ($P<0.0001$) and the shape of BBSS did not differ substantially

depending on the conversion factors used (mean sieve, mean shape or mean major taxon biomasses) among and within sites (Figures 3.8, 3.9). Secondly, that there was a significant difference among seasons within the marine site (one site in four seasons) in terms of abundance and biomass size spectra separately ($P<0.0001$) for each conversion factor (Figure 3.10 - 3.12). This may be due to the taxonomic variation among seasons (i.e. the absence or reduced abundance of some taxa in a particular season) which were abundant in the season (summer) where organisms were measured). For example, the presence of low abundance of polychaetes (high mean biomass) and high abundance of nematodes (low mean biomass) in the 355 μm sieve in autumn and spring relative to those in summer may explain the different pattern in the taxon curve in these seasons compared with the "sieve" and "shape" curves (Figure 3.10 B&D). However, in winter season, the presence of amphipods and ostracods (37.5% and 12.5%) respectively in addition to nematodes (50%) decreased the gap between the taxon curve and the "sieve" and "shape" curves (Figure 3.10 C).

BBSS in general (sieve, shape or taxon) were significantly different among seasons, this relates to the observed low abundance in winter (Figures 3.11).

Table 3.2. Regression equations for the major taxa in the Yealm in freshwater (FW), middle estuary (ME) and marine site (MA) in relation to the sieve size. R square is the regression coefficient which explains how much is the varation in the dependant variable, $\log_e$ (biomass).

Taxon	Site	R square	Regression equation	Appendix No.
Nematoda	All sites	98%	$\log_e$ (biomass)= -18.6393+2.07674*$\log_e$(sieve size)	3.1
Copepoda	FW	97%	$\log_e$ (biomass)= -18.99675+2.3778*$\log_e$(sieve size)	3.2
	ME	97%	$\log_e$ (biomass)= -18.2441+2.37779*$\log_e$(sieve size)	
	MA	97%	$\log_e$ (biomass)= -18.7963+2.37779*$\log_e$(sieve size)	
Oligochaeta	FW	97%	$\log_e$ (biomass)= -15.4245+1.70691*$\log_e$(sieve size)	3.3
	ME	97%	$\log_e$ (biomass)= -14.4073+1.70691*$\log_e$(sieve size)	
	MA	97%	$\log_e$ (biomass)= -14.6687+1.70691*$\log_e$(sieve size)	
Hydracarina	FW&MA	96%	$\log_e$ (biomass)= -20.5904+2.62575*$\log_e$(sieve size)	3.4
Ostracoda	All sites	97%	$\log_e$ (biomass)= -23.7819+3.40813*$\log_e$(sieve size)	3.5
Polychaeta	ME&MA	90%	$\log_e$ (biomass)= -18.0585+2.31616*$\log_e$(sieve size)	3.6
Amphipoda	ME	96%	$\log_e$ (biomass)= -19.7505+3.02439*$\log_e$(sieve size)	3.7
	MA	96%	$\log_e$ (biomass)= -21.5177+3.02439*$\log_e$(sieve size)	
Tricladida	FW	95%	$\log_e$ (biomass)= -15.1243+2.04161*$\log_e$(sieve size)	3.8
Nemertea	MA	95%	$\log_e$ (biomass)= -13.6975+1.55893*$\log_e$(sieve size)	3.9
Bivalvae	FW&MA	98%	$\log_e$ (biomass)= -22.7654+3.22507*$\log_e$(sieve size)	3.10
Coleoptera larvae	FW	96%	$\log_e$ (biomass)= -16.4393+2.21185*$\log_e$(sieve size)	3.11
Coleoptera adult	FW	66%	$\log_e$ (biomass)= -5.03067+0.85879*$\log_e$(sieve size)	3.12
Cladocera	FW	96%	$\log_e$ (biomass)= -19.7017+2.5169*$\log_e$(sieve size)	3.13
Chironomid	FW	98%	$\log_e$ (biomass)= -18.9652+2.45257*$\log_e$(sieve size)	3.14
Diptera larvae	FW	85%	$\log_e$ (biomass)= -18.1642+2.53619*$\log_e$(sieve size)	3.15
Plecoptera	FW	90%	$\log_e$ (biomass)= -18.7314+2.23902*$\log_e$(sieve size)	3.16
Gastropod	FW	99%	$\log_e$ (biomass)= -19.5023+2.48319*$\log_e$(sieve size)	3.17
Tardigrada	FW	86%	$\log_e$ (biomass)= -21.2553+2.84178*$\log_e$(sieve size)	3.18
Collembola	FW	95%	$\log_e$ (biomass)= -15.0187+1.77507*$\log_e$(sieve size)	3.19
Diptera pupae	FW	82%	$\log_e$ (biomass)= -6.75745+0.79331*$\log_e$(sieve size)	3.20

Table 3.3. The number of individuals for which length-mass relationships were used (power equation) and for which simple geometric shape categories were applied, ratio of body length to mesh size for each sieve, ratio of body width to mesh size, ratio of [body length/mesh size]/[body width/mesh size] and the mean individiual ESD values (mm) for each shape.

	Mesh size (μm)												
	2000	*1400*	*1000*	*710*	*500*	*355*	*250*	*180*	*125*	*90*	*63*	*45*	*Overall*
No. of individuals													
Power equa	8	12	20	26	16	42	201	301	402	184	46		1258
Cylinder	126	181	159	253	353	413	705	722	679	413	419	222	4645
Half cylinde	14	7	3	1	6	26		14	17	13			101
Sphere	1					3		21	11	19			55
Total	149	200	182	280	375	484	906	1058	1109	629	465	222	6059
Ratio of body length to mesh size													
Power equa	5.1	4.1	4.1	4.4	5	2.6	3	3.1	3	3	3		3.1
Cylinder	6.9	6.6	7.4	7.7	7.5	5.9	6.6	7.3	7.3	7.6	8.2	9.2	7.3
Half cylinde	6.1	2.6	2.3	5.8	3.8	2.7		2.8	2.8	2.5			3.2
Sphere	2					1.1		0.2	1.6	1.9			1.9
Overall	6.65	6.29	6.94	7.4	7.3	5.39	5.77	5.96	5.61	5.94	7.68	9.18	6.3
Ratio of body width to mesh size													
Power equa	1.08	0.44	0.51	0.53	0.45	0.71	0.92	0.96	1.06	0.99	1.16		1.0
Cylinder	0.24	0.2	0.21	0.27	0.32	0.42	0.4	0.39	0.33	0.33	0.34	0.33	0.3
Half cylinde	2.69	1.54	2	1.22	0.72	0.71		1.21	1.36	1.16			1.3
Sphere	1.84					1.07		1.28	1.14	1.15			1.2
Overall	0.5	0.3	0.3	0.3	0.3	0.5	0.5	0.6	0.6	0.6	0.4	0.3	0.5
Ratio of (Body length/mesh size)/(Body width/mesh size)													
Power equa	4.9	12.8	11.5	10.8	11.7	4.1	4.4	5.1	3.4	3.7	3.5		4.5
Cylinder	50.3	42.7	45.1	37.6	29.8	24.3	35.1	31.9	33.7	33.2	30.7	35.6	33.7
Half cylinde	4.4	2.2	1.2	4.8	12.1	8.6		2.5	2.1	2.3			4.8
Sphere	1.1					1.1		1.6	1.5	1.7			1.6
Overall	43.2	39.5	40.6	35.0	28.8	21.6	28.3	23.3	22.0	22.9	28.0	35.6	26.8
Mean individual ESD values (mm)													
Power equa	2.85	0.92	0.78	0.57	0.39	0.24	0.22	0.16	0.12	0.08	0.07		0.19
Cylinder	0.88	0.55	0.42	0.36	0.29	0.22	0.15	0.11	0.07	0.05	0.04	0.03	0.18
Half cylinde	3.47	1.23	1.01	0.70	0.29	0.18		0.14	0.10	0.06			0.71
Sphere	2.32					0.20		0.13	0.08	0.06			0.14
Overall	1.24	0.59	0.47	0.38	0.29	0.22	0.16	0.13	0.09	0.06	0.04	0.03	0.19

Note: The overall values were calculated by pooling all samples.

Figure 3.5 The mean sieve (ESD) values of organisms collected in 12 mesh sizes showing high significant difference among the sieve sizes.

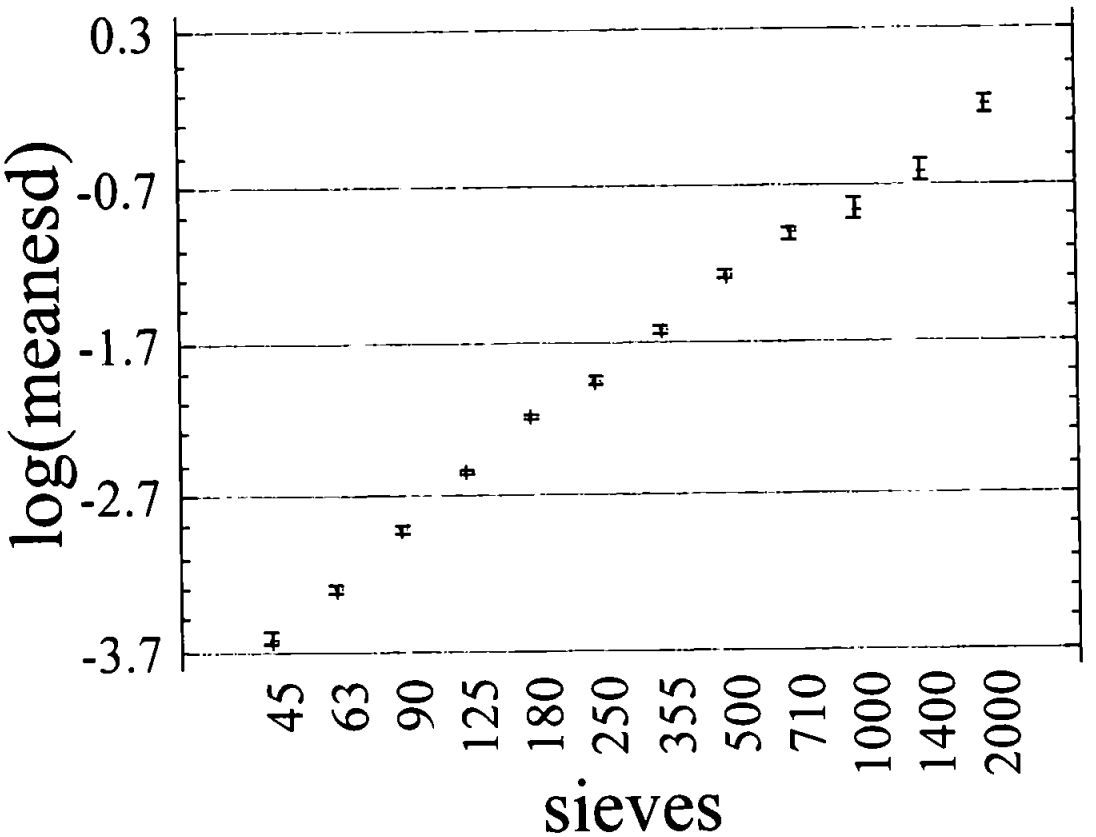

Figure 3.6 Overall Percentage of the measured major taxa per sieve in all sites.

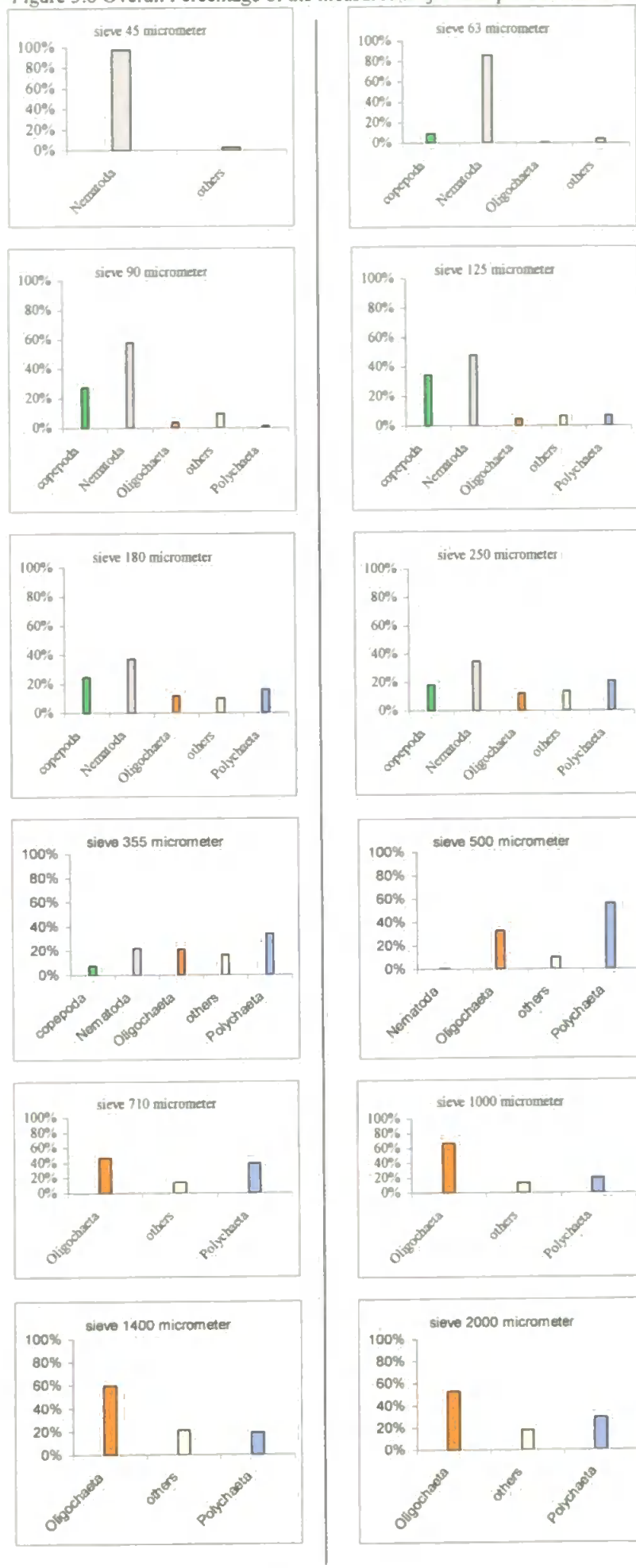

Table 3.4. Overall percentage of the measured organisms per sieve in (freshwater, middle estuary and marine sites).

Sieve size (µm)	taxon	overall % of measured organisms	Sieve size (µm)	taxon	overall % of measured organisms
45	Nematoda	97.7%	250	others	13.8%
45	others	2.3%	250	Polychaeta	20.8%
63	copepoda	9.2%	355	copepoda	7.4%
63	Nematoda	86.2%	355	Nematoda	21.9%
63	Oligochaeta	0.4%	355	Oligochaeta	20.7%
63	others	4.1%	355	others	16.5%
90	copepoda	27.5%	355	Polychaeta	33.5%
90	Nematoda	57.9%	500	Nematoda	1.1%
90	Oligochaeta	3.7%	500	Oligochaeta	32.8%
90	others	9.7%	500	others	10.1%
90	Polychaeta	1.3%	500	Polychaeta	56.0%
125	copepoda	34.4%	710	Oligochaeta	46.8%
125	Nematoda	47.6%	710	others	13.9%
125	Oligochaeta	4.5%	710	Polychaeta	39.3%
125	others	6.5%	1000	Oligochaeta	67.0%
125	Polychaeta	6.9%	1000	others	13.2%
180	copepoda	24.7%	1000	Polychaeta	19.8%
180	Nematoda	37.2%	1400	Oligochaeta	59.8%
180	Oligochaeta	11.8%	1400	others	21.1%
180	others	10.1%	1400	Polychaeta	19.1%
180	Polychaeta	16.2%	2000	Oligochaeta	52.7%
250	copepoda	18.3%	2000	others	18.2%
250	Nematoda	34.8%	2000	Polychaeta	29.1%
250	Oligochaeta	12.4%			

Figure 3.7 Log transformed total (ESD) values of the study sites (Yealm) across the sieve sizes.

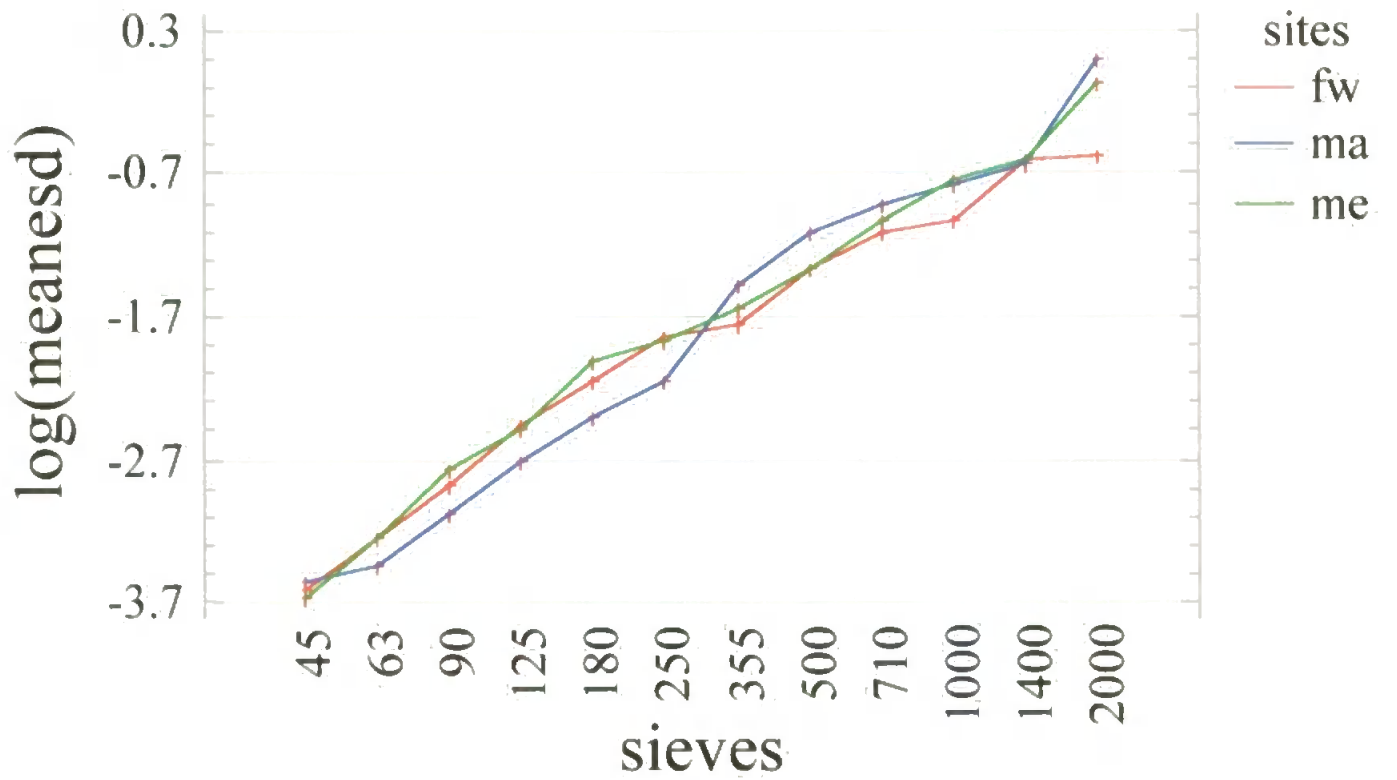

Table 3.5. (F) Values of ANOVA for the log transformed ESD and biomass values in the Yealm (P values) are represented by stars (*<0.05, **<0.001, ***<0.0001).

	Factor	Sites	Df	Sieves	Df	Interaction	Df	Appendix No.
Total	ESD	15.94***	2	1293.09***	11	13.37***	22	3.21
	Biomass	20.34***	2	1239.10***	11	13.37***	22	3.22
Shape	CYL ESD	17.61***	2	1219.83***	11	14.91***	22	3.23
	CYL Biomass	21.14***	2	1219.83***	11	14.91***	22	3.24
	Others ESD	45.14***	2	501.09***	5	2.81**	10	3.25
	Others Biomass	43.54***	2	501.09***	5	2.81**	10	3.26
Taxonomy	Nematoda ESD	1.83	2	291.95***	5	2.85**	10	3.27
	Nematoda Biomass	0.72	2	291.95***	5	2.85**	10	3.28
	Copepoda ESD	54.11***	2	161.59***	4	4.36***	8	3.29
	Copepoda Biomass	51.55***	2	161.59***	4	4.36***	8	3.30
	Oligochaeta ESD	31.11***	2	36.19***	4	2.01*	10	3.31
	Oligochaeta Biomass	32.85***	2	36.19***	4	2.01*	10	3.32
	Polychaeta ESD	0.46	1	188.11***	9	5.91***	9	3.33
	Polychaeta Biomass	1.28	1	188.11***	9	5.91***	9	3.34
Biology	Nematoda length	20.27***	2	457.08***	5	4.62***	10	3.35
	Nematoda width	24.64***	2	103.60***	5	4.58***	10	3.36
	Copepoda length	66.38***	2	457.66***	4	9.35***	8	3.37
	Copepoda width	88.57***	2	200.79***	4	10.85***	8	3.38
	Oligochaeta length	25.14***	2	56.86***	4	14.59***	10	3.39
	Oligochaeta width	14.22***	2	7.91***	4	1.85	10	3.40
	Polychaeta length	29.27***	1	157.71***	9	11.42***	9	3.41
	Polychaeta width	7.8**	1	39.44***	9	12.7***	9	3.42

Table 3.6. (F) values of multifactor ANOVA of total BBSS resulted from using the three means of biomass for three different sites in one season, (P) values were *<0.05, **<0.001 and ***<0.0001. DF (degree of freedom).

Sites	Mean sieve biomass	Mean shape biomass	Mean taxon biomass	DF of biomass levels	Appendix No.
Freshwater	2.06			2	3.43
Middle estuary	1.15			2	3.44
Marine	1.22			2	3.45
All sites	4.17*			2	3.46
All sites	165.39***	120.42***	143.04***		
DF for sites	2	2	2		
Appendix No.	3.47	3.48	3.49		

Table 3.7. (F) values of multifactor ANOVA of total BBSS resulted from using the three means of biomass for one site in all seasons, (P) values were *<0.05, **<0.001 and ***<0.0001. DF (degree of freedom).

Season	Mean sieve biomass	Mean shape biomass	Mean taxon biomass	DF of biomass levels	Appendix No.
Winter	4.56*			2	3.50
Spring	8.93**			2	3.51
Autumn	19.19***			2	3.52
Summer	1.22			2	3.45
All seasons	27.36***			2	3.53
All seasons	170.85***	126.50***	85.01***		
DF for seasons	3	3	3		
Appendix No.	3.54	3.55	3.56		

Figure 3.8. Total biomass size spectra constructed using (mean sieve, mean shape & mean major taxon) biomass in summer for freshwater (A), middle estuary (B) and marine sites (C).

A)

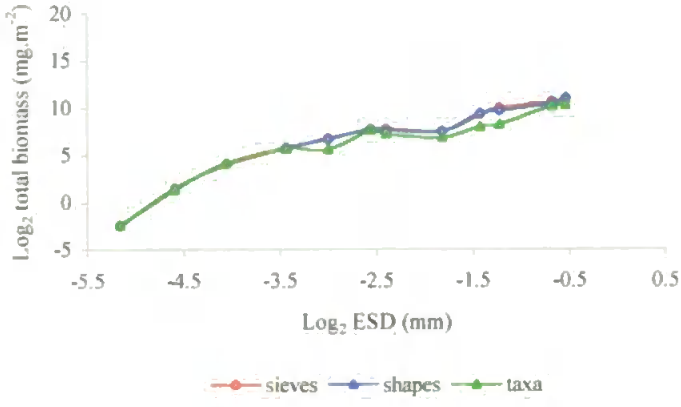

B)

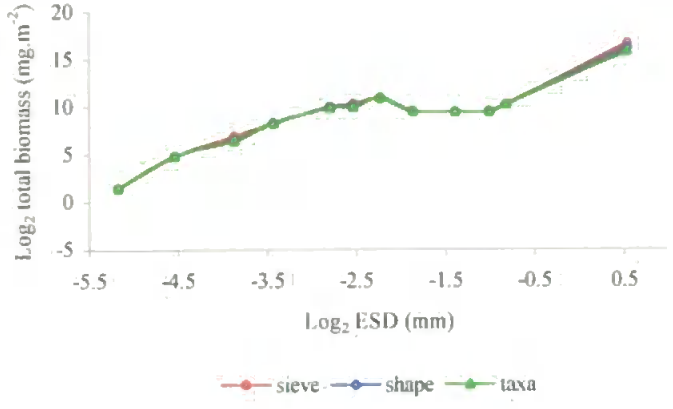

C)

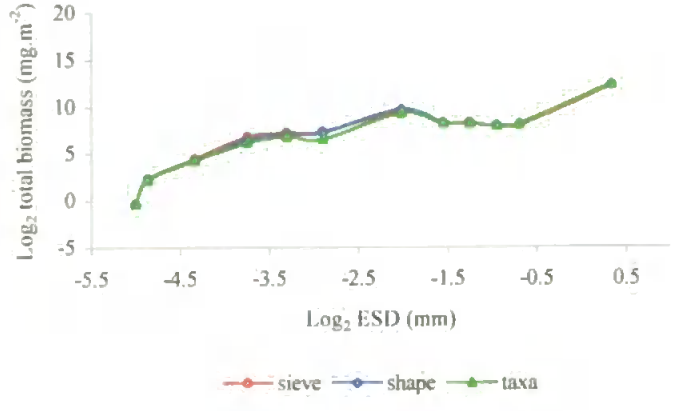

Figure 3.9 Benthic size spectra for FW-freshwater, ME-middle estuary and MA-marine sites in summer: A) abundance; and total biomass constructed using B) mean sieve biomass, C) mean shape biomass and D) mean taxon biomass.

A) mean abundance size spectra

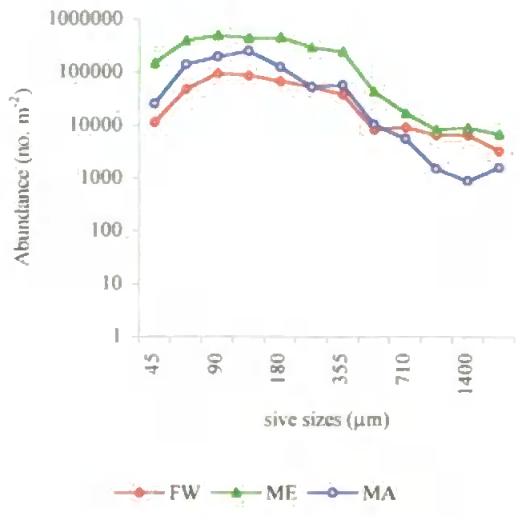

B) mean sieve biomass

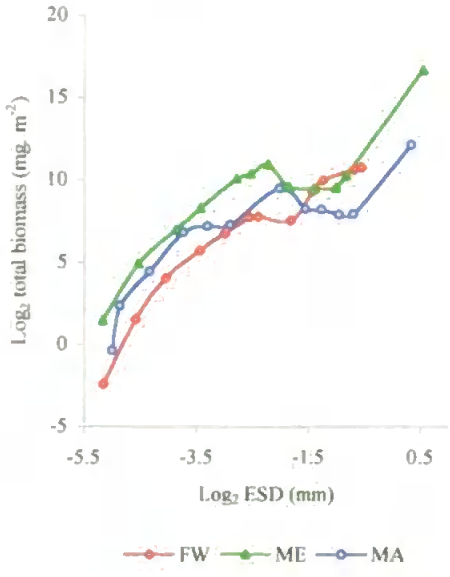

C) mean shape biomass

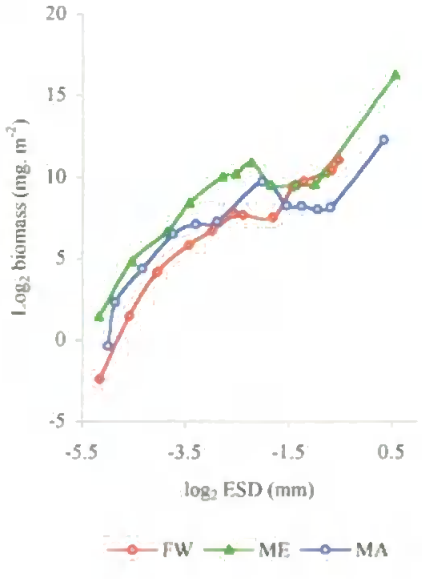

D) mean taxon biomass

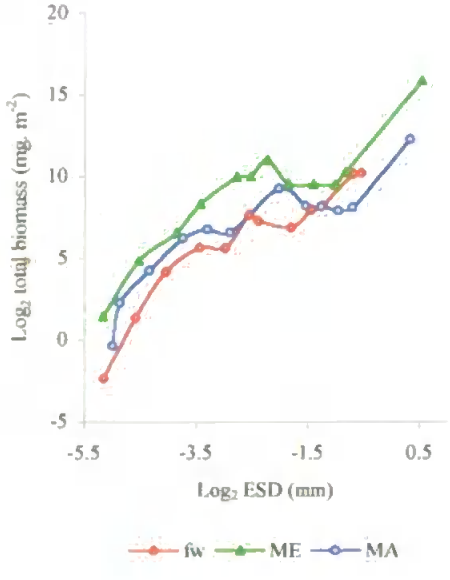

Figure 3.10. Total biomass size spectra constructed using mean (sieve, shape and taxon) biomass for marine site in summer (A), autumn (B), winter (C) and spring (D).

A)

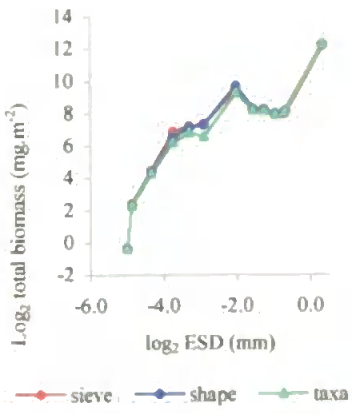

B)

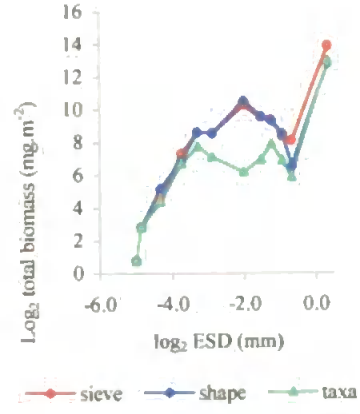

C)

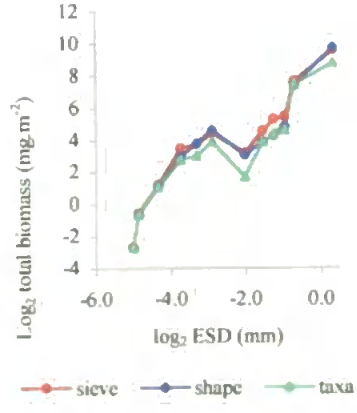

D)

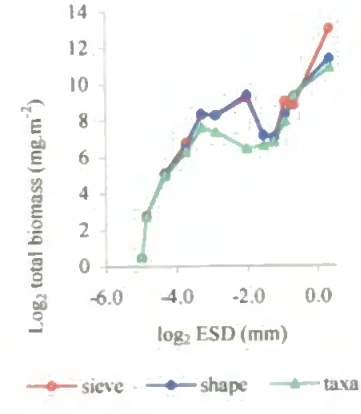

Figure 3.11 Seasonal mean abundance in the marine site.

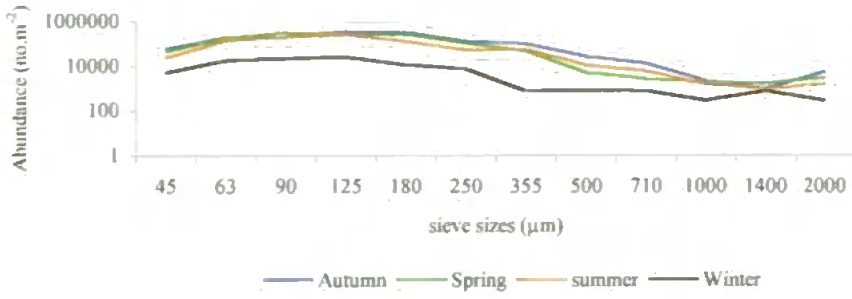

Figure 3.12 Seasonal biomass size spectra for marine site constructed using mean sieve biomass (A), mean shape biomass (B) and mean taxon biomass (C).

A)

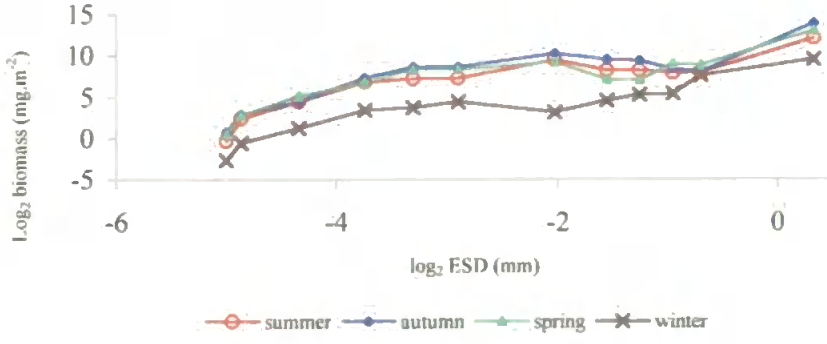

B)

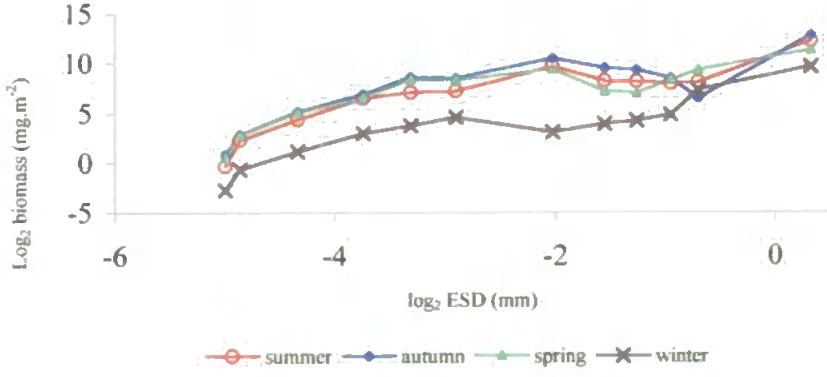

C)

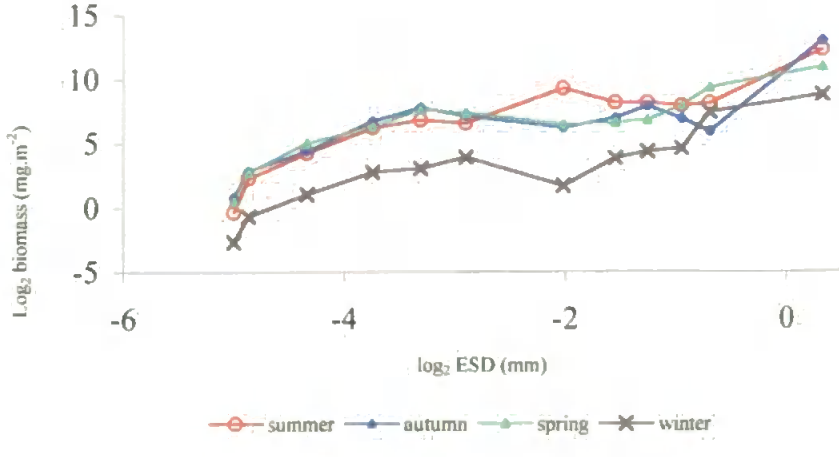

3.7. Discussion

The results of this chapter provide important supplementary information to the methodology given by Ramsay *et al* (1997) in terms of comparing the shapes of benthic biomass size spectra in different sites and seasons. Application of multiple regression analysis reduced the variation in taxon biomass values across the sieve sizes, giving standard values to be used as conversion factors within sites and among seasons assuming that mean major taxon biomass is invariable among seasons. This was achieved by predicting the mean major taxon biomass per sieve per site from the measured values.

Although there was no significant difference in BBSS within sites (freshwater, middle estuary and marine) in summer or between measures (mean sieve, mean shape and mean major taxon biomasses), there was a difference in BBSS between sites for each measure and between measures and seasons for each measure within one site (marine) (Tables 3.6 & 3.7).

The significant low BBSS constructed using the mean taxon biomass within one site (marine) for all seasons except in summer, relative to those constructed using the other biomass conversion factors may be as a result of the overestimation of BBSS using the mean sieve or mean shape biomass as conversion factors. For the same season, total abundance is the same within the same site and using mean sieve or mean shape biomass as conversion factors may include other taxa which were present in summer (where organisms were measured) and absent or reduced in abundance in other seasons. This could result in an overestimation of the BBSS, if compared with that constructed using the mean major taxon biomass, which is the real representation of the taxa present. Therefore, mean major taxon biomass is going to be used as the valid conversion factor throughout the current study.

Despite the similarity between this study with that of Ramsay *et al* (1997) in terms of the overall ratios of the organism body length to mesh size and the closeness of the overall mean ESD values for the different body shapes (Table 3.3), cylindrically shaped organisms

behaved differently through the sieving process than other shapes. Mean ESD values for the cylindrically shaped organisms were consistently smaller than both that of the other shapes within the same sieve size and that of the organisms allocated the category of the power equation in the next smaller sieve size. This may be explained by these long and thin taxa becoming coiled around the mesh wires, especially in coarse sieves as suggested by Edgar (1990), thus reducing the mean organism weight. This artefact became less obvious for meiofauna, so it could be deducted that the pattern was due to the dominance of Oligochaeta and Polychaeta in the macrofauna category (Table 3.4 & Figure 3.5), which were gradually replaced by other cylindrically shaped organisms, like Ostracoda, Tardigrada, Collembola, etc. These are characterised by their body length not exceeding their width, the organisms therefore behaving to some extent as other body shapes, reducing the difference between the mean ESD for the cylindrically shaped organisms and that of the other body shapes in the meiofauna category. Edgar (1990) and Bachelet (1990) suggested that, in marine systems, different body shapes of the same biomass might be caught in different sieves, particularly Polychaeta, Oligochaeta and Nematoda. This suggestion might support the findings of the current study. However, the overall mean ESD values for the sieve sizes were significantly different from each other (Figure 3.5).

The percentage of the different body shapes measured in Ramsay *et al.*'s (1997) study, (72% as power equation and 22% as cylinders) may explain any contrasting results with the current study (i.e. there being no difference between mean ESD values for cylindrically shaped organisms and that of the other shapes). In the current study, organisms represented by power equations were about 20.8% and 76.7% were cylinders. The low percentage of the measured cylinders in the study of Ramsay *et al* (1997) might underestimate the influence of these body shapes on the final biomass size spectra in habitats containing large numbers of polychaetes, oligochaetes and nematodes.

The significant difference in mean sieve biomass among sites observed in the current study contrasts with the results of Ramsay *et al* (1997) which could be explained by the large

difference in the sites of the current study from freshwater to marine compared with freshwater and upper estuarine sites (Ramsay *et al.*, 1997).

Different taxonomic distribution in both categories of meiofauna and macrofauna may be the reason of the overlap between freshwater site and marine site (Figure 3.7). i.e. in the marine site, most of the meiofaunal organisms were nematodes compared with that of freshwater, where oligochaeta, ostracoda and tardigrada were abundant, in contrast, the presence of nemertea in the macrofaunal category in the marine site resulted in relatively high mean ESD values if compared with that of freshwater, while in the middle estuary site, taxa represented in both freshwater and marine site were present especially in the meiofauna category, therefore, its mean ESD values were high. Despite the underestimation of the size of cylindrical organisms, the described method is valuable for quick, direct comparison of sites, but any comparison with spectra derived using alternative methods should be treated with caution.

In conclusion, this chapter provides supplementary information to that given by Ramsay *et al* (1997) for comparing the shapes of the plots of benthic biomass size spectra in different sites and seasons. Temporal and spatial taxonomic variability within and between sites can be taken into account by using mean major taxon biomass per sieve as a conversion factor for calculating total biomass. Although this technique may underestimate the size of cylindrically shaped organisms, it is still a useful tool for comparing the shapes of benthic biomass size spectra from different geographical locations. Regression models also allow a robust means of generating major taxon mean biomass values.

3.8. The recommended method for BBSS construction

For constructing BBSS using this method, the following outlined procedures are advisable:

1. Collection of sample while low tide.
2. Macrofauna separation from meiofauna using 500 and 45 μm mesh sizes.

3. Fixing meiofauna and sediments in the plastic pots with 10% formalin until finishing the macrofaunal processing (separation from the sediments, washing into 2000, 1400, 1000, 710 and 500 μm mesh sizes and then fixing each size category by 70 % alcohol).
4. Separating meiofauna from the sediments by floatation on Ludox™ (McIntyre and Warwick 1984) three subsequent times to ensure complete extraction of meiofauna from the sediments.
5. Washing the extracted meiofauna through 355, 250, 180, 125, 90, 63 and 45 μm mesh sizes and then collecting these organisms within each size category in a separate tube to be fixed by 70 % alcohol.
6. Direct counting or subsampling in case of macrofauna and large meiofauna or small meiofauna respectively to be performed using binocular stereomicroscope.
7. Measurement of organisms to be achieved using a *camera lucida* connected to laptop programmed for measuring the organisms' body dimension (taking into account the curvatures of the organisms) drawn on a digitising pad.
8. Ten organisms are enough for getting accurate result of either mean sieve, shape or major taxon biomass. However, the more measurements the more accuracy.
9. Where no published data for density or the dry/wet weight ratio for organisms in sites like the estuary, these values might be predicted from the published data in other sites (freshwater and marine) as a function of salinity.
10. Mean major taxon biomass is the best conversion factor to be used for converting total abundance into total biomass.
11. Multiple regression analysis could be used to overcome the variability of the conversion factors across the mesh sizes.

CHAPTER 4

Variation in Benthic Size Spectra Across A Full Salinity Gradient

4.Variation in benthic size spectra across a full salinity gradient

4.1. Introduction

Size spectra are a tool that is being used increasingly to evaluate and compare the structure of aquatic communities (Hanson, 1990). It is important to quantify the seasonal and spatial variations of benthic biomass size spectra in order that they may be incorporated in environmental assessment programs as diagnostic measures of community or ecosystem structure (Morin *et al.* 1995). To date, however, benthic size spectra studies have tended to focus on one type of aquatic system, for example, Strayer (1986) and Poff *et al.* (1993) for freshwaters and Warwick (1984) and Drgas *et al.* (1998) for marine systems. Any possible impact of a salinity gradient within the same system on the benthic size spectra has been neglected.

Few studies on temporal and spatial variability of size spectra exist. Strayer (1986) found no obvious change in biomass and abundance size spectra between the littoral sediments (1m through 5m) and oxygenated gyttia (7.5 m) of Mirror Lake, New Hampshire. In contrast, he reported abrupt spatial changes between depths of 7.5 m and 10.5 m. He suggested that these differences were not related to body size, but instead were a result of the low number of species, which are able to tolerate the seasonal anoxia at 10.5 m.

Similarly, Drgas *et al.* (1998) reported that benthic biomass spectra conformed to a common pattern in the Gulf of Gdansk (Southern Baltic Sea) and could be represented by a single "averaged" spectrum, despite differences in habitat and community structure between the studied sites. Other studies for freshwater habitats have shown consistent patterns in the distribution of biomass between sites and dates, despite large differences in taxonomic composition (Cattaneo, 1993, Bourassa and Morin, 1995). Benthic biomass size spectra (BBSS) in nine freshwater habitat types investigated by Poff *et al.* (1993) were similar to those observed for the marine benthos but not to other freshwater benthic systems, being bimodal instead of unimodal. In marine sites, workers have concluded that

biomass distribution patterns are a consistent, conservative and predictable feature of communities (Schwinghamer, 1981, 1985). Warwick (1984) stated that species body size distributions from eight temperate marine benthic communities showed a highly conservative pattern with two separate log-normal distributions, corresponding to the traditional categories of meiofauna and macrofauna. More recently, however, Duplisea (1998) concluded that BBSS had a consistent pattern along a salinity gradient arguing that the bimodal 'common' pattern did not exist in like regions / conditions throughout the world.

However, other studies reported differences in size spectra for different habitats. For example, Morin and Nadon (1991), showed that there was significant difference in size structure of epilithic lotic organisms among 12 streams and Hanson (1990) recorded significant differences between two weed-bed habitats in terms of macrobenthos size spectra. Similarly, Shirayama and Horikoshi (1989) pointed out that benthic size spectra varied between different depths (sublittoral, upper-slope and deep sea areas) of the Western Pacific Ocean, with the average size of individuals decreasing with increasing water depth. Other studies have reported both temporal and spatial variability in biomass size spectra. For example, Hanson *et al.* (1989) for lake macrofauna, Aller and Stupakoff (1996) for the whole marine benthic community and Soltwedel *et al.* (1996) for benthic Nematoda.

The inconsistency in benthic size spectra among the different habitats may result from an inconsistency in the methodology used. This chapter will compare and estimate the variation of benthic size spectra (if any) across a full salinity gradient using a consistent methodology.

4.2. Aims

The main goal of this chapter was to study the seasonal variation in benthic size spectra (abundance and biomass) across a full salinity gradient (i.e. from freshwater to marine) within the same river/coastal system.

4.3. Materials and methods

Five sites were sampled in the Yealm system, (freshwater, upper estuary, middle estuary, lower estuary and marine - See chapter 2 & 3 for sampling and sample processing). Abundance and biomass size spectra were standardized by calculating the percentage of abundance or biomass in each sieve relative to the total (sum of all abundance or biomass in all sieves) (Hanson 1990). Normalized benthic biomass size spectra were also constructed (Rodriguez and Magnan, 1993) to facilitate comparison among sites.

Differences between sieves, sites, seasons and their interaction in terms of abundance, biomass were examined by ANOVA using log (N+1) transformed data. Abundance and biomass data were tested for normality visually to confirm homogeneity of variance.

4.4. Results

4.4.1. Seasonal and spatial variations in abundance size spectra

Multifactor analysis of variance of log (N+1) transformed abundance values for all sites in all seasons revealed that there were significant differences between sieves ($P<0.0001$), sites ($P<0.0001$), seasons ($P<0.0001$) and their interactions ($P<0.0001$) (appendix (4.1)).

Generally, benthic abundance size spectra (Figure 4.1) showed a conservative pattern across the different sites of increasing abundance with decreasing body size. However, this pattern broke down in winter, where there was a trough corresponding to the 355 μm size class and where macrofaunal and meiofaunal size categories were relatively equal (Figure 4.1). Moreover, the abundance of meiofauna in the freshwater site in autumn was lower than those of summer and spring seasons.

Standardized abundance size spectra for summer did not differ markedly in shape among the study sites (Figure 4.2) and peaked in the 90 μm (for freshwater and middle estuary sites) and 125 μm sieves (for upper, lower estuary and marine sites). Macrofauna were represented at all sites by only a small fraction (2.4-9.3 %) of the total abundance in the size range 500 – 2000 μm.

Standardized abundance size spectra in autumn peaked in the 125 μm size class for upper, middle, lower estuary and marine sites (Figure 4.2). The freshwater site showed a different pattern, with peaks in 355 and 125 μm size classes (Figure 4.2). Again, macrofauna were represented by a small fraction of the total abundance, except for the freshwater site where 24 % of organisms were retained by the 355 μm sieve. In winter, standardized abundance size spectra showed a completely different pattern compared with other seasons in all sites except marine (Figure 4.3): freshwater, upper, middle estuary abundance size spectra showed a higher macrofaunal abundance compared with the meiofaunal abundance, while in lower estuary site macrofauna and meiofauna were fairly equal.

In spring there was a similar pattern to that of summer and autumn (Figure 4.3) with a peak abundance in the meiofaunal size range (63 μm for the freshwater site; 90 μm for upper, middle estuary and the marine site; and 125 μm for the lower estuary site). Macrofauna represented only a small fraction of the total abundance (Figure 4.3).

4.4.2 Taxa driving patterns in abundance and biomass size spectra

Abundance spectra for the individual major taxa within the different sites and seasons (Figures 4.4, 4.5) provide important information on which organisms were driving the patterns observed. Some major taxa were abundant across most of the sites, for example nematodes, copepods in the meiofaunal size range and oligochaetes (except the marine site) and polychaetes (except in the freshwater site) in the macrofauna (Figures 4.4, 4.5). Some taxa did have a site-specific distribution, however, insect larvae for example were abundant in the freshwater site and amphipods in the lower estuary and marine sites. Oligochaetes were also dominant in the freshwater site whilst Polychaetes dominated in the marine site (Figure 4.4, 4.5).

Variation in the abundance of the major taxon may influence the biomass spectra. For example, in summer, the observed peak in the 355 μm size class was due to oligochaetes and dipteran larvae in the freshwater site, and polychaetes and nematodes in the middle

estuary site and polychaetes, nematodes and copepods in the marine site (Figure 4.4). In autumn, the observed high biomass in the 1000 μm size class in the freshwater site is related to the presence of bivalves with high mean biomass, whilst the biomass peak in the 355 μm size class in the middle estuary site is mainly due to high abundance of polychaetes. Moreover, the flatness of the biomass in the 180-500 μm size range in the marine site is probably due to the combined effect of abundant nematodes, copepods, bivalves, amphipods and polychaetes (Figure 4.4).

In winter, where the shape of the spectra broke down, the irregularity in BBSS in freshwater is probably due to the presence of Coleoptera in the 500-1000 μm size range compared with that in the 1400 μm size class. Irregularity in the meiofaunal category was mainly due to the presence of just one taxon (nematodes) which was the main meiofaunal constituent (Figure 4.5). In the middle estuary site, the detected biomass trough in the 355 μm size class is due to the low nematode and copepod abundance and absence of oligochaetes and polychaetes in this size class. In the marine site, the presence of polychaetes only in the 1000 μm size class relative to the other macrofaunal size classes is responsible for the detected low biomass in this size class, while lower nematode and ostracod abundances in the 355 μm size class relative to those in the next smaller size class (250 μm) lowed the biomass value in the 355 μm size class. In spring, in the freshwater site, the co-presence of oligochaetes along with dipteran larvae and bivalves in a wide size spectrum (180-2000 μm) may result in the regular biomass increase in this size range. The presence of polychaetes in the 250 μm size class increases the biomass in this size class, while in the 45-125 μm size range, nematodes, oligochaetes and copepods were the shaping factors for the biomass spectrum in this size range (Figure 4.5). Similarly, in the middle estuary site, the persistent presence of oligochaetes and polychaetes in a wide range of size classes, approximately the whole size range studied, resulted in the regularity in biomass spectrum. Moreover, the presence of amphipods in the 1000 μm size class and ostracods in

Figure 4.1 Abundance size spectra in the Yealm (fw-freshwater, ue-upper estuary, me-middle estuary, le-lower estuary, ma-marine site). A) summer; B) autumn; C) winter; and D) spring. (Note differences in Y-axis scale).

A)

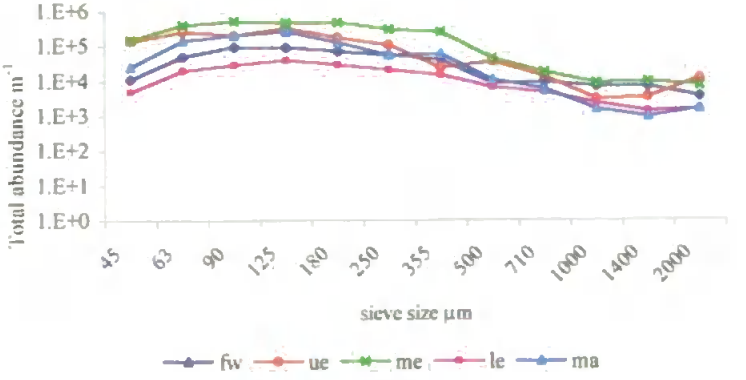

B)

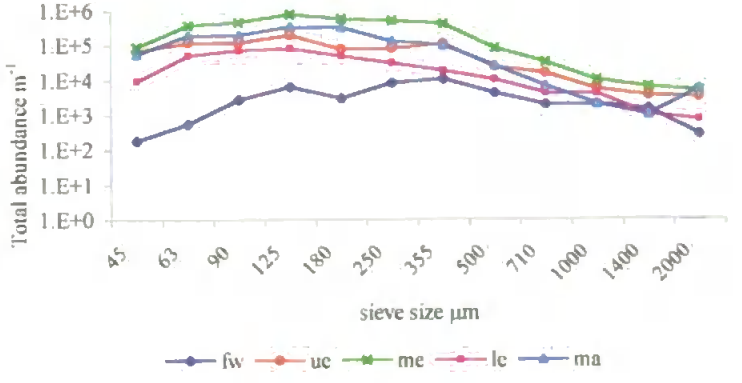

C)

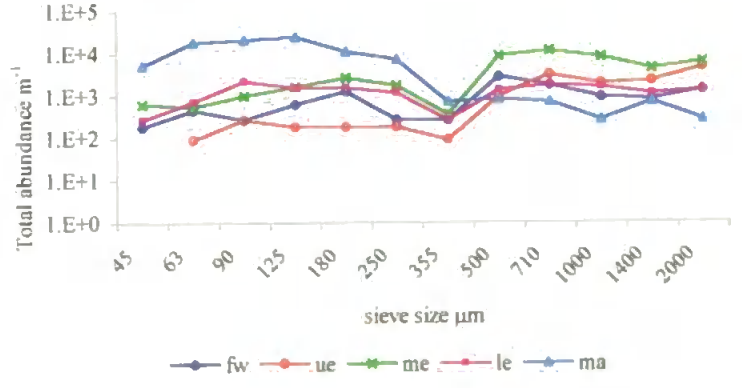

D)

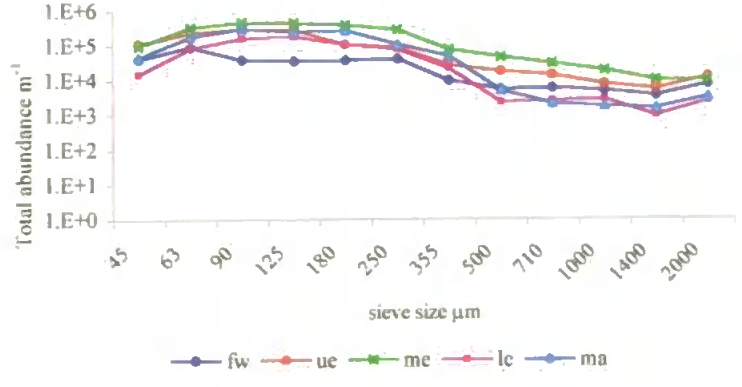

the 250 μm size class may be related to the relative high biomass in these size classes. In the marine site, the gradual decrease in the nematode and copepod abundance in the 180-500 μm size range may be the reason for the counterpart biomass spectrum in the same site and season (Figure 4.5).

4.4.3 Seasonal and spatial variation in absolute BBSS

Three sites were chosen for studying biomass size spectra (freshwater, middle estuary and marine) representing the full salinity gradient.

Despite the significant differences between sieves ($P<0.0001$), sites ($P<0.0001$), seasons ($P<0.0001$) and their interactions ($P<0.0001$) in terms of log transformed biomass values for freshwater, middle estuary and marine sites over the year as a whole (appendix (4.2)), a conservative pattern of increasing biomass with increasing body size was found across sites and seasons. The BBSS interaction plot for sites and seasons revealed that the BBSS for the freshwater site were significantly lower than those of the marine site, which in turn, was significantly lower than those of the middle estuary site, for all seasons (Figures 4.6, 4.7). Biomass size spectra in winter were significantly lower than those of the other seasons (Figure 4.6).

Although there were shallow troughs in BBSS which varied among sites and seasons (Figures 4.8, 4.9), these troughs were less than half an order of magnitude in relation to the biomass represented in the $\log_2$ ESD category of -2.4 (sieve size 355 μm) and −1.2 (sieve size 1000 μm) in the freshwater site in summer and autumn, respectively. Similarly, in the middle estuary site in summer and autumn, and marine site in all seasons, the troughs were also less than half an order of magnitude for BBSS in relation to the biomass represented in the $\log_2$ ESD category of −2.2 (sieve size 355 μm) in the middle estuary in both seasons and in the marine site, in the $\log_2$ ESD categories of −2.0, -3.3, (-1.3 & -2.9) and −3.3 in summer, autumn, winter and spring, respectively. The two drops in the freshwater BBSS in winter were less than an order of magnitude in relation to the biomass represented by $\log_2$

Figure 4.2 Standardized abundance size spectra for all sites in the Yealm in 1) summer, 2) autumn for fw-freshwater; ue-upper estuary; me-middle estuary; le-lower estuary; and ma-marine site.

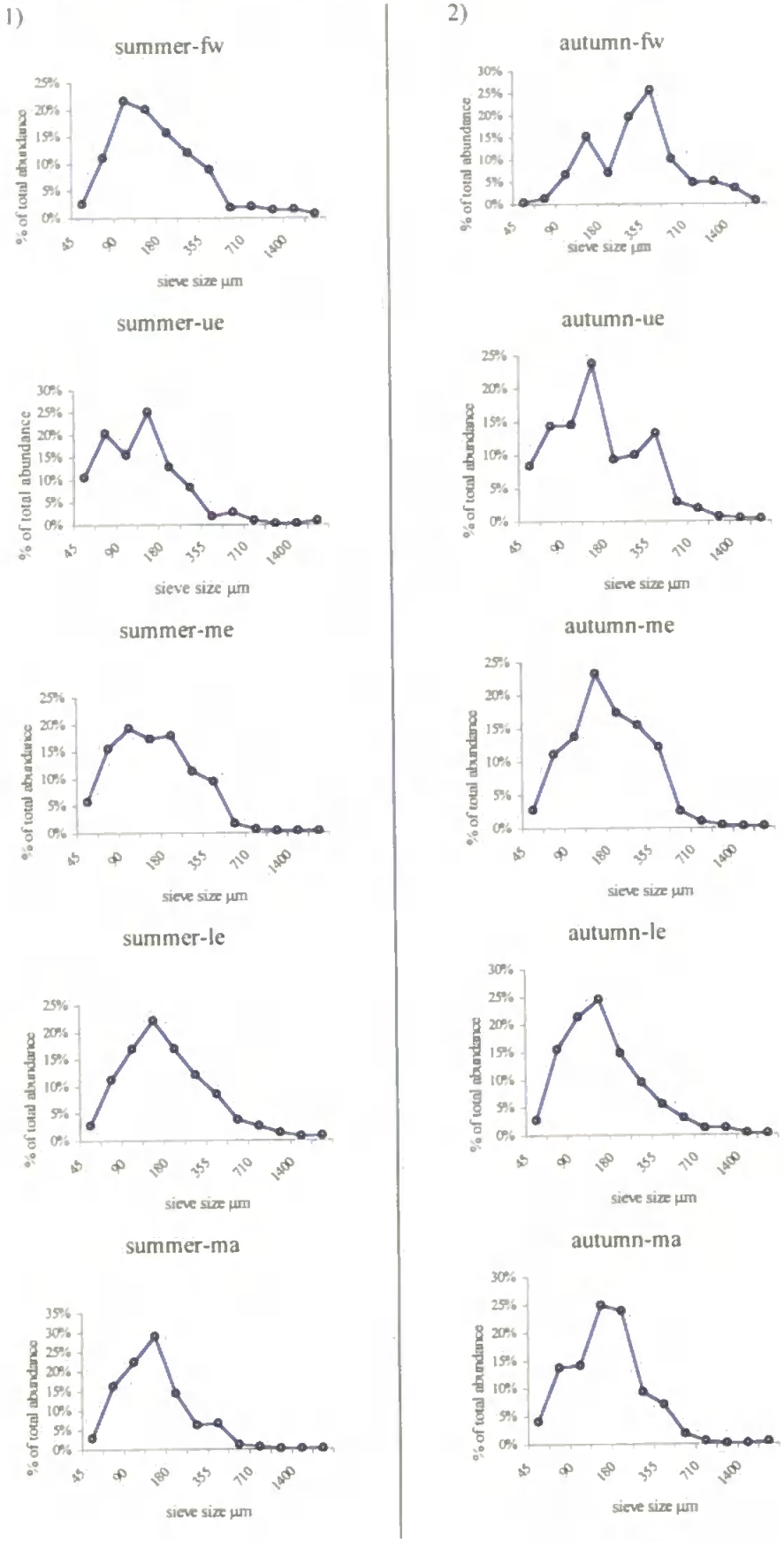

Figure 4.3 Standardized abundance size spectra for all sites in the Yealm in (1) winter, 2) spring for fw-freshwater; ue-upper estuary; me-middle estuary; le-lower estuary; and ma-marine site. (note differences in Y-axis scale).

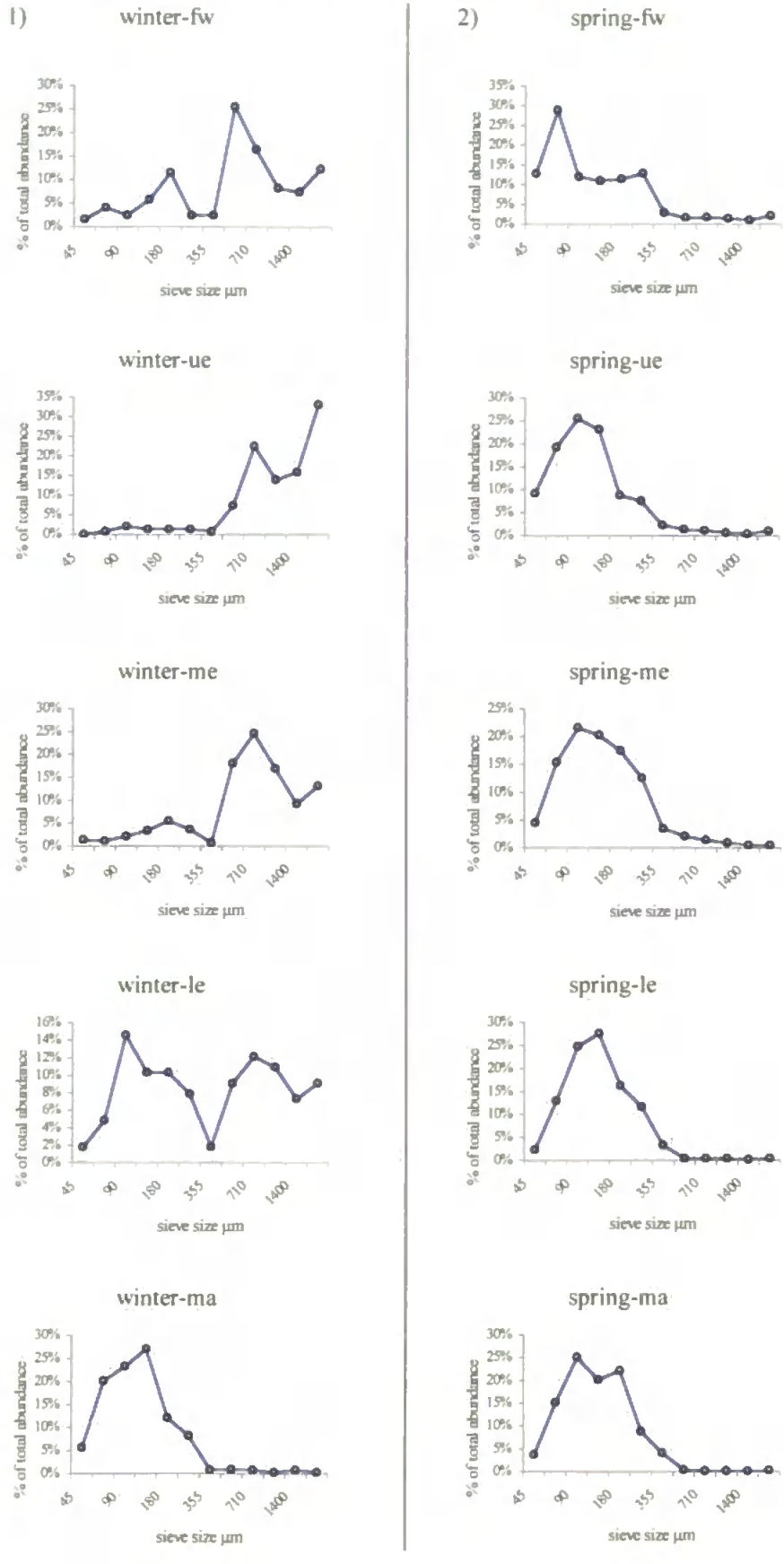

Figure 4.4 Mean abundance of the major taxa in the Yealm in 1) summer and 2) autumn in freshwater, upper, middle, lower estuarine and marine sites.

1) summer freshwater site.

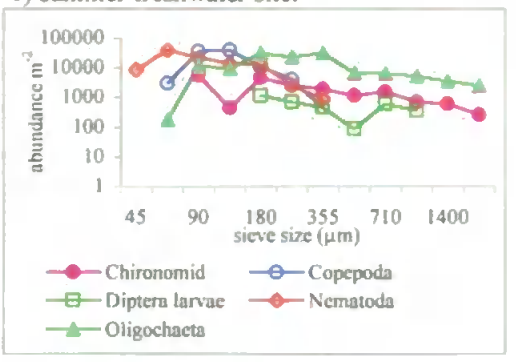

2) autumn freshwater site

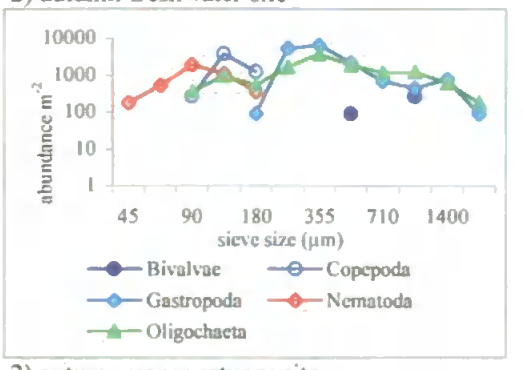

1) summer upper estuary site

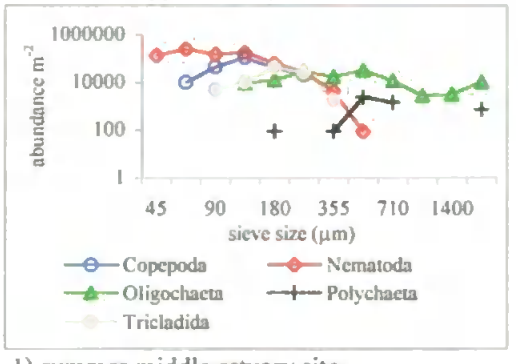

2) autumn upper estuary site

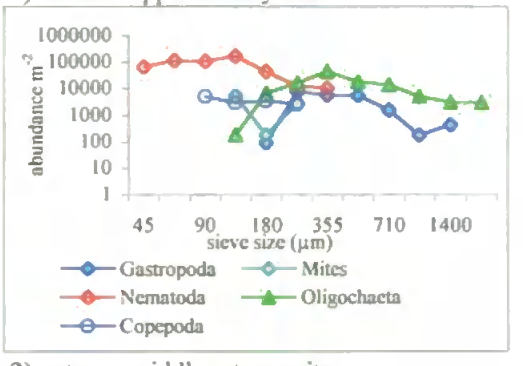

1) summer middle estuary site

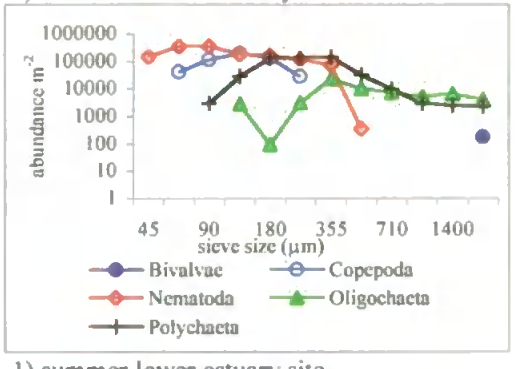

2) autumn middle estuary site

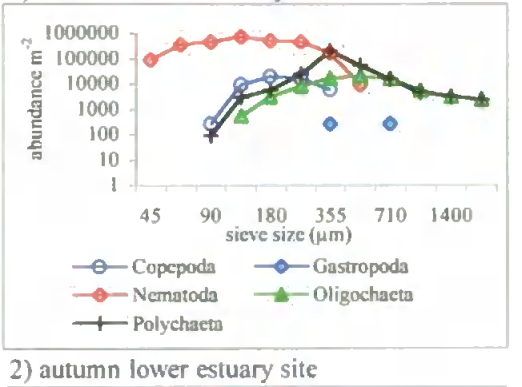

1) summer lower estuary site

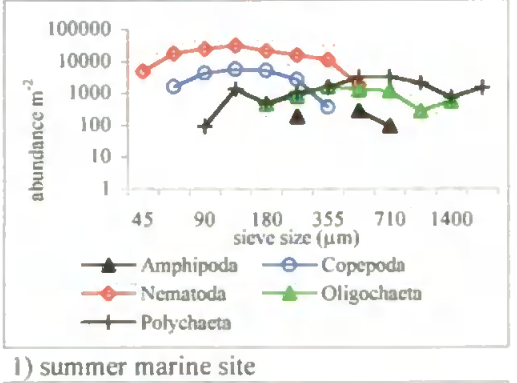

2) autumn lower estuary site

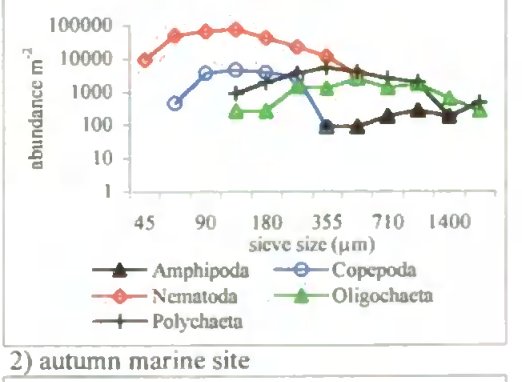

1) summer marine site

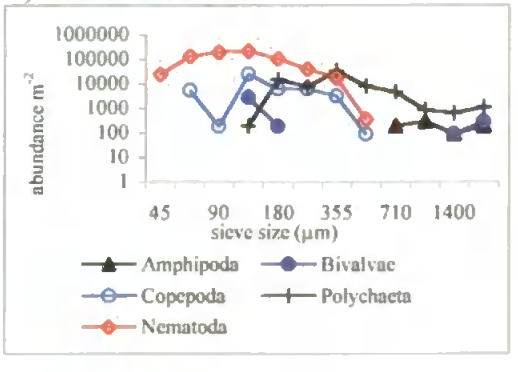

2) autumn marine site

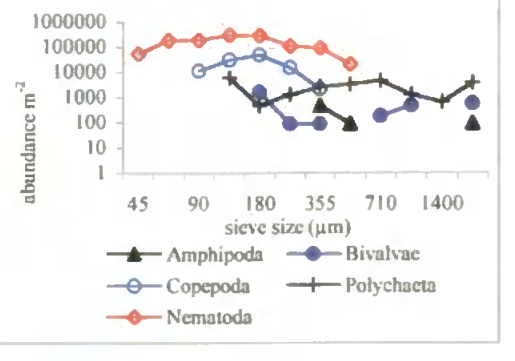

Figure 4.5 Mean abundance of the major taxa in the Yealm in 1) winter and 2) spring in freshwater, upper, middle, lower estuarine and marine sites.

1) winter freshwater site.

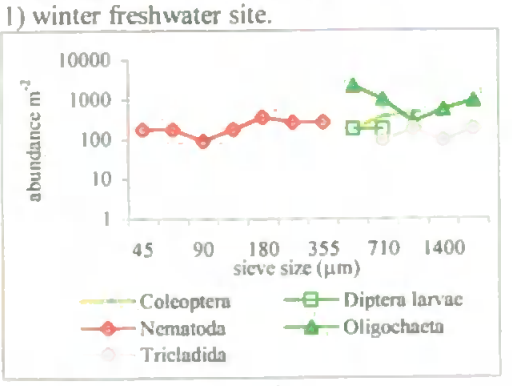

2) spring freshwater site

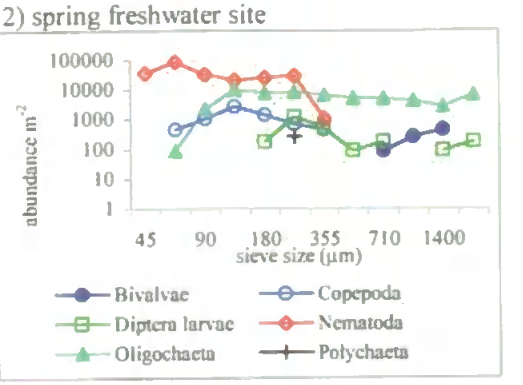

1) winter upper estuary site

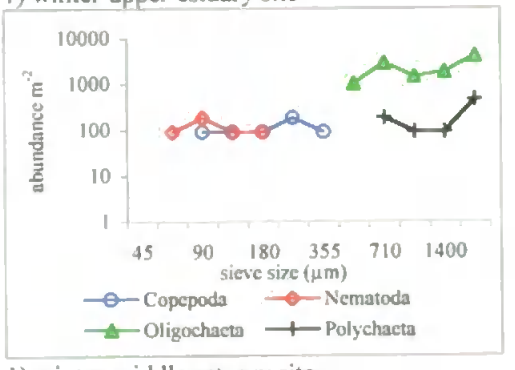

2) spring upper estuary site

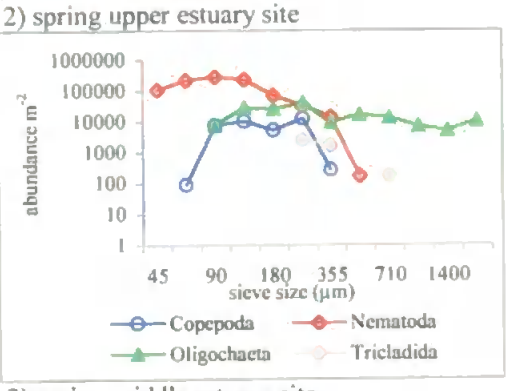

1) winter middle estuary site

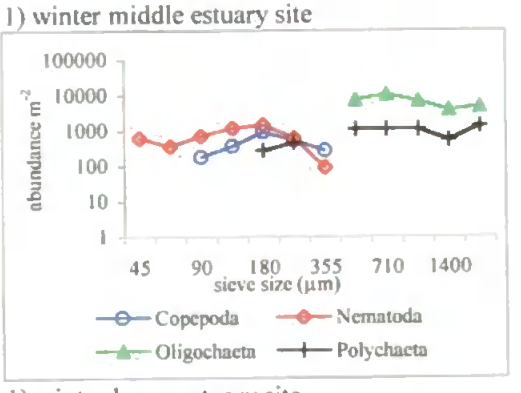

2) spring middle estuary site

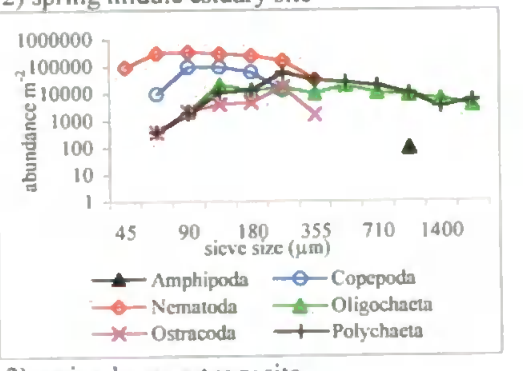

1) winter lower estuary site

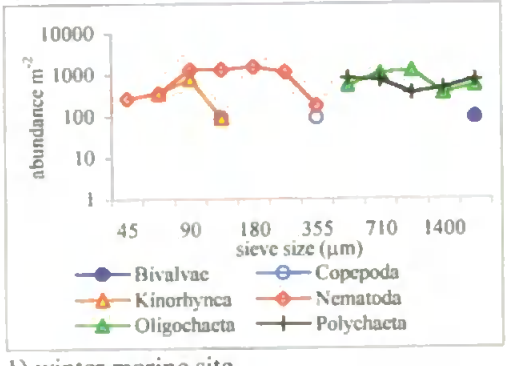

2) spring lower estuary site

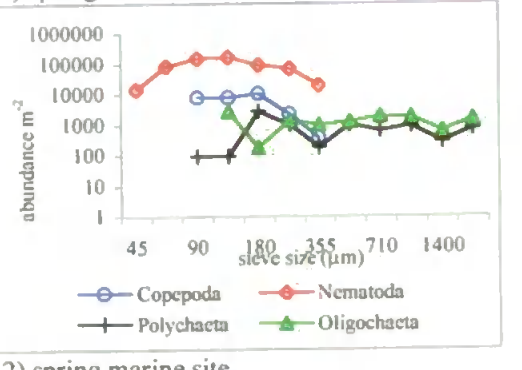

1) winter marine site

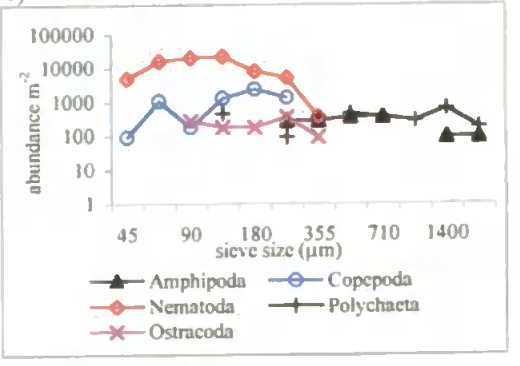

2) spring marine site

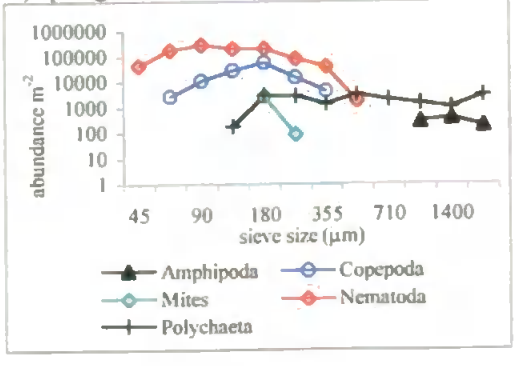

Figure 4.6 Log biomass (N+1) interaction plot of seasons and sites in the Yealm. fw-freshwater site, me-middle estuary site and ma-marine site.

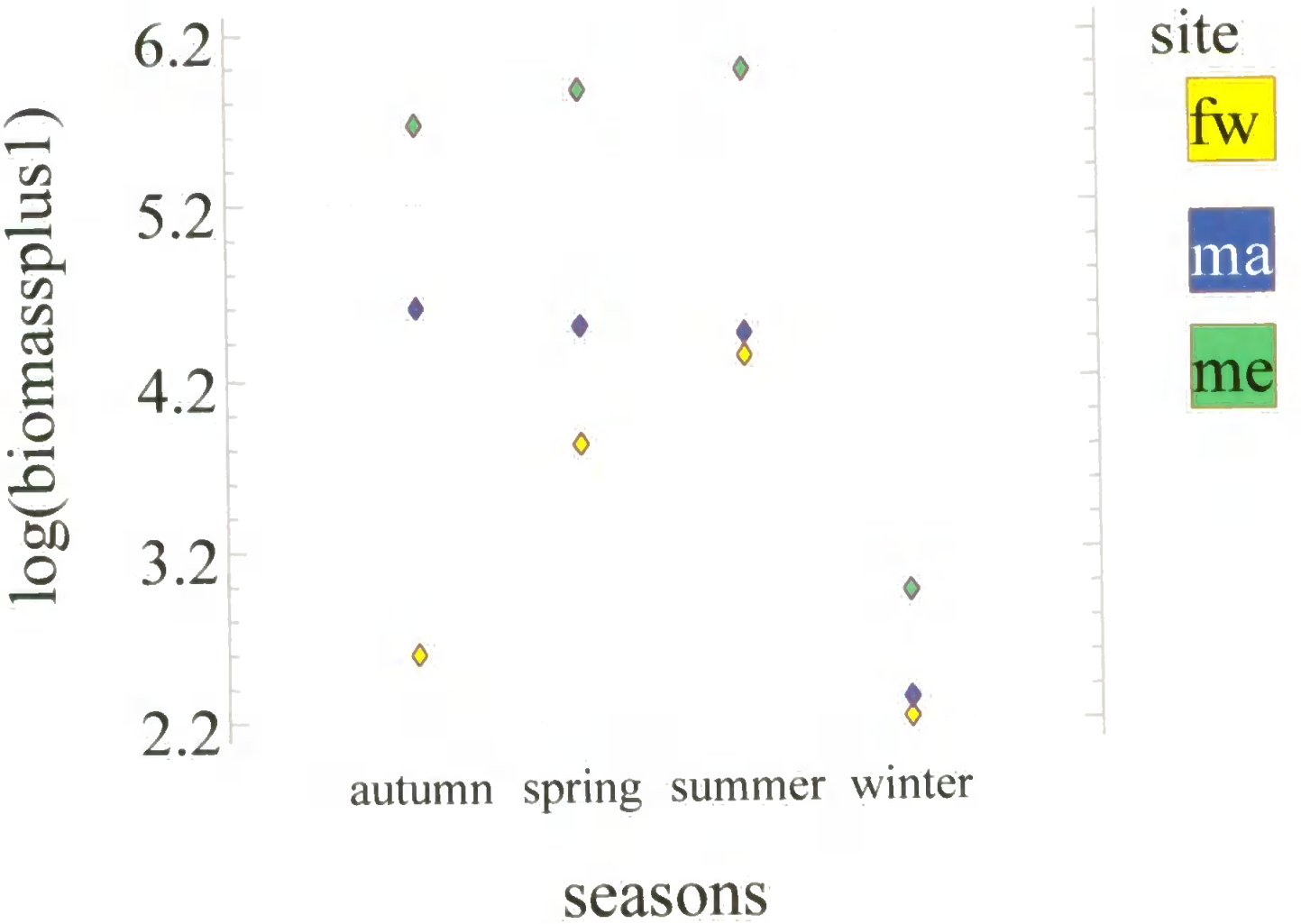

Figure 4.7 Absolute benthic biomass size spectra for all sites in the Yealm in summer, fw-freshwater, me-middle estuary and ma-marine sites.

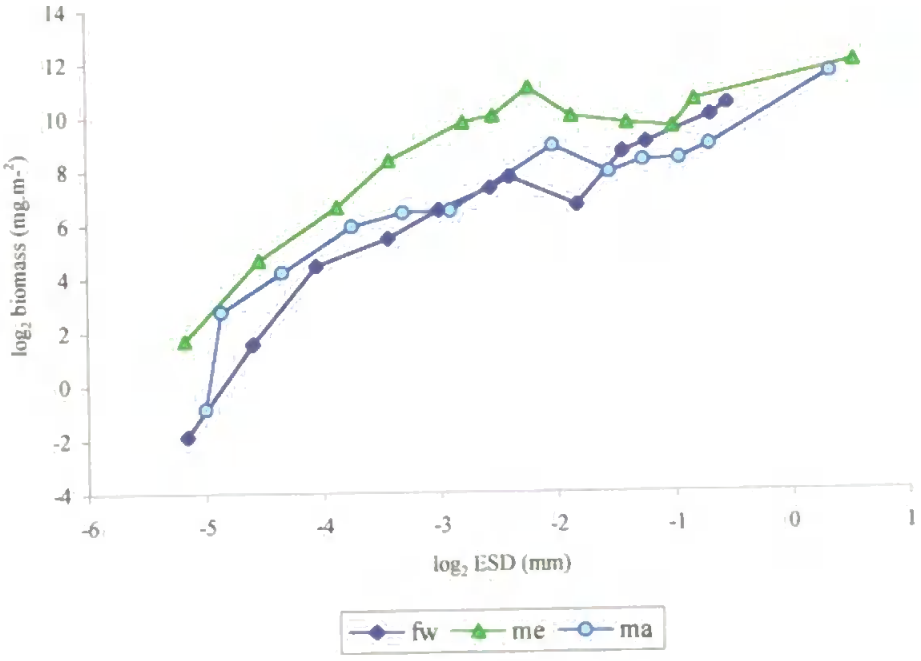

Figure 4.8 Absolute benthic biomass size spectra for all sites in the Yealm in 1) summer; 2) autumn. fw-freshwater; me-middle estuary; and ma-marine sites (Note differences in Y-axis scale).

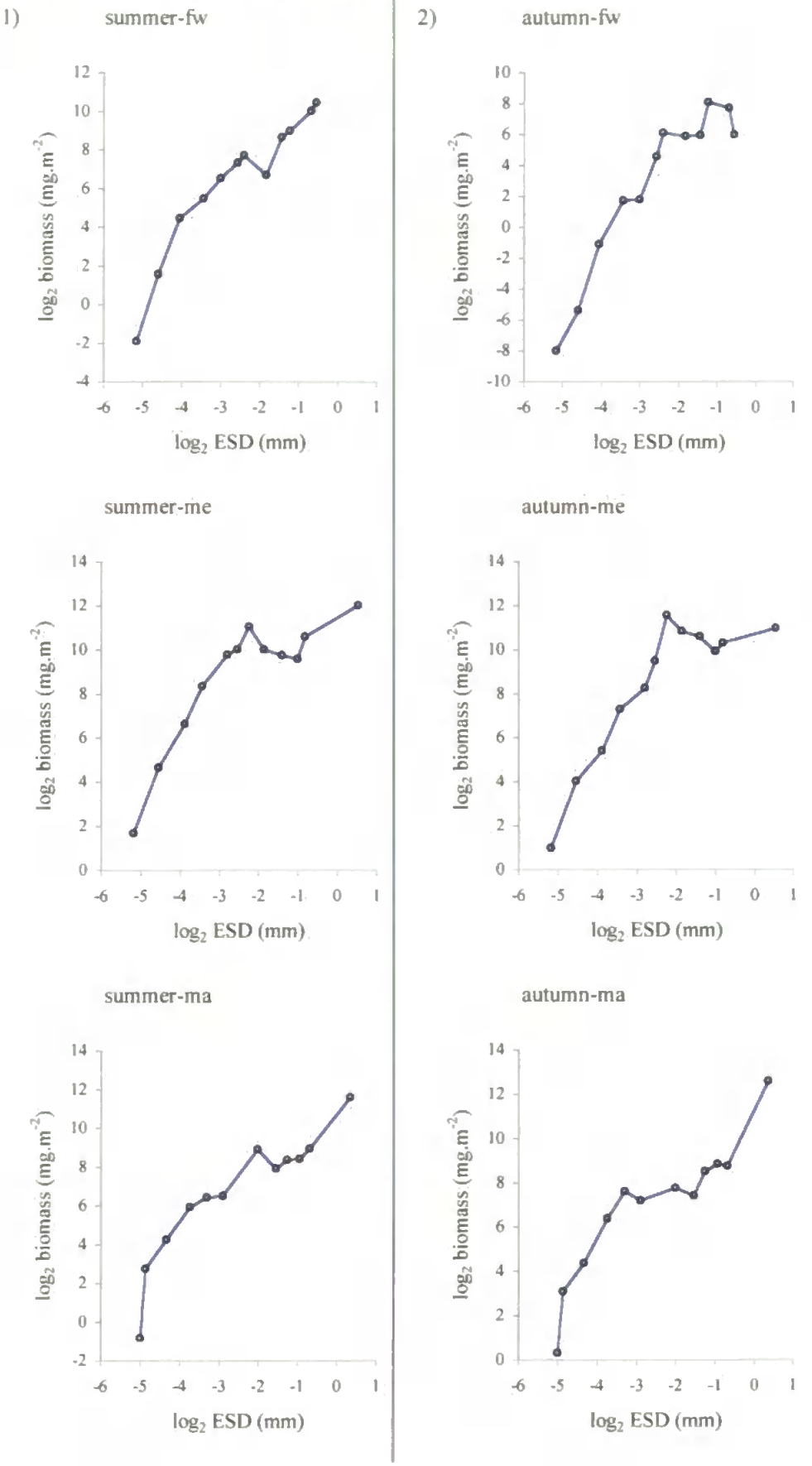

Figure 4.9 Absolute benthic biomass size spectra for all sites in the Yealm in 1) winter: and 2) spring. fw-freshwater; me-middle estuary; and ma-marine site.
(Note differences in Y-axis scale).

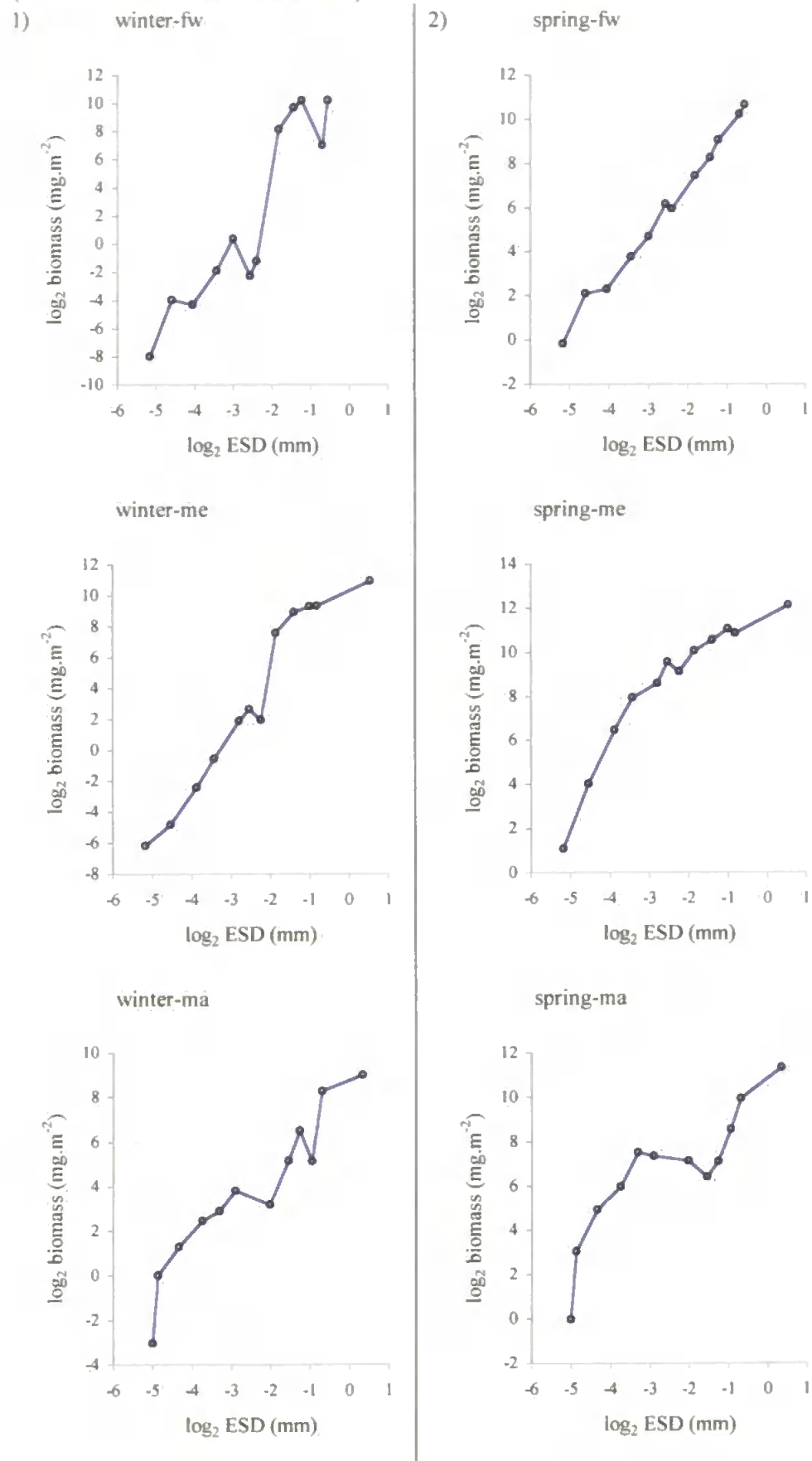

ESD categories of –1.2 and –3.0 (sieve sizes 1000 and 180), respectively. (Figures 4.9). Visual comparison of the spectra (Figures 4.8, 4.9) reveals that the meiofaunal ranges of the spectrum were relatively consistent compared with the macrofaunal ranges which varied among sites and seasons.

4.4.4 Seasonal and spatial variation in standardized BBSS

Generally, standardized benthic biomass size spectra showed a relatively consistent pattern across sites (freshwater, middle estuary and marine sites) and seasons; biomass increasing with size class. Most of the biomass fraction was concentrated in the macrofaunal size range 500 – 2000 μm (Table 4.1).

In summer, standardized benthic biomass size spectra peaked in the size category of 2000 μm at all sites (Figure 4.10). There was a small trough in the size range of 1400-355 μm (equivalent to the $\log_2$ ESD values of (–0.8) – (–2.2) and (–0.7) – (–2.0)) in middle estuary and marine sites, respectively. In autumn, although most of the biomass was concentrated in the macrofaunal category in the three sites, middle estuary biomass size structure had a trough in the same size range. However, there were no clear peaks other than that in the 2000 μm size class in the marine site and in the size class 1000 μm in case of freshwater site (Figure 4.10).

In winter, and spring, patterns of biomass size spectra have the same conservative shape, that is a gradual increase of the percentage of biomass with increasing size, apart from the biomass drop in the size class 1400 and 1000 μm in the freshwater and marine sites, respectively, in winter, and the trough in the size range of 250-500 μm (Figure 4.11).

Table 4.1. Seasonal sum of the % of biomass in the sieve size category 500 - 2000 µm for the different sites.

Site	summer	autumn	winter	spring
Freshwater	86.6%	86.9%	99.9%	95.4%
Middle estuary	65.0%	64.1%	99.6%	84.4%
Marine site	85.7%	91.8%	96.1%	87.6%

Figure 4.10. standardized benthic biomass size spectra for all sites in the Yealm in 1) summer, 2) autumn. fw-freshwater; me-middle estuary and ma-marine sites.
(Note differences in Y-axis scale).

1) summer-fw

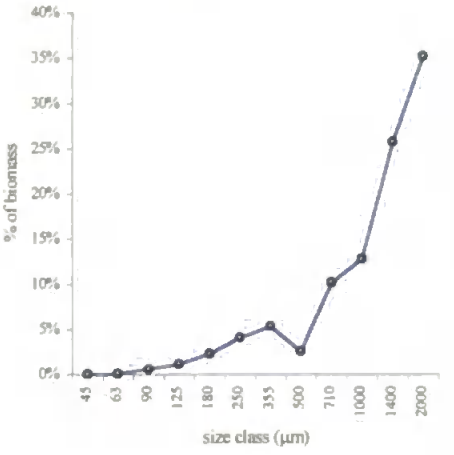

2) autumn-fw

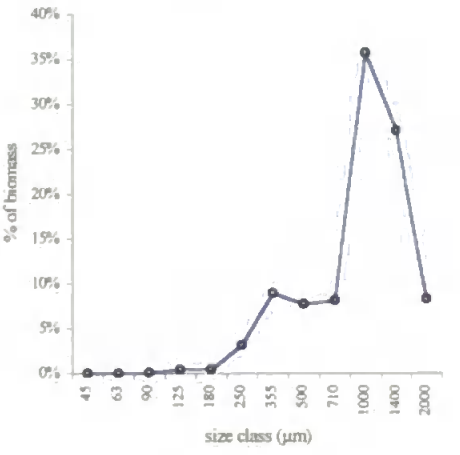

summer-me

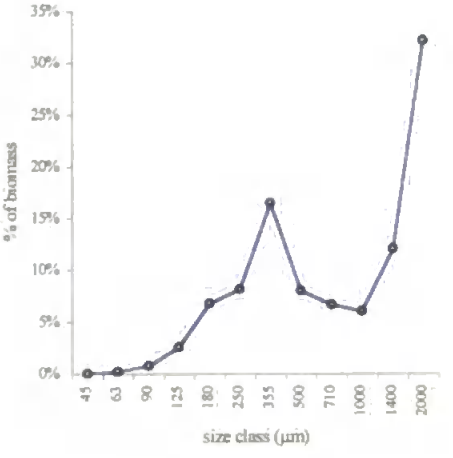

autumn-me

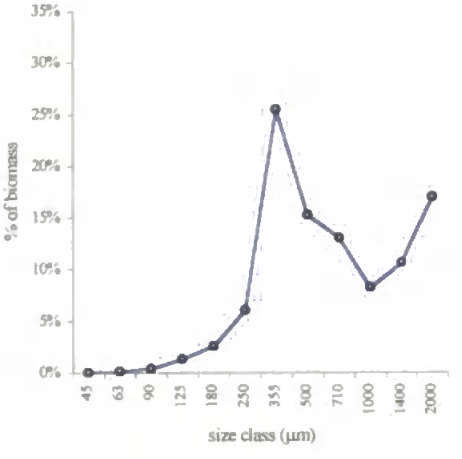

summer-ma

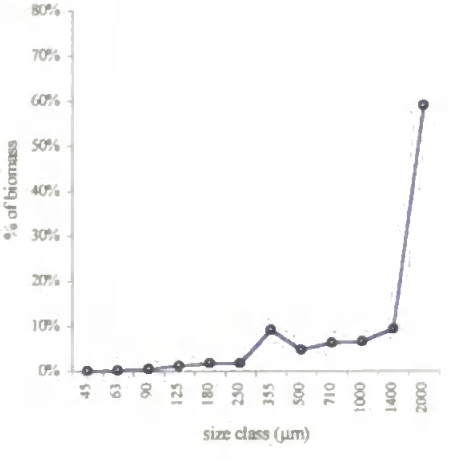

autumn-ma

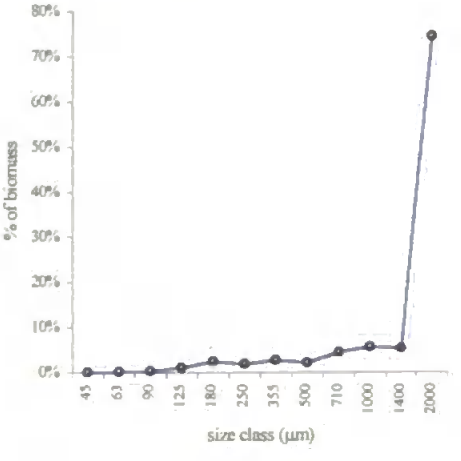

Figure 4.11 Standardized benthic biomass size spectra for all sites in the Yealm in 1) winter, 2) spring. Fw-freshwater; me-middle estuary and ma-marine sites. (Note differences in Y-axis scale).

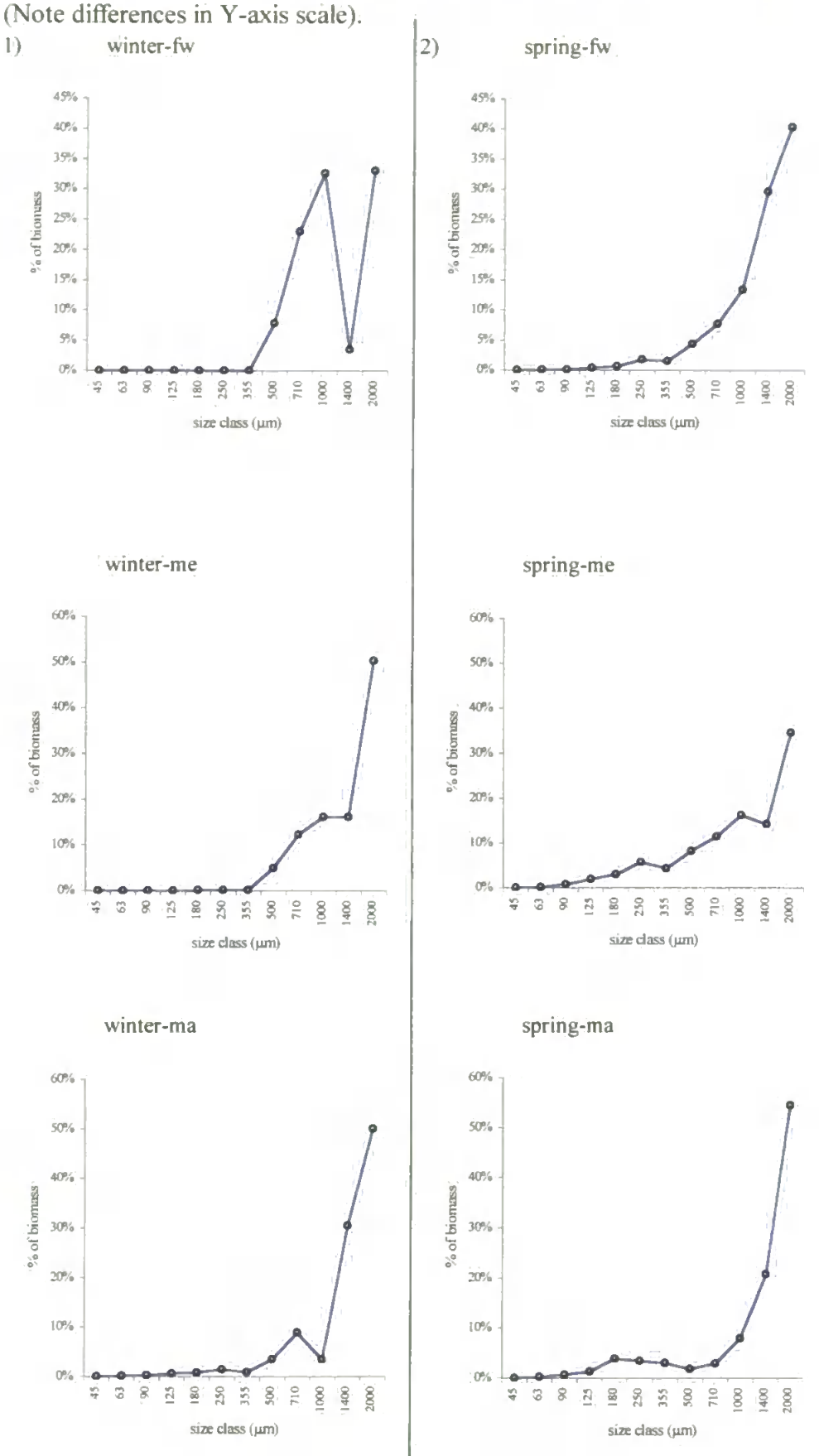

4.4.5 Normalized biomass size spectra

Normalized biomass size spectra were constructed to facilitate a more quantitative comparison of biomass distributions among sites (see chapter 3).

The normalized size spectra mirrored closely the changing trends in the biomass profiles of the benthic communities (Figures 4.12 to 4.13) (Table 4.2) (appendixes 4.3-4.14). The slopes of the normalized spectra for all sites and seasons were shallower than -1.0 (steady state, i.e. biomass being evenly distributed among sieve sizes), indicating the influential effect of macrofauna in the benthic biomass size spectra. The intercepts of the normalized spectra also varied among sites and seasons. The highest intercept value was in the middle estuary, indicating a higher abundance in this site. Intercepts values were lowest during winter indicating lower abundance in this season.

Figure 4.12 Normalised benthic biomass size spectra for all sites in Yealm in 1) summer; 2) autumn, fw-freshwater; me-middle estuary; and ma-marine sites.

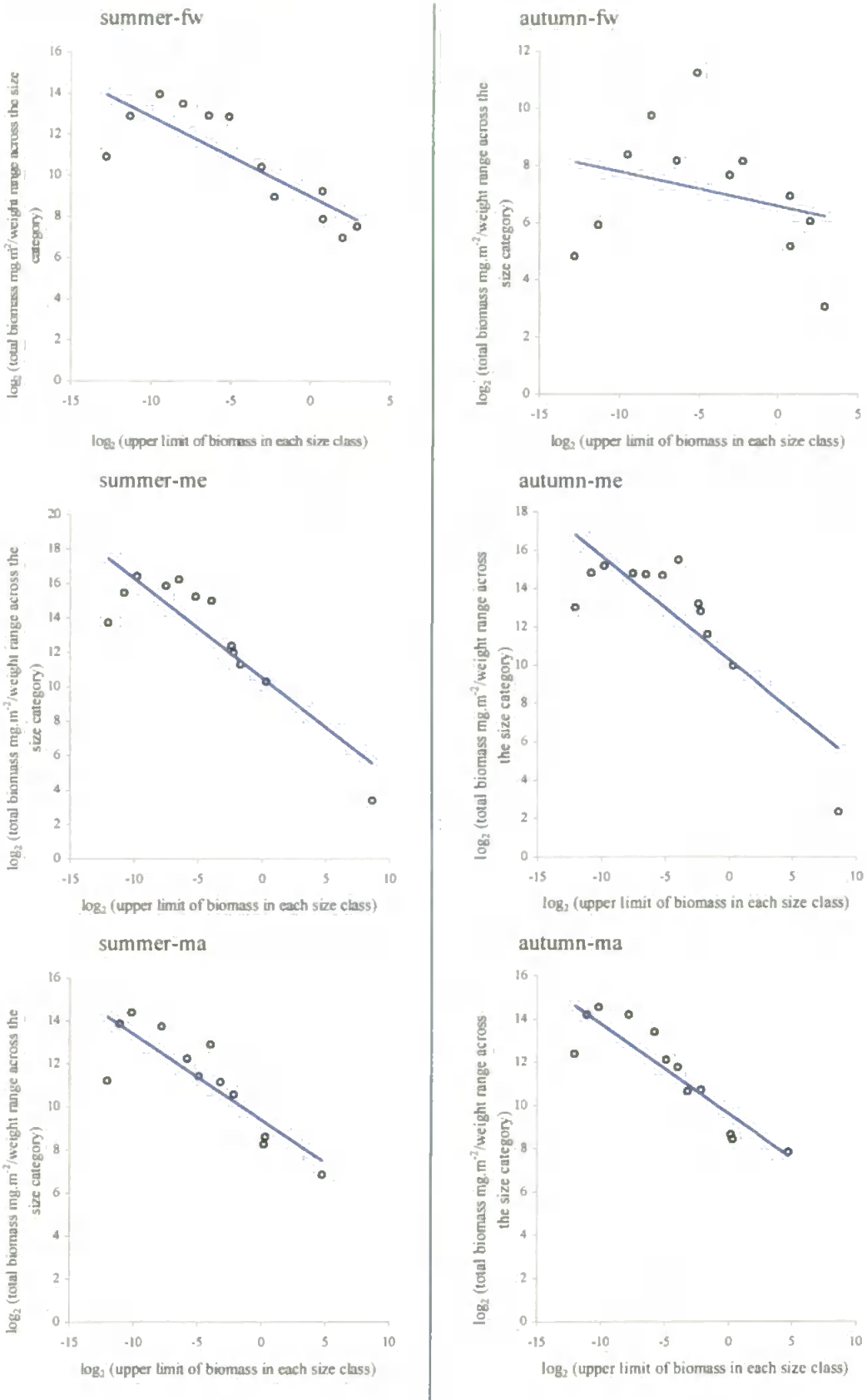

Figure 4.13 Normalized benthic biomass size spectra for all sites in Yealm in 1) winter; 2) spring, fw-freshwater; me-middle estuary; and ma-marine sites.

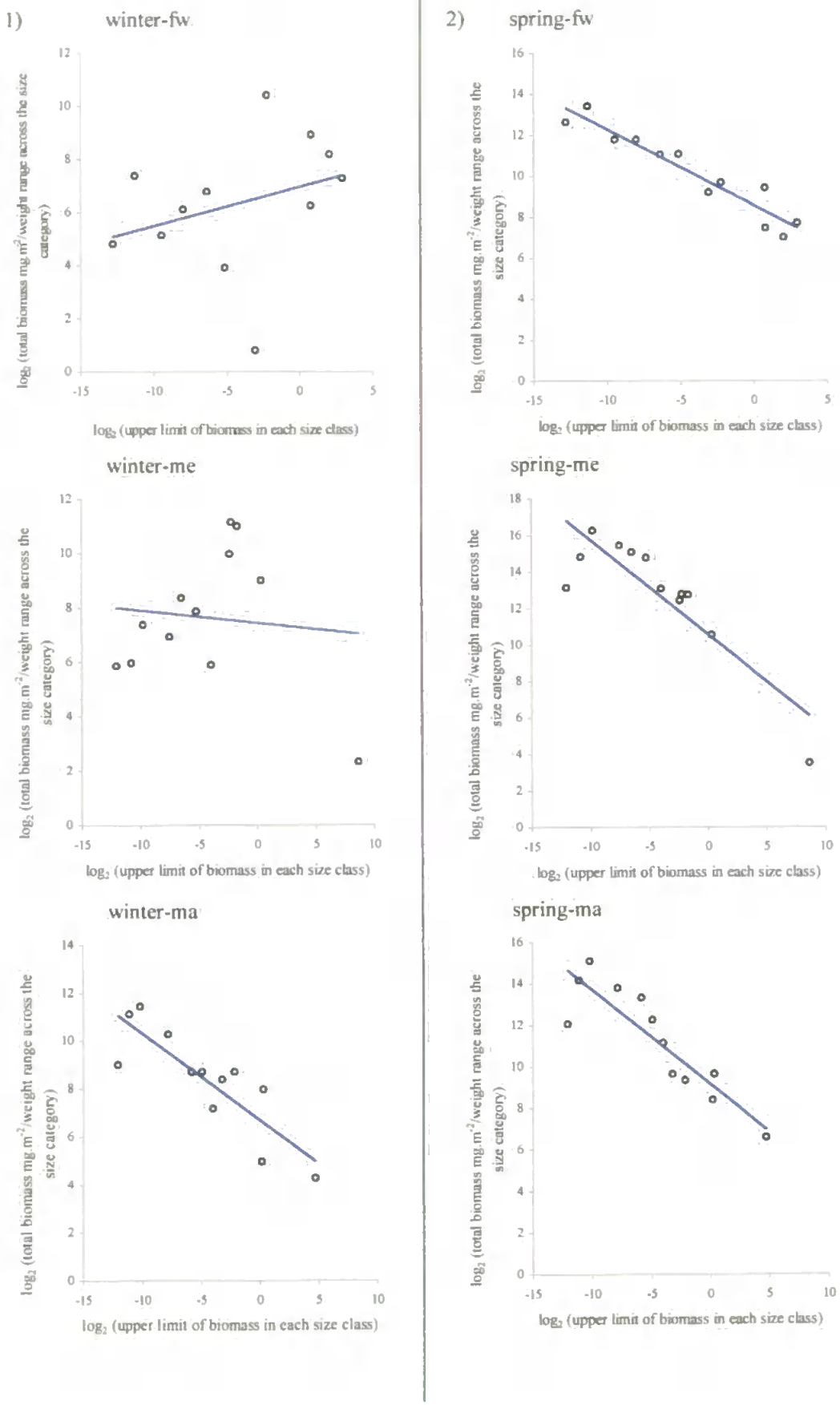

Table 4.2. Normalized biomass size spectra: slopes, intercepts, correlation coefficients (r^2) and the P values for the study sites in the different seasons. (*) = not significant.

Season		Site					
		freshwater	Appendix No.	middle estuary	Appendix No.	marine site	Appendix No.
Summer	Slope	-0.3877	4.3	-0.5763	4.7	-0.3984	4.11
	intercept	8.9828		10.5493		9.3870	
	r^2	0.6840		0.7795		0.7181	
	P value	0.0009		0.0001		0.0005	
Autumn	Slope	-0.1195	4.4	-0.5403	4.8	-0.4161	4.12
	intercept	6.5881		10.3319		9.6127	
	r^2	0.0813		0.6999		0.8056	
	P value	0.3688 *		0.0007		0.0001	
Winter	Slope	0.1471	4.5	-0.0466	4.9	-0.3639	4.13
	intercept	6.9571		7.4316		6.6795	
	r^2	0.1000		0.0111		0.7255	
	P value	0.3165 *		0.7445 *		0.0004	
Spring	Slope	-0.3706	4.6	-0.5156	4.10	-0.4567	4.14
	intercept	8.5837		10.5945		9.1303	
	r^2	0.9075		0.7585		0.7930	
	P value	0.0000		0.0002		0.0001	

4.5. Discussion

Abundance size spectra showed a general conservative pattern of increasing abundance with decreasing body size (Strayer 1994, Cotgreave 1993, Blackburn *et al.* 1993) across all sites in all seasons with a peak in the 63–125 μm sieve size range (see Figures 4.4 & 4.5). However, there were some exceptions to this pattern, most notably in winter when abundances were low.

This pattern in abundance was reflected in biomass spectra. Hence, despite the big differences in salinity regime and community structure across the study sites and seasons, the shape of abundance and biomass size spectra was consistent; biomass increased with size and showed no evidence for bimodality as shown by Schwinghamer (1981). Moreover, biomass size spectra in the current study were not similar to those of Schwinghamer (1981, 1985) in that there was an absence of large biomass troughs. Despite the presence of biomass troughs in the different sites and seasons the most extreme trough was less than an order of magnitude relative to the observed peaks. This level of difference in the order of magnitude between troughs and peaks was not the same as those of Schwinghamer (1985) who showed that the biomass troughs of BBSS were 2-3 orders of magnitude lower than the adjacent peaks.

This lack of bimodality and of significant troughs in BBSS was similar to other studies, such as those detected in the Baltic Sea (Duplisea, 1998; Duplisea and Drgas, 1999), in a freshwater lake (Strayer, 1986) and in freshwater stream and the top end of an estuary (Ramsay *et al.* 1997). The probable reason for the differences between the findings of Schwinghamer (1981, 1985), and those of the current study may be due to inconsistency in the methodology used, which might result in biomass drop in certain size categories. Similarly, the fluctuation of the BBSS pattern among sites being bimodal at only some sites and unimodal at the other sites in a Piedmont stream (Poff *et al.* 1993) was thought to be due to differences in the nature of the mineral sedimentary habitats which probably accommodate a wide range of organism sizes (sensu Schwinghamer, 1981, 1985).

However, this seems unlikely to be a reason for this fluctuation, since the current thesis provides evidence for the consistency of BBSS in the natural and artificial substrata (chapter 6).

The relatively consistent shapes of meiofaunal biomass spectra compared with those of macrofauna (Figures 4.8 & 4.9), suggests that macrofauna are probably more sensitive than meiofauna to seasonal variation in environmental factors. Moreover, macrobenthic life history patterns may explain the detected fluctuation in the biomass spectra of the macrofaunal size categories. Macrobenthic species have planktotrophic larvae which fall within the adult meiobenthic size distribution. After attaining a size which enables them to compete with the holoplankton, the macrofaunal larvae settle to the bottom (Warwick *et al.* 1986).

The low abundance and consequently altered biomass spectra in all sites in winter (Figures 4.2, 4.3) might be related to three possible factors. Firstly, the sediment instability which is at a maximum in winter due to the impact of winds and increased flows (Aller and Stupakoff, 1996; Garcia *et al.*, 1995). Secondly, in winter, most of meiobenthos may migrate deeper down in the sediments (Giere, 1993). Thirdly, life cycle strategies might result in low growth rates and abundances in cold seasons. These suggestions are supported by Wiedenbrug *et al.* (1997) who reported that neither abundance nor composition of the macrobenthos of a coastal lake in southern Brazil differed significantly between seasons (summer and winter). They argued that their result might be as a result of the permanent exposure to the blowing winds. Similarly, Tokeshi (1995) reported that populations of polychaete taxa demonstrated moderate seasonal fluctuations, with numbers generally low in winter and reaching maxima in spring and summer in a pacific South-American rocky shore. Moreover, Beukema *et al.* (1993) reported that biomass fluctuations were stronger in nearly all individual benthos species and size classes than those in total macrobenthos. They showed that minimal biomass values were caused as a response to winter character over the entire Wadden Sea.

The detected differences in the biomass size spectra between the study sites in the current study may be related to the differences in the abundance size spectra, with abundance having an influential impact on benthic biomass size spectra (Ramsay *et al.* 1997). Therefore, low abundance in winter and in freshwater in autumn may consequently result in low biomass in the same seasons and sites.

Despite the known effects of environmental factors such as organic carbon on benthic biomass size spectra BBSS (Soltwedel *et al.* (1996) for benthic nematodes), differences in BBSS between sites in the current study are not simply a function of such environmental factors. The percentage of organic carbon in summer, spring and winter in freshwater and marine sites was not correlated with the BBSS in the same seasons for these sites (see Figure 4.6 in the current chapter & Table 2.5 in chapter 2). However, differences in abundance of the different taxa with different mean biomass seem to be the key factor for temporal and spatial variation of BBSS (see section 4.4.2 in the current chapter). This suggestion may support the findings of Duplisea and Drgas, (1999) who referred to the presence or absence of some organisms and hydrodynamics as more likely to be the important factors determining the community structure and hence the differences between sites in terms of BBSS.

Normalized spectra as a mean of quantitative comparison supported the finding of the current study, which is the concentration of most of the biomasses in the macrofaunal category. The slopes in summer, autumn and spring seasons were all in the range detected by Drgas *et al.* (1998) who reached the same result. Similar to other biomass spectra, patterns of normalized spectra broke down in winter (i.e. at low abundances) compared with those of the other seasons (see above).

CHAPTER 5

Benthic Bacterial Biomass Size Spectra

5. Benthic bacterial size spectra

5.1. Introduction

Studies of bacterial size distributions in aquatic systems were initiated by Azam and Hodson (1977) in an investigation of size distributions and activities of marine microheterotrophs. They used the approach of size fractionation of natural populations of marine microorganisms using Nuclepore filters, to separate the bacterial fraction from other organisms and to determine the importance of bacteria in the heterotrophic activity in a variety of oceanic and neritic environments. They considered organisms passing through 1-μm-pore filters to be bacteria, with the reservations that bacteria attached firmly to larger particles will be retained by such filters, and that some organisms other than bacteria might pass through 1-μm-pores.

The importance of the size structure approach in aquatic microbial ecology has increased recently due to its usefulness in evaluating the relationships between the bacterial activity and size (Gasol *et al.* 1995 and Servais and Garnier, 1993), or in the estimation of the proportion of the metabolically active cells (Delgiorgio and Scarborough, 1995) which could be used as a stress indicator (Goulder, 1991). For example, Gilmour and Henry (1991) have shown that an alteration in population size and/or structure of sulfate-reducing bacteria could be one of the explanations for increased bioaccumulation of mercury as a contaminant in fish. Furthermore, enzyme activities within different sizes could be determined through bacterial size structure leading to a better understanding of how and why the bacteria "sediment chemists" perform their essential roles in the environment (Berman *et al.* 1990).

Bacteria are described as "microscopic organisms", but this conveys little quantitative meaning and more definitive remarks concerning their dimensions must be made. It is difficult to obtain anything other than representative or average values, not only because individual bacterial cells vary in dimensions, but also because the methods employed for

measuring them yield only approximations. Bacteria range from 0.15 to 4.0 μm in width and from 0.2 to 50 μm in length (Doetsch and Cook, 1973). In cylindrical forms, length appears more variable than width.

5.1.1. The choice of bacterial size categories

Williams (1970) used Millipore filters to size-fractionate natural marine microbial populations after incubation with ^{14}C-labeled D-glucose or a ^{14}C-labeled amino acid mixture. He found that an average of 49.5% of assimilated ^{14}C was associated with organisms passing through 1.2 μm, 68% through 3 μm and 80% through 8 μm effective–pore–size membrane filters and concluded that at least 50% of activity was almost certainly due to bacteria. Azam and Holm-Hansen (1973) reached a similar conclusion from their work in the central North Pacific gyre, using Millipore filters. These reported similarities may be as a result of using the same filter (Millipore filters), where only a minimum estimate could be made compared with that resulted from using the more advanced filters (Nuclepore filters) (Bowden, 1977). This could be confirmed by comparing their results (49.5%) with that of Azam and Hadson (1977) (90%) who used Nuclepore filters that resulted in better estimation of the bacterial activity (from 49.5 % to 90 %).

As the 1 μm filterable size fraction appears to contain a high proportion of bacteria (Azam and Hadson 1977), it was the focus for this study and was further fractionated into three size categories. The proposed sizes were on Wentworth filter-size series, with a doubling of filter-pore area at each stage (0.2 μm, 0.4 μm, and 0.8 μm), the same approach used for the other chapters in the current study.

5.2. Aims

This study aims to compare: 1) abundance and biomass size spectra; and 2) Adenosine Triphosphate concentrations (ATP, i.e. the activity measure) within the different size classes, for benthic bacteria in a freshwater and a marine site within the same system (Yealm).

5.3. Methods

5.3.1. Biotic and Abiotic Sampling

Sediment samples were collected in June 1998 from the marine (5/6/1998) and freshwater site (8/6/1998) in the Yealm system. 3 replicate samples were taken using a sterile cylindrical corer (5.3 cm in diameter and 10 cm in length) from land in the case of the freshwater site or by a diver in case of the marine site. This sample was then placed in a sterile pot and homogenised using a sterile spatula. 1 cm^3 of this homogenized sediment sample was taken from the first replicate in the two study sites using sterile plastic medical syringe (with the needle end cut off as coring device) and was placed in a sterile universal tube to be processed live in the laboratory. The remaining sediment samples were fixed with formaldehyde (3.7% final concentration).

This sampling strategy was repeated at weekly intervals for the following two weeks giving 3 live replicates and 9 preserved replicates for each site. Finally, three fresh replicates of 5 cm^3 sediments were collected from the marine site on 24/6/1998 and the freshwater site on 29/6/1998 to be processed for ATP analysis. Two of these three replicates were kept in the fridge while processing the third replicate to prevent bacterial proliferation.

Environmental variables (salinity, conductivity, temperature and pH) were measured in the field before taking the sediment samples. The percentage of organic carbon in the sediments of both sites was measured using the same method described in chapter 2.

5.3.2. Sample processing

Microorganisms were separated from sediments using density gradient centrifugation. This method has been used for extraction of protists from aquatic sediments (Alongi, 1993); the efficiency of this method has also been approved for extracting bacteria from the sediments in the current study by applying it, in the laboratory, on controlled sediment (autoclaved, defaunated sediments with a known number of bacteria and pre-known average cell

volume). This controlled experiment revealed that the average increase in number of bacteria and the average cell volume (control) were lower than 1%. Therefore, this method has been adopted for the extraction of bacteria from the sediments in the current study.

5.3.2.1. Extracting microorganisms from sediments

5 cm^3 of Percoll–sorbitol mixture were added to the unpreserved 1 cm^3 sediment sample in the universal tube. The sample was then mixed thoroughly using vortex at slow speed for 1 to 2 min. and left to stand for 1 hour to allow the density gradient to develop. The sample was then centrifuged at 3000 rpm for 30 minutes. The resultant supernatant was filtered through three different pore sized Nuclepore filters (0.8-, 0.4- & 0.2 μm). The remaining pellets in the centrifuge tube were fixed with formaldehyde (3.7% final concentration) to be processed again as a recovery run, (to extract as much adherent bacteria as possible) using an improved sample preparation for enumeration of aggregated aquatic substrate bacteria (Velji and Albright 1993), (see section 5.3.2.2).

The Nuclepore filters (0.8, 0.4 & 0.2 μm) were eluted separately in 20 ml of the suitable diluent (filtered sterile physiological saline in case of freshwater samples and filtered sterile sea water in case of marine samples) (a filter per tube). The contents of each of these tubes were homogenized by vortex and divided between new 4 sterile tubes (5 cm^3 each). Table 5.1 and Figure 5.1 shows the fate of each (5 cm^3) within the same size category, and for the three different size categories separately in freshwater and marine sites. Details of the techniques used for enumerating and measuring cell volume, image analysis and the Adenosine Triphosphate (ATP) extraction and measurement are listed in sections 5.2.4.and 5.2.5. respectively.

Table 5.1. The fate of each 5 cm^3 aliquots in each size category in the first run.

<table>
<tr><td colspan="5">first 5 cm^3</td><td>second 5 cm^3</td><td>third 5 cm^3</td><td>fourth 5 cm^3</td></tr>
<tr><td colspan="5">Qualitative estimation (not fixed)</td><td>Quantitative and biovolume estimation (fixed)</td><td>Activity estimation</td><td>Spare (Quantitative and biovolume estimation (fixed))</td></tr>
<tr><td rowspan="2">4 cm^3 (spare)</td><td colspan="4">1 cm^3 (serial dilutions)</td><td>epifluorescence</td><td>ATP</td><td rowspan="2">spare (epifluorescence (AODC))</td></tr>
<tr><td colspan="3">bacteria</td><td>protista</td><td rowspan="2">Acridine Orange Direct Count (AODC)</td><td rowspan="2">extraction with boiling buffer, then kept frozen.</td></tr>
<tr><td>(10^{-1})</td><td>(10^{-2})</td><td>(10^{-7})</td><td>(10^{-1})</td></tr>
</table>

Figure 5.1a processing of the unpreserved sediment sample for Qualitative, Quantitative and ATP estimation

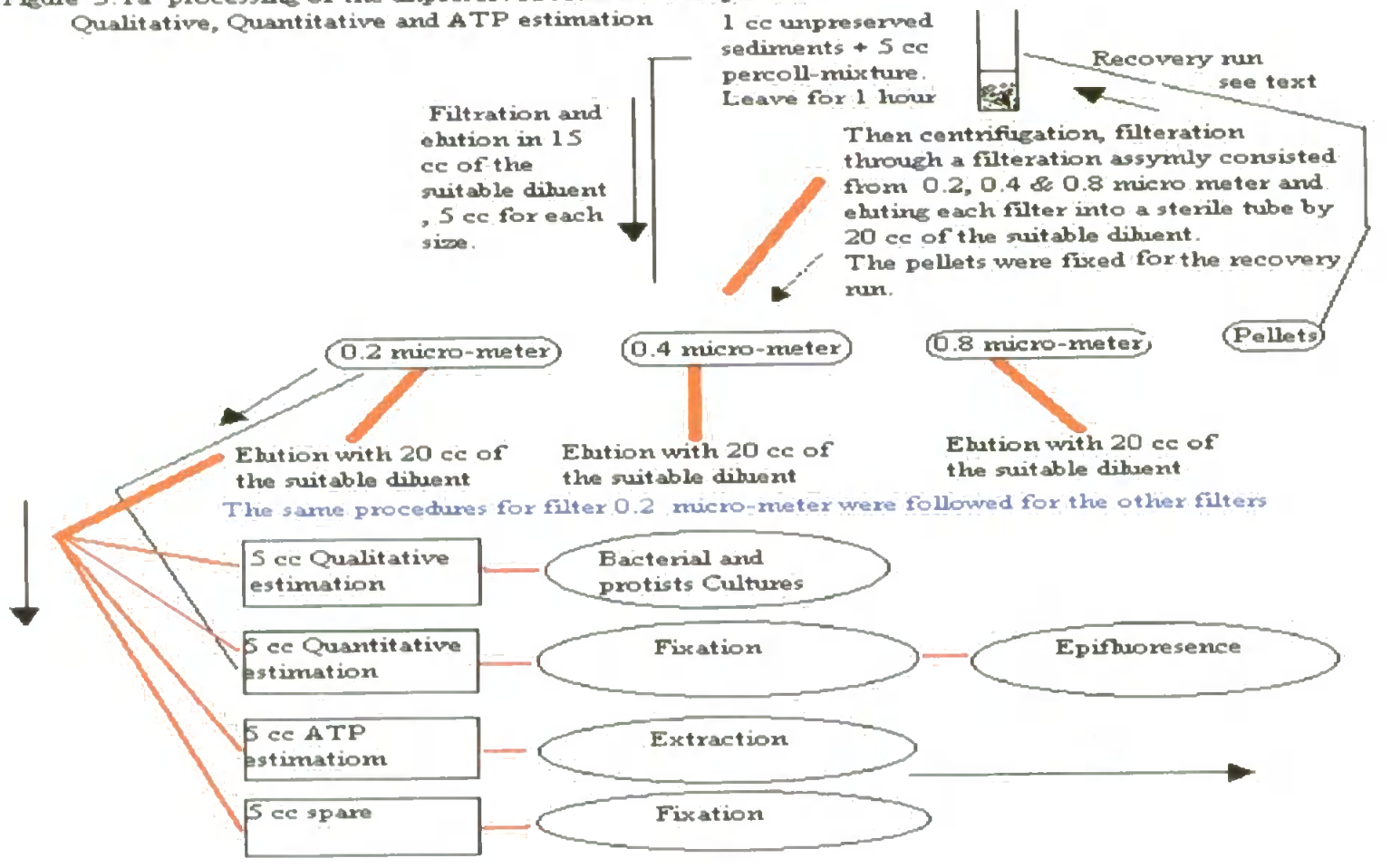

Figure 5.1b processing of the preserved sediment sample for Quantitative estimation

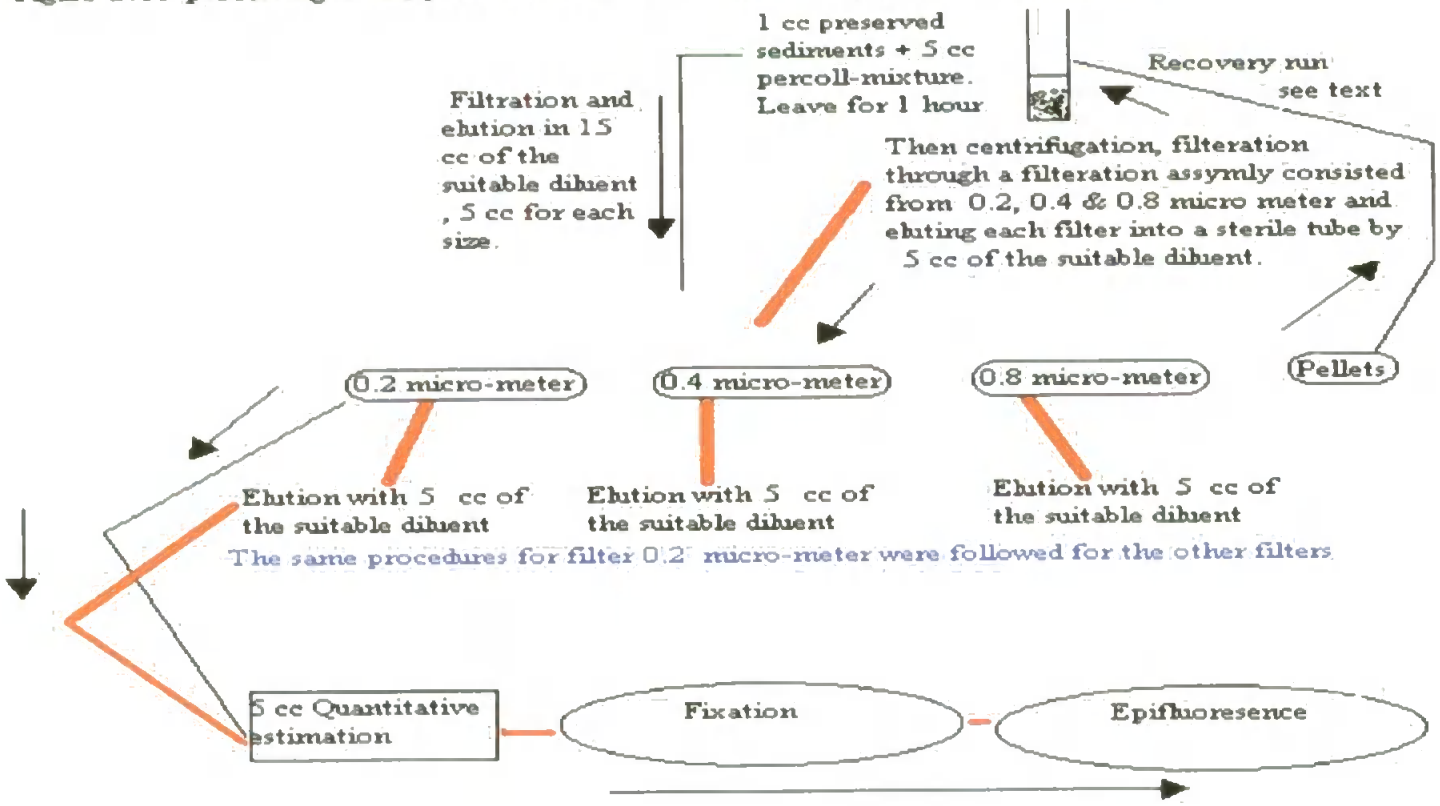

Figure 5. 1c processing of the unpreserved sediment sample for ATP estimation

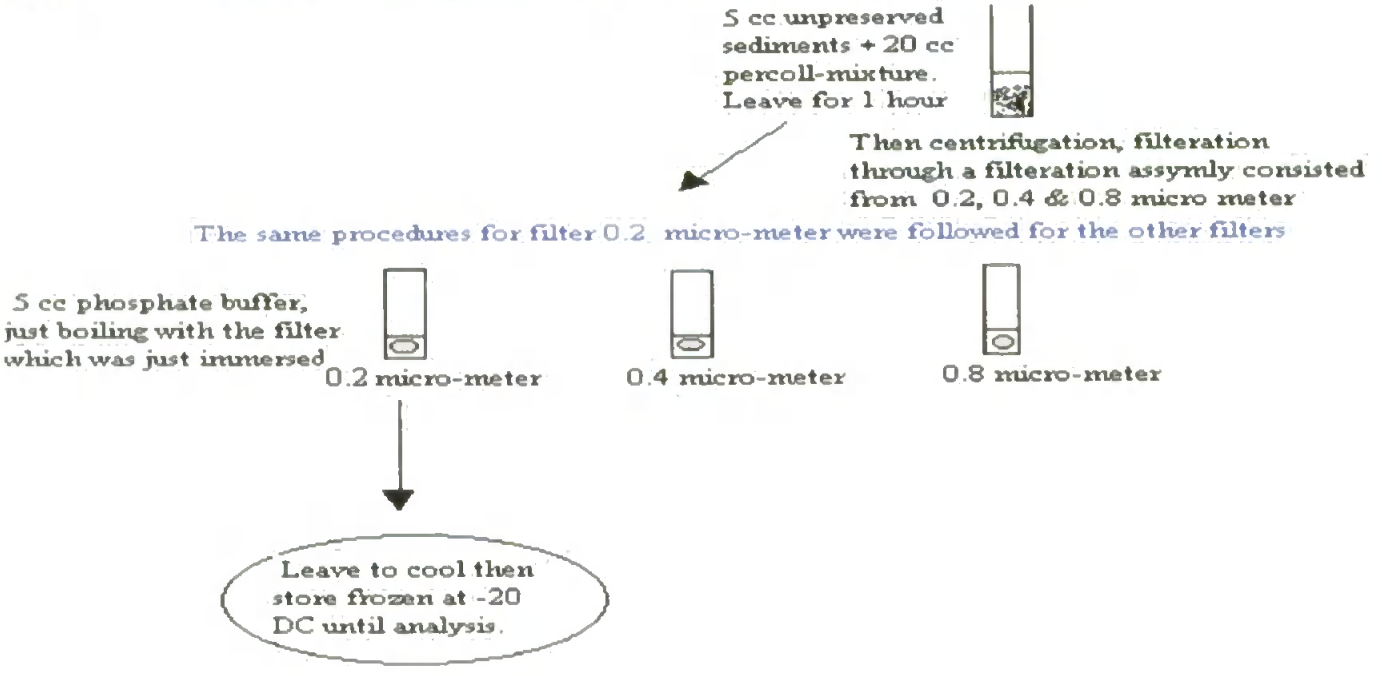

- For qualitative estimates 1 cm^3 from the first 5 cm^3 was used for serial dilutions using the appropriate diluent (filtered sterile physiological saline in case of freshwater samples and filtered sterile sea water in case of marine samples). Suitable ten-fold serial dilutions were made for culturing bacteria and protista. Protista were cultured so that they could be excluded from the counting and body dimension measurements using the epifluorescence technique.
- For quantitative and biovolume estimation, the second 5 cm^3 was washed to remove any traces of percoll–mixture, which may gel on adding preservative (Alongi, 1993), by vacuum filtration of the sample through the appropriate filter size by adding enough amount of the suitable sterile diluent (~5 – 10 cm^3). The washed organisms on the filter were then resuspended in 5 cm^3 of the appropriate sterile diluent and fixed by adding ~ 0.26 ml concentrated formaldehyde to produce a final concentration of 2% formaldehyde. They were kept in the fridge before processing by the Acridine Orange Direct Count (AODC), according to Hobbie *et al.* (1977) and Heldal *et al.* (1985), using image analysis.
- For quantitative estimate of ATP concentration, microbes (bacteria plus others) from the third 5 cm^3 aliquot were concentrated onto the appropriate pore sized Nuclepore filter membrane by vacuum filtration. The filter with the organisms was then immersed in 5 cm^3 of boiling phosphate (60 mM, pH 7.4) buffer, following the recommendations of Karl, (1993). The results of this portion (representing a quarter of the original sample) indicated that there was no ATP at all, this may have been due to the very dilute sample or due to the fact that the ATP concentration in the volume of the sediment was too small. To overcome this problem, a larger volume (5 cm^3) of the sediment (allocated entirely for ATP estimation) was resampled and processed the same way.
- The fourth 5 cm^3 aliquot was fixed and kept as a spare for the epifluorescence pathway.

5.3.2.2. Re-extraction of adherent microorganisms from sediments

The scheme of this experiment followed that of Velji and Albright, (1993). It overcomes the problems of enumeration of attached bacteria, which can be problematic using standard epifluorescent methods. This is due to aggregation and layering of microbes embedded in colloidal matrices, or the presence of opaque particulate matter which caused interference with the observation of bacteria. This method utilizes a combination of chemical and physical procedures for dispersing the bacteria from their attached sites or aggregated forms. This involves initial fixation and strengthening of bacteria in the sample with formaldehyde, followed by the addition of the dispersant tetrasodium pyrophosphate (PPi), and the use of ultrasound, to separate bacterial cells. Bacteria were then enumerated using a standard epifluorescence method (see below). The advantages of this method are : 1) it allows for bacterial enumeration from aquatic substrates that are difficult or impossible to enumerate via the use of standard methods; 2) the even dispersion of bacteria decreases variance in bacterial counts between microscopic fields reducing the time required for enumeration. The disadvantages of this method are that: 1) the bacteria are no longer viable after being subjected to the treatment regime; and that 2) the use of PPi in samples with a high concentration of multivalent cations in water can cause precipitation which would interfere with the observation of bacteria. Therefore, minimal artificial seawater had been prepared to be used to avoid this latter problem.

The fixed pellets retained from the first run experiment were prepared by suspending in 5 cm^3 of 128 mM PPi (freshwater) and 93 mM PPi (marine) (Velji and Albright, 1993). The contents of each tube were mixed using a vortex mixer and incubated at room temperature (22 °C) for 15 – 30 minutes with shaking. The sample was precooled to 4 °C, packed with crushed ice, and then sonicated at a power level of 100 W for 30–60 seconds. A 1 cm^3 subsample was then processed using density gradient centrifugation (see first run experiment). This recovery experiment was allocated entirely to the AODC technique (i.e.

the sample was not divided into four sections like the first run experiment) according to Hobbie *et al.* (1977).

5.3.3. Qualitative estimation of microorganisms

The diluted microbial suspensions from the first 5 cm^3 aliquot (Table 5.1) were cultured in order to identify the main types of bacteria present in the different size classes in the two study sites.

Two media were tested for bacteria cultures: minimal and enriched sediment media. The first media was from the natural habitats without addition of any nutrients (minimal sediment medium), and the second media was supplemented with nutrients (enriched sediment medium).

5.3.3.1. The minimal sediment medium

500 g of sediment was steamed in 1 L of Instant Ocean (marine sample) or physiological saline (freshwater sample) for 1 hour. The supernatant was then decanted off and made up to 1 L using instant ocean or physiological saline. The resultant solution was allowed to cool, then pH was adjusted to be the same as that of the natural environment where the organisms were living. Then 15 g of agar powder per liter was added (to solidify the medium) and dissolved by heating. Finally, the media was distributed in pre-labeled bottles and autoclaved.

5.3.3.2. The enriched sediment medium

The enriched sediment medium was prepared as the minimal sediment medium except that, after cooling, 3g of yeast extract and 5g of peptone were added and dissolved by heating if necessary. Then pH was adjusted to be the same as that of the natural environment. The resultant solution was boiled for 3-5 minutes, filtered and pH was readjusted. Then 15g of agar powder was added (to solidify the medium) and dissolved by heating. The final solution was distributed in pre-labeled bottles and autoclaved.

Two types of bacterial cultures were performed (aerobic and anaerobic cultures). For aerobic cultures (spread plate), a 0.5 ml of bacterial suspension was transferred to the surface of the solidified medium in a Petri plate, then it was evenly distributed over the surface of the plate using the sterile spreader. The medium was allowed to absorb the distributed bacterial suspension, then the media were transferred to the incubator at the same temperature as that of the natural environment.

For anaerobic cultures, 1 ml of bacterial suspension was poured onto a sterile petri dish, then molten medium was added. The medium was then allowed to set and incubated in an anaerobic cabinet at the same temperature as that of the natural environment.

5.3.4. Quantitative estimation and biovolume measurements

It is imperative to calibrate size measurement procedures against fluorescent latex beads with a known diameter. The latex beads are very bright and will therefore appear larger than they really are. The fluorescence intensity of the beads should be reduced to a level more like the bacteria by inserting a natural gray filter in the light path. Preparations of latex beads for calibration of size measurements are made in the same way as the bacterial preparations, but staining is omitted. The beads' stock solutions should be diluted 10^{-4}-10^{-5} fold in distilled water before use and then mixed to make a preparation containing different bead sizes. It is important that the filter membrane and the cellulose–backing filter be pre–wetted with deionized or filtered seawater and that bubbles be excluded when mounting the filters on the filtration assembly.

The reliability of Acridine Orange Direct Count (AODC) for counting and measuring bacterial cells was suggested by Bowden, (1977). He found an agreement between AODC and Scanning Electron Microscope (SEM) techniques if 0.2 μm Nuclepore filters were used. AODC is preferable for routine ecological sampling.

Epifluorescence procedures:

A volume of Acridine Orange (AO) solution (0.1% w/v in distilled water, preserved with 1% formaldehyde or glutaraldehyde) equal to 10% of the sample volume was added to the sample. After staining for 3 min. the sample was gently filtered down using the appropriate Polycarbonate Nuclepore black filter pore size, and 2 cm^3 of either filtered seawater (marine samples) or filtered physiological saline (freshwater samples) was then added to the sample as a rinse when the meniscus of the sample reaches the filter surface. The filter was gently removed from the tower while still under vacuum to minimize water retention and prevent cells from floating off the filter surface. The filter was then mounted onto a glass slide by smearing a small drop of non–fluorescent immersion oil onto the slide, placing the filter onto the area of the slide covered with oil, and then placing another drop of oil and a cover slip onto the top of the filter. The mounted filter was then examined using an Olympus BH compound microscope with epifluorescent attachment with blue excitation to fluoresce the microbes at either 1000x or 400x magnification. This was connected to the image analyzer unit by a trinocular BH with a 3.3 photoeyepiece and a low light level video camera (Fujitsu CCD TCZ-230EA) to acquire the image (see Figure 5.2). The image was then directly imported to the Quantimet Q570 image analyzer programmed for recording the counts and the cell dimensions in an ASCII delimited savable file that could be read into MS Excel for analysis. Final magnification to the monitor screen was 6330 for the 100x objective and 2530 for the 40x objective.

For estimation of bacterial numbers and cell dimension measurements, the whole filter was scanned by moving the microscope stage with the slide through a regular and constant movement of the stage glider. This was repeated for at least 70 microscopic fields with an average countable bacterial number for the scanned microscopic fields ranging from 40 (0.2 μm filter size) to 140 (0.8 μm filter size) cells (first run) and from 4 (0.2 μm filter size) to 70 (0.8 μm filter size) cells (recovery run).

The total number of bacteria / ml (#) was calculated using the formula of Sherr *et al.* (1993).

$$\#/ml = \frac{(cells/field\ of\ wiew)\times(area\ of\ filter\ covered\ by\ sample)}{(field\ of\ view\ area)\times(DF)\times(ml\ filtered)}$$

Where "*DF*" is the preservative dilution factor, "*ml filtered*" is the bacterial suspension volume filtered. At a given magnification using the same area of filter and dilution technique a constant can be derived from the formula of Sherr *et al.* (1993):

At magnification of 100 objective the constant = 161,513

At magnification of 40 objective the constant = 25,375

For biomass estimation, the cell dimensions were then used for calculating the biovolume. Cell shape was approximated to simple geometric shapes (cylindrical or spherical), which was then transformed to biomass (dry weight) assuming that freshwater and marine bacteria have a specific gravity of 1.1 and a dry- to wet-weight ratio of 0.3 (Batterton and Van Baalen (1968), Warwick and Joint (1987)).

Total biomass was calculated by multiplying abundance per filter size x mean cell biomass for that filter size (Maclean *et al.* (1994), Cole *et al.* (1993)).

Figure 5.2 The image analyses unit used

5.3.5. ATP extraction (activity measure)

5 cm^3 of sediment were added to 20 cm^3 of percol–mixture, centrifuged after 1 hour as previously described. The supernatant was then filtered through the three subsequent Nuclepore membrane filters (0.8, 0.4 & 0.2 µm pore size). Meanwhile, 3 aliquots (5 cm^3) of phosphate (60 mM, pH 7.4) buffer were placed in 3 separate pre-labeled sterile universal tubes and allowed to boil. Filters with concentrated microbes were immersed separately into the boiling buffers as quickly as possible, to avoid loss of viability due to desiccation. The filters with microbes in the boiling buffers were heated for an additional 5 minutes, during which time the tubes were partially covered to minimize evaporation and resultant volume change. Following extraction, the samples were cooled then stored frozen (-20°C) until assays were performed. Such sample extracts are extremely stable with ATP losses of less than 1% $year^{-1}$ in properly buffered solutions (Karl, 1993).

At the time of analysis, the samples were left to thaw at room temperature, and ATP was measured using an ADENOSINE 5'–TRIPHOSPHATE (ATP) BIOLUMINESCENT ASSAY KIT. The idea of ATP measurement using this kit is that ATP is consumed and light is emitted when firefly luciferase catalyzes the oxidation of D-luciferin. For full details (see the technical Bulletin No. BAAB-1, for the stock No. FL-AA ADENOSINE 5'–TRIPHOSPHATE (ATP) BIOLUMINESCENT ASSAY KIT).

Estimation of ATP does not distinguish between bacteria and other organisms, therefore, the values of ATP reported in the current study cover all organisms in the processed sample.

5.3.6. Statistical Analysis:

Differences between filter sizes, sites and their interaction in terms of bacterial abundance, ESD, mean cell biomass, total biomass and ATP were examined by ANOVA using log (N) transformed data. These data were tested for normality using residuals plots visually to confirm homogeneity of variance.

5.4. Results

5.4.1. Bacterial culturing

The minimal sediment medium did not provide any microbial growth. However, there was an obvious growth in the enriched sediment medium. Although, there is no universal growth medium for all the bacteria, the second growth medium was chosen to grow the dominant bacteria for both freshwater and marine sites.

There were two dominant cell shapes (Rods and Cocci) in both marine and freshwater sites Tables (5.2 & 5.3). Rod shaped bacteria dominated the population. For example, in the scanned areas of the filter, the percentage of rod shaped organisms in marine and freshwater sites of the total number within each filter were 50%, 80% and 100% in 0.2, 0.4 and 0.8 μm filter sizes respectively. Although some bacteria appeared similar, they differed in one of the physical or the biochemical characters such as Gram stain reaction, cell shape, colony diameter, color, shape, transparency, consistency, pigmentation, oxidase and fermentation tests, which were measured using the standard microbiological methods. Marine bacterial colonies exhibited more variety in their consistency, (the state of being mucoid, dry, shiny etc.). Most of the bacteria were aerobic, (the majority of bacteria were grown in the aerobic conditions), this is probably because the samples were taken from the water–sediment interface (oxic layer).

5.4.2. Physico-chemical characterization of freshwater and marine sites

In addition to the physicochemical differences between sites (i.e. marine and freshwater) reported in chapter 2 percentage of organic carbon in marine sediments was approximately twice as that of freshwater sediments.

Table 5.2 : Freshwater bacteria cultivated in the enriched sediment medium

Filter size	Gram stain	Bactrial shape	Diameter of the colony (mm)	Color of the colony	shape of the colony	Transparency	Consistency	Pigments		Oxidase test	Fermentation test	
Aerobic bacteria								Exo.	Endo.		Glucose	mannitol
0.2 µm	(+ve)	Cocci	1.3	Dark cream	Circular Convex	Opaque	Mucoid	(-)	(+)	(-ve)	(-ve)	(-ve)
0.2 µm	(+ve)	Rod	1.5	light cream	Circular Convex	Translucent	Mucoid	(-)	(+)	(-ve)	(-ve)	(-ve)
0.2 µm	(+ve)	Rod	2.0	Dark cream	Circular Convex	Opaque	Mucoid	(-)	(+)	(+ve)	(-ve)	(-ve)
0.2 µm	(+ve)	Rod	3.0	Dark cream	Circular Convex	Opaque	Mucoid	(-)	(+)	(-ve)	(-ve)	(-ve)
0.4 µm	(+ve)	Rod	2.5	Dark cream	Circular Convex	Opaque	Mucoid	(-)	(+)	(+ve)	(-ve)	(-ve)
0.4 µm	(-ve)	Rod	2.5	Orange	Circular Convex	Opaque	Mucoid	(-)	(+)	(+ve)	(-ve)	(-ve)
0.4 µm	(-ve)	Rod	2.0	Dark cream	Circular Convex	Translucent	Mucoid	(-)	(+)	(+ve)	(-ve)	(-ve)
0.4 µm	(-ve)	Rod	3.5	Dark cream	Circular Convex	Opaque	Mucoid	(-)	(+)	(+ve)	(-ve)	(-ve)
0.4 µm	(-ve)	Rod	4.3	Dark cream	Circular Convex	Opaque	Mucoid	(-)	(+)	(-ve)	(-ve)	(-ve)
0.4 µm	(+ve)	Rod	4.5	Dark cream	Circular Convex	Opaque	Mucoid	(-)	(+)	(-ve)	(-ve)	(-ve)
0.4 µm	(-ve)	Rod	4.0	light cream	Circular Convex	Translucent	Mucoid	(-)	(+)	(+ve)	(-ve)	(-ve)
0.8 µm	(+ve)	Rod	1.5	light cream	Circular effuse	Translucent	Mucoid	(-)	(+)	(+ve)	(-ve)	(-ve)
0.8 µm	(+ve)	Rod	2.8	Dark cream	Circular Convex	Opaque	Mucoid	(-)	(+)	(+ve)	(-ve)	(-ve)
0.8 µm	(-ve)	Rod	2.0	Dark cream	Circular Convex	Opaque	Mucoid	(-)	(+)	(+ve)	(-ve)	(-ve)
0.8 µm	(+ve)	Rod	3.0	light cream	Circular Convex	Translucent	Mucoid	(-)	(+)	(+ve)	(-ve)	(-ve)
0.8 µm	(+ve)	Rod	4.8	light cream	Circular umbonate	Translucent	Mucoid	(-)	(+)	(+ve)	(-ve)	(-ve)
Anaerobic bacteria												
0.2 µm	(-ve)	Rod	1.2	light cream	Circular Convex	Translucent	Mucoid	(-)	(+)	(-ve)	(+ve)	(+ve)
0.4 µm	(-ve)	Rod	1.0	Dark cream	Circular Convex	Translucent	Mucoid	(-)	(+)	(-ve)	(+ve)	(+ve)
0.8 µm	(-ve)	Rod	1.5	Dark cream	Circular Convex	Translucent	Mucoid	(-)	(+)	(-ve)	(+ve)	(+ve)

Table 5.3. Marine bacteria cultivated in the enriched sediment medium

Filter size	Gram stain	Bactrial shape	Diameter of the colony (mm)	Color of the colony	shape of the colony	Transparency	Consistency	Pigments		Oxidase test	Fermentation test	
Aerobic bacteria								Exo.	Endo.		Glucose	mannitol
0.2 µm	(+ve)	Rod	2.0	light cream	Circular Convex	Transparent	Mucoid	(-)	(+)	(-ve)	(-ve)	(-ve)
0.2 µm	(-ve)	Cocci	2.2	Dark cream	Circular Convex	Opaque	Mucoid	(-)	(+)	(+ve)	(-ve)	(-ve)
0.2 µm	(-ve)	Rod	2.3	light cream	Circular Convex	Transparent	Mucoid	(-)	(+)	(+ve)	(-ve)	(-ve)
0.2 µm	(-ve)	Rod	3.4	light cream	Circular umbonate	Translucent	Dry	(-)	(+)	(+ve)	(-ve)	(-ve)
0.2 µm	(-ve)	Rod	3.5	Dark cream	Circular Convex	Opaque	Mucoid	(-)	(+)	(+ve)	(-ve)	(-ve)
0.2 µm	(+ve)	Rod	4.0	Dark cream	Circular Convex	Opaque	Mucoid	(-)	(+)	(+ve)	(-ve)	(-ve)
0.4 µm	(-ve)	Rod	1.7	Dark cream	Circular pulvinate	Opaque	Dry	(-)	(+)	(-ve)	(-ve)	(-ve)
0.4 µm	(-ve)	Rod	1.9	Dark cream	Circular Convex	Opaque	Mucoid	(-)	(+)	(-ve)	(-ve)	(-ve)
0.4 µm	(-ve)	Cocci	2.5	Dark cream	Circular Convex	Opaque	Mucoid	(-)	(+)	(+ve)	(-ve)	(-ve)
0.4 µm	(-ve)	Rod	2.5	Dark cream	Circular umbonate	Translucent	Dry	(-)	(+)	(+ve)	(-ve)	(-ve)
0.4 µm	(+ve)	Rod	2.8	light cream	Circular Convex	Translucent	Mucoid	(-)	(+)	(-ve)	(-ve)	(-ve)
0.4 µm	(-ve)	Rod	4.8	Dark cream	Circular umbonate	Translucent	Dry	(-)	(+)	(+ve)	(-ve)	(-ve)
0.8 µm	(-ve)	Rod	2.5	light cream	Circular Convex	Transparent	Mucoid	(-)	(+)	(-ve)	(-ve)	(-ve)
0.8 µm	(-ve)	Rod	3.3	light cream	Circular umbonate	Transparent	Dry	(-)	(+)	(+ve)	(-ve)	(-ve)
0.8 µm	(-ve)	Rod	3.8	Dark cream	Circular Convex	Translucent	Mucoid	(-)	(+)	(+ve)	(-ve)	(-ve)
0.8 µm	(+ve)	Rod	4.3	Dark cream	Circular umbonate	Opaque	Mucoid	(-)	(+)	(+ve)	(-ve)	(-ve)
Anaerobic bacteria												
0.2 µm	(-ve)	Rod	1.8	light cream	Circular umbonate	Translucent	Mucoid	(-)	(+)	(-ve)	(-ve)	(-ve)
0.4 µm	(-ve)	Rod	1.7	light cream	Circular umbonate	Translucent	Mucoid	(-)	(+)	(-ve)	(-ve)	(-ve)
0.8 µm	(+ve)	Rod	1.9	Dark cream	Circular Convex	Opaque	Mucoid	(-)	(+)	(-ve)	(-ve)	(-ve)

5.4.3. Epifluorescence technique

5.4.3.1. Bacterial abundance

Acridine orange direct count (AODC) revealed that the bacterial counts in freshwater and marine sites were of the same order of magnitude ($10^5 cm^{-3}$), (Figure 5.3). Bacterial abundance in the 0.8 μm size category, however, was about a third of that in the size categories of 0.2- or 0.4-μm in both freshwater and marine sites. Analysis of variance (ANOVA) revealed that there was a significant difference in abundance between sites ($P=0.0001$) (abundance in the marine site was higher than that of the freshwater site) filter sizes ($P<0.0001$) (abundance on both 0.2 and 0.4 μm filter sizes were higher than that of the 0.8 μm) and a significant interaction among these two factors ($P<0.0001$) (see Appendix 5.1).

5.4.3.2. Bacterial biomass

To standardize for the variety of cell shapes, bacterial sizes on each filter were expressed as an Equivalent Spherical Diameter (ESD). Analysis of variance demonstrated a clear significant difference in both mean ESD and mean cell biomass values between sites ($P<0.0001$) (marine site was higher than freshwater site in terms of mean ESD and mean cell biomass) and filter sizes ($P<0.0001$) (all filter sizes were different $0.8 > 0.4 > 0.2$ μm) , although the interaction term was not significant ($P>0.05$) (see Appendices 5.2 and 5.3, respectively).

Bacterial cells inhabiting freshwater sediments showed a lower mean cell biomass compared with that of the marine site (Figure 5.4). Multifactor analysis of variance showed that there was a significant difference in the total biomass between sites ($P<0.0001$) (total biomass in the marine site was higher than that of the freshwater site), filter sizes ($P<0.0001$) (all filter sizes were different $0.8 > 0.4 > 0.2$ μm) and their interaction ($P<0.0001$). However, total biomass spectra were consistent in their shape (Figure 5.5 and Appendix 5.4).

Figure 5.3. Bacterial abundance in freshwater and marine sites per 1cm^3 of sediments.

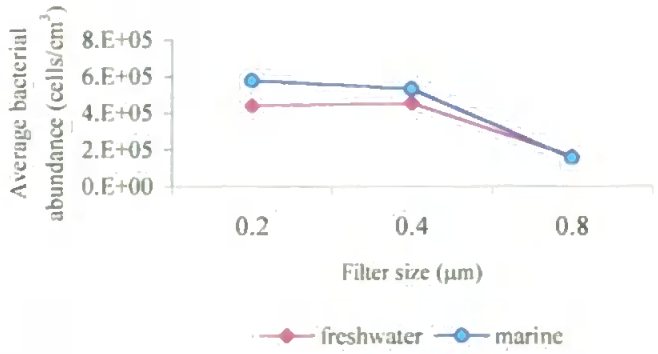

Figure 5.4. Mean bacterial cell biomass in freshwater and marine sediments (pg).

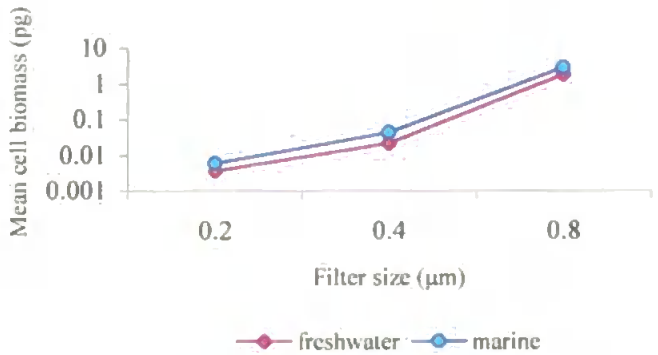

Figure 5.5.Average total bacterial biomass (ng) in freshwater and marine sediments (in Log2 - scale) per 1 cm3. ESD (Equivalent Spherical Diameter) expressed as mm to be consistent with other chapters.

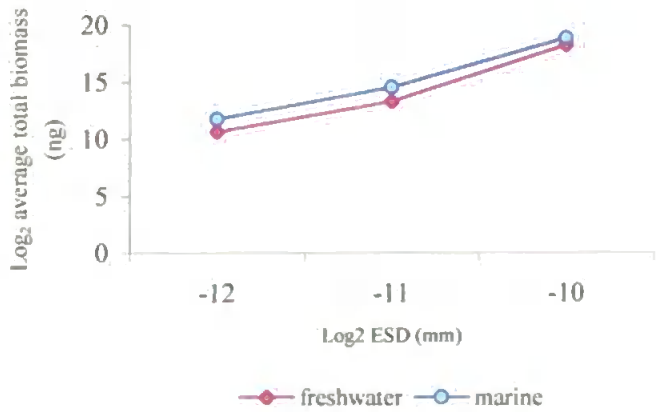

Table 5.4 ATP (ng/litre) concentration in each size category for the freshwater and marine sediments.

Size	freshwater site	marine site
0.2 µm	0.0	0.0
0.4 µm	13.47	18.83
0.8 µm	15.89	23.17

Figure 5.6. ATP concentration (ng/litre) for freshwater and marine sites.

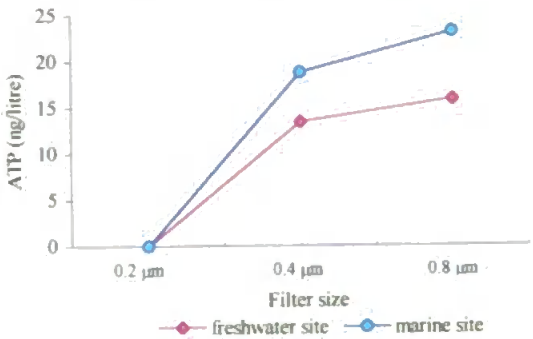

5.4.4. ATP estimation

Despite the similarity in the 0.2 μm size category in both sites, ATP contents in the marine site were consistently, and significantly, higher than that of freshwater site (Table 5.4). The values ranged from 0.0 – 15.89 ng/l in freshwater sediments and from 0.0 – 23.17 ng/l in marine sediments. Figure 5.6 shows the relative distribution of ATP among the size categories in both sites.

Statistical analysis (ANOVA) revealed that there was a significant difference in ATP concentration between the sites ($P<0.05$), but no significant difference among the filter sizes ($P=0.13$) or for the interaction term ($P=0.83$) (see Appendix 5.5).

No ATP was detected in the 0.2 μm organisms, while about 48% and 46% were found in the size category of 0.4 μm in freshwater and marine sites, respectively. The 0.8 μm size category was represented by 52% and 54% for freshwater and marine sites, respectively.

5.5. Discussion

Most previous size fractionations of microbes in aquatic systems have been performed for bacteria in the water column (Cole *et al.* 1993, Saliot *et al.* 1996; Lind and Davalos-Lind 1991; Azam and Hodson, 1977, Ishizaka *et al.* 1997 and Viles and Sieracki, 1992). This does not mean that benthic bacteria are unimportant. On the contrary, benthic bacteria are higher in abundance than those in the water column (Drake *et al.* 1998) and may have uses in a variety of useful fields, as biodegradation and contamination biomarkers.

5.5.1. Bacterial abundance

The statistical difference in abundance between study sites may be explained by differences in organic carbon. Organic carbon is considered as a limiting factor for microbial activity (Aller and Stupakoff 1996; Jurgens *et al.* 1994 a, Wright and Coffin 1984, Cole *et al.* 1988; Billen *et al.* 1990 and Maclean *et al.* 1994).

The estimated bacterial abundance in the current study for both sites (overall values were 3.2×10^8 and 4.1×10^8 cell per l in freshwater and marine sites, respectively) lies in the

range obtained by Azam and Hodson (1977) who estimated the number of bacteria in seawater to be $1x10^8$ cells per l which was similar to that estimated by Ferguson and Rublee (1976).

Hobbie *et al.* (1977) reported that, in one lake, $8.1x10^5$, $4.6x10^5$ and $1.1x10^5$ cells ml^{-1} were found for filters of 0.2 μm, 0.4 μm and 1.0 μm, respectively, which are values in the same order of magnitude as those observed in the current study (4.4×10^5, 4.6×10^5, and $1.7x10^5$ cell ml^{-1} for, freshwater site, and 5.8×10^5, 5.3×10^5 and 1.6×10^5 cell ml^{-1} for, marine site, in 0.2, 0.4 and 0.8 μm filter sizes respectively). They argued that filtration onto Nuclepore filters was the best technique for direct counts of bacteria. The fact that estimated abundances for the current study in the different size categories, especially on 0.4 and 0.8 μm filter sizes, were higher than that of Hobbie *et al.* (1977) may be due to the relatively high content of organic carbon in the sediments compared with the water column (Drake *et al.* 1998). Lind and Dávalos-Lind (1991) hypothesized that the bacterial communities associated with suspended clay–organic aggregates would be numerous and large celled compared with those living free in the water.

Similarly, Saliot *et al.* (1996) reported that the availability of dissolved organic carbon is a limiting factor for bacterial abundance and hence bacterial activity. They found that total bacterial abundance (in their study) in the Lena River and delta ($6.0x10^8$-$8.3x10^9$ cell L^{-1}) was higher than that of the Laptev Sea ($2.0x10^8$-$2.0x10^9$ cell L^{-1}) which they attributed to the fact that organic carbon was higher in the river site. However, total bacterial abundance in the current study ($1.37x10^9$-$2.1x10^9$ and $9x10^8$-$1.5x10^9$ cells per liter for freshwater and marine sites, respectively) was in the same order of magnitude as those reported in Saliot *et al.* (1996). Therefore, organic carbon may be one of the important factors controlling the spatial distribution of bacteria.

This explanation has been supported by Aller and Stupakoff (1996) who suggested that the significant elevation of the bacterial inventories throughout the upper 0–10 cm of the sea bed as a result of more utilizable organic matter. Moreover, Maclean *et al.* (1994) found

that bacterial abundance and mean cell volumes were generally greatest in sediments receiving the greatest input of organic fertilizer, at the faculty of Fisheries and marine Science in trials with the freshwater prawn.

Bacterial abundance on the 0.8 μm filter was significantly lower than that reported on the other filter sizes (0.2 & 0.4 μm). This may be explained by the fact that large bacteria (between 0.8-1.2 μm^3) are more likely to be consumed by predators such as protozoa Chrzanowski and Šimek (1990) and may be more susceptible to viral infection (Weinbauer and Höfle, 1998).

Moreover, bacterial resistance mechanisms towards grazing by higher trophic levels may be through reducing the cell size (Jürgens, 1994). Therefore, the preferential consumption of large sized bacteria by higher trophic levels shifts the bacterial community to the dominance of smaller cells (Jürgens *et al.* 1994 b and Perlmutter and Meyer, 1991).

5.5.2. Bacterial biomass

Bacterial cell biomass values have been expressed using a variety of terms, (mean diameter, cell volume, dry mass, weight of C/cell, etc). In this study, the dry weight has been adopted for expressing bacterial biomass, to be consistent with the other chapters.

The result of this study revealed that there was difference in the overall mean cell dry weight between the marine site (1.35 pg) and that of the freshwater site (0.76 pg) ($P<0.0001$) and between filter sizes ($P<0.0001$). This may be attributed to the difference in the percentage of organic carbon present in the sediments between sites. This explanation was supported by Aller and Stupakoff (1996) who reported that high bacterial biomass on the Amazon shelf is possible, due to the rapid response time of bacteria to disturbance and organic–matter inputs. Moreover, the three parameters (cell size, abundance and the calculated biomass) were significantly related to elevated nutrient concentrations (Cole *et al.* 1993).

Further support for the role of the richness of nutrients on bacterial biomass was given by Letarte and Pinel-Alloul (1991), who suggested that reduced cell dimensions are an adaptive mechanism of bacteria under starvation, increasing the cell surface: volume ratio (allowing a higher substrate incorporation rate per unit of biomass) and protection from zooplankton grazing (Wiebe, 1984).

Schwinghamer (1981) reported that variation of bacterial biomass in marine sediments including deep sea ocean areas is likely to exhibit less than two orders of magnitude. This is confirmed by the current study, where the variation between freshwater and marine sites in total bacterial biomass was less than two orders of magnitude within the same filter size. He added that bacterial biomass peaked in the 0.5 to 1 μm equivalent spherical diameter (ESD). Although, the current study did not account for size class bigger than 0.8 μm, it seems that the size 0.8 μm (where ESD was 1.04 and 1.37 in freshwater and marine sites, respectively) has the highest biomass value. This may be due to the presence of a significant portion of bacterial carbon stored in large cells (Weinbauer and Höfle, 1998). Despite this clear influence of organic carbon, salinity and conductivity may influence both bacterial abundance and biomass.

5.5.3. ATP analysis

The results of ATP analysis revealed that a small cell size tends to be inactive, the degree of activity decreasing from 0.8 μm till it became zero on the 0.2 μm filter size. This result was supported by Pernthaler *et al.* (1996), Posch *et al.* (1997) who reported that small cells are frequently less active than medium–size cells although they did not specify the size range involved. Azam and Hodson (1977) in their study on seawater samples, reported that there was insignificant activity in the 0.1, 0.2, or 0.4 μm filterable organisms, while about 70% of the activity was due to those in the size range of 0.4 – 0.6 μm. This is in agreement with the current study where no activity was detectable in 0.2 μm sized filters in both sites. The amounts of ATP obtained in this study (13.47, 15.89 ng L^{-1} and 18.83, 23.17 ng L^{-1} in

freshwater and marine sites in 0.4 and 0.8 μm filter sizes respectively) were less than 1 order of magnitude than that estimated in Azam and Hodson (1977) (113 ng / liter) in 0.6 μm filtrates. This may be due to lower activity possibly due to bacterial dormancy in the current study where ATP test depends on the physiological state of the population (Watson *et al.* 1977).

The method of extracting ATP in this study from the filter might explain low levels of ATP detected. Two explanations might explain this difference. Firstly, the presence of the filter during extraction may either reduce the extractability of ATP or retain ATP by adsorption. Secondly, there may be a change in the cellular ATP level owing to the additional manipulation of bacteria on the filter (Bulleid, 1978).

Another possibility for the low levels of ATP in this study is the fact that analysis of ATP in sediments has proved more difficult owing to mobilization of anions and cations, which can interfere with the bioluminescent reaction (Aledort *et al.* 1966). The presence of significant difference between the study sites may be due to what has been found in the current study in terms of that the mean cell volume, total abundance and total biomass were higher in the marine site than those of the freshwater site.

5.6. Summary

1. Cylindrical and spherical bacterial cells dominated populations in freshwater and marine site.
2. The marine site was significantly higher than the freshwater site in terms of abundance, mean ESD, mean cell size, total biomass and ATP.
3. All filter sizes were significantly different 0.8 > 0.4 > 0.2 μm in terms of mean ESD, mean and total biomass, except for total abundance where there was no difference between 0.2 and 0.4 μm and for ATP where there was no difference between 0.4 and 0.8 μm.

CHAPTER 6

A Comparison of Standardised Benthic Biomass Size Spectra Across A Salinity Gradient Using Artificial Substrata

6-A comparison of standardised benthic biomass size spectra across a salinity gradient using artificial substrata

6.1. Introduction

The effect of sediment granulometry on benthic biomass size spectra is unclear at present. Schwinghamer (1981) was the first to suggest that sediment grain size was an important factor that underpinned the modality of BBSS. However, Duplisea and Drgas (1999) showed that benthic biomass size spectra from sites with different grain size were not bimodal or significantly different. Similarly, Drgas *et al* (1998) stated that, regardless of the differences in the granulomtery of sites in the shallow coastal area of the Gulf of Gdansk (Southern Baltic Sea), benthic biomass spectra of all stations conformed to a common pattern and could be represented by a single, averaged spectrum.

One approach to assessing the influence of sediment granulometry on benthic communities (including their size structure) is to use a standard artificial substrata across sites with a range of different substrata types and then to compare the community colonosing these substrata with those from the "natural" environment. This chapter extends the study of size spectra across a salinity gradient presented in chapter 4 by assessing both abundance and biomass size spectra in the same sites using artificial substrata.

6.2. Aims

The main aim of this chapter is to compare the benthic size spectra in artificial substrata with those in the natural sediments at the sites representing a range of salinities and heavy metal contamination.

6.3. Materials and methods

The experimental design and sample processing is recorded in chapter 2 and 3. The sampling units used were plastic pan scourers, that have a network of interstices

resembling sponges/algal tufts that have been used previously in studies of biodiversity (Gee and Warwick 1996). Five replicate pan scourers were used at each site in the same season one year after collection of the sediment samples (see table 2.1 in chapter 2). Due to the long time period required to process the standard corer samples for estimating abundance and measuring organisms for 12 sieve sizes (see chapter 3) it was assumed that there was no difference in the standard corer samples over a year for the same sites and the same season (summer). The artificial substratum units (ASU) were positioned in spring 1997 and collected in summer 1997 allowing three months for colonisation. In the marine and lower estuarine sites in the Yealm they were deployed by SCUBA divers, whilst in the other sites in the Yealm and the Fal, the ASUs were placed and collected by accessing these sites as for the normal sediment sampling by the standard corer. Collection of the ASUs was performed by detaching them from the brick by a sharp cutter, transferring them as soon as possible into plastic pots, and fixing by adding 10 % formalin. The fauna was then extracted from these artificial substrata by unravelling and agitating the pan scourers and was sieved using a set of twelve sieves, (see chapter 3). Meiofauna were extracted from any sediment that may have accumulated in these artificial substrata by floatation in Ludox™ made up to a specific gravity of 1.15 (see chapter 3). Organisms were then stored in 70% alcohol.

Analysis of variance and multiple range tests were used to compare relative abundance and relative biomass separately between corer samples and artificial substrata samples within the study sites. Abundance and biomass values were standardised to % of total to allow comparison, (especially they were generated from two different samplers) and log (N+1) transformed to normalise their distribution. Relative abundance and relative biomass data were tested for normality visually using residuals plots to confirm homogeneity of variance. For biomass size spectra, only freshwater and middle estuary sites were studied, as there were no conversion factors (mean major taxon biomasses) from total abundance to total biomass in upper and lower estuary sites in the Yealm. The middle estuary site in the

Fal was omitted from analysis due to a lack of replicates. This was due to their loss during the colonisation period.

6.4. Results

Analysis of variance and multiple range tests revealed that there was no significant difference between relative abundance in artificial substrata and the natural substratum in the freshwater or upper and middle estuarine sites in the Yealm system and the upper estuary site in the Fal. However, relative abundance in artificial substrata was significantly lower than that in the sediment in the lower estuarine site in the Yealm and higher in artificial substrata than that of the sediment in the lower estuary site in the Fal ($P<0.05$) (Figure 6.1, 6.2) appendix (6.1 and 6.2).

Analysis of variance and multiple range tests for relative biomass data revealed that there was no significant effect of substratum type on the biomass size spectra in the freshwater and middle estuarine sites in Yealm (Figure 6.3). However, relative biomass size spectra in artificial substrata were generally significantly different than those of the natural substratum in the case of the upper and lower estuarine site in the Fal ($P<0.05$) (Figure 6.4) appendices (6.3 and 6.4). The significant difference in the upper estuary site in the Fal might be due to the disappearance of the two largest size classes (2000 and 1400 μm mesh sizes) as well as the apparent low relative biomass values in the small meiofaunal categories in the natural substratum. In the lower estuary site, the difference probably as a result of the biomass peak in the size class 355 μm.

Figure 6.1 Abundance size spectra as % of total in the yealm system per sampling unit in A) fw-freshwater site, B) ue-upper estuary, C) me-middle and D) le-lower estuary sites. a.s.-artificial substrata.

A)

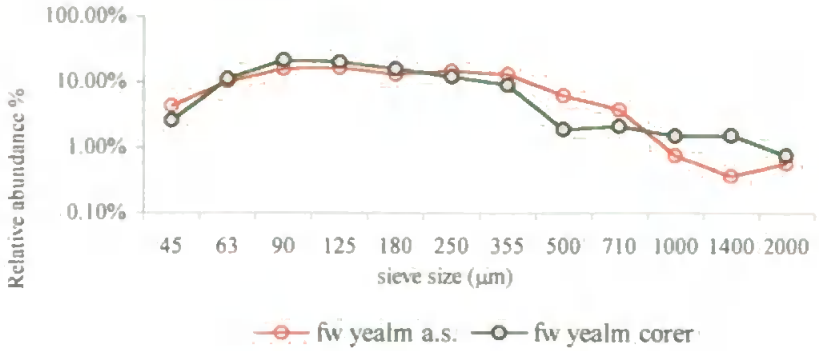

B)

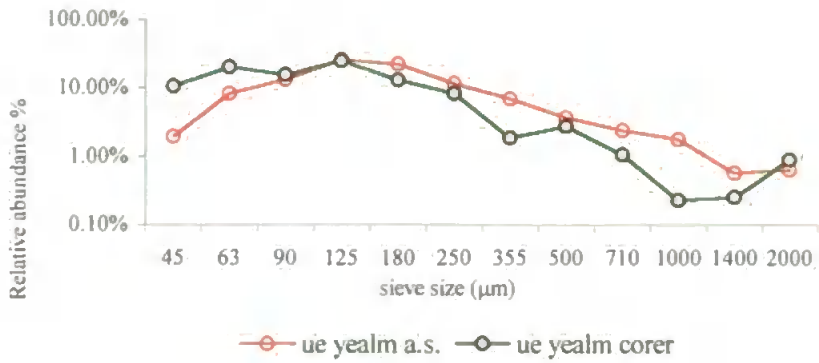

C)

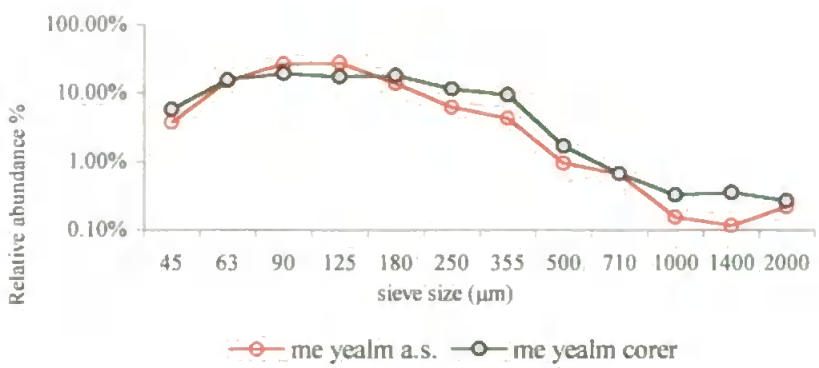

D)

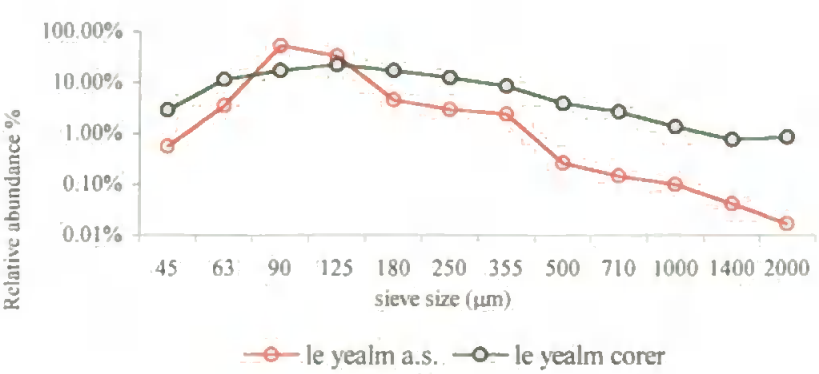

Figure 6.2 Abundance size spectra as % of total in the Fal system per sampling unit in A) ue-upper estuary, B) le-lower estuary sites. a.s.- artificial substrata.

A)

B)

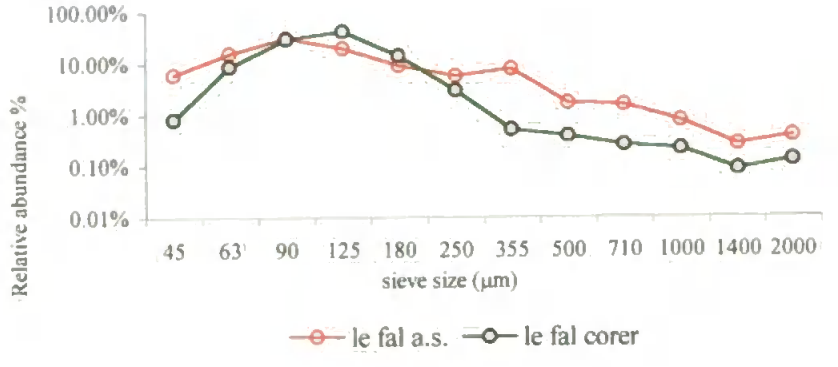

Figure 6.3 Biomass size spectra as % of total in the yealm system per sampling unit in A) fw-freshwater site and B) me-middle estuary sites.
a.s.- artificial substrata.

A)

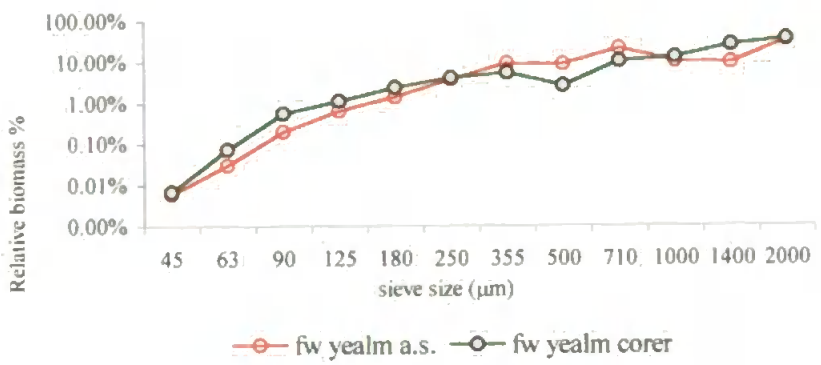

B)

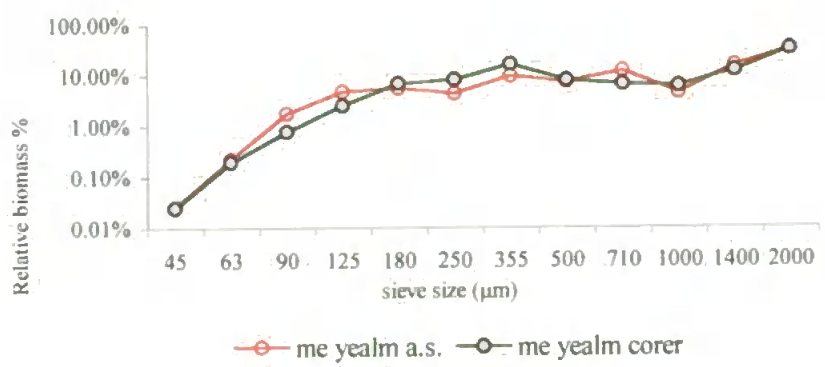

Figure 6.4 Biomass size spectra as % of total in the Fal system per sampling unit in A) ue-upper estuary, B) le-lower estuary sites.
a.s.-artificial substrata.

A)

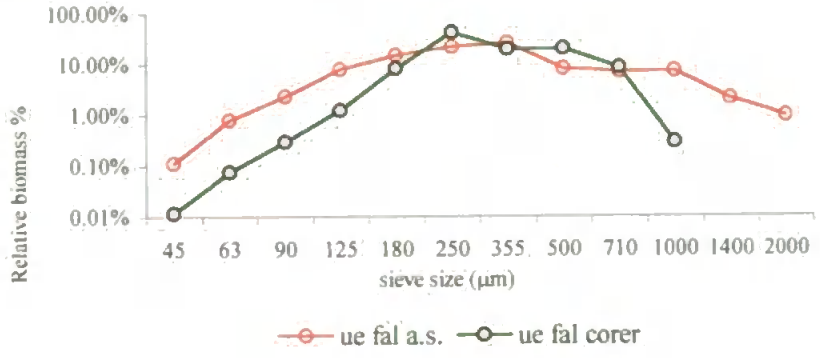

B)

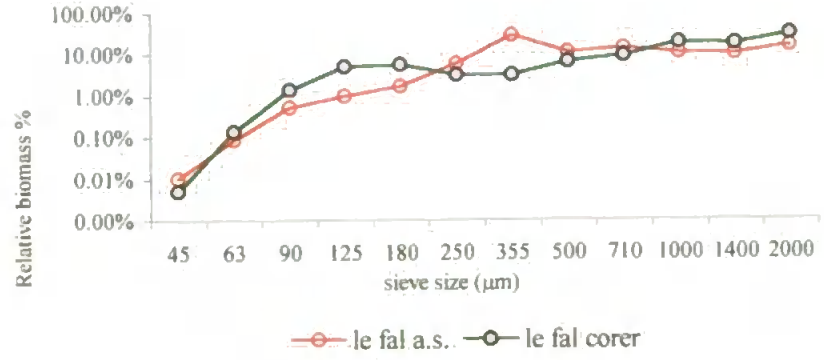

6.5. Discussion

There were no significant differences in the relative abundance in artificial substrata and that of the natural substrata in freshwater, upper, and middle estuary sites in the Yealm and upper estuary site in the Fal. However, relative abundance in lower estuary sites in both systems (Yealm and Fal) in artificial substrata were significantly different from those of the natural substrata i.e., relative abundance in artificial substrata in the Yealm was lower that that of the natural substratum and the opposite was the case in the lower estuary in the Fal. In terms of relative biomass, there were no significant differences in artificial substrata and those of the natural substratum in the Yealm. However, in the Fal relative biomass in artificial substrata were generally significantly higher that those of the natural substrata.

The consistency in the lower estuary sites in both systems where significant differences in relative abundance between artificial and in natural substrata occurred may be due to two factors. Lower relative abundance in artificial substrata in the Yealm compared with that of natural substrata could be as a result of the way divers collected and handled the samples under the water, i.e. organisms had the chance to escape from the artificial substrata units through the big or wide cavities (interstices) within artificial substrata. In the lower estuary site in the Fal, the situation was the opposite with relative abundance in artificial substrata significantly higher than that of the natural substrata. This may be due to differences in the sampling methodology in lower estuarine sites between systems (i.e., diving and land sampling). The high relative abundance in artificial substrata compared with the natural substratum in the lower estuary site in the Fal may reflect the movement of benthic organisms away from highly toxic natural sediments.

For the other sites (freshwater, upper and middle estuary in the Yealm), where there were no significant differences in the relative abundance in artificial substrata and natural substratum, this may be due to conditions of sampling which were nearly the same. In other words, the possibility of organisms to escape was minimum due to the absence of both the extra mechanical work (which was done under water in case of lower estuary site

in the Yealm to untie the pan scourers) and the water interference, which probably enabled organisms to escape. Beside this, high toxicity in the upper estuary site in the Fal might be an indirect reason for the similarity between relative abundance in artificial substrata and that of the natural substratum despite the absence of two size classes (2000 & 1400 μm) from that of the natural substratum. The high toxicity levels detected in the sediment of the upper estuary site in the Fal (see chapter 2) compared with those of the other sites, might have influenced the water sediment interface area, reducing relative abundance in the artificial substrata to be similar to that of the natural substratum.

The possibility of artificial substrata being filled with the natural substratum may be another explanation for the lack of difference in relative abundance in upper estuary in both artificial and natural substratum in the Fal. This similarity may highlight the responsiveness of organisms to the sediments within scourers rather than scourers themselves.

Relative biomass size spectra in artificial substrata were not significantly different from those in the sediment in freshwater and middle estuary sites respectively in the Yealm. Conversely, in the Fal, biomass was significantly higher in artificial compared with natural substrata. This could be attributed firstly to the influence of contamination with high toxicity levels leading to a migration of the benthos to less-polluted substrates.

The results of the current study support those from other studies that have demonstrated a lack of influence of sediment granulometry on benthic size spectra. For example, Rodriguez and Magnan (1993) indicated that macrobenthic size spectra were invariant regardless the differences in the substrata. Bourassa and Morin (1995) showed that abundance size distribution was similar on all substrates. Drgas *et al* (1998) pointed out that benthic biomass size spectra in the shallow coastal area of the Gulf of Gdansk (Southern Baltic Sea) conformed to a common pattern and could be represented by a single, averaged spectrum regardless of the differences in the granulometry of the study sites. More recently, Duplisea and Drgas (1999) stated that benthic biomass size spectra

from different grained sized sites were not bimodal; furthermore, the shape of the spectra was not consistently different. The pattern of benthic biomass size spectra was described as an irregular increase of biomass with increasing body size peaking near the ultimate weight class. This suggests that the benthic community in aquatic system may not have evolved into three distinct size fractions as suggested by Schwinghamer (1981).

The results of the current chapter may illustrate that the sediment granulometry has no structuring effect on the benthic size spectra. Moreover, variability in benthic size spectra is not as simple as to be interpreted by the variability in the sediment granulometry.

One of the most important results in the current chapter is that ASUs provide modelling size spectra to that obtained from the natural substrata. Therefore, ASUs are valuable and very useful in benthic size spectra studies especially in the freshwater, upper and middle estuary sites.

CHAPTER 7

The Influence of Heavy Metal Concentration on Benthic Size Spectra

7.The influence of heavy metal contamination on benthic size spectra.

7.1. Introduction

Studying the impact of contamination on the abundance and/or biomass of benthic organisms has been a popular method for biomonitoring of contamination in aquatic systems. For example, Raffaelli and Mason (1981) and Raffaelli (1982) considered the ratio of the benthic free living nematodes to copepods as an organic pollution indicator. Similarly, Warwick (1986) and Warwick *et al* (1987) developed the ABC (Abundance Biomass Comparison) method for pollution detection using marine macrobenthos, suggesting that the distribution of the numbers of individuals among species should behave differently from the distribution of biomass among species when influenced by pollution-induced disturbance. The majority of benthic size spectra (BSS), however, have shown a characteristic and conservative pattern over a wide range of highly fluctuating environmental conditions, e.g. Strayer (1986) for freshwater, Ramsay *et al* (1997) for freshwater and brackish water, Warwick (1984), Duplisea (1998) and Drgas *et al* (1998) for marine. This consistency suggests that BSS might provide a reference against which environmental impacts can be gauged.

Schwinghamer (1988) pioneered the use of benthic biomass size spectra for biomonitoring in a study of the impact of mixture of diesel oil and copper contamination at the head of Frierfjord/Langesundfjord (Norway). The main conclusion from his study was that the pollution-induced changes in communities were equally well detected using benthic biomass size spectra as in the more time consuming analyses involving species identification. However, his method had some limitations. For example, only nematodes and harpacticoid copepods were measured in the meiofaunal field samples which may have resulted in biomass underestimation in the size classes where organisms other than

nematodes and harpacticoids were significant. Schwinghamer (1988) also suggested that benthic biomass size spectra became increasingly 'bumpy' with increasing sediment pollution i.e. biomass trends from size class to another were less consistent for polluted sites than they were for the control basin.

More recently, Duplisea and Hargrave (1996) studied the meiofaunal biomass and respiration size structure in response to sediment organic enrichment near a salmon aquaculture farm in Bliss Harbour, Bay of Fundy, Canada. They concluded that biomass size spectra were not significantly different between sites, despite a decrease in taxon diversity with increasing sediment organic enrichment. The single largest contributor to biomass and respiration in this case was the small nematodes, particularly at the most polluted sites.

In terms of heavy metal contamination, Stark (1998a) stated that the patterns of macrobenthic assemblage distribution and abundance in two Sydney estuaries, Australia, were found to vary significantly at several spatial scales which were related to the significant differences in the heavy metals concentrations in the sediments, concluding that there was a significant correlation between patterns of assemblages and concentrations of heavy metals. Similarly, Stark (1998b) showed experimentally that assemblages of marine benthic organisms differed in areas with or without heavy metals contamination.

Therefore, if benthic biomass size spectra are consistent across different sites in both the current study and in other studies (see earlier), they might provide a valuable method for biomonitoring through the probable different sensitivities of large and small bodied organisms.

7.2. Aims

The main aim of this chapter is to assess the impact of heavy metal contamination on the shape of benthic biomass size spectra across a salinity gradient within the polluted Fal estuary by making a comparison with the benthic biomass size spectra across a salinity gradient in an uncontaminated system (the Yealm).

7.3. Materials and methods

Details of the sample sites, sample collection and processing are given in chapter 2. The methodology used for the uncontaminated Yealm system was adopted for the contaminated Fal system. This included the generation of site-specific mean values for individual major taxon biomass in each sieve from the measured mean major taxon biomass by multiple regression analysis as in (chapter 3) as a conversion factor from abundance to biomass.

In terms of comparison between the Fal study sites, log transformed ESD and biomass values for each sieve in the Fal study sites were compared using multifactor analyses of variance for: 1) all organisms (total); 2) different shapes of organisms; 3) major taxa; and 4) body dimensions (body length and width). Tests for normality were conducted visually using residuals plots to confirm homogeneity of variance prior to ANOVA. This was to support the usage of multiple regression analysis for deriving site-specific biomass values as the Yealm study sites were significantly different in terms of biomass (mean sieve, mean shape, mean major taxon and organisms body dimensions).

Multifactor analysis of variance of the log transformed total abundance and total biomass was used for comparing the Fal study sites.

Multifactor analysis of variance was used for comparing the log transformed ESD values among the sieve sizes and the study sites of Yealm and Fal systems. Finally, log transformed abundance and biomass values were compared among sieves, sites and seasons within and between the two systems (Yealm and Fal) using multifactor analysis of variance. Comparisons between the two systems (Yealm and Fal) in terms of biomass,

were achieved only between freshwater and middle estuary sites as these were the only measured sites in Yealm equivalent to sites in the Fal.

7.4. Results

Results will deal firstly with the Fal system alone and secondly compare the two systems (Fal, contaminated and Yealm, control).

7.4.1. Fal system

7.4.1.1. Mean ESD, biomass comparisons among sites and sieves

Multifactor analysis of variance (ANOVA) of log transformed values of ESD and biomass per sieve for the Fal system for all four measurement parameters (i.e. all organisms (total), different shaped organisms, major taxa, and body dimensions) revealed significant differences among the study sites ($P<0.0001$) and sieves ($P<0.0001$) (Table 7.1), with the exception of mean copepod ESD and oligochaeta body length which were not significantly different among sites ($P>0.05$).

Due to the significant differences in the ESD and biomass among the study sites of Fal system, multiple regression analysis (see chapter 3 for the same case in Yealm system) was used to predict the mean major taxon biomass from the measured values for each site to be used as a conversion factor from abundance to biomass (Table 7.2).

7.4.1.2. Abundance size spectra

In the Fal system, there were no significant differences in abundance between lower, middle and upper estuarine sites but abundances at these sites were significantly higher than that of the freshwater site ($P<0.05$) (see appendices 7.37, 7.38), (Figure 7.1) regardless of season. There was no significant difference between seasons (summer and autumn) ($P=0.864$) (see appendix 7.39). Hence data were pooled for Figure (7.1). Benthic abundance size spectra in the Fal showed a general pattern among seasons and

Table 7.1. (F) values for the ANOVA in the Fal system; for testing ESD and biomass values for four different levels, Total (all organisms within the sieve), Shape (cylinder or the other shapes pooled), Taxonomy (mean ESD and mean biomass for individual major taxa) and Biology (organisms body dimensions), P values are represented by stars (*<0.05, **<0.001 & ***<0.0001).

	Factor	site	Df	sieves	Df	Appendix number
Total	ESD	56.55***	3	527.66***	11	7.1
	Biomass	63.01***	3	527.66***	11	7.2
Shape	Cyl ESD	46.97***	3	447.85***	11	7.3
	Cyl biomass	20.68***	3	144***	11	7.4
	Others ESD	7.21**	3	259.49***	9	7.5
	Others Biomass	8.80***	3	259.49***	9	7.6
Taxonomy	Nematoda ESD	36.39***	3	225.35***	6	7.7
	Nematoda Biomass	42.06***	3	225.35***	6	7.8
	Copepod ESD	1.78	3	92.57***	4	7.9
	Copepod Biomass	2.86*	3	92.57***	4	7.10
	Oligochaeta ESD	5.69*	3	90.18***	7	7.11
	Oligochaeta biomass	6.53**	3	90.18***	7	7.12
	Polychaetra ESD	21.63***	2	13.49***	6	7.13
	Polychaeta Biomass	23.48***	2	13.49***	6	7.14
Biology	Nematoda length	12.51***	3	449.67***	6	7.15
	Nematoda width	24.82***	3	128.26***	6	7.16
	Copepod length	22.22***	3	155.98***	4	7.17
	Copepod width	3.89*	3	124.35***	4	7.18
	Oligochaeta length	0.31	3	110.49***	7	7.19
	Oligochaeta width	3.33*	3	47.57***	7	7.20
	Polychaetra length	65.48***	2	74.08***	6	7.21
	Polychaeta width	6.46*	2	20.84***	6	7.22

Table (7.2): Regression equations for biomass of the major taxa in the Fal system in freshwater (FW), upper estuary (UE), middle estuary (ME) and lower estuary site (LE) in relation to sieve size, In case of R=100%, just two points were available for the regression.

Taxon	Site	R square	Regression equation	Appendix No.
Nematoda	FW	96%	log (biomass)=-22.07519+2.83909*log(sieve size)	7.23
	UE	96%	log (biomass)=-16.35087+1.58425*log(sieve size)	
	ME	96%	log (biomass)=-18.20202+1.87607*log(sieve size)	
	LE	96%	log (biomass)=-21.1081+2.75259*log(sieve size)	
Oligochaeta	FW	94%	log (biomass)=-18.64894+2.45616*log(sieve size)	7.24
	UE	94%	log (biomass)=-18.8871+2.45616*log(sieve size)	
	ME	94%	log (biomass)=-18.77352+2.45616*log(sieve size)	
	LE	94%	log (biomass)=-17.7691+2.45616*log(sieve size)	
Polychaeta	UE	95%	log (biomass)=-9.59244+0.9237*log(sieve size)	7.25
	ME	95%	log (biomass)=-8.69099+0.971355*log(sieve size)	
	LE	95%	log (biomass)=-16.3777+2.18574*log(sieve size)	
Hydracarina	FW,ME&LE	84%	log (biomass)=-28.4447+4.28019*log(sieve size)	7.26
Tardigrada	FW	100%	log (biomass)=-16.628+2.00822*log(sieve size)	7.27
Tricladida	FW,UE,ME&LE	93%	log (biomass)=-15.9928+2.20088*log(sieve size)	7.28
Copepod	FW,UE,ME&LE	90%	log (biomass)=-20.4348+2.82021*log(sieve size)	7.29
Ostracoda	UE	96%	log (biomass)=-18.15744+2.37843*log(sieve size)	7.3
	ME	96%	log (biomass)=-17.51754+2.37843*log(sieve size)	
	LE	96%	log (biomass)=-17.309+2.37843*log(sieve size)	
Rotifera	FW	98%	log (biomass)=-23.8224+3.5412*log(sieve size)	7.31
Mysides	LE	99%	log (biomass)=-21.7479+3.1273*log(sieve size)	7.32
Ephemeroptera	FW	88%	log (biomass)=-19.5411+2.63976*log(sieve size)	7.33
Diptera larvae	FW	87%	log (biomass)=-22.9771+3.34006*log(sieve size)	7.34
Chironomid	FW	100%	log (biomass)=-17.6133+2.31755*log(sieve size)	7.35
Amphipoda	ME	100%	log (biomass)=-23.99982+3.50819*log(sieve size)	7.36
	LE	100%	log (biomass)=-6.42452+0.65032*log(sieve size)	

sites of decreasing abundance with increasing organism size. However, this pattern showed some deviations, such as the abrupt increase in abundance in the 45 μm sieve size in the freshwater site in summer. Moreover, there was a complete absence of organisms in some sieve sizes in some sites (e.g. 2000, 1400 μm in case of freshwater and upper estuary sites). Similarly, organisms were completely absent in the 2000 μm sieve size in the middle estuary site in both study seasons (summer and autumn). Additionally, during Autumn there was a trough in the sieve size 500 μm, where macrofaunal categories in the different sites in the Fal systems started to increase (Figures 7.2, 7.3).

Nematodes, copepods, and to a lesser degree oligochaetes dominated meiofaunal size classes (Figure 7.4). Oligochaetes and polychaetes were the main representatives of the macrofauna, although the latter was present in the larger meiofaunal categories, especially at the three estuary sites (Figure 7.4).

7.4.1.3. Biomass size spectra

Multifactor analysis of variance of log transformed biomass of all Fal sites (freshwater, upper, middle and lower estuary) revealed that the biomass at upper and lower estuarine sites were not significantly different, but were significantly higher ($P<0.05$) than those of the middle estuarine and freshwater site. Biomass of the middle estuary site was also significantly higher than that of the freshwater site ($P<0.05$). Additionally, there was no significant difference in biomass between seasons (i.e. summer and autumn) ($P=0.98$) (see appendices 7.40, 7.41).

Some sites showed high values of abundance and biomass in some sieve sizes, for example the upper estuary site revealed highest values from 710 μm to 180 μm in summer and in the size classes 45 μm to 180 μm in autumn (Figures 7.5 & 7.6).

Figure 7.1 Interaction plot of log transformed abundance size spectra in the Fal sites, freshwater (fw), lower estuary (le), middle estuary (me) and upper estuary (ue) with sieve sizes (summer and autumn data were pooled).

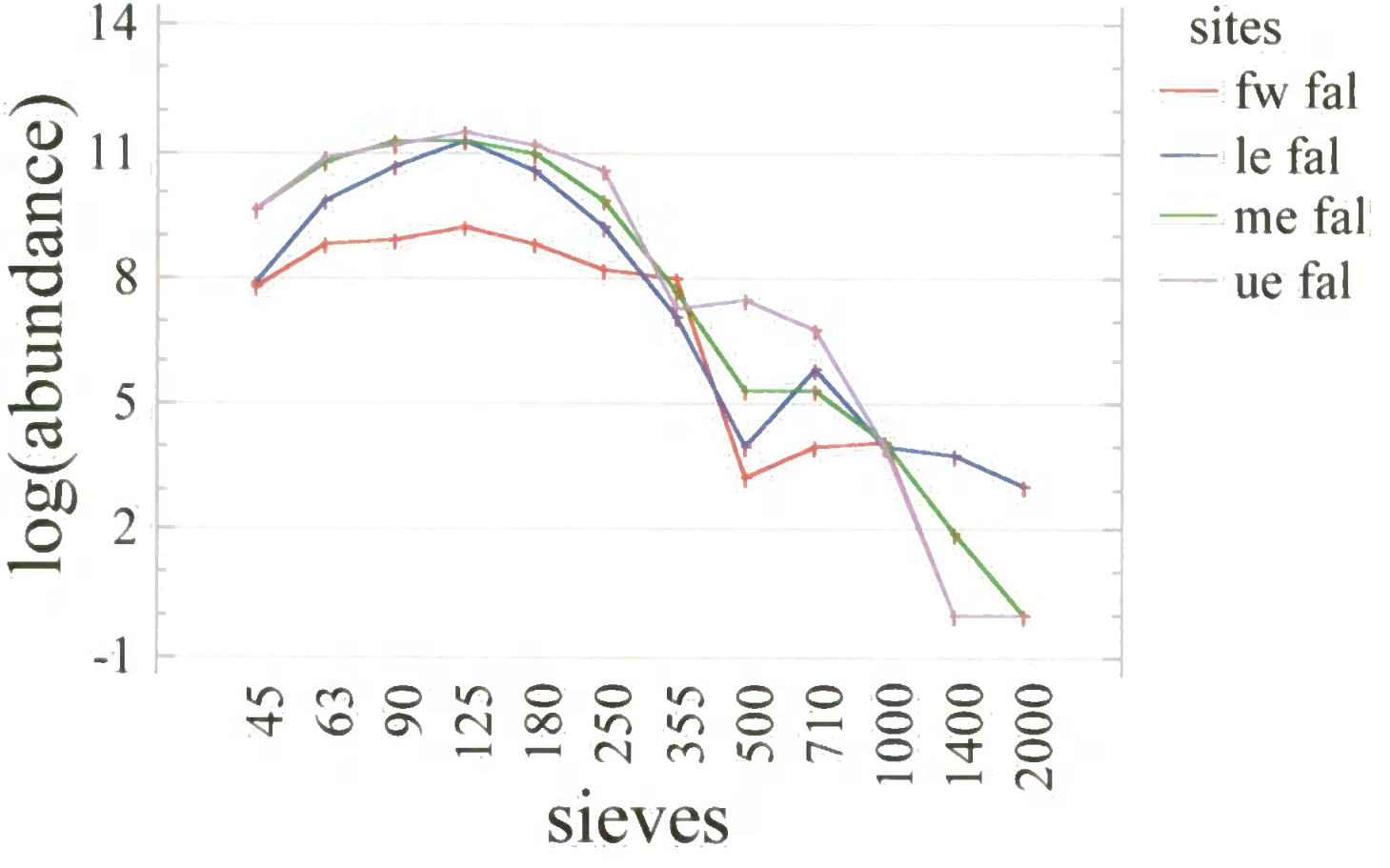

Figure 7.2 Abundance size spectra for four sites in the Fal system (fw- freshwater site, ue- upper estuary, me- middle estuary and le- lower estuary sites) in A) summer, B) autumn.

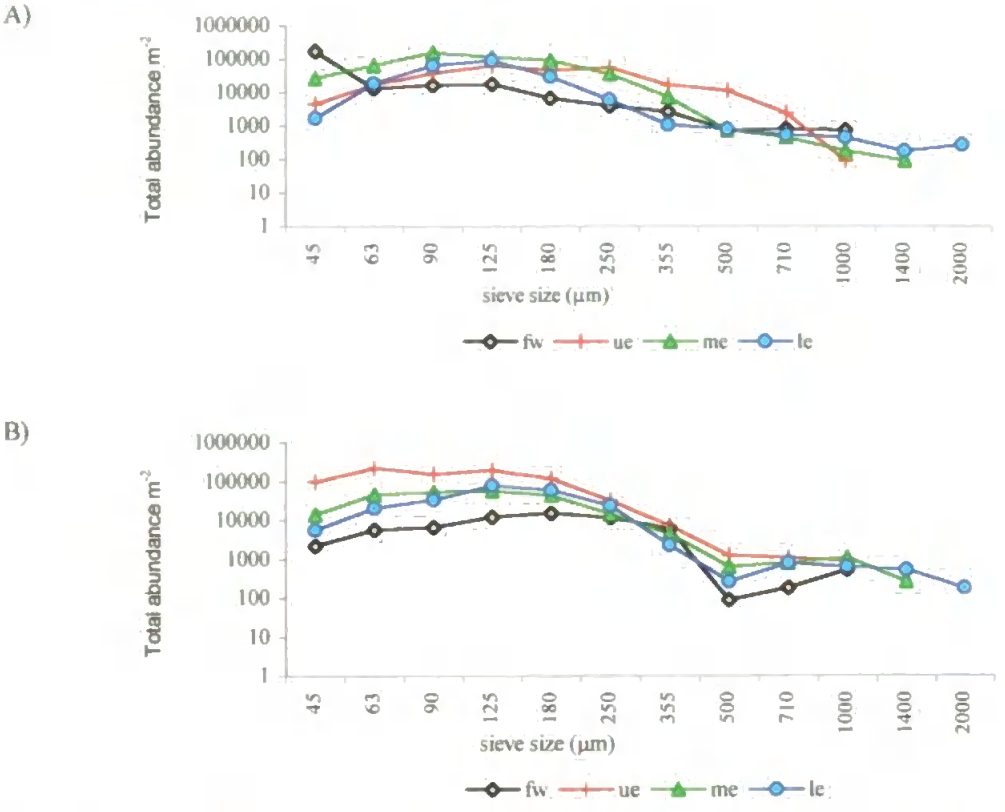

Figure 7.3 Standardized (% of total) abundance size spectra for four sites in the Fal system (fw- freshwater site, ue- upper estuary, me- middle estuary and le- lower estuary sites) in A) summer, B) autumn. (note differences in the Y-axis scale).

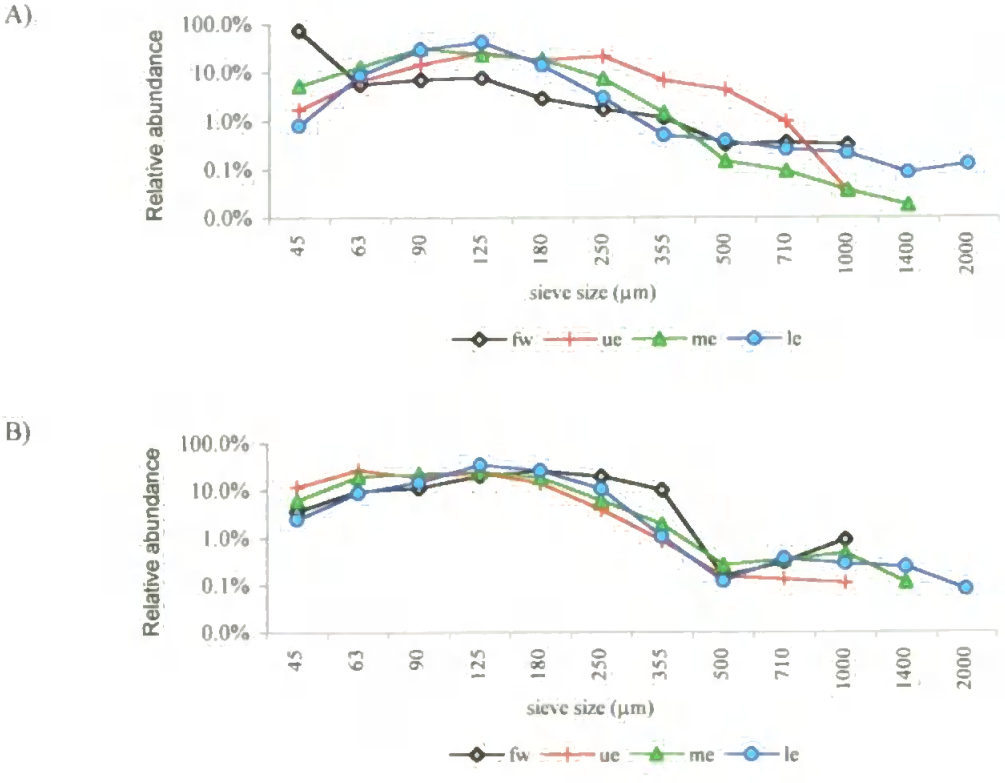

Figure 7.4. Mean abundance of most abundant major taxa in the Fal in 1) Summer and 2) Autumn.

1)summer freshwater site

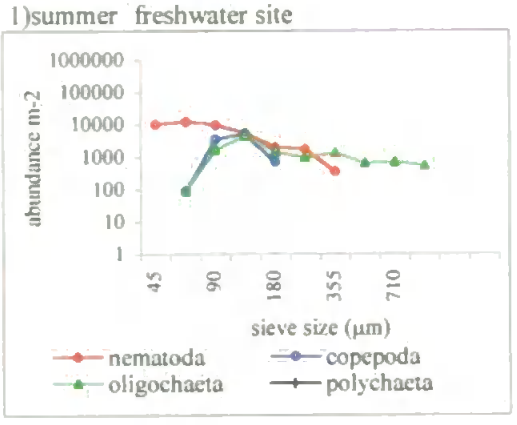

2)autumn freshwater site

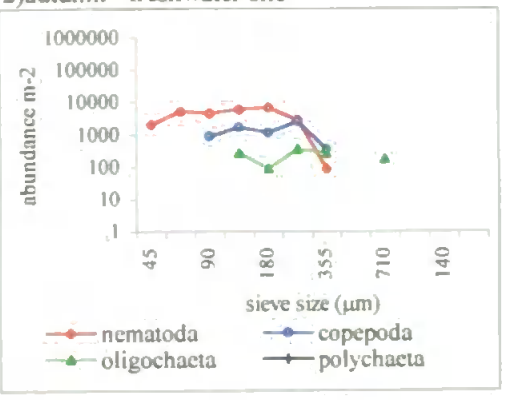

1)summer upper estuary site

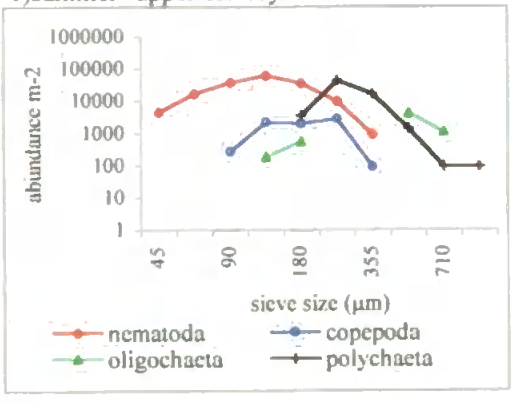

2)autumn upper estuary site

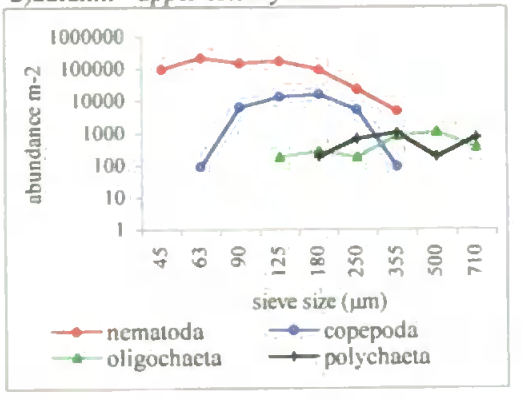

1)summer middle estuary site

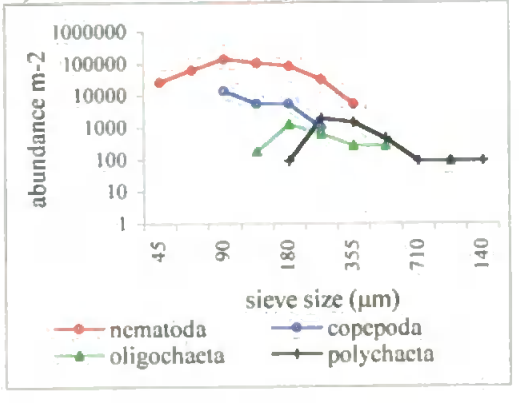

2)autumn middle estuary site

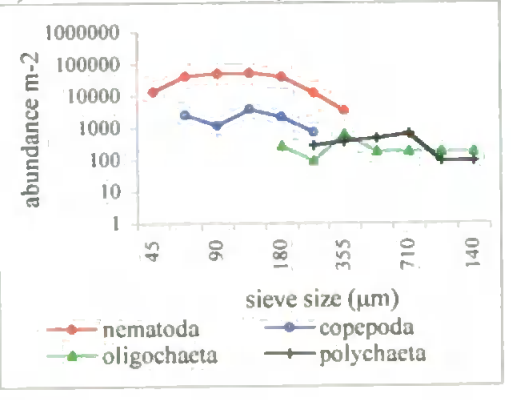

1)summer lower estuary site

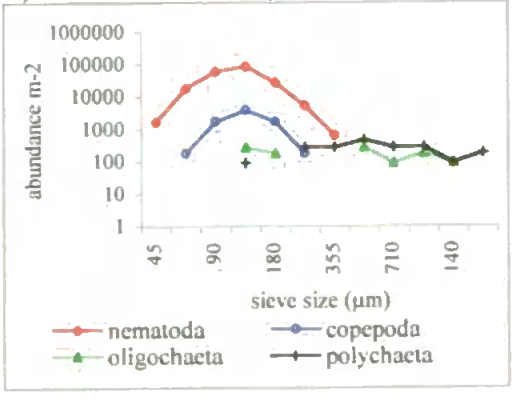

2)autumn lower estuary site

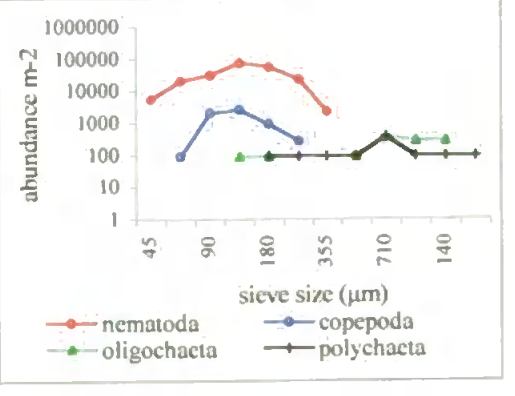

Figure 7.5 Absolute biomass size spectra for four sites in the Fal system (fw-freshwater site, ue-upper estuary, me-middle estuary and le-lower estuary sites) in A) summer, B) autumn. (note differences in Y-axis scale).

A)

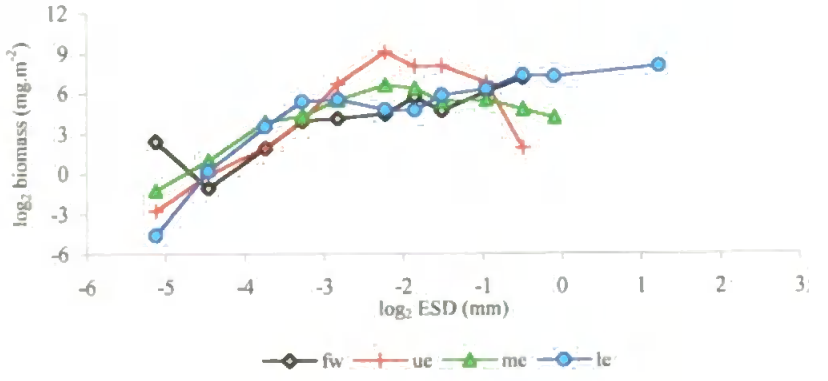

B)

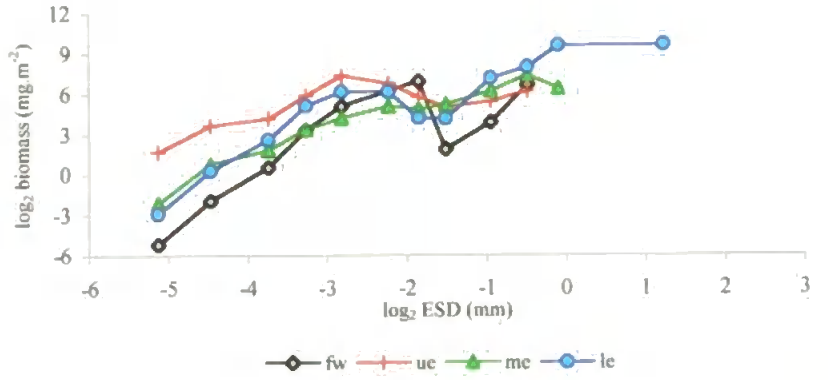

Figure 7.6 Standardized biomass size spectra for four sites in the Fal system (fw, freshwater site, ue, upper estuary, me, middle estuary and le, lower estuary sites) in A) summer; B) autumn. (note differences in Y-axis scale).

A)

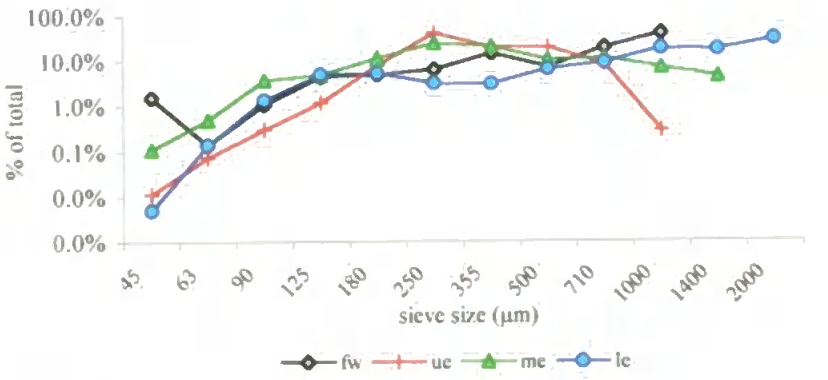

B)

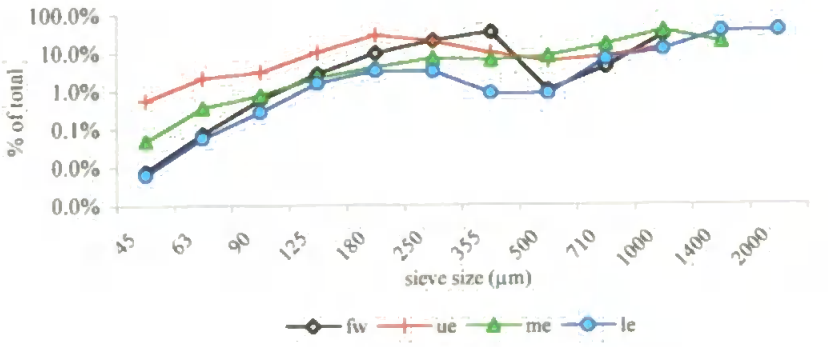

7.4.2. Comparison of Fal and Yealm systems

7.4.2.1. Mean ESD comparison between the two systems

Multiple factor analysis of variance and multiple range tests for the log transformed mean sieve ESD values in Yealm and Fal sites revealed significant differences between sites in the Fal ($P<0.05$) (i.e. ESD values of the different sites in Fal were in the following sequence, upper estuary < freshwater site ≤ middle estuary < lower estuary). Moreover, ESD values of the Yealm system were significantly higher than those of the upper estuary, freshwater or middle estuary site in the Fal system, but smaller than that of the lower estuary site in the Fal ($P<0.05$) (see appendices 7.42, 7.43). However, the interaction plot of the log transformed ESD for sieve sizes and the sites (Figure 7.7) revealed that the ESD values in the lower estuary site in the Fal system were the highest along the size range 250-2000 μm. Similarly, ESD values of the middle estuary and the freshwater sites in the same system had a similar pattern, with highest ESD values in the size range 500-1000 μm and 355-1000 μm, respectively. These differences between the two systems, in terms of among sieve ESD differences could be attributed to the differences in the organisms body dimensions (length & width) among sites of the two systems. Table 7.3 gives an example for two sites (freshwater and middle estuarine site). Due to these differences between systems, separate ESD values for each system were used as the x-axis to plot the biomass size spectra.

7.4.2.2. Abundance size spectra

Log transformed abundance values were significantly different between sieves, sites and seasons ($P<0.0001$, $P<0.0001$ and $P=0.049$, respectively) and there was also a significant interaction among these factors ($P<0.0001$) (see appendix 7.44).

Abundances in all sites of the Yealm system were significantly higher than those of the equivalent (in terms of salinity) sites in the Fal system ($P<0.05$) (Figures 7.8) (see

Figure 7.7 Interaction plot of the log transformed (ESD+1) values with the sieve sizes for all sites in both systems, Yealm and Fal.

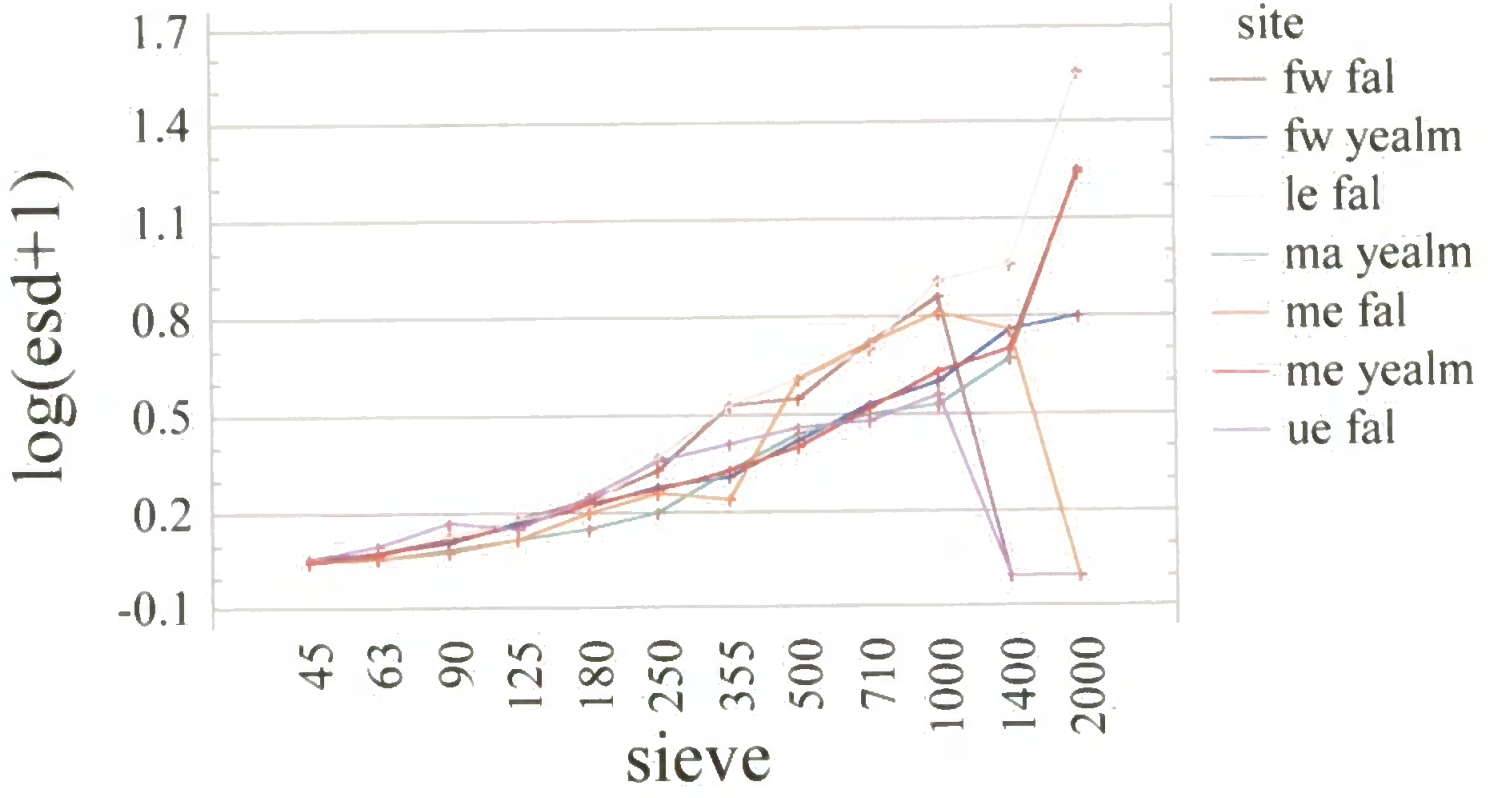

Table 7.3. Differences in organisms body lengths and widths (in cm) affecting the ESD values between Yealm and Fal resulting in an increase in the Fal's ESD values.

		YEALM SYSTEM						FAL SYSTEM					
		Freshwater site			Middle estuary site			Freshwater site			Middle estuary site		
Sieve size (μm)	Taxa	B.length	B.width	Mean ESD	B.length	B.width	Mean ESD	B.length	B.width	Mean ESD	B.length	B.width	Mean ESD
1000	Oligochaeta	0.52	0.02	0.56	1.02	0.02	0.93	0.70	0.03	0.85			
	Tricladida	0.27	0.07	1.27				0.45	0.09	1.69			
	Chironomid	0.43	0.03	1.07									
	Mysides										0.26	0.04	1.24
	Mollusca	0.23	0.20	1.90									
710	Chironomid	0.33	0.03	0.86				0.41	0.03	1.04			
	Oligochaeta	0.44	0.02	0.51	0.72	0.02	0.69	0.88	0.03	0.99	0.77	0.03	1.05
	Collembolla				0.16	0.03	0.56						
	Polychaeta				0.57	0.02	0.67				0.53	0.04	1.08
500	Oligochaeta	0.32	0.01	0.43	0.56	0.02	0.61	0.50	0.03	0.76	0.58	0.02	0.68
	Chironomid	0.24	0.02	0.65									
	Mollusca	0.13	0.10	1.01									
	Nematoda	0.30	0.01	0.27									
	Polychaeta				0.35	0.01	0.46				0.54	0.04	0.99
	Ampipoda										0.21	0.03	0.97
355	Oligochaeta	0.22	0.01	0.33	0.30	0.02	0.54	0.27	0.02	0.55	0.17	0.02	0.41
	Chironomid							0.21	0.02	0.59			
	Nematoda	0.31	0.00	0.18	0.22	0.01	0.24				0.17	0.01	0.19
	Copepoda	0.10	0.03	0.40	0.07	0.03	0.45						

Figure 7.8. Abundance size spectra in A) summer, B) autumn in both systems (Yealm and Fal).

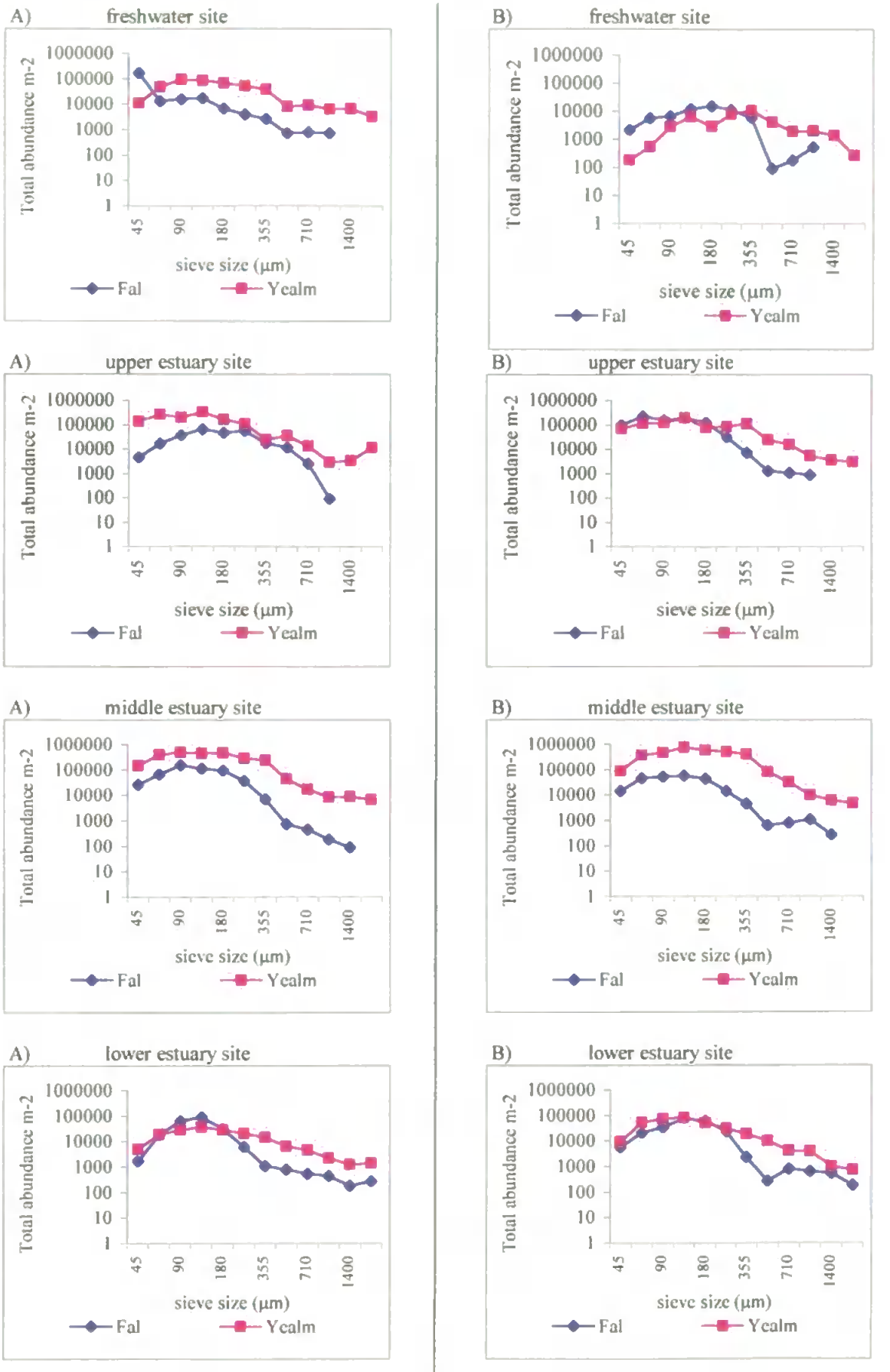

appendix 7.45). Differences between seasons were less significant (P=0.049), although abundances were higher in both systems in autumn, except in upper estuary and freshwater sites in the Yealm and the freshwater site in the Fal (see appendix 7.46).

One major difference between the Fal and the Yealm was the absence (from the Fal) of large macrofauna in the freshwater and upper estuary sites (1400 and 2000 μm) and middle estuary site (2000 μm) in both seasons (summer and autumn).

Benthic abundance size spectra in the Fal (contaminated system) showed a similar shape as for the Yealm of decreasing abundance with increasing organism size, but there were large, significant differences in abundance across sieves in most sites. For example, in the case of the middle estuary site in both systems, macrofaunal and meiofaunal abundances were higher in the Yealm, with a similar pattern in the freshwater and upper estuary sites in summer. In contrast, meiofaunal abundance in the Fal in freshwater and upper estuary sites was higher or equal to the equivalent sites in the Yealm. Moreover, lower estuary macrofaunal abundance in the Yealm was higher than that of the lower estuary in the Fal, but for meiofaunal abundance the two sites were fairly similar in both systems.

Abundance size spectra within the Fal system showed different patterns within the different size classes. For example, in the summer freshwater samples, the high recorded abundance in the 45 μm size class was due to high numbers of Rotifers. Also, the upper estuary showed higher abundance in the size classes 710-250 μm in the same season compared with those of the other sites, whilst, there was a trough in the size class 500 μm in all sites in autumn except the upper estuary site (Figure 7.2, 7.3).

7.4.2.3. Biomass size spectra

Comparison of the equivalent sites (i.e. freshwater and middle estuary sites) in both systems using multifactor analysis of variance on log transformed biomass data revealed that biomass values at the Fal sites were significantly lower than those of Yealm sites, except for the meiofaunal category in Yealm freshwater site in autumn and the 45 μm size

category at the same site in summer (Figure 7.9). Moreover, middle estuary biomass was significantly higher than that of freshwater site in both systems ($P<0.05$) (see appendices 7.47, 7.48).

Seasonal variability among the equivalent sites in both systems in terms of biomass was not consistent. For example, despite the clear difference between summer and autumn biomasses (i.e. summer biomass being higher), the difference was more pronounced at freshwater sites than in middle estuary sites within both systems (Figure 7.10).

The detected difference in behaviour of abundance size spectra for some size classes in Fal as reported in section 7.4.2.2. was apparent in the benthic biomass size spectra. The differences between the study sites in the two systems (Yealm & Fal) could be confirmed by the results of the normalized biomass size spectra (Figures 7.11, 7.12). For example, the slopes of the normalized biomass size spectra in the contaminated system (Fal) were not consistent within the same site or between the different sites, when compared with that of the clean system (Yealm) (Table 7.4). The values of the correlation coefficient (R^2) in the contaminated system were small. Therefore, the slopes can not be relied on. This probably reveals that the normalized biomass size spectra have broken down, as a result of environmental stresses or heavy metal contamination.

Figure 7.9 Benthic biomass size spectra in A) summer , B) autumn for freshwater and middle estuary sites in Yealm and Fal systems.
(note differences in ESD values between the two systems in the x-axis).

A) freshwater site

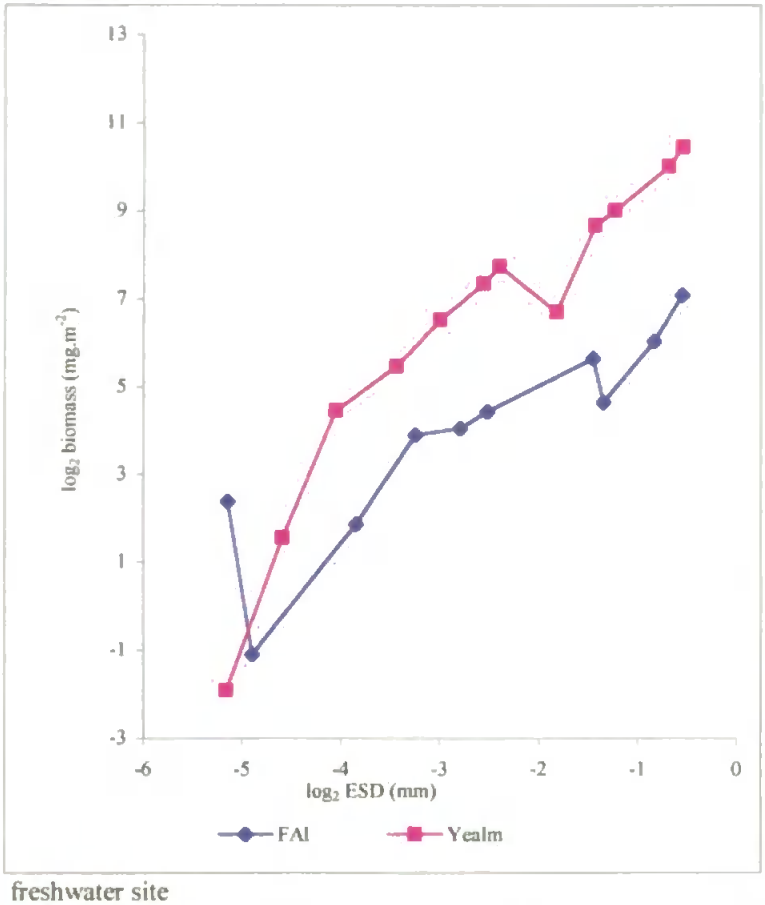

B) freshwater site

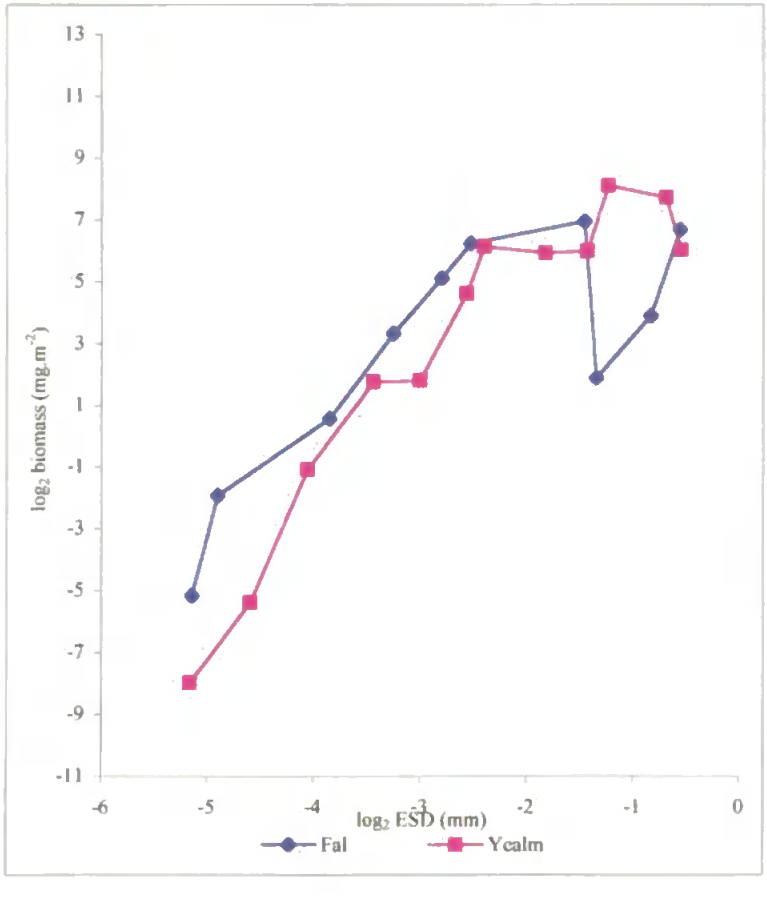

Figure 7.9 continued.

A) middle estuary site

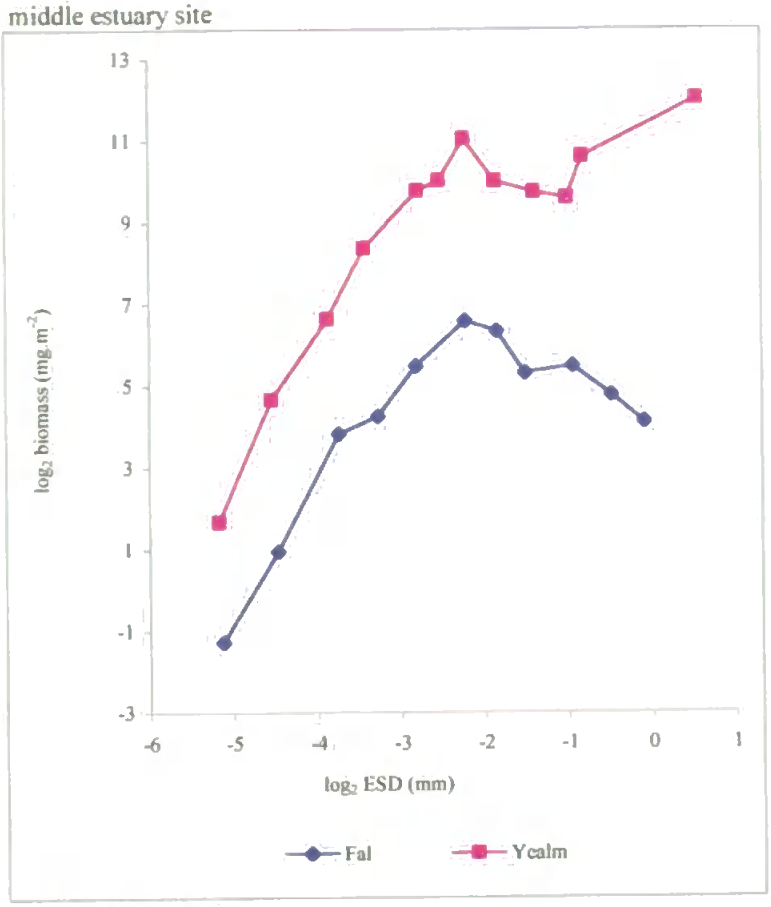

B) middle estuary site

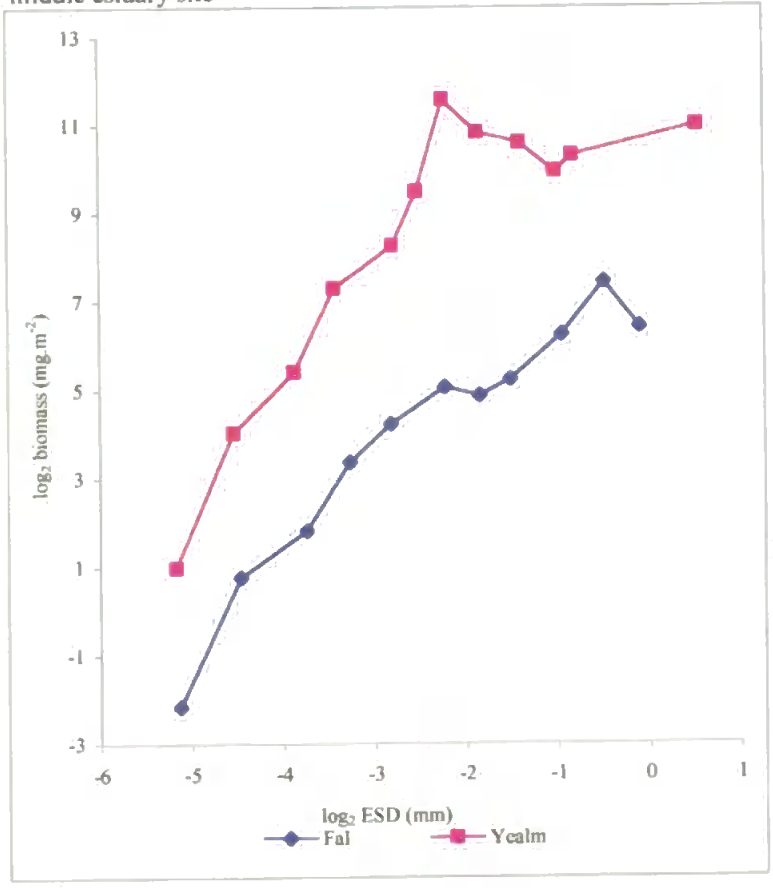

Figure 7.10 Interaction plot of log transformed biomass values with seasons (autumn and summer) for freshwater and middle estuary sites in Yealm and Fal

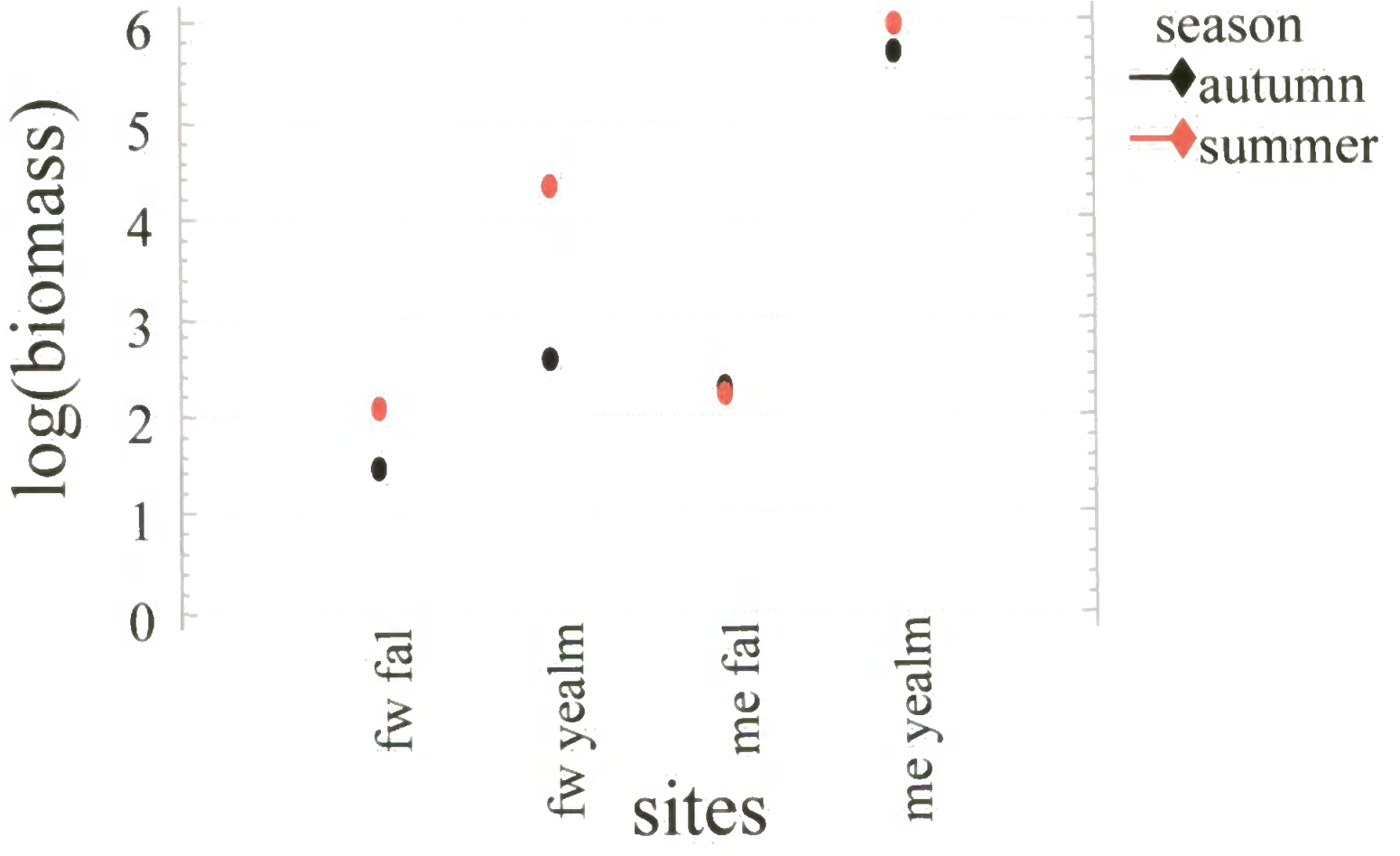

Figure 7.11. Normalized benthic biomass size spectra (BBSS) in A) summer, B) autumn in freshwater and middle estuary sites in Yealm system

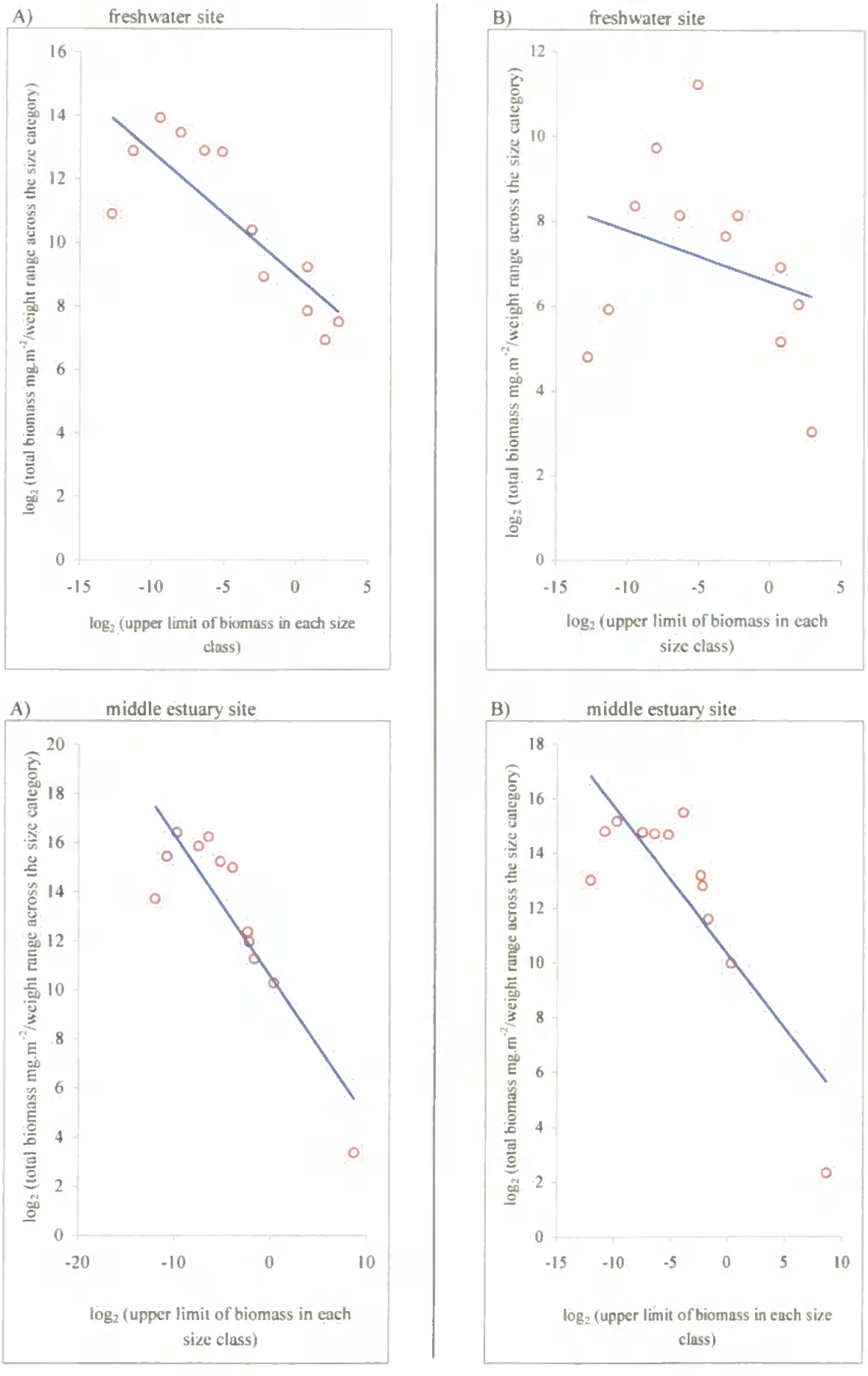

Figure 7.12. Normalized benthic biomass size spectra (BBSS) in A) summer, B) autumn in freshwater, upper estuary, middle estuary and lower estuary sites in the Fal system.

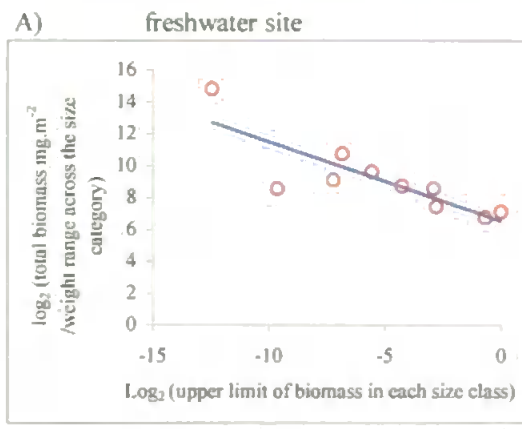

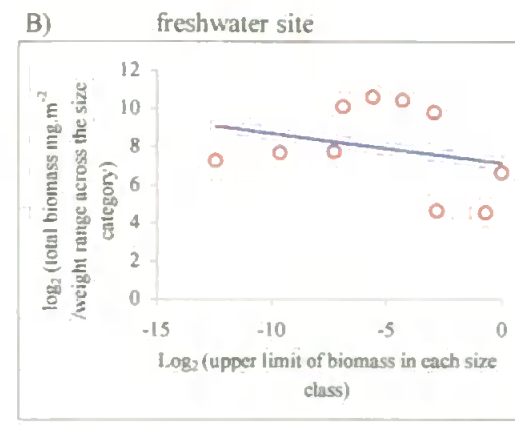

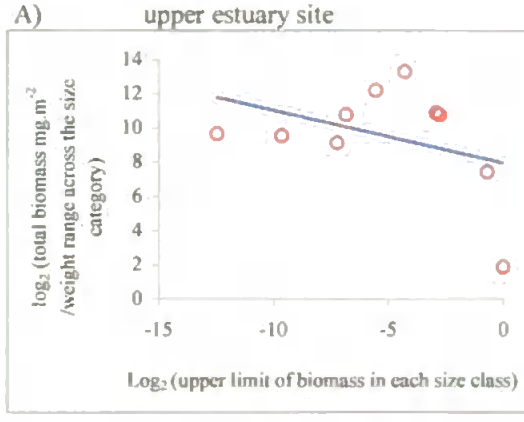

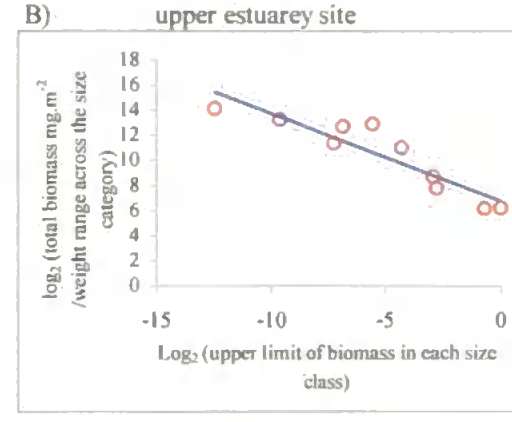

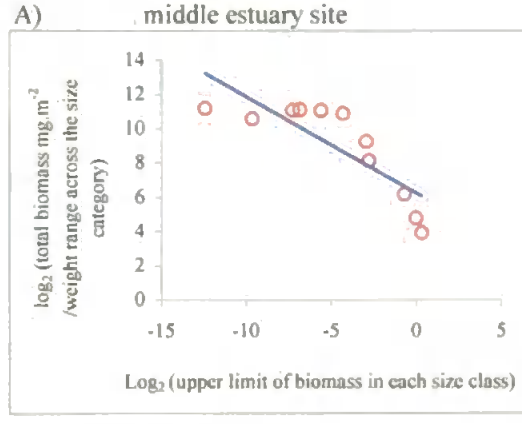

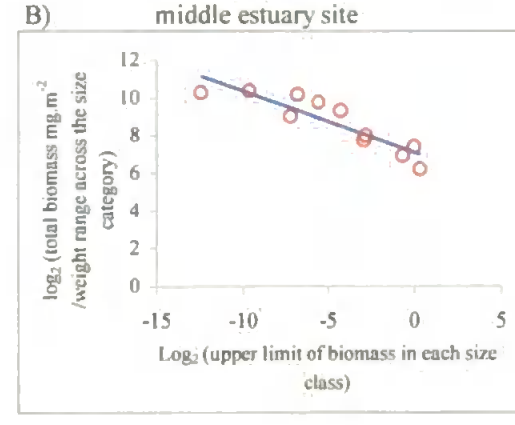

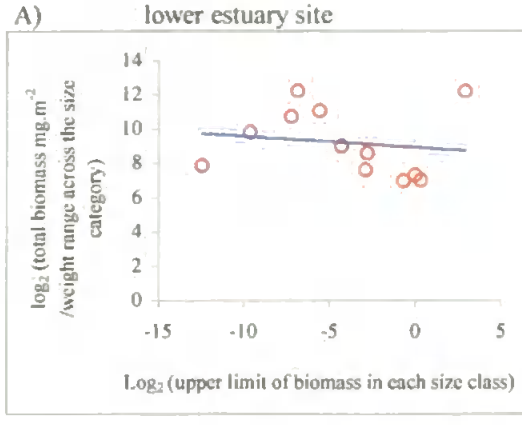

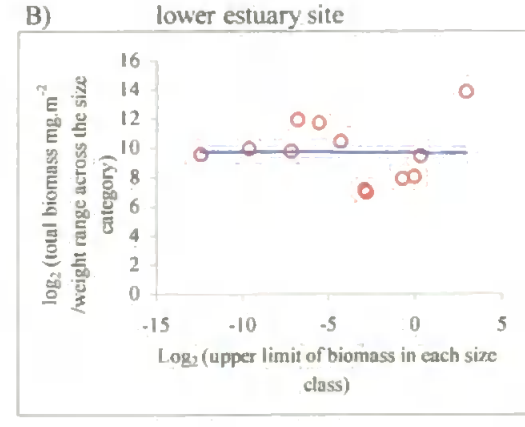

Table 7.4 Slopes, intercepts and R^2 values of the normalized benthic biomass size spectra in Yealm and Fal systems in both autumn and summer.
fw-freshwater site, ue-upper estuary, me-middle estuary, le-lower estuary and ma-marine site. (* denotes not significant). Ch-4, appendix number in Chapter 4

		Fal system (contaminated)				Yealm system (clean)		
	Season	fw	ue	me	le	fw	me	ma
Slope	summer	-0.49	-0.30	-0.56	-0.07	-0.39	-0.58	-0.40
	autumn	-0.15	-0.70	-0.32	-0.01	-0.12	-0.54	-0.42
Intercept	summer	6.55	7.96	6.27	8.92	8.98	10.54	9.39
	autumn	7.16	6.78	7.14	9.69	6.59	10.33	9.62
R^2	summer	0.69	0.14	0.69	0.02	0.68	0.77	0.72
	autumn	0.07	0.84	0.81	0.00	0.08	0.70	0.81
P value	summer	0.0027	0.2750	0.0015	0.6330	0.0009	0.0001	0.0005
	autumn	0.4573	0.0002	0.0001	0.9568	0.3688*	0.0007	0.0001
Appendix No.	summer	7.49	7.51	7.53	7.55	4.3 ch-4	4.7 ch-4	4.11 ch-4
	autumn	7.50	7.52	7.54	7.56	4.4 ch-4	4.8 ch-4	4.12 ch-4

7.5. Discussion

7.5.1 The Fal

The significant differences in the mean ESD values and consequently the mean biomass for the different organismal measures might be explained by three complementary scenarios. The first is that differences in organisms body dimensions (length and width), (which might be an output of the presence of different hosts of species within the different sites), resulted in differences in the ESD values. The second is that contamination might have a significant effect on the organisms body dimensions, for example, amphipods (*Themisto libellula)* in the Greenland Sea experienced exponential relationships between Cd, Pb, Cu and Ni concentrations and their body length, while for Zn no length dependency was noted (Ritterhoff and Zauke, 1997). The later scenario may explain the higher ESD values in the lower estuary site in the Fal, due to the significant presence of amphipods in this site relative to that of the other sites. Unfortunately, species level identification was not possible in the current study, but would allow better understanding of the mechanisms controlling organismal size in benthic communities. The third scenario might be related to the different availability of food among the study sites, resulting in differences in the organism body dimensions, mean ESD or biomass. For example mean individual nematode body weights has been shown to be significantly smaller at an oligotrophic site compared with a site of higher trophic status in the Northeast Atlantic (Vanreusel *et al.*, 1995).

The low abundances at the freshwater site in the Fal may be attributed to two main factors: Low numbers of nematodes, which are an important constituent of the meiofauna. Or the complete absence of polychaetes from the freshwater site compared with other sites in the Fal. Also, the lower abundance detected in autumn may be due to the higher Pb concentrations relative to that of the other sites in the same season.

Food supply may also have a significant influence on benthic densities (DeBovee *et al.*, 1996). Which might explain the low abundances in the freshwater site in the Fal where the

percentage of organic carbon was lowest. This suggests that the variability of abundance size spectra is not simply a function of heavy metal concentration and that factors such as organic carbon may alter the tolerance of the benthos towards heavy metal toxicity.

The higher biomass in the upper estuary site in both seasons (summer and autumn) appears to be due to the responses of different components of the biota. In summer, the biomass increase was mainly due to polychaeta in the size range 180-710 μm, but in autumn, increases in copepods and nematodes in the size range 45-250 μm significantly increased total biomass in this site comparative to the other sites. The higher biomass in the lower estuary site in both seasons, was mainly due to the presence of polychaetes in the 2000 μm size class.

The detected variability of benthic biomass size spectra modes in the Fal across seasons (for example, 250 μm sieve size in upper estuary site had a clear mode of biomass in summer while in autumn, the 45-180 μm size category in the same site had the highest meiofaunal biomass across the system, are in agreement with the findings of other workers (Schwinghamer, 1988; Duplisea and Hargrave, 1996). such variations may be a result of differential responses of the different size classes to heavy metal contamination (i.e. complete absence of certain macrofaunal size classes). This highlights the importance of such sensitive size classes organism as potentially important tools for monitoring programs.

7.5.2 Comparison of the Fal and the Yealm

The clear difference in metal concentrations between the Fal and Yealm was reflected in abundance and biomass spectra. However, the variability in biomass spectra among the contaminated sites support the findings of Schwinghamer (1988) and Duplisea and Hargrave (1996) in that there is no clear correlation between the distance from the contamination source and the biomass size spectra response.

Abundance size spectra in the Fal were generally lower than those of the equivalent sites

in terms of salinity in the Yealm. The high variability of abundance size spectra in the Fal compared with that of Yealm may be due to the fact that macrofaunal size categories were generally lower in the Fal than those in the Yealm (Figure 7.8). This may be due to the high sensitivity of macrofauna to contamination compared with that of meiofauna (Josefson and Widbom (1988), for hypoxia; Somerfield *et al* (1995) for metals and dredging disposal; Duplisea and Hargrave, (1996) for sediment organic enrichment and Schwinghamer (1988) for diesel oil and copper pollution). However, other studies highlighted the importance of meiofauna as a sensitive indicator of pollution (Moore and Bett, 1989).

Despite the fact that, meiofaunal abundance and biomass were similar in the Fal and the Yealm, these parameters did vary within the same site, especially in upper and middle estuary sites. This may be due to seasonal variability in heavy metal concentrations. For example, in upper estuary site in the Fal, Cu concentrations were the highest in autumn while Zn was the highest in summer. Also, in the middle estuary site in the Fal, Cu and Zn concentrations were higher in autumn relative to summer, which was characterised by higher Pb concentration. Hence, meiofauna may respond differently to different types of heavy metals. Alternatively, variability of meiofauna might be a result of hydrodynamic disturbance (Aller and Stupakoff 1996), which may explain the lower meiofaunal abundance in the Yealm freshwater site in autumn.

The significantly lower abundance recorded in all sites of the contaminated system (Fal) compared with the reference system (Yealm), concur with the other studies which investigated the response of the benthos to contamination. For example, Fabrikant (1984) reported that the population density of the clam *Parvilucina tenuisculpta* decreased dramatically when organic nitrogen concentration increased to critical level. Similarly, Grassle *et al* (1980) pointed out a highly significant reduction in macrofaunal and meiofaunal abundances in experimental tanks contaminated with oil compared with controls. The same result was reported by Scullion and Edwards (1980) who reported a

pronounced faunal abundance reduction in the reaches silted by ferric hydroxide or coal in a small river in the South Wales coalfield.

Benthic biomass size spectra, whether absolute or standardized as percentage of total in each size class, were an inverted mirror of the abundance size spectra (Ramsay *et al* 1997). The relative consistency of the shape of meiofaunal biomass spectra may be due to the meiofaunal higher rate of tolerance compared with that of macrofauna (see above). The lowest meiofaunal biomass spectra in freshwater in both the Yealm and the Fal in autumn compared with those of the other sites and seasons may be as a result of lower meiofaunal abundance. While in summer, probably only contamination effects exist resulting in lower biomass in the Fal compared with that of the Yealm in freshwater site.

Seasonal shifts in macrofaunal biomass switch in the middle estuary site in the Fal (Figure 7.9), may resulted from the presence of polychaeta and oligochaeta in the macrofaunal categories in autumn while in summer oligochaeta were relatively low (Figure 7.4) resulting in general decline in the macrofaunal size categories. Whilst in the same site in the Yealm, oligochaeta and polychaeta were consistently present in all macrofaunal categories. This heads to the same suggestion, which is benthos respond differently to the different types and concentrations of heavy metals, where Cu and Zn concentrations were higher in autumn and Pb was higher in summer in the same site.

The inconsistency of the slopes of the normalised biomass size spectra alongside the low values of the correlation coefficient (R^2), both within and among contaminated sites in the current study, indicates that environmental stresses (contamination, in the current chapter and hydrodynamic forces in autumn and winter especially in freshwater and estuarine sites, in chapter 4) may result in the breaking down of the normalised BBSS. This suggests that the normalised size spectra should be used as an early warning of stresses. These findings support those of Sprules and Munawar (1986) who highlighted the importance of normalised size spectra as a stress monitor. Moreover, absolute benthic biomass size spectra or standardised as percentage of total can be used as a sensitive contamination

predictor.

7.6. Conclusion

1) Comparison within the Fal

a) Both mean ESD and mean biomass per sieve were significantly different among the Fal study sites on four different levels: 1) all organisms; 2) different shaped organisms; 3) major taxa; and 4) body dimensions (length and width).

b) There were no significant differences in abundance size spectra among lower, middle and upper estuarine sites but the latter sites were significantly higher than that of freshwater site.

c) Biomass size spectra of upper and lower estuarine sites in Fal were not significantly different, but higher than that of the middle estuary which in turn was significantly higher than that of the freshwater site. No significant difference was detected between the two studied seasons.

2) Comparison between the Yealm and Fal

a) ESD values of the Yealm sites were significantly lower than that of the Fal lower estuary site but higher than those of the other Fal sites.

b) Abundances in all sites of the Fal system were significantly lower than those of the equivalent (in terms of salinity) sites in the Yealm system ($P<0.0001$).

c) Biomass of all Yealm study sites were significantly higher than those of the Fal system except the freshwater site in Yealm in autumn which might be attributed to the hydrodynamic stress in that season.

CHAPTER 8

General Discussion and Conclusion

8. General discussion and conclusion

The main objectives of this thesis were, firstly, to investigate the seasonal variability in benthic size spectra (BSS) across a full salinity gradient (i.e. from freshwater to marine) within the same system. In a second study, size spectra in artificial substrata were assessed in order to investigate the role of sediment grain size on the shape of BSS. Thirdly, the microbial (bacterial) size distribution in freshwater and marine sites of the same system were investigated. Finally, the influence of metal contamination on benthic size spectra patterns was assessed. This chapter reviews the temporal and spatial patterns in metazoan and microbial benthic size spectra and discusses the potential importance of benthic size spectra as a contamination biomonitor. Further, technical developments in benthic size spectra construction are suggested that could save time and effort.

8.1 Variation in benthic size spectra between highly contrasting sites

Despite the high variability between sites in the River Yealm in terms of their salinity and organismal evolutionary history, metazoan and microbial benthic size spectra showed a conservative pattern between sites. There was no tendency to bimodality in biomass size spectra (chapter 4). Although the size range studied for the microbial realm was narrow, the shape of the detected spectra was conservative (chapter 5) with increasing biomass and decreasing abundance with increasing size. Previous studies of metazoan size spectra have shown considerable variability among sites in benthic size spectra. This variability was obvious even between microhabitats in the same site (Table 8.1). This high variability of benthic size spectra among different studies may be due to the differences in the methodologies used. The adoption of a consistent methodology in this thesis should have resulted in a more robust view of inter site variation.

Table 8.1 some examples for the variability in benthic size spectra.

Reference	Site	Benthic size spectra shape
Strayer (1986)	Freshwater	Unimodal
Ramsay *et al.* (1997)	Freshwater	Unimodal
Poff *et al.* (1993)	Freshwater	Bimodal
Ramsay *et al.* (1997)	Upper estuary	Unimodal
Schwinghamer (1981, 1985)	Marine	Trimodal including microbenthos.
Warwick (1984)	Marine	Bimodal for species size distribution.
Duplisea and Drgas (1999)	Marine	Unimodal
Drgas *et al* (1998)	Marine	Unimodal

This consistency of BBSS was extremely interesting considering the differences in the communities sampled. Moreover, fundamental differences in the organismal evolutionary history did not influence the pattern of biomass size distribution. It has been suggested previously that macrobenthic organisms in marine systems have different life histories compared with those in freshwater sites, which might be reflected in size spectra. Marine macrofaunal organisms have a planktonic larval stage corresponding in size to the biomass trough between macrobenthos and meiobenthos (Warwick, 1986). The lack of planktonic larval stages in freshwater, macrofaunal organisms implies that the shape of size spectra here might be very different to those in marine systems (Strayer, 1991). No such differences were found in this study.

It might also be predicted that the emergence of adult insects from freshwater systems might influence the shape of BBSS seasonally, especially in the macrofaunal category, as the larval stages of aquatic insects switch from an aquatic to terrestrial mode of life (Poff *et al.* 1993). However, no such influence was evident in the current study where BBSS were consistent in all the study sites (freshwater, estuary and marine) throughout the year.

Other authors have highlighted the role of sediment grain size as a limiting factor for the shape of benthic biomass size spectra in both freshwater (Poff *et al.* 1993) and marine sites (Schwinghamer, 1981, 1985). This point of view is unlikely to explain the variability of biomass size spectra in this thesis, where biomass spectra in both artificial substrata and the natural substratum in most sites were not significantly different. Additionally, some authors like Poff *et al.* (1993) have found unimodal spectra in some of their study sites, despite the general overall bimodal spectra detected in sites of different grain size. Moreover, Duplisea and Drgas, (1999) reported a unimodal biomass size spectra in the Baltic Sea regardless of differences in the median grain size among their study sites.

According to Schwinghamer (1981, 1985) the three biomass modes in size spectra correspond to micro-, meio- and macrobenthos and their response to the structure of natural sediments. Biomass spectra might therefore be predicted to be different in natural substrata from those in artificial substrata where interstices are of a consistent size. However, the similarities of BBSS in artificial substrata and natural substrata in this thesis (chapter 6) may indicate that sediment grain size has no major effect on the shape of biomass size spectra.

These findings suggest that other factors may influence the biomass spectra shape, for example, different site-specific biomass inputs from microorganisms (bacterial biomass) to the higher trophic levels. BBSS were higher in the marine site than those in the freshwater site in both microbial and metazoan size categories (chapters 4 and 5), which may be linked to the higher organic carbon levels available to marine microbes. This organic carbon will be available to the higher trophic levels through the food chain, resulting in the detected biomass increase in the marine site compared with the freshwater site. This may highlight the more sensitivity of microbial (bacterial) organisms to organic carbon than that of the metazoan organisms (chapters 4 and 5) and that role of microbes as a mediator between organic carbon and the higher trophic levels.

8.2 Are benthic size spectra useful for contamination monitoring?

Many studies have investigated the effects of contamination on benthic organisms, including macrofauna (Warwick, 1986; Warwick *et al.* 1987) and meiofauna (Warwick *et al.* 1988; Somerfield *et al.* 1994; Moore and Bett. 1989). Some of these studies for macrofauna led to the production of an index (ABC index), which was suggested as being possible contamination biomonitor. Other studies (Raffaelli and Mason, 1981; Raffaelli, 1982; Raffaelli, 1987 and Lambshead, 1984) highlighted another index, which used meiofauna and the ratio of Nematode abundance to Copepod abundance (N/C). Despite the importance of such indices in terms of their simplicity, they focus on only one component of the benthic community. The adoption of an approach like abundance or biomass size fractionation may provide a more reliable biomonitoring tool, as it includes all benthic metazoans and, potentially, microorganisms.

Comparison of benthic size spectra between a relatively clean and metal-contaminated system (chapter 7) offered a realistic indication of contamination effects. The observed effects were quantitative, in the form of lower abundance and consequently lower biomass in the contaminated sites, and qualitative in terms of a lack of consistency in the slope of normalised size spectra both within the contaminated (Fal) system sites and between the contaminated (Fal system) sites and the clean (Yealm system) sites. Such quantitative and qualitative effects could be used as indicators of contamination. This study also revealed that macrofauna were more sensitive to metal contamination compared with meiofauna; and there was consistency in meiofaunal biomass between sites. These findings support the conclusion of other workers. For example, Grassle *et al.* (1980), Scullion and Edwards (1980) and Fabrikant (1984) all showed lower overall abundance and biomass in contaminated sites. Moreover, Josefson and Widbom (1988), Somerfield *et al.* (1995), Schwinghamer (1988) and Duplisea and Hargrave (1996) found that macrofauna were more sensitive than meiofauna to contamination. Acquiring such information in a single study using a size spectra approach adds to the credits of this approach as a biomonitor.

Although there is a shortage of studies dealing with benthic size spectra as a biomonitor (but see Schwinghamer (1988) for macro-, meio- and microbenthos, and Duplisea and Hargrave (1996) for meiofauna), this approach seems promising as a contamination biomonitor. This study demonstrated clear responses of benthic size spectra to contamination (chapter 7). The coverage of all benthic components (from microorganisms to macrofauna) in one approach (size spectra) might evaluate the response of each of these components to environmental and contamination stresses on both a temporal and spatial basis. Additionally, as a non-taxonomic approach BBSS have an advantage in that no taxonomic expertise is required, which could save considerable time in training and sample processing. The sensitivity of some size classes in size spectra also allows the identification of size classes of organisms that might be suitable for further research as sensitive components of the benthic community.

8.3 Further technical developments

In the current study, multiple regression analysis was used to derive site-specific mean major taxon biomasses from measured values (chapter 3). These predicted values were found to be the best conversion factors from total abundance to total biomass (chapter 3). Ramsay *et al.* (1997) found that there was no significant difference in the size of organisms between their study sites, which may be due to the relative similarity of these sites to each other in terms of their salinity and geographical location. They used the mean sieve biomass as a conversion factor from total abundance to total biomass. However, in this thesis, more sites with a greater variability, especially in salinity, were included (chapter 2). This might explain the significant differences detected in the site-specific mean sieve biomass, which were in disagreement with Ramsay *et al.* (1997) (chapter 3). However, site-specific mean sieve biomass could be used as a conversion factor in the same season, where the organisms were measured (summer in this thesis) but, if a study is to be performed on a seasonal basis, site-specific mean major taxon biomass should be used as a conversion factor from total abundance to total biomass. This may be due to the seasonal

variation of the community structure in terms of both the major taxa and species make up, which may influence the organismal distribution in the different sieve sizes. Therefore, to develop this technique further, measuring representative organisms from each site in each season to produce site-specific mean major taxon biomasses as conversion factors, may improve biomass size spectra construction. This will, however, make the process of BBSS construction more time consuming.

The possibility of using abundance size spectra instead of biomass size spectra would save time and effort but may be justified considering the similar response of both abundance and biomass, with abundance size spectra a mirror image of biomass size spectra (chapters 4,5,6,7).

The microbiological techniques employed in this thesis (chapter 5) allowed the qualitative and quantitative estimation of bacteria and the estimation of ATP in different size components of the "micro" community. Microorganism cell measurements could be automated by using an automoving stage in an epiflourescent microscope attached to the image analysis unit. This method is currently used to measure the darkness of the stained blood cells, so may increase the accuracy of slide scanning. However, the application of this method would need some caution, so that detrital or non-organismal bodies were not included in calculations.

More research is needed to incorporate other microbial and Protozoan organisms to enhance understanding of their importance in the community.

Macrofaunal and meiofaunal biomass calculation and construction might also be automated by generating an index of the mean major taxon biomass for the different habitats (freshwater, estuary and marine) from different geographical regions on a seasonal basis. These overall mean biomass values could be directly inputted to computer programs e.g. Excel, to speed up the process.

Finally, further research is needed to focus on factors other than sediment grain size that might influence benthic size spectra. Trophic influences might be particularly important.

For example, high predation pressure on a specific size class or size range might result in a biomass trough. Alternatively, differences in primary productivity due to microbenthic algae might also alter the shape of size spectra and bioturbation might also affect certain size components of the benthic community.

8.4 Further research

Within the framework of this thesis, important information has been generated which might be used as a base line for further research in developing this new size fractionation approach to benthic studies. Further work includes:

1. Inclusion of all microbial sized organisms (including algae) in BBSS construction to check for the microbenthic-meiobenthic biomass gap founded in previous studies (Schwinghamer, 1981, 1985).
2. Generating a mean major taxon biomass index, which might automate the process of biomass calculation and construction.
3. BBSS comparison of sites at a range of spatial scales.
4. Testing BBSS (including microbial category) sensitivity to pollutants other than metals (e.g. oil, organic pollution, and eutrophication).
5. Assessing the utility of active microbial size classes for solving environmental problems (i.e. biodegradation of contaminants).

8.5 Conclusion

1. Metazoan size spectra

The shapes of benthic size spectra were remarkably similar between sites of contrasting salinity and in all seasons except in winter. Moreover, sediment grain size has no major influence on the shape of benthic size spectra. Generally, abundance decreased and biomass increased with increasing body size and there was no evidence for modality in spectra.

Accurate estimates of abundance are necessary as abundance size spectra are a mirror image of the biomass size spectra and underpin their shape.

Site-specific mean major taxon biomass was the most reliable conversion factor from total abundance to total biomass. If a seasonal study of biomass size spectra is to be achieved using the same technique, site-specific mean major taxon biomass in one season (when organisms were abundant) would need to be calculated, or representative organisms from each site in each season measured and mean major taxon biomass values used as a conversion factors.

2. Microbial size spectra

Bacterial size spectra might be more sensitive than those for metazoa to organic carbon. This may be indirectly recognised by the possible link of bacterial biomass to metazoan biomass in terms of higher metazoan biomass in sites characterised by higher bacterial biomass. Active microbial size classes (ATP levels) could be used in the activity needed processes like, biodegradation etc.

3. Size spectra as a biomonitor

Benthic biomass and normalised biomass size spectra are useful, sensitive, nontaxonomic and universal tool for comparing community structures as well as contamination biomonitoring. This could be achieved through quantitative and qualitative comparison of both BBSS and normalised size spectra. Inconsistency and reduction of BBSS and the slope of its normalised spectra are a good monitor for contamination.

APPENDICES

Appendix 2.1 Concentration of eleven heavy metals in all sites of the Yealm and Fal systems as μg/g. FW-freshwater, UE-upper estuary, ME-middle estuary, LE-lower estuary and MA-marine sites.

Site	Season	System	Cu μg/g	Pb μg/g	Cd μg/g	Zn μg/g	Cr μg/g	Mn μg/g	Fe μg/g	Ni μg/g	Mg μg/g	Co μg/g	Al μg/g
FW	winter	Yealm	49.437	45.157	1.815	148.662	15.766	406.707	27347.57	116.806	4233.232	16.741	25434.77
UE	winter	Yealm	27.375	43.039	1.435	118.062	12.667	469.528	28688.5	31.732	4229.727	14.405	16149.14
ME	winter	Yealm	49.062	77.852	2.671	157.842	28.167	415.054	31056.72	38.674	11158.55	16.532	30124.36
LE	winter	Yealm	19.43	32.928	2.916	71.335	22.321	292.178	23365.25	34.159	8846.622	13.724	21213.3
MA	winter	Yealm	7.33	28.88	1.114	39.577	6.035	213.79	2149.891	20.099	5634.946	8.703	6758.962
FW	spring	Yealm	24.941	31.132	1.023	108.923	12.842	550.599	23983.5	27.934	3625.141	14.376	16316.64
UE	spring	Yealm	27.435	36.613	0.832	116.936	16.397	341.997	24629.54	30.592	6420.803	14.66	15789.28
ME	spring	Yealm	29.775	50.914	3.239	263.557	20.812	5233.581	53142.27	100.045	5863.477	147.771	21363.48
LE	spring	Yealm	12.465	27.676	2.622	59.309	16.2	236.545	16896.59	27.355	6013.9	11.748	15343.05
MA	spring	Yealm	8.014	24.766	1.714	34.952	9.559	179.202	9932.485	17.162	6834.846	7.241	7920.971
FW	summer	Yealm	24.97	41.894	1.316	118.372	17.81	393.088	24448.42	28.613	4167.982	12.422	13804.34
UE	summer	Yealm	37.942	87.279	1.683	146.82	18.595	346.214	26685.93	28.851	4846.991	15.021	24773.59
ME	summer	Yealm	46.3	69.68	2.137	151.233	26.95	268.962	28163.47	33.553	9166.553	13.329	25627.8
LE	summer	Yealm	9.63	26.834	2.971	77.953	14.754	307.159	17665.04	29.112	7643.133	11.858	11740.22
MA	summer	Yealm	8.886	32.706	3.659	57.721	19.29	373.556	19952.14	31.81	9277.977	13.914	15356.38
FW	autumn	Yealm	25.054	27.812	1.469	119.832	14.641	428.085	27672.88	28.56	5566.347	13.197	13474.53
UE	autumn	Yealm	23.473	29.707	1.391	92.764	19.253	292.222	23439.08	24	6328.57	10.813	10742.74
ME	autumn	Yealm	52.921	72.895	2.474	154.974	26.553	272.842	30484.13	33.158	8967.158	13.5	30041
LE	autumn	Yealm	14.559	38.798	4.419	73.534	21.123	375.153	22435.56	32.489	7804.25	15.887	18324.94
MA	autumn	Yealm	15.923	35.339	2.915	80.82	19.585	348.718	20267.68	29.052	9324.292	11.707	21919.25
FW	autumn	Fal	676.928	493.566	2.079	205.013	10.467	371.573	48375.53	12.892	1790.31	13.041	10583.79
UE	autumn	Fal	2813.552	247.49	5.241	2965.567	28.012	572.631	57150.58	43.733	8203.056	31.407	48195.75
ME	autumn	Fal	1924.695	267.683	4.522	2946.011	22.18	433.079	43570.93	36.026	7191.819	25.178	34982.52
LE	autumn	Fal	559.263	67.446	2.181	941.434	17.311	796.448	40102.34	40.737	8702.113	17.941	16837.05
FW	summer	Fal	1065.131	148.364	5.386	824.731	17.978	554.209	42084.38	23.888	3332.087	16.657	15881.51
UE	summer	Fal	2526.75	243.892	5.118	3491.545	26.722	547.902	50349.28	40.069	9723.73	28.277	30112.88
ME	summer	Fal	1767.277	217.907	4.789	2269.949	27.543	542.28	45373.9	39.607	9182.718	27.172	30635.83
LE	summer	Fal	1485.103	151.449	2.908	1341.035	14.673	935.537	41794.58	24.895	4506.352	19.214	14514.45

Appendix 3.1 Multiple regression analysis for predicting mean Nematode biomass in the three study sites in the Yealm system. fw-freshwater, me-middle estuary and ma-marine sites.

Multiple Regression Analysis

Dependent variable: log(nematode biomass)

Parameter	Estimate	Standard Error	T Statistic	P-Value
CONSTANT	-18.6393	0.332438	-56.0685	0.0000
log(size size)	2.07674	0.0677514	30.6523	0.0000

Analysis of Variance

Source	Sum of Squares	Df	Mean Square	F-Ratio	P-Value
Model	46.5383	1	46.5383	939.56	0.0000
Residual	0.941104	19	0.0495318		
Total (Corr.)	47.4794	20			

R-squared = 98.0179 percent
R-squared (adjusted for d.f.) = 97.9135 percent
Standard Error of Est. = 0.222557
Mean absolute error = 0.181196
Durbin-Watson statistic = 2.34584

The equation of the fitted model is

log(nematod biomass) = -18.6393 + 2.07674*log(size size)

Appendix 3.2 Multiple regression analysis for predicting mean Copepod biomass in the three study sites in the Yealm system. fw-freshwater, me-middle estuary and ma-marine sites.

Multiple Regression Analysis

Dependent variable: log(Copepoda biomass)

Parameter	Estimate	Standard Error	T Statistic	P-Value
CONSTANT	-18.7963	0.614158	-30.605	0.0000
log(sieve size)	2.37779	0.116205	20.462	0.0000
site Yealm="fw"	-0.200455	0.163971	-1.2225	0.2432
site Yealm="me"	0.552123	0.163971	3.3672	0.0051

Analysis of Variance

Source	Sum of Squares	Df	Mean Square	F-Ratio	P-Value
Model	32.1343	3	10.7114	148.32	0.0000
Residual	0.93887	13	0.0722207		
Total (Corr.)	33.0732	16			

R-squared = 97.1612 percent
R-squared (adjusted for d.f.) = 96.5061 percent
Standard Error of Est. = 0.268739
Mean absolute error = 0.198885
Durbin-Watson statistic = 2.44662

The equation of the fitted model is

log(Copepoda biomass) = -18.7963 + 2.37779*log(sieve size) -
0.200455*site Yealm="fw" + 0.552123*site Yealm="me"

Appendix 3.3 Multiple regression analysis for predicting mean Oligochaeta biomass in the three study sites in the Yealm system. fw-freshwater, me-middle estuary and ma-marine sites.

Multiple Regression Analysis

Dependent variable: log(Oligochaeta biomass)

Parameter	Estimate	Standard Error	T Statistic	P-Value
CONSTANT	-14.6687	0.401072	-36.5737	0.0000
log(sieve size)	1.70691	0.0659622	25.877	0.0000
site Yealm="fw"	-0.755792	0.1608	-4.7002	0.0001
site Yealm="me"	0.261367	0.169539	1.54164	0.1374

Analysis of Variance

Source	Sum of Squares	Df	Mean Square	F-Ratio	P-Value
Model	79.9478	3	26.6493	266.07	0.0000
Residual	2.20349	22	0.100159		
Total (Corr.)	82.1513	25			

R-squared = 97.3178 percent
R-squared (adjusted for d.f.) = 96.952 percent
Standard Error of Est. = 0.316479
Mean absolute error = 0.22182
Durbin-Watson statistic = 1.69062

The equation of the fitted model is

log(Oligochaeta biomass) = -14.6687 + 1.70691*log(sieve size) -
0.755792*site Yealm="fw" + 0.261367*site Yealm="me"

Appendix 3.4 Multiple regression analysis for predicting mean Hydracarina biomass in fw-freshwater and ma-marine sites in the Yealm system.

Multiple Regression Analysis

Dependent variable: log(Hydracarina biomass)

Parameter	Estimate	Standard Error	T Statistic	P-Value
CONSTANT	-20.5904	1.29193	-15.9377	0.0001
log(sieve size)	2.62575	0.253947	10.3397	0.0005

Analysis of Variance

Source	Sum of Squares	Df	Mean Square	F-Ratio	P-Value
Model	7.69133	1	7.69133	106.91	0.0005
Residual	0.287768	4	0.0719421		
Total (Corr.)	7.9791	5			

R-squared = 96.3935 percent
R-squared (adjusted for d.f.) = 95.4918 percent
Standard Error of Est. = 0.26822
Mean absolute error = 0.216095
Durbin-Watson statistic = 1.55312

The equation of the fitted model is

log(Hydracarina biomass) = -20.5904 + 2.62575*log(sieve size)

Appendix 3.5 Multiple regression analysis for predicting mean Ostracoda biomass in the three study sites in the Yealm system. fw-freshwater, me-middle estuary and ma-marine sites.

Multiple Regression Analysis

Dependent variable: log(Ostracoda biomass)

Parameter	Estimate	Standard Error	T Statistic	P-Value
CONSTANT	-23.7819	0.955172	-24.898	0.0000
log(sieve size)	3.40813	0.180206	18.9125	0.0000

Analysis of Variance

Source	Sum of Squares	Df	Mean Square	F-Ratio	P-Value
Model	75.0208	1	75.0208	357.68	0.0000
Residual	2.51691	12	0.209742		
Total (Corr.)	77.5377	13			

R-squared = 96.754 percent
R-squared (adjusted for d.f.) = 96.4835 percent
Standard Error of Est. = 0.457976
Mean absolute error = 0.317029
Durbin-Watson statistic = 2.07034

The equation of the fitted model is

log(Ostracoda biomass) = -23.7819 + 3.40813*log(sieve size)

Appendix 3.6 Multiple regression analysis for predicting mean Polychaeta biomass in me-middle estuary and ma-marine sites in the Yealm system.

Multiple Regression Analysis

Dependent variable: log(Polychaete biomass)

Parameter	Estimate	Standard Error	T Statistic	P-Value
CONSTANT	-18.0585	1.12009	-16.1224	0.0000
log(sieve Size)	2.31616	0.182864	12.666	0.0000

Analysis of Variance

Source	Sum of Squares	Df	Mean Square	F-Ratio	P-Value
Model	105.153	1	105.153	160.43	0.0000
Residual	11.7982	18	0.655453		
Total (Corr.)	116.951	19			

R-squared = 89.9119 percent
R-squared (adjusted for d.f.) = 89.3514 percent
Standard Error of Est. = 0.809601
Mean absolute error = 0.448084
Durbin-Watson statistic = 1.85508

The equation of the fitted model is

log(Polychaete biomass) = -18.0585 + 2.31616*log(sieve Size)

Appendix 3.7 Multiple regression analysis for predicting mean Amphipoda biomass in me-middle estuary and ma-marine sites in the Yealm system.

Multiple Regression Analysis

Dependent variable: log(Amphipoda biomass)

Parameter	Estimate	Standard Error	T Statistic	P-Value
CONSTANT	-21.5177	1.84853	-11.6404	0.0001
log(sieve size)	3.02439	0.285575	10.5905	0.0001
site Yealm="me"	1.76719	0.598759	2.95142	0.0318

Analysis of Variance

Source	Sum of Squares	Df	Mean Square	F-Ratio	P-Value
Model	70.5574	2	35.2787	67.45	0.0002
Residual	2.61536	5	0.523072		
Total (Corr.)	73.1728	7			

R-squared = 96.4258 percent
R-squared (adjusted for d.f.) = 94.9961 percent
Standard Error of Est. = 0.723237
Mean absolute error = 0.454904
Durbin-Watson statistic = 1.50282

The equation of the fitted model is

log(Amphipoda biomass) = -21.5177 + 3.02439*log(sieve size) + 1.76719*site Yealm="me"

Appendix 3.8 Multiple regression analysis for predicting mean Tricladida biomass in fw-freshwater site in the Yealm system.

Multiple Regression Analysis

Dependent variable: log(Tricladida biomass)

Parameter	Estimate	Standard Error	T Statistic	P-Value
CONSTANT	-14.9903	3.1147	-4.81275	0.1304
log(sieve size)	1.99601	0.478407	4.1722	0.1498

Analysis of Variance

Source	Sum of Squares	Df	Mean Square	F-Ratio	P-Value
Model	9.64332	1	9.64332	17.41	0.1498
Residual	0.553984	1	0.553984		
Total (Corr.)	10.1973	2			

R-squared = 94.5673 percent
R-squared (adjusted for d.f.) = 89.1347 percent
Standard Error of Est. = 0.744301
Mean absolute error = 0.377719
Durbin-Watson statistic = 2.73837

The equation of the fitted model is

log(Tricladida biomass) = -14.9903 + 1.99601*log(sieve size)

Appendix 3.9 Multiple regression analysis for predicting mean Nemertea biomass in ma-marine site in the Yealm system.

Multiple Regression Analysis

Dependent variable: log(Nemertea biomass)

Parameter	Estimate	Standard Error	T Statistic	P-Value
CONSTANT	-13.6975	1.51348	-9.0503	0.0120
log(sieve size)	1.55893	0.249921	6.23768	0.0248

Analysis of Variance

Source	Sum of Squares	Df	Mean Square	F-Ratio	P-Value
Model	1.46645	1	1.46645	38.91	0.0248
Residual	0.0753791	2	0.0376896		
Total (Corr.)	1.54183	3			

R-squared = 95.1111 percent
R-squared (adjusted for d.f.) = 92.6666 percent
Standard Error of Est. = 0.194138
Mean absolute error = 0.117193
Durbin-Watson statistic = 3.27968

The equation of the fitted model is

log(Nemertea biomass) = -13.6975 + 1.55893*log(sieve size)

Appendix 3.10 Multiple regression analysis for predicting mean Bivalve biomass in fw-freshwater and ma-marine sites in the Yealm system.

Multiple Regression Analysis

Dependent variable: log(Bivalve biomass)

Parameter	Estimate	Standard Error	T Statistic	P-Value
CONSTANT	-22.7654	2.2373	-10.1754	0.0005
log(sieve size)	3.22507	0.325449	9.9096	0.0006

Analysis of Variance

Source	Sum of Squares	Df	Mean Square	F-Ratio	P-Value
Model	23.2772	1	23.2772	98.20	0.0006
Residual	0.948152	4	0.237038		
Total (Corr.)	24.2253	5			

R-squared = 96.086] percent
R-squared (adjusted for d.f.) = 95.1076 percent
Standard Error of Est. = 0.486866
Mean absolute error = 0.318165
Durbin-Watson statistic = 2.23476

The equation of the fitted model is

log(Bivalve biomass) = -22.7654 + 3.22507*log(sieve size)

Appendix 3.11 Multiple regression analysis for predicting mean Coleoptera larvae biomass in fw-freshwater site in the Yealm system.

Multiple Regression Analysis

Dependent variable: log(Coleoptra larvae)

Parameter	Estimate	Standard Error	T Statistic	P-Value
CONSTANT	-16.4393	1.26273	-13.0189	0.0000
log(sieve size)	2.21185	0.213576	10.3563	0.0001

Analysis of Variance

Source	Sum of Squares	Df	Mean Square	F-Ratio	P-Value
Model	16.3601	1	16.3601	107.25	0.0001
Residual	0.762684	5	0.152537		
Total (Corr.)	17.1227	6			

R-squared = 95.5458 percent
R-squared (adjusted for d.f.) = 94.6549 percent
Standard Error of Est. = 0.39056
Mean absolute error = 0.266499
Durbin-Watson statistic = 2.86554

The equation of the fitted model is

log(Coleoptra larvae) = -16.4393 + 2.21185*log(sieve size)

Appendix 3.12 Multiple regression analysis for predicting mean Coleoptera adult biomass in fw-freshwater site in the Yealm system.

Multiple Regression Analysis

Dependent variable: log(Coleoptra adult)

Parameter	Estimate	Standard Error	T Statistic	P-Value
CONSTANT	-5.03067	4.3705	-1.15105	0.4554
log(sieve size)	0.858792	0.621	1.38292	0.3986

Analysis of Variance

Source	Sum of Squares	Df	Mean Square	F-Ratio	P-Value
Model	0.410628	1	0.410628	1.91	0.3986
Residual	0.214712	1	0.214712		
Total (Corr.)	0.625339	2			

R-squared = 65.6648 percent
R-squared (adjusted for d.f.) = 31.3295 percent
Standard Error of Est. = 0.46337
Mean absolute error = 0.247541
Durbin-Watson statistic = 2.92638

The equation of the fitted model is

log(Coleoptra adult) = -5.03067 + 0.858792*log(sieve size)

Appendix 3.13 Multiple regression analysis for predicting mean Cladocera biomass in fw-freshwater site in the Yealm system.

Multiple Regression Analysis

Dependent variable: log(Cladocera biomass)

Parameter	Estimate	Standard Error	T Statistic	P-Value
CONSTANT	-19.7017	1.83241	-10.7518	0.0085
log(sieve size)	2.5169	0.357633	7.03767	0.0196

Analysis of Variance

Source	Sum of Squares	Df	Mean Square	F-Ratio	P-Value
Model	6.58083	1	6.58083	49.53	0.0196
Residual	0.265738	2	0.132869		
Total (Corr.)	6.84657	3			

R-squared = 96.1187 percent
R-squared (adjusted for d.f.) = 94.178 percent
Standard Error of Est. = 0.364512
Mean absolute error = 0.253394
Durbin-Watson statistic = 1.97339

The equation of the fitted model is

log(Cladocera biomass) = -19.7017 + 2.5169*log(sieve size)

Appendix 3.14 Multiple regression analysis for predicting mean Chironomid biomass in fw-freshwater site in the Yealm system.

Multiple Regression Analysis

Dependent variable: log(Chironomid biomass)

Parameter	Estimate	Standard Error	T Statistic	P-Value
CONSTANT	-18.9652	0.683806	-27.7348	0.0000
log(sieve size)	2.45257	0.118419	20.711	0.0000

Analysis of Variance

Source	Sum of Squares	Df	Mean Square	F-Ratio	P-Value
Model	58.7449	1	58.7449	428.94	0.0000
Residual	0.958664	7	0.136952		
Total (Corr.)	59.7035	8			

R-squared = 98.3943 percent
R-squared (adjusted for d.f.) = 98.1649 percent
Standard Error of Est. = 0.37007
Mean absolute error = 0.25294
Durbin-Watson statistic = 0.76469

The equation of the fitted model is

log(Chironomid biomass) = -18.9652 + 2.45257*log(sieve size)

Appendix 3.15 Multiple regression analysis for predicting mean Diptera larvae biomass in fw-freshwater site in the Yealm system.

Multiple Regression Analysis

Dependent variable: log(Diptera larvae biomass)

Parameter	Estimate	Standard Error	T Statistic	P-Value
CONSTANT	-18.1642	3.54405	-5.12526	0.0144
log(sieve size)	2.53619	0.62464	4.06024	0.0269

Analysis of Variance

Source	Sum of Squares	Df	Mean Square	F-Ratio	P-Value
Model	28.1874	1	28.1874	16.49	0.0269
Residual	5.12946	3	1.70982		
Total (Corr.)	33.3168	4			

R-squared = 84.604 percent
R-squared (adjusted for d.f.) = 79.472 percent
Standard Error of Est. = 1.3076
Mean absolute error = 0.900997
Durbin-Watson statistic = 1.39191

The equation of the fitted model is

log(Diptera larvae biomass) = -18.1642 + 2.53619*log(sieve size)

Appendix 3.16 Multiple regression analysis for predicting mean Plecoptera biomass in fw-freshwater site in the Yealm system.

Multiple Regression Analysis

Dependent variable: log(Plecoptera biomass)

Parameter	Estimate	Standard Error	T Statistic	P-Value
CONSTANT	-18.7314	4.1087	-4.55896	0.1375
log(sieve size)	2.23902	0.742205	3.01671	0.2038

Analysis of Variance

Source	Sum of Squares	Df	Mean Square	F-Ratio	P-Value
Model	1.15661	1	1.15661	9.10	0.2038
Residual	0.127092	1	0.127092		
Total (Corr.)	1.2837	2			

R-squared = 90.0996 percent
R-squared (adjusted for d.f.) = 80.1991 percent
Standard Error of Est. = 0.356499
Mean absolute error = 0.194019
Durbin-Watson statistic = 2.99929

The equation of the fitted model is

log(Plecoptera biomass) = -18.7314 + 2.23902*log(sieve size)

Appendix 3.17 Multiple regression analysis for predicting mean Gastropoda biomass in fw-freshwater site in the Yealm system.

Multiple Regression Analysis

Dependent variable: log(Gastropoda biomass)

Parameter	Estimate	Standard Error	T Statistic	P-Value
CONSTANT	-19.5023	1.03719	-18.803	0.0028
log(sieve size)	2.48319	0.160182	15.5023	0.0041

Analysis of Variance

Source	Sum of Squares	Df	Mean Square	F-Ratio	P-Value
Model	27.0283	1	27.0283	240.32	0.0041
Residual	0.224934	2	0.112467		
Total (Corr.)	27.2532	3			

R-squared = 99.1747 percent
R-squared (adjusted for d.f.) = 98.762 percent
Standard Error of Est. = 0.335361
Mean absolute error = 0.233677
Durbin-Watson statistic = 3.26592

The equation of the fitted model is

log(Gastropoda biomass) = -19.5023 + 2.48319*log(sieve size)

Appendix 3.18 Multiple regression analysis for predicting mean Tardigrada biomass in fw-freshwater site in the Yealm system.

Multiple Regression Analysis

Dependent variable: log(Tardigrada biomass)

Parameter	Estimate	Standard Error	T Statistic	P-Value
CONSTANT	-21.2553	4.69368	-4.52849	0.1384
log(sieve size)	2.84178	1.12842	2.51837	0.2406

Analysis of Variance

Source	Sum of Squares	Df	Mean Square	F-Ratio	P-Value
Model	1.94055	1	1.94055	6.34	0.2406
Residual	0.305976	1	0.305976		
Total (Corr.)	2.24653	2			

R-squared = 86.3801 percent
R-squared (adjusted for d.f.) = 72.7601 percent
Standard Error of Est. = 0.553151
Mean absolute error = 0.301055
Durbin-Watson statistic = 2.99943

The equation of the fitted model is

log(Tardigrada biomass) = -21.2553 + 2.84178*log(sieve size)

Appendix 3.19 Multiple regression analysis for predicting mean Collembolla biomass in fw-freshwater site in the Yealm system.

Multiple Regression Analysis

Dependent variable: log(Collembolla biomass)

Parameter	Estimate	Standard Error	T Statistic	P-Value
CONSTANT	-15.0187	2.31154	-6.49726	0.0972
log(sieve size)	1.77507	0.426116	4.16569	0.1500

Analysis of Variance

Source	Sum of Squares	Df	Mean Square	F-Ratio	P-Value
Model	1.77807	1	1.77807	17.35	0.1500
Residual	0.102465	1	0.102465		
Total (Corr.)	1.88054	2			

R-squared = 94.5513 percent
R-squared (adjusted for d.f.) = 89.1026 percent
Standard Error of Est. = 0.320102
Mean absolute error = 0.171197
Durbin-Watson statistic = 2.93071

The equation of the fitted model is

log(Collembolla biomass) = -15.0187 + 1.77507*log(sieve size)

Appendix 3.20 Multiple regression analysis for predicting mean Diptera pupae biomass in fw-freshwater site in the Yealm system.

Multiple Regression Analysis

Dependent variable: log(Diptra pupae biomass)

Parameter	Estimate	Standard Error	T Statistic	P-Value
CONSTANT	-6.75745	2.57037	-2.62898	0.2314
log(sieve size)	0.793305	0.37694	2.10459	0.2824

Analysis of Variance

Source	Sum of Squares	Df	Mean Square	F-Ratio	P-Value
Model	0.653944	1	0.653944	4.43	0.2824
Residual	0.14764	1	0.14764		
Total (Corr.)	0.801584	2			

R-squared = 81.5815 percent
R-squared (adjusted for d.f.) = 63.1629 percent
Standard Error of Est. = 0.38424
Mean absolute error = 0.201129
Durbin-Watson statistic = 2.84949

The equation of the fitted model is

log(Diptra pupae biomass) = -6.75745 + 0.793305*log(sieve size)

Appendix 3.21 ANOVA table for Total (ESD).

Analysis of Variance for log(meanesd) - Type III Sums of Squares

Source	Sum of Squares	Df	Mean Square	F-Ratio	P-Value
MAIN EFFECTS					
A:sieves	2855.84	11	259.622	1293.15	0.0000
B:sites	6.40212	2	3.20106	15.94	0.0000
INTERACTIONS					
AB	59.0535	22	2.68425	13.37	0.0000
RESIDUAL	1209.22	6023	0.200767		
TOTAL (CORRECTED)	5014.9	6058			

All F-ratios are based on the residual mean square error.

Appendix 3.22 ANOVA table for Total (Biomass).

Analysis of Variance for Log(mean biomass) - Type III Sums of Squares

Source	Sum of Squares	Df	Mean Square	F-Ratio	P-Value
MAIN EFFECTS					
A:sieves	23533.2	11	2139.38	1239.10	0.0000
B:sites	70.2532	2	35.1266	20.34	0.0000
INTERACTIONS					
AB	520.401	22	23.6546	13.70	0.0000
RESIDUAL	10236.8	5929	1.72656		
TOTAL (CORRECTED)	41343.0	5964			

All F-ratios are based on the residual mean square error.

Appendix 3.23 ANOVA table for shape (Cyl) (ESD).

Analysis of Variance for log(meanesdCYL) - Type III Sums of Squares

Source	Sum of Squares	Df	Mean Square	F-Ratio	P-Value
MAIN EFFECTS					
A:sieves	2430.0	11	220.909	1219.83	0.0000
B:sites	6.37968	2	3.18984	17.61	0.0000
INTERACTIONS					
AB	59.4176	22	2.7008	14.91	0.0000
RESIDUAL	834.685	4609	0.181099		
TOTAL (CORRECTED)	4204.87	4644			

All F-ratios are based on the residual mean square error.

Appendix 3.24 ANOVA table for shape (Cyl) (Biomass).

Analysis of Variance for log(meanbiomassCYL) - Type III Sums of Squares

Source	Sum of Squares	Df	Mean Square	F-Ratio	P-Value
MAIN EFFECTS					
A:sieves	21870.0	11	1988.18	1219.83	0.0000
B:sites	68.924	2	34.462	21.14	0.0000
INTERACTIONS					
AB	534.758	22	24.3072	14.91	0.0000
RESIDUAL	7512.16	4609	1.62989		
TOTAL (CORRECTED)	37757.9	4644			

All F-ratios are based on the residual mean square error.

Appendix 3.25 ANOVA table for shape (Others) (ESD).

Analysis of Variance for log(esdothers) - Type III Sums of Squares

Source	Sum of Squares	Df	Mean Square	F-Ratio	P-Value
MAIN EFFECTS					
A:sieves	233.976	5	46.7952	501.09	0.0000
B:sites	8.43117	2	4.21558	45.14	0.0000
INTERACTIONS					
AB	2.623	10	0.2623	2.81	0.0019
RESIDUAL	117.574	1259	0.0933872		
TOTAL (CORRECTED)	489.039	1276			

All F-ratios are based on the residual mean square error.

Appendix 3.26 ANOVA table for shape (Others) (Biomass).

Analysis of Variance for log(biomassothers) - Type III Sums of Squares

Source	Sum of Squares	Df	Mean Square	F-Ratio	P-Value
MAIN EFFECTS					
A:sieves	2105.78	5	421.157	501.09	0.0000
B:sites	73.1824	2	36.5912	43.54	0.0000
INTERACTIONS					
AB	23.607	10	2.3607	2.81	0.0019
RESIDUAL	1058.17	1259	0.840485		
TOTAL (CORRECTED)	4411.22	1276			

All F-ratios are based on the residual mean square error.

Appendix 3.27 ANOVA table for Nematode (ESD).

Analysis of Variance for log(nematodesd) - Type III Sums of Squares

Source	Sum of Squares	Df	Mean Square	F-Ratio	P-Value
MAIN EFFECTS					
A:sieves	199.739	5	39.9477	291.95	0.0000
B:sites	0.499438	2	0.249719	1.83	0.1615
INTERACTIONS					
AB	3.89496	10	0.389496	2.85	0.0016
RESIDUAL	301.163	2201	0.13683		
TOTAL (CORRECTED)	635.459	2218			

All F-ratios are based on the residual mean square error.

Appendix 3.28 ANOVA table for Nematode (Biomass).

Analysis of Variance for log(nematodbiomass) - Type III Sums of Squares

Source	Sum of Squares	Df	Mean Square	F-Ratio	P-Value
MAIN EFFECTS					
A:sieves	1797.65	5	359.53	291.95	0.0000
B:sites	1.76663	2	0.883315	0.72	0.4882
INTERACTIONS					
AB	35.0546	10	3.50546	2.85	0.0016
RESIDUAL	2710.46	2201	1.23147		
TOTAL (CORRECTED)	5745.35	2218			

All F-ratios are based on the residual mean square error.

Appendix 3.29 ANOVA table for Copepod (ESD).

Analysis of Variance for log(copepodesd) - Type III Sums of Squares

Source	Sum of Squares	Df	Mean Square	F-Ratio	P-Value
MAIN EFFECTS					
A:sieves	48.3752	4	12.0938	161.59	0.0000
B:sites	8.09979	2	4.0499	54.11	0.0000
INTERACTIONS					
AB	2.61069	8	0.326337	4.36	0.0000
RESIDUAL	75.0648	1003	0.0748403		
TOTAL (CORRECTED)	211.244	1017			

All F-ratios are based on the residual mean square error.

Appendix 3.30 ANOVA table for Copepod (Biomass).

Analysis of Variance for log(copepodbiomass) - Type III Sums of Squares

Source	Sum of Squares	Df	Mean Square	F-Ratio	P-Value
MAIN EFFECTS					
A:sieves	435.376	4	108.844	161.59	0.0000
B:sites	69.4418	2	34.7209	51.55	0.0000
INTERACTIONS					
AB	23.4962	8	2.93703	4.36	0.0000
RESIDUAL	675.583	1003	0.673562		
TOTAL (CORRECTED)	1908.08	1017			

All F-ratios are based on the residual mean square error.

Appendix 3.31 ANOVA table for Oligochaeta (ESD).

Analysis of Variance for log(oligochaetaesd) - Type III Sums of Squares

Source	Sum of Squares	Df	Mean Square	F-Ratio	P-Value
MAIN EFFECTS					
A:sieves	16.3245	4	4.08113	36.19	0.0000
B:sites	7.01744	2	3.50872	31.11	0.0000
INTERACTIONS					
AB	1.94467	8	0.243084	2.16	0.0296
RESIDUAL	55.4844	492	0.112773		
TOTAL (CORRECTED)	157.372	506			

All F-ratios are based on the residual mean square error.

Appendix 3.32 ANOVA table for Oligochaeta (Biomass).

Analysis of Variance for log(oligocaetabiomass) - Type III Sums of Squares

Source	Sum of Squares	Df	Mean Square	F-Ratio	P-Value
MAIN EFFECTS					
A:sieves	146.921	4	36.7302	36.19	0.0000
B:sites	66.691	2	33.3455	32.85	0.0000
INTERACTIONS					
AB	17.502	8	2.18775	2.16	0.0296
RESIDUAL	499.359	492	1.01496		
TOTAL (CORRECTED)	1426.4	506			

All F-ratios are based on the residual mean square error.

Appendix 3.33 ANOVA table for Polychaeta (ESD).

Analysis of Variance for log(polychaeta esd) - Type III Sums of Squares

Source	Sum of Squares	Df	Mean Square	F-Ratio	P-Value
MAIN EFFECTS					
A:sieves	192.175	9	21.3528	188.11	0.0000
B:sites	0.0524366	1	0.0524366	0.46	0.4967
INTERACTIONS					
AB	6.03274	9	0.670304	5.91	0.0000
RESIDUAL	116.008	1022	0.11351		
TOTAL (CORRECTED)	381.169	1041			

All F-ratios are based on the residual mean square error.

Appendix 3.34 ANOVA table for Polychaeta (Biomass).

Analysis of Variance for log(polychaeta biomass) - Type III Sums of Squares

Source	Sum of Squares	Df	Mean Square	F-Ratio	P-Value
MAIN EFFECTS					
A:sieves	1729.58	9	192.175	188.11	0.0000
B:sites	1.30972	1	1.30972	1.28	0.2575
INTERACTIONS					
AB	54.2946	9	6.03274	5.91	0.0000
RESIDUAL	1044.07	1022	1.02159		
TOTAL (CORRECTED)	3443.88	1041			

All F-ratios are based on the residual mean square error.

Appendix 3.35 ANOVA table for Nematode (body length).

Analysis of Variance for nematodelength - Type III Sums of Squares

Source	Sum of Squares	Df	Mean Square	F-Ratio	P-Value
MAIN EFFECTS					
A:sieves	2.39837	5	0.479673	457.08	0.0000
B:sites	0.0425401	2	0.0212701	20.27	0.0000
INTERACTIONS					
AB	0.0484915	10	0.00484915	4.62	0.0000
RESIDUAL	2.30979	2201	0.00104943		
TOTAL (CORRECTED)	7.38228	2218			

All F-ratios are based on the residual mean square error.

Appendix 3.36 ANOVA table for Nematode (body width).

Analysis of Variance for nematodewidth - Type III Sums of Squares

Source	Sum of Squares	Df	Mean Square	F-Ratio	P-Value
MAIN EFFECTS					
A:sieves	0.00121852	5	0.000243704	103.60	0.0000
B:sites	0.000115936	2	0.0000579679	24.64	0.0000
INTERACTIONS					
AB	0.000107722	10	0.0000107722	4.58	0.0000
RESIDUAL	0.00517742	2201	0.0000023523		
TOTAL (CORRECTED)	0.0071031	2218			

All F-ratios are based on the residual mean square error.

Appendix 3.37 ANOVA table for Copepod (body length).

Analysis of Variance for copepodlength - Type III Sums of Squares

Source	Sum of Squares	Df	Mean Square	F-Ratio	P-Value
MAIN EFFECTS					
A:sieves	0.126872	4	0.0317181	457.66	0.0000
B:sites	0.00920052	2	0.00460026	66.38	0.0000
INTERACTIONS					
AB	0.00518555	8	0.000648194	9.35	0.0000
RESIDUAL	0.0695131	1003	0.0000693052		
TOTAL (CORRECTED)	0.310237	1017			

All F-ratios are based on the residual mean square error.

Appendix 3.38 ANOVA table for Copepod (body width).

Analysis of Variance for copepodwidth - Type III Sums of Squares

Source	Sum of Squares	Df	Mean Square	F-Ratio	P-Value
MAIN EFFECTS					
A:sieves	0.012524	4	0.00313099	200.79	0.0000
B:sites	0.00276235	2	0.00138118	88.57	0.0000
INTERACTIONS					
AB	0.00135408	8	0.00016926	10.85	0.0000
RESIDUAL	0.0156403	1003	0.0000155936		
TOTAL (CORRECTED)	0.0522215	1017			

All F-ratios are based on the residual mean square error.

Appendix 3.39 ANOVA table for Oligochaeta (body length).

Analysis of Variance for oligochaeta length - Type III Sums of Squares

Source	Sum of Squares	Df	Mean Square	F-Ratio	P-Value
MAIN EFFECTS					
A:sieves	4.97864	4	1.24466	56.86	0.0000
B:sites	1.10072	2	0.550362	25.14	0.0000
INTERACTIONS					
AB	2.55555	8	0.319444	14.59	0.0000
RESIDUAL	10.769	492	0.0218881		
TOTAL (CORRECTED)	48.3796	506			

All F-ratios are based on the residual mean square error.

Appendix 3.40 ANOVA table for Oligochaeta (body width).

Analysis of Variance for oligochaeta width - Type III Sums of Squares

Source	Sum of Squares	Df	Mean Square	F-Ratio	P-Value
MAIN EFFECTS					
A:sieves	0.00119543	4	0.000298858	7.91	0.0000
B:sites	0.0010745	2	0.000537251	14.22	0.0000
INTERACTIONS					
AB	0.000557849	8	0.0000697311	1.85	0.0665
RESIDUAL	0.0185842	492	0.0000377727		
TOTAL (CORRECTED)	0.0295667	506			

All F-ratios are based on the residual mean square error.

Appendix 3.41 ANOVA table for Polychaeta (body length).

Analysis of Variance for polychaeta length - Type III Sums of Squares

Source	Sum of Squares	Df	Mean Square	F-Ratio	P-Value
MAIN EFFECTS					
A:sieves	90.9515	9	10.1057	157.71	0.0000
B:sites	1.87576	1	1.87576	29.27	0.0000
INTERACTIONS					
AB	6.58893	9	0.732103	11.42	0.0000
RESIDUAL	65.4891	1022	0.0640794		
TOTAL (CORRECTED)	199.988	1041			

All F-ratios are based on the residual mean square error.

Appendix 3.42 ANOVA table for Polychaeta (body width).

Analysis of Variance for polychaeta width - Type III Sums of Squares

Source	Sum of Squares	Df	Mean Square	F-Ratio	P-Value
MAIN EFFECTS					
A:sieves	0.138275	9	0.0153639	39.44	0.0000
B:sites	0.00303712	1	0.00303712	7.80	0.0052
INTERACTIONS					
AB	0.0445371	9	0.00494856	12.70	0.0000
RESIDUAL	0.398161	1022	0.00038959		
TOTAL (CORRECTED)	0.672198	1041			

All F-ratios are based on the residual mean square error.

Appendix 3.43 ANOVA table for testing differences between BBSS constructed from the three conversion factors in the freshwater site in summer.

Analysis of Variance for log(biomass) - Type III Sums of Squares

Source	Sum of Squares	Df	Mean Square	F-Ratio	P-Value
MAIN EFFECTS					
A:sieves	995.266	11	90.4787	144.17	0.0000
B:levels	2.58431	2	1.29216	2.06	0.1314
INTERACTIONS					
AB	5.22179	22	0.237354	0.38	0.9950
RESIDUAL	88.4912	141	0.627597		
TOTAL (CORRECTED)	1091.67	176			

All F-ratios are based on the residual mean square error.

Appendix 3.44 ANOVA table for testing differences between BBSS constructed from the three conversion factors in the middle estuary site in summer.

Analysis of Variance for log(biomass) - Type III Sums of Squares

Source	Sum of Squares	Df	Mean Square	F-Ratio	P-Value
MAIN EFFECTS					
A:sieves	976.972	11	88.8156	384.53	0.0000
B:levels	0.530009	2	0.265004	1.15	0.3208
INTERACTIONS					
AB	1.70297	22	0.0774077	0.34	0.9979
RESIDUAL	33.2598	144	0.230971		
TOTAL (CORRECTED)	1012.46	179			

All F-ratios are based on the residual mean square error.

Appendix 3.45 ANOVA table for testing differences between BBSS constructed from the three conversion factors in the marine site in summer.

Analysis of Variance for log(biomass) - Type III Sums of Squares

Source	Sum of Squares	Df	Mean Square	F-Ratio	P-Value
MAIN EFFECTS					
A:sieves	837.576	11	76.1433	169.58	0.0000
B:levels	1.09567	2	0.547837	1.22	0.2983
INTERACTIONS					
AB	1.93499	22	0.0879539	0.20	1.0000
RESIDUAL	63.3099	141	0.449006		
TOTAL (CORRECTED)	903.897	176			

All F-ratios are based on the residual mean square error.

Appendix 3.46 ANOVA table for testing differences between BBSS constructed from the three conversion factors in the freshwater,middle estuary and marine sites in summer.

Analysis of Variance for log(biomass) - Type III Sums of Squares

Source	Sum of Squares	Df	Mean Square	F-Ratio	P-Value
MAIN EFFECTS					
A:sieves	2650.97	11	240.998	554.76	0.0000
B:sites	367.032	2	183.516	422.44	0.0000
C:levels	3.62591	2	1.81296	4.17	0.0160
INTERACTIONS					
AB	153.971	22	6.99867	16.11	0.0000
AC	2.83966	22	0.129075	0.30	0.9993
BC	0.604006	4	0.151002	0.35	0.8457
ABC	6.0637	44	0.137811	0.32	1.0000
RESIDUAL	185.061	426	0.434415		
TOTAL (CORRECTED)	3354.58	533			

All F-ratios are based on the residual mean square error.

Appendix 3.47 ANOVA table for testing differences between BBSS constructed from mean sieve biomass as a conversion factor in the freshwater,middle estuary and marine sites in summer.

Analysis of Variance for log(biomass) - Type III Sums of Squares

Source	Sum of Squares	Df	Mean Square	F-Ratio	P-Value
MAIN EFFECTS					
A:sieves	914.434	11	83.1304	230.70	0.0000
B:sites	119.191	2	59.5953	165.39	0.0000
INTERACTIONS					
AB	61.4897	22	2.79499	7.76	0.0000
RESIDUAL	51.1686	142	0.360342		
TOTAL (CORRECTED)	1140.89	177			

All F-ratios are based on the residual mean square error.

Appendix 3.48 ANOVA table for testing differences between BBSS constructed from mean shape biomass as a conversion factor in the freshwater,middle estuary and marine sites in summer.

Analysis of Variance for log(biomass) - Type III Sums of Squares

Source	Sum of Squares	Df	Mean Square	F-Ratio	P-Value
MAIN EFFECTS					
A:sieves	901.137	11	81.9216	173.94	0.0000
B:sites	113.43	2	56.7149	120.42	0.0000
INTERACTIONS					
AB	53.3129	22	2.42331	5.15	0.0000
RESIDUAL	66.8768	142	0.470963		
TOTAL (CORRECTED)	1129.17	177			

All F-ratios are based on the residual mean square error.

Appendix 3.49 ANOVA table for testing differences between BBSS constructed from mean major taxon biomass as a conversion factor in the freshwater,middle estuary and marine sites in summer.

Analysis of Variance for log(biomass) - Type III Sums of Squares

Source	Sum of Squares	Df	Mean Square	F-Ratio	P-Value
MAIN EFFECTS					
A:sieves	838.242	11	76.2038	161.47	0.0000
B:sites	135.015	2	67.5077	143.04	0.0000
INTERACTIONS					
AB	45.2318	22	2.05599	4.36	0.0000
RESIDUAL	67.0155	142	0.47194		
TOTAL (CORRECTED)	1080.86	177			

All F-ratios are based on the residual mean square error.

Appendix 3.50 ANOVA table for testing differences between BBSS constructed from the three conversion factors in the marine site in winter.

Analysis of Variance for log(biomass) - Type III Sums of Squares

Source	Sum of Squares	Df	Mean Square	F-Ratio	P-Value
MAIN EFFECTS					
A:sieves	719.164	11	65.3786	206.02	0.0000
B:levels	2.89376	2	1.44688	4.56	0.0124
INTERACTIONS					
AB	4.36305	22	0.19832	0.62	0.8983
RESIDUAL	36.4936	115	0.317335		
TOTAL (CORRECTED)	764.392	150			

All F-ratios are based on the residual mean square error.

Appendix 3.51 ANOVA table for testing differences between BBSS constructed from the three conversion factors in the marine site in spring.

Analysis of Variance for log(biomass) - Type III Sums of Squares

Source	Sum of Squares	Df	Mean Square	F-Ratio	P-Value
MAIN EFFECTS					
A:sieves	645.038	11	58.6398	122.57	0.0000
B:levels	8.54396	2	4.27198	8.93	0.0002
INTERACTIONS					
AB	21.4915	22	0.976885	2.04	0.0068
RESIDUAL	68.8945	144	0.478434		
TOTAL (CORRECTED)	743.968	179			

All F-ratios are based on the residual mean square error.

Appendix 3.52 ANOVA table for testing differences between BBSS constructed from the three conversion factors in the marine site in autumn.

Analysis of Variance for log(biomass) - Type III Sums of Squares

Source	Sum of Squares	Df	Mean Square	F-Ratio	P-Value
MAIN EFFECTS					
A:sieves	807.409	11	73.4008	137.96	0.0000
B:levels	20.4169	2	10.2084	19.19	0.0000
INTERACTIONS					
AB	31.1345	22	1.4152	2.66	0.0003
RESIDUAL	74.4866	140	0.532047		
TOTAL (CORRECTED)	934.769	175			

All F-ratios are based on the residual mean square error.

Appendix 3.53 ANOVA table for testing differences between BBSS constructed from the three conversion factors in the marine site in all seasons.

Analysis of Variance for log(biomass) - Type III Sums of Squares

Source	Sum of Squares	Df	Mean Square	F-Ratio	P-Value
MAIN EFFECTS					
A:sieves	2835.71	11	257.792	572.44	0.0000
B:season	485.357	3	161.786	359.25	0.0000
C:levels	24.6471	2	12.3235	27.36	0.0000
INTERACTIONS					
AB	137.443	33	4.16494	9.25	0.0000
AC	28.8557	22	1.31162	2.91	0.0000
BC	7.14878	6	1.19146	2.65	0.0154
ABC	27.5712	66	0.417746	0.93	0.6386
RESIDUAL	243.185	540	0.450342		
TOTAL (CORRECTED)	4054.95	683			

All F-ratios are based on the residual mean square error.

Appendix 3.54 ANOVA table for testing differences between BBSS constructed from mean sieve biomass as a conversion factor in the marine site in all seasons.

Analysis of Variance for log(biomass) - Type III Sums of Squares

Source	Sum of Squares	Df	Mean Square	F-Ratio	P-Value
MAIN EFFECTS					
A:sieves	1071.19	11	97.3807	273.33	0.0000
B:season	182.616	3	60.872	170.85	0.0000
INTERACTIONS					
AB	53.9269	33	1.63415	4.59	0.0000
RESIDUAL	65.5556	184	0.35628		
TOTAL (CORRECTED)	1445.73	231			

All F-ratios are based on the residual mean square error.

Appendix 3.55 ANOVA table for testing differences between BBSS constructed from mean shape biomass as a conversion factor in the marine site in all seasons.

Analysis of Variance for log(biomass) - Type III Sums of Squares

Source	Sum of Squares	Df	Mean Square	F-Ratio	P-Value
MAIN EFFECTS					
A:sieves	949.475	11	86.3159	184.23	0.0000
B:season	177.8	3	59.2667	126.50	0.0000
INTERACTIONS					
AB	60.4964	33	1.83322	3.91	0.0000
RESIDUAL	84.3325	180	0.468514		
TOTAL (CORRECTED)	1361.98	227			

All F-ratios are based on the residual mean square error.

Appendix 3.56 ANOVA table for testing differences between BBSS constructed from mean major taxon biomass as a conversion factor in the marine site in all seasons.

Analysis of Variance for log(biomass) - Type III Sums of Squares

Source	Sum of Squares	Df	Mean Square	F-Ratio	P-Value
MAIN EFFECTS					
A:sieves	846.69	11	76.9718	145.20	0.0000
B:season	135.188	3	45.0626	85.01	0.0000
INTERACTIONS					
AB	56.673	33	1.71736	3.24	0.0000
RESIDUAL	93.2965	176	0.530094		
TOTAL (CORRECTED)	1222.52	223			

All F-ratios are based on the residual mean square error.

Appendix 4.1 ANOVA table for log (N+1) transformed abundance values for all sites in all seasons in the Yealm system.

Analysis of Variance for log(abundplus1) - Type III Sums of Squares

Source	Sum of Squares	Df	Mean Square	F-Ratio	P-Value
MAIN EFFECTS					
A:sieves	1344.45	11	122.223	51.57	0.0000
B:sites	822.325	4	205.581	86.74	0.0000
C:seasons	3955.98	3	1318.66	556.36	0.0000
INTERACTIONS					
AB	656.846	44	14.9283	6.30	0.0000
AC	1461.26	33	44.2806	18.68	0.0000
BC	635.406	12	52.9505	22.34	0.0000
ABC	979.281	132	7.4188	3.13	0.0000
RESIDUAL	2275.33	960	2.37014		
TOTAL (CORRECTED)	12130.9	1199			

All F-ratios are based on the residual mean square error.

Appendix 4.2 ANOVA table for log (N+1) transformed biomass values for fw-freshwater, me-middle estuary and ma-marine sites in all seasons in the Yealm.

Analysis of Variance for log(biomassplus1) - Type III Sums of Squares

Source	Sum of Squares	Df	Mean Square	F-Ratio	P-Value
MAIN EFFECTS					
A:sieves	2393.8	11	217.618	256.70	0.0000
B:site	431.438	2	215.719	254.46	0.0000
C:seasons	656.64	3	218.88	258.19	0.0000
INTERACTIONS					
AB	101.238	22	4.60173	5.43	0.0000
AC	242.153	33	7.33796	8.66	0.0000
BC	115.213	6	19.2022	22.65	0.0000
ABC	218.748	66	3.31437	3.91	0.0000
RESIDUAL	488.304	576	0.84775		
TOTAL (CORRECTED)	4647.54	719			

All F-ratios are based on the residual mean square error.

Appendix 4.3 Statistics of the normalised biomass size spectra in the fw-freshwater site in the Yealm system in summer.

Regression Analysis - Linear model: Y = a + b*X

Dependent variable: FWy axissummer
Independent variable: FWx axis

Parameter	Estimate	Standard Error	T Statistic	P-Value
Intercept	8.98281	0.560019	16.0402	0.0000
Slope	-0.387742	0.0833369	-4.65271	0.0009

Analysis of Variance

Source	Sum of Squares	Df	Mean Square	F-Ratio	P-Value
Model	47.9822	1	47.9822	21.65	0.0009
Residual	22.165	10	2.2165		
Total (Corr.)	70.1473	11			

Correlation Coefficient = -0.827056
R-squared = 68.4021 percent
Standard Error of Est. = 1.48879

The equation of the fitted model is

FWy axissummer = 8.98281 - 0.387742*FWx axis

Appendix 4.4 Statistics of the normalised biomass size spectra in the fw-freshwater site in the Yealm system in autumn.

Regression Analysis - Linear model: Y = a + b*X

Dependent variable: FWy axisautumn
Independent variable: FWx axis

Parameter	Estimate	Standard Error	T Statistic	P-Value
Intercept	6.58812	0.853846	7.71581	0.0000
Slope	-0.119586	0.127062	-0.941162	0.3688

Analysis of Variance

Source	Sum of Squares	Df	Mean Square	F-Ratio	P-Value
Model	4.56407	1	4.56407	0.89	0.3688
Residual	51.5256	10	5.15256		
Total (Corr.)	56.0897	11			

Correlation Coefficient = -0.285256
R-squared = 8.13709 percent
Standard Error of Est. = 2.26993

The equation of the fitted model is

FWy axisautumn = 6.58812 - 0.119586*FWx axis

Appendix 4.5 Statistics of the normalised biomass size spectra in the fw-freshwater site in the Yealm system in winter.

Regression Analysis - Linear model: Y = a + b*X

Dependent variable: FWy axiswinter
Independent variable: FWx axis

Parameter	Estimate	Standard Error	T Statistic	P-Value
Intercept	6.95716	0.937657	7.41973	0.0000
Slope	0.147117	0.139534	1.05435	0.3165

Analysis of Variance

Source	Sum of Squares	Df	Mean Square	F-Ratio	P-Value
Model	6.9075	1	6.9075	1.11	0.3165
Residual	62.1372	10	6.21372		
Total (Corr.)	69.0447	11			

Correlation Coefficient = 0.316297
R-squared = 10.0044 percent
Standard Error of Est. = 2.49273

The equation of the fitted model is

FWy axiswinter = 6.95716 + 0.147117*FWx axis

Appendix 4.6 Statistics of the normalised biomass size spectra in the fw-freshwater site in the Yealm system in spring.

Regression Analysis - Linear model: Y = a + b*X

Dependent variable: FWy axisspring
Independent variable: FWx axis

Parameter	Estimate	Standard Error	T Statistic	P-Value
Intercept	8.58376	0.251489	34.1317	0.0000
Slope	-0.370695	0.0374243	-9.90518	0.0000

Analysis of Variance

Source	Sum of Squares	Df	Mean Square	F-Ratio	P-Value
Model	43.8558	1	43.8558	98.11	0.0000
Residual	4.46994	10	0.446994		
Total (Corr.)	48.3257	11			

Correlation Coefficient = -0.95263
R-squared = 90.7504 percent
Standard Error of Est. = 0.668576

The equation of the fitted model is

FWy axisspring = 8.58376 - 0.370695*FWx axis

Appendix 4.7 Statistics of the normalised biomass size spectra in the me-middle estuary site in the Yealm system in summer.

Regression Analysis - Linear model: Y = a + b*X

Dependent variable: MEy axissummer
Independent variable: MEx axis

Parameter	Estimate	Standard Error	T Statistic	P-Value
Intercept	10.5493	0.677829	15.5633	0.0000
Slope	-0.576343	0.0969342	-5.94571	0.0001

Analysis of Variance

Source	Sum of Squares	Df	Mean Square	F-Ratio	P-Value
Model	117.445	1	117.445	35.35	0.0001
Residual	33.2222	10	3.32222		
Total (Corr.)	150.668	11			

Correlation Coefficient = -0.882893
R-squared = 77.95 percent
Standard Error of Est. = 1.8227

The equation of the fitted model is

MEy axissummer = 10.5493 - 0.576343*MEx axis

Appendix 4.8 Statistics of the normalised biomass size spectra in the me-middle estuary site in the Yealm system in autumn.

Regression Analysis - Linear model: Y = a + b*X

Dependent variable: MEy axisautumn
Independent variable: MEx axis

Parameter	Estimate	Standard Error	T Statistic	P-Value
Intercept	10.3319	0.782376	13.2058	0.0000
Slope	-0.540391	0.111885	-4.82987	0.0007

Analysis of Variance

Source	Sum of Squares	Df	Mean Square	F-Ratio	P-Value
Model	103.25	1	103.25	23.33	0.0007
Residual	44.2608	10	4.42608		
Total (Corr.)	147.511	11			

Correlation Coefficient = -0.83663
R-squared = 69.9949 percent
Standard Error of Est. = 2.10382

The equation of the fitted model is

MEy axisautumn = 10.3319 - 0.540391*MEx axis

Appendix 4.9 Statistics of the normalised biomass size spectra in the me-middle estuary site in the Yealm system in winter.

Regression Analysis - Linear model: Y = a + b*X

Dependent variable: MEy axiswinter
Independent variable: MEx axis

Parameter	Estimate	Standard Error	T Statistic	P-Value
Intercept	7.43167	0.974436	7.62664	0.0000
Slope	-0.0466903	0.139351	-0.335056	0.7445

Analysis of Variance

Source	Sum of Squares	Df	Mean Square	F-Ratio	P-Value
Model	0.770775	1	0.770775	0.11	0.7445
Residual	68.6584	10	6.86584		
Total (Corr.)	69.4292	11			

Correlation Coefficient = -0.105364
R-squared = 1.11016 percent
Standard Error of Est. = 2.62028

The equation of the fitted model is

MEy axiswinter = 7.43167 - 0.0466903*MEx axis

Appendix 4.10 Statistics of the normalised biomass size spectra in the me-middle estuary site in the Yealm system in spring.

Regression Analysis - Linear model: Y = a + b*X

Dependent variable: MEy axisspring
Independent variable: MEx axis

Parameter	Estimate	Standard Error	T Statistic	P-Value
Intercept	10.5945	0.643347	16.4678	0.0000
Slope	-0.515617	0.092003	-5.60435	0.0002

Analysis of Variance

Source	Sum of Squares	Df	Mean Square	F-Ratio	P-Value
Model	94.0002	1	94.0002	31.41	0.0002
Residual	29.928	10	2.9928		
Total (Corr.)	123.928	11			

Correlation Coefficient = -0.870922
R-squared = 75.8505 percent
Standard Error of Est. = 1.72997

The equation of the fitted model is

MEy axisspring = 10.5945 - 0.515617*MEx axis

Appendix 4.11 Statistics of the normalised biomass size spectra in the ma-marine site in the Yealm system in summer.

Regression Analysis - Linear model: Y = a + b*X

Dependent variable: MAv axissummer
Independent variable: MAx axis

Parameter	Estimate	Standard Error	T Statistic	P-Value
Intercept	9.38703	0.532196	17.6383	0.0000
Slope	-0.398496	0.0789377	-5.04823	0.0005

Analysis of Variance

Source	Sum of Squares	Df	Mean Square	F-Ratio	P-Value
Model	44.969	1	44.969	25.48	0.0005
Residual	17.6456	10	1.76456		
Total (Corr.)	62.6146	11			

Correlation Coefficient = -0.84746
R-squared = 71.8188 percent
Standard Error of Est. = 1.32837

The equation of the fitted model is

MAv axissummer = 9.38703 - 0.398496*MAx axis

Appendix 4.12 Statistics of the normalised biomass size spectra in the ma-marine site in the Yealm system in autumn.

Regression Analysis - Linear model: Y = a + b*X

Dependent variable: MAv axisautumn
Independent variable: MAx axis

Parameter	Estimate	Standard Error	T Statistic	P-Value
Intercept	9.6127	0.435778	22.0587	0.0000
Slope	-0.416179	0.0646366	-6.43875	0.0001

Analysis of Variance

Source	Sum of Squares	Df	Mean Square	F-Ratio	P-Value
Model	49.0485	1	49.0485	41.46	0.0001
Residual	11.831	10	1.1831		
Total (Corr.)	60.8796	11			

Correlation Coefficient = -0.897588
R-squared = 80.5665 percent
Standard Error of Est. = 1.08771

The equation of the fitted model is

MAv axisautumn = 9.6127 - 0.416179*MAx axis

Appendix 4.13 Statistics of the normalised biomass size spectra in the ma-marine site in the Yealm system in winter.

Regression Analysis - Linear model: Y = a + b*X

Dependent variable: MAv axiswinter
Independent variable: MAx axis

Parameter	Estimate	Standard Error	T Statistic	P-Value
Intercept	6.67957	0.477151	13.9988	0.0000
Slope	-0.363908	0.0707733	-5.14188	0.0004

Analysis of Variance

Source	Sum of Squares	Df	Mean Square	F-Ratio	P-Value
Model	37.5015	1	37.5015	26.44	0.0004
Residual	14.1842	10	1.41842		
Total (Corr.)	51.6857	11			

Correlation Coefficient = -0.851803
R-squared = 72.5568 percent
Standard Error of Est. = 1.19097

The equation of the fitted model is

MAv axiswinter = 6.67957 - 0.363908*MAx axis

Appendix 4.14 Statistics of the normalised biomass size spectra in the ma-marine site in the Yealm system in spring.

Regression Analysis - Linear model: Y = a + b*X

Dependent variable: MAv axisspring
Independent variable: MAx axis

Parameter	Estimate	Standard Error	T Statistic	P-Value
Intercept	9.13034	0.497491	18.3528	0.0000
Slope	-0.456789	0.0737901	-6.19039	0.0001

Analysis of Variance

Source	Sum of Squares	Df	Mean Square	F-Ratio	P-Value
Model	59.0879	1	59.0879	38.32	0.0001
Residual	15.4192	10	1.54192		
Total (Corr.)	74.5071	11			

Correlation Coefficient = -0.890534
R-squared = 79.305 percent
Standard Error of Est. = 1.24174

The equation of the fitted model is

MAv axisspring = 9.13034 - 0.456789*MAx axis

Appendix 5.1 ANOVA table for bacterial log transformed abundance in fw-freshwater and ma-marine sites.

Analysis of Variance for log(total abundance) - Type III Sums of Squares

Source	Sum of Squares	Df	Mean Square	F-Ratio	P-Value
MAIN EFFECTS					
A:filtersize	20.3535	2	10.1768	709.18	0.0000
B:sites	0.253874	1	0.253874	17.69	0.0001
INTERACTIONS					
AB	0.354917	2	0.177458	12.37	0.0000
RESIDUAL	0.9471	66	0.01435		
TOTAL (CORRECTED)	21.9094	71			

All F-ratios are based on the residual mean square error.

Appendix 5.2 ANOVA table for bacterial log transformed (ESD) in fw-freshwater and ma-marine sites.

Analysis of Variance for log(esd) - Type III Sums of Squares

Source	Sum of Squares	Df	Mean Square	F-Ratio	P-Value
MAIN EFFECTS					
A:filtersize	443.883	2	221.941	1500.73	0.0000
B:sites	8.81339	1	8.81339	59.59	0.0000
INTERACTIONS					
AB	0.569435	2	0.284717	1.93	0.1464
RESIDUAL	134.727	911	0.147889		
TOTAL (CORRECTED)	645.63	916			

All F-ratios are based on the residual mean square error.

Appendix 5.3 ANOVA table for bacterial log transformed (mean cell biomass) in fw-freshwater and ma-marine sites.

Analysis of Variance for log(mean biomass) - Type III Sums of Squares

Source	Sum of Squares	Df	Mean Square	F-Ratio	P-Value
MAIN EFFECTS					
A:filtersize	3995.56	2	1997.78	1500.57	0.0000
B:sites	79.2612	1	79.2612	59.53	0.0000
INTERACTIONS					
AB	5.14282	2	2.57141	1.93	0.1455
RESIDUAL	1212.85	911	1.33134		
TOTAL (CORRECTED)	5811.73	916			

All F-ratios are based on the residual mean square error.

Appendix 5.4 ANOVA table for bacterial log transformed (total biomass) in fw-freshwater and ma-marine sites.

Analysis of Variance for log(total biomass) - Type III Sums of Squares

Source	Sum of Squares	Df	Mean Square	F-Ratio	P-Value
MAIN EFFECTS					
A:filtersize	314.263	2	157.131	10949.92	0.0000
B:sites	8.5017	1	8.5017	592.45	0.0000
INTERACTIONS					
AB	0.690246	2	0.345123	24.05	0.0000
RESIDUAL	0.9471	66	0.01435		
TOTAL (CORRECTED)	324.402	71			

All F-ratios are based on the residual mean square error.

Appendix 5.5 ANOVA table for microbial log transformed (ATP) in fw-freshwater and ma-marine sites.

Note that the filter size 0.2 μm has been removed from analysis.

Analysis of Variance for log(ATP) - Type III Sums of Squares

Source	Sum of Squares	Df	Mean Square	F-Ratio	P-Value
MAIN EFFECTS					
A:filter	0.0961192	1	0.0961192	2.88	0.1284
B:sites	0.395027	1	0.395027	11.82	0.0089
INTERACTIONS					
AB	0.0016715	1	0.0016715	0.05	0.8287
RESIDUAL	0.267397	8	0.0334246		
TOTAL (CORRECTED)	0.760214	11			

All F-ratios are based on the residual mean square error.

Appendix 5.6 the composition of the artificial minimum sea water
it is 34g per litre of the following composition

Element	% total weight
chloride	47.47
sodium ions	26.28
sulphate	6.602
magnesium ions	3.23
calcium ions	1.013
potassium ions	1.015
bicarbonate	0.491
borate	0.015
strontium ions	0.001
water	13.9

Appendix 6.1 ANOVA table for log transformed (relative abundance) in artificial substrata and natural substrata within the study sites in both systems (Yealm and Fal).

Analysis of Variance for log(abundance) - Type III Sums of Squares

Source	Sum of Squares	Df	Mean Square	F-Ratio	P-Value
MAIN EFFECTS					
A:sieves	739.65	11	67.2409	483.48	0.0000
B:sites	28.6081	11	2.60074	18.70	0.0000
INTERACTIONS					
AB	90.9519	121	0.751669	5.40	0.0000
RESIDUAL	76.7709	552	0.139078		
TOTAL (CORRECTED)	939.706	695			

All F-ratios are based on the residual mean square error.

Appendix 6.2 Multiple range tests for log transformed (relative abundance) in artificial substrata and natural substrata within the study sites in both systems (Yealm and Fal).
le-lower estuary, ue-upper estuary, me-middle estuary, fw-freshwater, y-Yealm system, f_Fal system, A-artificial substrata, C-standard corer.

Multiple Range Tests for log(abundance) by sites

Method: 95.0 percent LSD

sites	Count	LS Mean	Homogeneous Groups
leyA	60	1.20064	X
lefC	60	1.27696	X
uefA	48	1.43068	X
uefC	60	1.54375	XX
meyA	60	1.62652	XX
ueyC	60	1.65908	XX
lefA	60	1.71527	XX
meyC	60	1.71943	XX
ueyA	60	1.73848	XX
leyC	60	1.80569	X
fwyA	48	1.81523	X
fwyC	60	1.84274	X

Appendix 6.3 ANOVA table for log transformed (relative biomass) in artificial substrata and natural substrata within the study sites in both systems (Yealm and Fal).

Analysis of Variance for log(biomass) - Type III Sums of Squares

Source	Sum of Squares	Df	Mean Square	F-Ratio	P-Value
MAIN EFFECTS					
A:sieves	301.251	11	27.3865	76.00	0.0000
B:sites	15.5951	7	2.22787	6.18	0.0000
INTERACTIONS					
AB	192.297	77	2.49736	6.93	0.0000
RESIDUAL	129.725	360	0.360347		
TOTAL (CORRECTED)	641.709	455			

All F-ratios are based on the residual mean square error.

Appendix 6.4 Multiple range tests for log transformed (relative biomass) in artificial substrata and natural substrata within the study sites in both systems (Yealm and Fal).
le-lower estuary, ue-upper estuary, me-middle estuary, fw-freshwater, y-Yealm system, f_Fal system, A-artificial substrata, C-standard corer.

Multiple Range Tests for log(biomass) by sites

Method: 95.0 percent LSD

sites	Count	LS Mean	Homogeneous Groups
uefC	60	1.15801	X
lefC	60	1.44986	X
fwyC	60	1.54209	XX
fwyA	48	1.57275	XX
meyA	60	1.65635	XX
lefA	60	1.69207	X
uefA	48	1.72428	X
meyC	60	1.75386	X

Appendix 7.1 ANOVA table for Total (ESD).

Analysis of Variance for log(meanesd) - Type III Sums of Squares

Source	Sum of Squares	Df	Mean Square	F-Ratio	P-Value
MAIN EFFECTS					
A:sieves	1254.13	11	114.012	527.66	0.0000
B:sites	36.657	3	12.219	56.55	0.0000
RESIDUAL	446.832	2068	0.21607		
TOTAL (CORRECTED)	1772.44	2082			

All F-ratios are based on the residual mean square error.

Appendix 7.2 ANOVA table for Total (Biomass).

Analysis of Variance for log(mean biomass) - Type III Sums of Squares

Source	Sum of Squares	Df	Mean Square	F-Ratio	P-Value
MAIN EFFECTS					
A:sieves	11287.2	11	1026.1	527.66	0.0000
B:sites	367.619	3	122.54	63.01	0.0000
RESIDUAL	4021.49	2068	1.94463		
TOTAL (CORRECTED)	15955.7	2082			

All F-ratios are based on the residual mean square error.

Appendix 7.3 ANOVA table for shape (Cyl) (ESD).

Analysis of Variance for log(mean esd CYL) - Type III Sums of Squares

Source	Sum of Squares	Df	Mean Square	F-Ratio	P-Value
MAIN EFFECTS					
A:sieves	964.556	10	96.4556	447.85	0.0000
B:Sites	30.349	3	10.1163	46.97	0.0000
RESIDUAL	342.23	1589	0.215374		
TOTAL (CORRECTED)	1418.21	1602			

All F-ratios are based on the residual mean square error.

Appendix 7.4 ANOVA table for shape (Cyl) (Biomass).

Analysis of Variance for log(mean biomass CYL) - Type III Sums of Squares

Source	Sum of Squares	Df	Mean Square	F-Ratio	P-Value
MAIN EFFECTS					
A:sieves	8681.0	10	868.1	447.85	0.0000
B:Sites	302.816	3	100.939	52.07	0.0000
RESIDUAL	3080.07	1589	1.93837		
TOTAL (CORRECTED)	12753.4	1602			

All F-ratios are based on the residual mean square error.

Appendix 7.5 ANOVA table for shape (Others) (ESD).

Analysis of Variance for log(mean esd other shapes) - Type III Sums of Squares

Source	Sum of Squares	Df	Mean Square	F-Ratio	P-Value
MAIN EFFECTS					
A:Sieves	210.324	9	23.3694	259.49	0.0000
B:sites	1.9487	3	0.649565	7.21	0.0001
RESIDUAL	42.0579	467	0.0900598		
TOTAL (CORRECTED)	255.648	479			

All F-ratios are based on the residual mean square error.

Appendix 7.6 ANOVA table for shape (Others) (Biomass).

Analysis of Variance for log(mean biomass other shapes) - Type III Sums of Squares

Source	Sum of Squares	Df	Mean Square	F-Ratio	P-Value
MAIN EFFECTS					
A:Sieves	1892.92	9	210.324	259.49	0.0000
B:sites	21.4033	3	7.13443	8.80	0.0000
RESIDUAL	378.522	467	0.810539		
TOTAL (CORRECTED)	2307.97	479			

All F-ratios are based on the residual mean square error.

Appendix 7.7 ANOVA table for Nematode (ESD).

Analysis of Variance for log(Nematode ESD) - Type III Sums of Squares

Source	Sum of Squares	Df	Mean Square	F-Ratio	P-Value
MAIN EFFECTS					
A:sieves	169.117	6	28.1862	225.35	0.0000
B:sites	13.6535	3	4.55116	36.39	0.0000
RESIDUAL	112.07	896	0.125078		
TOTAL (CORRECTED)	284.038	905			

All F-ratios are based on the residual mean square error.

Appendix 7.8 ANOVA table for Nematode (Biomass).

Analysis of Variance for log(Nematode biomass) - Type III Sums of Squares

Source	Sum of Squares	Df	Mean Square	F-Ratio	P-Value
MAIN EFFECTS					
A:sieves	1522.05	6	253.676	225.35	0.0000
B:sites	142.049	3	47.3496	42.06	0.0000
RESIDUAL	1008.63	896	1.1257		
TOTAL (CORRECTED)	2565.98	905			

All F-ratios are based on the residual mean square error.

Appendix 7.9 ANOVA table for Copepod (ESD).

Analysis of Variance for log(Copepod ESD) - Type III Sums of Squares

Source	Sum of Squares	Df	Mean Square	F-Ratio	P-Value
MAIN EFFECTS					
A:sieves	22.2612	4	5.5653	92.57	0.0000
B:sites	0.321285	3	0.107095	1.78	0.1509
RESIDUAL	16.5935	276	0.0601212		
TOTAL (CORRECTED)	40.5882	283			

All F-ratios are based on the residual mean square error.

Appendix 7.10 ANOVA table for Copepod (Biomass).

Analysis of Variance for log(Copepod biomass) - Type III Sums of Squares

Source	Sum of Squares	Df	Mean Square	F-Ratio	P-Value
MAIN EFFECTS					
A:sieves	200.351	4	50.0877	92.57	0.0000
B:sites	4.64278	3	1.54759	2.86	0.0373
RESIDUAL	149.341	276	0.541091		
TOTAL (CORRECTED)	363.294	283			

All F-ratios are based on the residual mean square error.

Appendix 7.11 ANOVA table for Oligochaeta (ESD).

Analysis of Variance for log(Oligochaeta ESD) - Type III Sums of Squares

Source	Sum of Squares	Df	Mean Square	F-Ratio	P-Value
MAIN EFFECTS					
A:sieves	32.6356	7	4.66222	90.18	0.0000
B:sites	0.883087	3	0.294362	5.69	0.0010
RESIDUAL	8.22032	159	0.0517001		
TOTAL (CORRECTED)	51.2502	169			

All F-ratios are based on the residual mean square error.

Appendix 7.12 ANOVA table for Oligochaeta (Biomass).

Analysis of Variance for log(Oligochaeta biomass) - Type III Sums of Squares

Source	Sum of Squares	Df	Mean Square	F-Ratio	P-Value
MAIN EFFECTS					
A:sieves	293.72	7	41.96	90.18	0.0000
B:sites	9.11026	3	3.03675	6.53	0.0003
RESIDUAL	73.9829	159	0.465301		
TOTAL (CORRECTED)	463.833	169			

All F-ratios are based on the residual mean square error.

Appendix 7.13 ANOVA table for Polychaeta (ESD).

Analysis of Variance for log(Polychaeta ESD) - Type III Sums of Squares

Source	Sum of Squares	Df	Mean Square	F-Ratio	P-Value
MAIN EFFECTS					
A:sieves	11.6949	6	1.94916	13.49	0.0000
B:sites	6.24985	2	3.12493	21.63	0.0000
RESIDUAL	51.4238	356	0.144449		
TOTAL (CORRECTED)	91.0517	364			

All F-ratios are based on the residual mean square error.

Appendix 7.14 ANOVA table for Polychaeta (Biomass).

Analysis of Variance for log(Polychaeta biomass) - Type III Sums of Squares

Source	Sum of Squares	Df	Mean Square	F-Ratio	P-Value
MAIN EFFECTS					
A:sieves	105.254	6	17.5424	13.49	0.0000
B:sites	61.0589	2	30.5295	23.48	0.0000
RESIDUAL	462.814	356	1.30004		
TOTAL (CORRECTED)	832.048	364			

All F-ratios are based on the residual mean square error.

Appendix 7.15 ANOVA table for Nematode (body length).

Analysis of Variance for Nematode length - Type III Sums of Squares

Source	Sum of Squares	Df	Mean Square	F-Ratio	P-Value
MAIN EFFECTS					
A:sieves	1.25577	6	0.209295	449.67	0.0000
B:sites	0.0174655	3	0.00582184	12.51	0.0000
RESIDUAL	0.417034	896	0.000465439		
TOTAL (CORRECTED)	1.70993	905			

All F-ratios are based on the residual mean square error.

Appendix 7.16 ANOVA table for Nematode (body width).

Analysis of Variance for Nematode width - Type III Sums of Squares

Source	Sum of Squares	Df	Mean Square	F-Ratio	P-Value
MAIN EFFECTS					
A:sieves	0.00167005	6	0.000278341	128.26	0.0000
B:sites	0.000161571	3	0.0000538571	24.82	0.0000
RESIDUAL	0.00194442	896	0.00000217011		
TOTAL (CORRECTED)	0.00367383	905			

All F-ratios are based on the residual mean square error.

Appendix 7.17 ANOVA table for Copepod (body length).

Analysis of Variance for Copepod body length - Type III Sums of Squares

Source	Sum of Squares	Df	Mean Square	F-Ratio	P-Value
MAIN EFFECTS					
A:sieves	0.030955	4	0.00773875	155.98	0.0000
B:sites	0.00330656	3	0.00110219	22.22	0.0000
RESIDUAL	0.0136932	276	0.0000496129		
TOTAL (CORRECTED)	0.0520362	283			

All F-ratios are based on the residual mean square error.

Appendix 7.18 ANOVA table for Copepod (body width).

Analysis of Variance for Copepod body width - Type III Sums of Squares

Source	Sum of Squares	Df	Mean Square	F-Ratio	P-Value
MAIN EFFECTS					
A:sieves	0.00658267	4	0.00164567	124.35	0.0000
B:sites	0.000154474	3	0.0000514914	3.89	0.0095
RESIDUAL	0.0036526	276	0.000013234		
TOTAL (CORRECTED)	0.011516	283			

All F-ratios are based on the residual mean square error.

Appendix 7.19 ANOVA table for Oligochaeta (body length).

Analysis of Variance for Oligochaeta length - Type III Sums of Squares

Source	Sum of Squares	Df	Mean Square	F-Ratio	P-Value
MAIN EFFECTS					
A:sieves	7.65575	7	1.09368	110.49	0.0000
B:sites	0.00922735	3	0.00307578	0.31	0.8176
RESIDUAL	1.57392	159	0.00989886		
TOTAL (CORRECTED)	10.5768	169			

All F-ratios are based on the residual mean square error.

Appendix 7.20 ANOVA table for Oligochaeta (body width).

Analysis of Variance for Oligochaeta width - Type III Sums of Squares

Source	Sum of Squares	Df	Mean Square	F-Ratio	P-Value
MAIN EFFECTS					
A:sieves	0.00474618	7	0.000678026	47.57	0.0000
B:sites	0.000142465	3	0.0000474882	3.33	0.0211
RESIDUAL	0.0022665	159	0.0000142547		
TOTAL (CORRECTED)	0.00768048	169			

All F-ratios are based on the residual mean square error.

Appendix 7.21 ANOVA table for Polychaeta (body length).

Analysis of Variance for Polychaeta length - Type III Sums of Squares

Source	Sum of Squares	Df	Mean Square	F-Ratio	P-Value
MAIN EFFECTS					
A:sieves	2.88153	6	0.480255	74.08	0.0000
B:sites	0.848981	2	0.424491	65.48	0.0000
RESIDUAL	2.30795	356	0.006483		
TOTAL (CORRECTED)	10.8669	364			

All F-ratios are based on the residual mean square error.

Appendix 7.22 ANOVA table for Polychaeta (body width).

Analysis of Variance for Polychaeta width - Type III Sums of Squares

Source	Sum of Squares	Df	Mean Square	F-Ratio	P-Value
MAIN EFFECTS					
A:sieves	0.00890757	6	0.00148459	20.84	0.0000
B:sites	0.000920028	2	0.000460014	6.46	0.0018
RESIDUAL	0.0253628	356	0.0000712439		
TOTAL (CORRECTED)	0.0449595	364			

All F-ratios are based on the residual mean square error.

Appendix 7.23 Multiple regression analysis for predicting mean Nematode biomass in the four study sites in the Fal system. fw-freshwater, ue-upper estuary, me-middle estuary, le-lower estuary sites.

Multiple Regression Analysis

Dependent variable: log(Nematode biomass)

Parameter	Estimate	Standard Error	T Statistic	P-Value
CONSTANT	-21.1081	1.48787	-14.1868	0.0000
log(sieve size)*(site F	2.83909	0.24984	11.3636	0.0000
log(sieve size)*(site F	1.58425	0.251844	6.29058	0.0000
log(sieve size)*(site F	1.87607	0.197427	9.5026	0.0000
log(sieve size)*(site F	2.75259	0.329124	8.36339	0.0000
site Fal="fw"	-0.967091	1.89578	-0.510128	0.6174
site Fal="ue"	4.75723	1.90784	2.49351	0.0248
site Fal="me"	2.90608	1.77328	1.63882	0.1221

Analysis of Variance

Source	Sum of Squares	Df	Mean Square	F-Ratio	P-Value
Model	43.1255	7	6.16078	47.56	0.0000
Residual	1.94311	15	0.129541		
Total (Corr.)	45.0686	22			

R-squared = 95.6885 percent
R-squared (adjusted for d.f.) = 93.6765 percent
Standard Error of Est. = 0.359918
Mean absolute error = 0.220575
Durbin-Watson statistic = 2.9986

The equation of the fitted model is

log(Nematode biomass) = -21.1081 + 2.83909*log(sieve size)*(site Fal="fw") + 1.58425*log(sieve size)*(site Fal="ue") + 1.87607*log(sieve size)*(site_Fal="me") + 2.75259*log(sieve size)*(site Fal="le") - 0.967091*site_Fal="fw" + 4.75723*site_Fal="ue" + 2.90608*site_Fal="me"

Appendix 7.24 Multiple regression analysis for predicting mean Oligochaeta biomass in the four study sites in the Fal system. fw-freshwater, ue-upper estuary, me-middle estuary sites.

Multiple Regression Analysis

Dependent variable: log(Oligochaeta biomass)

Parameter	Estimate	Standard Error	T Statistic	P-Value
CONSTANT	-17.7691	0.796657	-22.3045	0.0000
log(sieve size)	2.45616	0.149679	16.4094	0.0000
site Fal="fw"	-0.879841	0.322895	-2.72485	0.0184
site Fal="ue"	-1.11799	0.347775	-3.21468	0.0074
site Fal="me"	-1.00442	0.343107	-2.92742	0.0127

Analysis of Variance

Source	Sum of Squares	Df	Mean Square	F-Ratio	P-Value
Model	46.4981	4	11.6245	80.53	0.0000
Residual	1.73229	12	0.144358		
Total (Corr.)	48.2304	16			

R-squared = 96.4083 percent
R-squared (adjusted for d.f.) = 95.2111 percent
Standard Error of Est. = 0.379944
Mean absolute error = 0.253595
Durbin-Watson statistic = 2.23079

The equation of the fitted model is

log(Oligochaeta biomass) = -17.7691 + 2.45616*log(sieve size) - 0.879841*site_Fal="fw" - 1.11799*site_Fal="ue" - 1.00442*site_Fal="me"

Appendix 7.25 Multiple regression analysis for predicting mean Polychaeta biomass in the three study sites in the Fal system. ue-upper estuary, me-middle estuary,le-lower estuary site.

Multiple Regression Analysis

Dependent variable: log(Polychaeta biomass)

Parameter	Estimate	Standard Error	T Statistic	P-Value
CONSTANT	-16.3777	1.50549	-10.8786	0.0000
log(sieve size)*(site F	0.9237	0.23515	3.92814	0.0028
log(sieve size)*(site F	0.971355	0.333477	2.91281	0.0155
log(sieve size)*(site F	2.18574	0.234695	9.31311	0.0000
site Fal="ue"	6.78526	2.07526	3.2696	0.0084
site Fal="me"	7.68671	2.63747	2.91443	0.0154

Analysis of Variance

Source	Sum of Squares	Df	Mean Square	F-Ratio	P-Value
Model	22.2574	5	4.45148	38.82	0.0000
Residual	1.14668	10	0.114668		
Total (Corr.)	23.4041	15			

R-squared = 95.1005 percent
R-squared (adjusted for d.f.) = 92.6507 percent
Standard Error of Est. = 0.338627
Mean absolute error = 0.223519
Durbin-Watson statistic = 2.13866

The equation of the fitted model is

log(Polychaeta biomass) = -16.3777 + 0.9237*log(sieve size)*(site Fal="ue") + 0.971355*log(sieve size)*(site Fal="me") + 2.18574*log(sieve size)*(site_Fal="le") + 6.78526*site Fal="ue" + 7.68671*site Fal="me"

Appendix 7.26 Multiple regression analysis for predicting mean Hydracarina biomass in the three study sites in the Fal system. fw-freshwater, me-middle estuary,le-lower estuary site.

Multiple Regression Analysis

Dependent variable: log(Hydracarina biomass)

Parameter	Estimate	Standard Error	T Statistic	P-Value
CONSTANT	-28.4447	4.04352	-7.03465	0.0009
log(sieve size)	4.28019	0.825655	5.184	0.0035

Analysis of Variance

Source	Sum of Squares	Df	Mean Square	F-Ratio	P-Value
Model	14.7715	1	14.7715	26.87	0.0035
Residual	2.7483	5	0.54966		
Total (Corr.)	17.5198	6			

R-squared = 84.3132 percent
R-squared (adjusted for d.f.) = 81.1758 percent
Standard Error of Est. = 0.741391
Mean absolute error = 0.593525
Durbin-Watson statistic = 1.33267

The equation of the fitted model is

log(Hydracarina biomass) = -28.4447 + 4.28019*log(sieve size)

Appendix 7.27 Multiple regression analysis for predicting mean Tardigrada biomass in the fw-freshwater site in the Fal system.

Multiple Regression Analysis

Dependent variable: log(Tardigrada biomass)

Parameter	Estimate	Standard Error	T Statistic	P-Value
CONSTANT	-16.628	0.650757	-25.5518	0.0249
log(sieve size)	2.00822	0.122428	16.4032	0.0388

Analysis of Variance

Source	Sum of Squares	Df	Mean Square	F-Ratio	P-Value
Model	2.26348	1	2.26348	269.07	0.0388
Residual	0.00841236	1	0.00841236		
Total (Corr.)	2.2719	2			

R-squared = 99.6297 percent
R-squared (adjusted for d.f.) = 99.2594 percent
Standard Error of Est. = 0.0917189
Mean absolute error = 0.0491867
Durbin-Watson statistic = 2.94125

The equation of the fitted model is

log(Tardigrada biomass) = -16.628 + 2.00822*log(sieve size)

Appendix 7.28 Multiple regression analysis for predicting mean Tricladida biomass in fw-freshwater, ue-upper estuary, me-middle estuary ans le-lower estuary sites in the Fal.

Multiple Regression Analysis

Dependent variable: log(Tricladida biomass)

Parameter	Estimate	Standard Error	T Statistic	P-Value
CONSTANT	-15.9928	0.870632	-18.3691	0.0000
log(sieve size)	2.20088	0.16607	13.2528	0.0000

Analysis of Variance

Source	Sum of Squares	Df	Mean Square	F-Ratio	P-Value
Model	48.3943	1	48.3943	175.64	0.0000
Residual	3.85754	14	0.275538		
Total (Corr.)	52.2518	15			

R-squared = 92.6174 percent
R-squared (adjusted for d.f.) = 92.0901 percent
Standard Error of Est. = 0.524917
Mean absolute error = 0.420698
Durbin-Watson statistic = 1.9887

The equation of the fitted model is

log(Tricladida biomass) = -15.9928 + 2.20088*log(sieve size)

Appendix 7.29 Multiple regression analysis for predicting mean Copepoda biomass in fw-freshwater, ue-upper estuary, me-middle estuary ans le-lower estuary sites in the Fal.

Multiple Regression Analysis

Dependent variable: log(Copepod biomass)

Parameter	Estimate	Standard Error	T Statistic	P-Value
CONSTANT	-20.4348	1.32487	-15.424	0.0000
log(sieve size)	2.82021	0.268098	10.5193	0.0000

Analysis of Variance

Source	Sum of Squares	Df	Mean Square	F-Ratio	P-Value
Model	21.6842	1	21.6842	110.66	0.0000
Residual	2.74344	14	0.19596		
Total (Corr.)	24.4277	15			

R-squared = 88.7691 percent
R-squared (adjusted for d.f.) = 87.9669 percent
Standard Error of Est. = 0.442674
Mean absolute error = 0.327647
Durbin-Watson statistic = 1.39016

The equation of the fitted model is

log(Copepod biomass) = -20.4348 + 2.82021*log(sieve size)

Appendix 7.30 Multiple regression analysis for predicting mean Ostracoda biomass in ue-upper estuary, me-middle estuary ans le-lower estuary sites in the Fal.

Multiple Regression Analysis

Dependent variable: log(Ostracoda biomass)

Parameter	Estimate	Standard Error	T Statistic	P-Value
CONSTANT	-17.309	0.822935	-21.0332	0.0000
log(sieve size)	2.37843	0.168385	14.1249	0.0000
site_Fal="ue"	-0.848444	0.166175	-5.10574	0.0009
site_Fal="me"	-0.208538	0.23663	-0.881286	0.4039

Analysis of Variance

Source	Sum of Squares	Df	Mean Square	F-Ratio	P-Value
Model	19.09	3	6.36332	92.18	0.0000
Residual	0.55228	8	0.069035		
Total (Corr.)	19.6422	11			

R-squared = 97.1883 percent
R-squared (adjusted for d.f.) = 96.1339 percent
Standard Error of Est. = 0.262745
Mean absolute error = 0.177223
Durbin-Watson statistic = 2.113

The equation of the fitted model is

log(Ostracoda biomass) = -17.309 + 2.37843*log(sieve size) - 0.848444*site_Fal="ue" - 0.208538*site_Fal="me"

Appendix 7.31 Multiple regression analysis for predicting mean Rotifera biomass in fw-freshwater site in the Fal.

Multiple Regression Analysis

Dependent variable: log(Rotifera biomass)

Parameter	Estimate	Standard Error	T Statistic	P-Value
CONSTANT	-23.8224	1.48408	-16.052	0.0005
log(sieve size)	3.5412	0.31298	11.3145	0.0015

Analysis of Variance

Source	Sum of Squares	Df	Mean Square	F-Ratio	P-Value
Model	25.612	1	25.612	128.02	0.0015
Residual	0.6002	3	0.200067		
Total (Corr.)	26.2122	4			

R-squared = 97.7102 percent
R-squared (adjusted for d.f.) = 96.947 percent
Standard Error of Est. = 0.447288
Mean absolute error = 0.321634
Durbin-Watson statistic = 2.95827

The equation of the fitted model is

log(Rotifera biomass) = -23.8224 + 3.5412*log(sieve size)

Appendix 7.32 Multiple regression analysis for predicting mean Mysides biomass in le-lower estuary site in the Fal.

Multiple Regression Analysis

Dependent variable: log(Mysides biomass)

Parameter	Estimate	Standard Error	T Statistic	P-Value
CONSTANT	-21.7479	2.24695	-9.67886	0.0655
log(sieve size)	3.1273	0.342072	9.14224	0.0694

Analysis of Variance

Source	Sum of Squares	Df	Mean Square	F-Ratio	P-Value
Model	2.34953	1	2.34953	83.58	0.0694
Residual	0.0281109	1	0.0281109		
Total (Corr.)	2.37764	2			

R-squared = 98.8177 percent
R-squared (adjusted for d.f.) = 97.6354 percent
Standard Error of Est. = 0.167663
Mean absolute error = 0.0912622
Durbin-Watson statistic = 2.99991

The equation of the fitted model is

log(Mysides biomass) = -21.7479 + 3.1273*log(sieve size)

Appendix 7.33 Multiple regression analysis for predicting mean Ephemeroptera biomass in fw-freshwater site in the Fal.

Multiple Regression Analysis

Dependent variable: log(Ephemeroptera biomass)

Parameter	Estimate	Standard Error	T Statistic	P-Value
CONSTANT	-19.5411	6.26576	-3.1187	0.1975
log(sieve size)	2.63976	0.95389	2.76736	0.2208

Analysis of Variance

Source	Sum of Squares	Df	Mean Square	F-Ratio	P-Value
Model	1.67405	1	1.67405	7.66	0.2208
Residual	0.218594	1	0.218594		
Total (Corr.)	1.89264	2			

R-squared = 88.4504 percent
R-squared (adjusted for d.f.) = 76.9007 percent
Standard Error of Est. = 0.46754
Mean absolute error = 0.254491
Durbin-Watson statistic = 2.99991

The equation of the fitted model is

log(Ephemeroptera biomass) = -19.5411 + 2.63976*log(sieve size)

Appendix 7.34 Multiple regression analysis for predicting mean Diptera larvae biomass in fw-freshwater site in the Fal.

Multiple Regression Analysis

Dependent variable: log(Diptera larvae biomass)

Parameter	Estimate	Standard Error	T Statistic	P-Value
CONSTANT	-22.9771	5.34465	-4.29907	0.0501
log(sieve size)	3.34006	0.932565	3.58159	0.0699

Analysis of Variance

Source	Sum of Squares	Df	Mean Square	F-Ratio	P-Value
Model	17.5147	1	17.5147	12.83	0.0699
Residual	2.73075	2	1.36537		
Total (Corr.)	20.2455	3			

R-squared = 86.5118 percent
R-squared (adjusted for d.f.) = 79.7677 percent
Standard Error of Est. = 1.16849
Mean absolute error = 0.686458
Durbin-Watson statistic = 3.3026

The equation of the fitted model is

log(Diptera larvae biomass) = -22.9771 + 3.34006*log(sieve size)

Appendix 7.35 Multiple regression analysis for predicting mean Chironomid biomass in fw-freshwater site in the Fal.

Multiple Regression Analysis

Dependent variable: log(chironomid biomass)

Parameter	Estimate	Standard Error	T Statistic	P-Value
CONSTANT	-17.6133	0.25267	-69.7087	0.0000
log(sieve size)	2.31755	0.0463117	50.0424	0.0000

Analysis of Variance

Source	Sum of Squares	Df	Mean Square	F-Ratio	P-Value
Model	14.9017	1	14.9017	2504.24	0.0000
Residual	0.0238024	4	0.0059506		
Total (Corr.)	14.9255	5			

R-squared = 99.8405 percent
R-squared (adjusted for d.f.) = 99.8007 percent
Standard Error of Est. = 0.0771401
Mean absolute error = 0.0443596
Durbin-Watson statistic = 2.79212

The equation of the fitted model is

log(chironomid biomass) = -17.6133 + 2.31755*log(sieve size)

Appendix 7.36 Multiple regression analysis for predicting mean Amphipoda biomass in me-middle estuary and le-lower estuary sites in the Fal.

Multiple Regression Analysis

Dependent variable: log(Amphipoda biomass)

Parameter	Estimate	Standard Error	T Statistic	P-Value
CONSTANT	-6.42452	5.06954	-1.26728	0.2609
log(sieve size)*(site F	3.50819	0.111055	31.5896	0.0000
log(size)*(site F	0.65032	0.838523	0.775554	0.4731
site Fal="me"	-17.5753	5.1222	-3.43121	0.0186

Analysis of Variance

Source	Sum of Squares	Df	Mean Square	F-Ratio	P-Value
Model	44.73	3	14.91	361.56	0.0000
Residual	0.20619	5	0.0412379		
Total (Corr.)	44.9361	8			

R-squared = 99.5411 percent
R-squared (adjusted for d.f.) = 99.2658 percent
Standard Error of Est. = 0.203071
Mean absolute error = 0.118996
Durbin-Watson statistic = 2.49089

The equation of the fitted model is

log(Amphipoda biomass) = -6.42452 + 3.50819*log(sieve size)*(site_Fal="me") + 0.65032*log(sieve size)*(site Fal="le") - 17.5753*site Fal="me"

Appendix 7.37 ANOVA table for comparing benthic abundance size spectra between the Fal study sites regardless of seasons.

Analysis of Variance for log(abundance) - Type III Sums of Squares

Source	Sum of Squares	Df	Mean Square	F-Ratio	P-Value
MAIN EFFECTS					
A:sieves	5690.02	11	517.275	119.34	0.0000
B:sites	194.876	3	64.9587	14.99	0.0000
INTERACTIONS					
AB	317.181	33	9.61154	2.22	0.0002
RESIDUAL	1872.48	432	4.33443		
TOTAL (CORRECTED)	8074.56	479			

All F-ratios are based on the residual mean square error.

Appendix 7.38 Multiple range test for comparing benthic abundance size spectra between the Fal study sites regardless of seasons. Fw-freshwater, le-lower estuary, me-middle estuary, ue-upper estuary sites.

Multiple Range Tests for log(abundance) by sites

Method: 95.0 percent LSD

sites	Count	LS Mean	Homogeneous Groups
fw fal	120	5.92216	X
le fal	120	7.28181	X
me fal	120	7.32431	X
ue fal	120	7.52765	X

Appendix 7.39 ANOVA table for comaring benthic abundance size spectra between the Fal study sites (considering seasons).

Analysis of Variance for log(abundance) - Type III Sums of Squares

Source	Sum of Squares	Df	Mean Square	F-Ratio	P-Value
MAIN EFFECTS					
A:sieves	5690.02	11	517.275	109.62	0.0000
B:sites	194.876	3	64.9587	13.77	0.0000
C:seasons	0.138675	1	0.138675	0.03	0.8640
RESIDUAL	2189.52	464	4.71879		
TOTAL (CORRECTED)	8074.56	479			

All F-ratios are based on the residual mean square error.

Appendix 7.40 ANOVA table for comparing BBSS between the Fal study sites (considering seasons).

Analysis of Variance for log(biomass) - Type III Sums of Squares

Source	Sum of Squares	Df	Mean Square	F-Ratio	P-Value
MAIN EFFECTS					
A:sieves	694.532	11	63.1392	29.62	0.0000
B:sites	79.9681	3	26.656	12.51	0.0000
C:season	0.00086944	1	0.00086944	0.00	0.9839
INTERACTIONS					
AB	247.397	33	7.49689	3.52	0.0000
AC	51.5456	11	4.68596	2.20	0.0138
BC	16.8276	3	5.60921	2.63	0.0497
RESIDUAL	888.863	417	2.13157		
TOTAL (CORRECTED)	1979.13	479			

All F-ratios are based on the residual mean square error.

Appendix 7.41 Multiple range test for comparing BBSS between the Fal study sites (considering seasons). fw-freshwater, ue-upper estuary, me-middle estuary, le-lower estuary sites in the Fal system.

Multiple Range Tests for log(biomass) by sites

Method: 95.0 percent LSD

sites	Count	LS Mean	Homogeneous Groups
fw fal	120	1.77566	X
me fal	120	2.25879	X
ue fal	120	2.64372	X
le fal	120	2.84576	X

Appendix 7.42 ANOVA table for comparing mean ESD between the Fal study sites and those of the Yealm.

Analysis of Variance for log(esd) - Type III Sums of Squares

Source	Sum of Squares	Df	Mean Square	F-Ratio	P-Value
MAIN EFFECTS					
A:sieve	22.6303	11	2.0573	279.03	0.0000
B:site	2.68969	6	0.448281	60.80	0.0000
INTERACTIONS					
AB	17.8196	66	0.269993	36.62	0.0000
RESIDUAL	2.47738	336	0.00737315		
TOTAL (CORRECTED)	45.6169	419			

All F-ratios are based on the residual mean square error.

Appendix 7.43 Multiple range test for comparing mean ESD between the Fal study sites and those of the Yealm. seasons). fw-freshwater, ue-upper estuary, me-middle estuary, le-lower estuary sites.

Multiple Range Tests for log(esd) by site

Method: 95.0 percent LSD

site	Count	LS Mean	Homogeneous Groups
ue fal	60	0.24713	X
fw fal	60	0.302423	X
me fal	60	0.324213	X
fw yealm	60	0.358301	X
ma yealm	60	0.362623	XX
me yealm	60	0.390957	X
le fal	60	0.522921	X

Appendix 7.44 ANOVA table for comparing log transformed abundance in both the Fal and the Yealm study sites in summer and autumn.

Analysis of Variance for log(abundance) - Type III Sums of Squares

Source	Sum of Squares	Df	Mean Square	F-Ratio	P-Value
MAIN EFFECTS					
A:sieves	6017.74	11	547.068	216.27	0.0000
B:sites	2862.09	8	357.761	141.43	0.0000
C:seasons	9.80562	1	9.80562	3.88	0.0490
INTERACTIONS					
AB	1743.08	88	19.8077	7.83	0.0000
AC	99.0405	11	9.00368	3.56	0.0001
BC	290.434	8	36.3043	14.35	0.0000
ABC	446.093	88	5.06924	2.00	0.0000
RESIDUAL	2185.57	864	2.52959		
TOTAL (CORRECTED)	13653.8	1079			

All F-ratios are based on the residual mean square error.

Appendix 7.45 Multiple range test for comparing abundance size spectra in both the Fal and the Yealm study sites. fw-freshwater, ue-upper estuary, me-middle estuary, le-lower estuary, ma-marine sites.

Multiple Range Tests for log(abundance) by sites

Method: 95.0 percent LSD

sites	Count	LS Mean	Homogeneous Groups
fw fal	120	5.92216	X
le fal	120	7.28181	X
me fal	120	7.32431	X
ue fal	120	7.52765	X
fw yealm	120	8.25925	X
le yealm	120	8.96814	X
ma yealm	120	10.0271	X
ue yealm	120	10.1265	X
me yealm	120	11.3546	X

Appendix 7.46: Interaction plot of log abundance with the study sites and seasons in both systems.

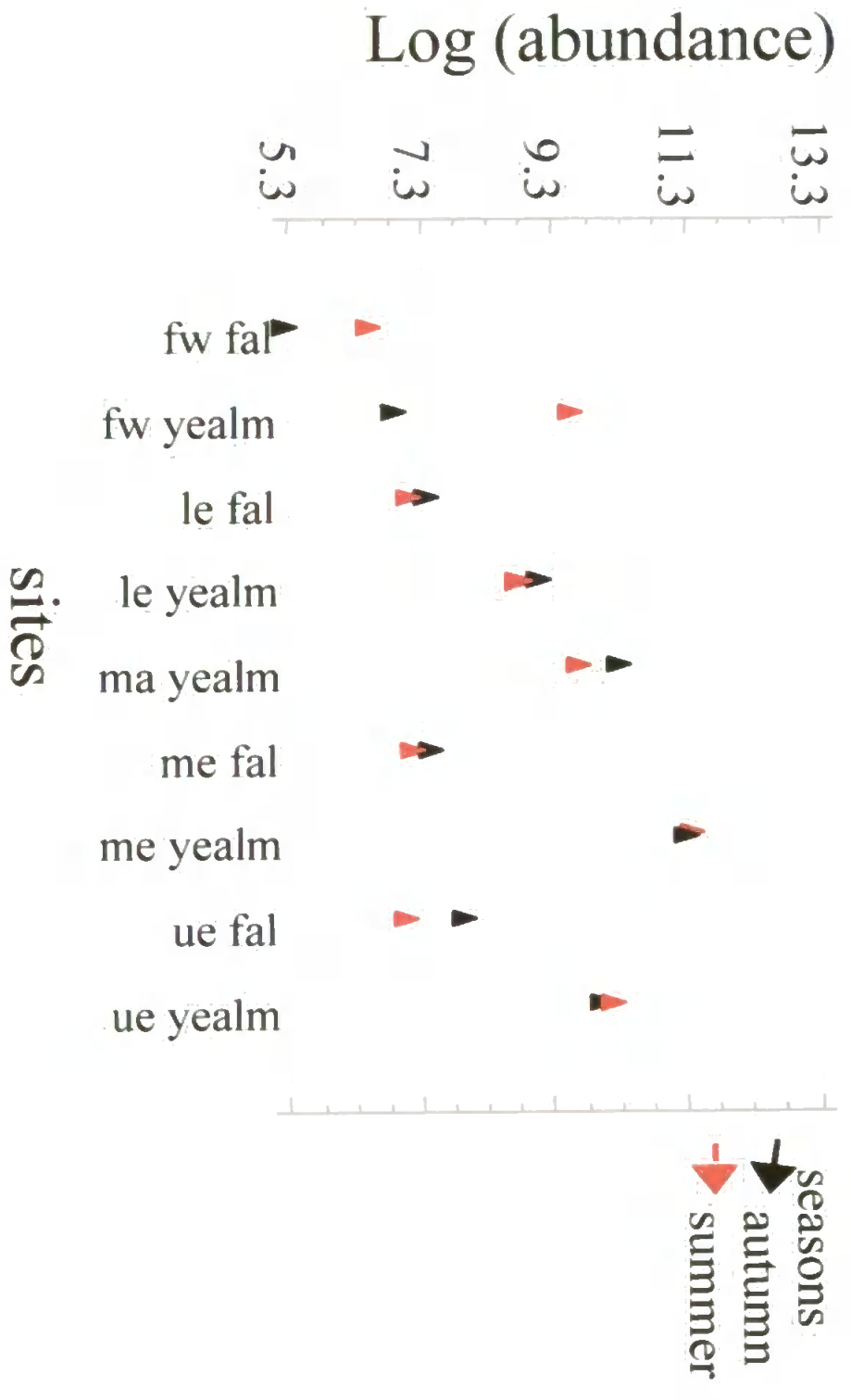

Appendix 7.47 ANOVA table for comparing log transformed BBSS between the study sites of both the Fal and the Yealm system.

Analysis of Variance for log(biomass) - Type III Sums of Squares

Source	Sum of Squares	Df	Mean Square	F-Ratio	P-Value
MAIN EFFECTS					
A:sieves	1306.91	11	118.81	85.41	0.0000
B:sites	1436.11	6	239.351	172.07	0.0000
C:season	15.2449	1	15.2449	10.96	0.0009
INTERACTIONS					
AB	922.897	66	13.9833	10.05	0.0000
AC	36.9377	11	3.35798	2.41	0.0060
BC	96.3056	6	16.0509	11.54	0.0000
ABC	191.302	66	2.89852	2.08	0.0000
RESIDUAL	934.758	672	1.39101		
TOTAL (CORRECTED)	4940.46	839			

All F-ratios are based on the residual mean square error.

Appendix 7.48 Multiple range test for comparing log trsnsformed BBSS between the study sites of both systems. fw-freshwater, ue-upper estuary, me-middle estuary, le-lower estuary, ma-marine sites.

Multiple Range Tests for log(biomass) by sites

Method: 95.0 percent LSD

sites	Count	LS Mean	Homogeneous Groups
fw fal	120	1.77566	X
me fal	120	2.25879	X
ue fal	120	2.64372	X
le fal	120	2.84576	X
fw yealm	120	3.45975	X
ma yealm	120	4.52685	X
me yealm	120	5.82989	X

Appendix 7.49 Normalised BBSS in the freshwater site in summer in the Fal.

Dependent variable: FWy axissummer
Independent variable: FWx axis

Parameter	Estimate	Standard Error	T Statistic	P-Value
Intercept	6.54806	0.744455	8.79578	0.0000
Slope	-0.49563	0.115922	-4.27553	0.0027

Analysis of Variance

Source	Sum of Squares	Df	Mean Square	F-Ratio	P-Value
Model	33.9553	1	33.9553	18.28	0.0027
Residual	14.86	8	1.8575		
Total (Corr.)	48.8153	9			

Correlation Coefficient = -0.834019
R-squared = 69.5588 percent
Standard Error of Est. = 1.3629

The equation of the fitted model is

FWy axissummer = 6.54806 - 0.49563*FWx axis

Appendix 7.50 Normalised BBSS in the freshwater site in autumn in the Fal.

Regression Analysis - Linear model: Y = a + b*X

Dependent variable: FWy axisautumn
Independent variable: FWx axis

Parameter	Estimate	Standard Error	T Statistic	P-Value
Intercept	7.1695	1.27074	5.64199	0.0005
Slope	-0.154525	0.197873	-0.780931	0.4573

Analysis of Variance

Source	Sum of Squares	Df	Mean Square	F-Ratio	P-Value
Model	3.30058	1	3.30058	0.61	0.4573
Residual	43.2967	8	5.41209		
Total (Corr.)	46.5973	9			

Correlation Coefficient = -0.266143
R-squared = 7.08321 percent
Standard Error of Est. = 2.32639

The equation of the fitted model is

FWy axisautumn = 7.1695 - 0.154525*FWx axis

Appendix 7.51 Normalised BBSS in the upper estuary site in summer in the Fal.

Regression Analysis - Linear model: Y = a + b*X

Dependent variable: UEv axissummer
Independent variable: UEx axis

Parameter	Estimate	Standard Error	T Statistic	P-Value
Intercept	7.96639	1.69043	4.71265	0.0015
Slope	-0.308452	0.263224	-1.17182	0.2750

Analysis of Variance

Source	Sum of Squares	Df	Mean Square	F-Ratio	P-Value
Model	13.1513	1	13.1513	1.37	0.2750
Residual	76.6186	8	9.57733		
Total (Corr.)	89.7699	9			

Correlation Coefficient = -0.382753
R-squared = 14.65 percent
Standard Error of Est. = 3.09473

The equation of the fitted model is

UEv axissummer = 7.96639 - 0.308452*UEx axis

Appendix 7.52 Normalised BBSS in the upper estuary site in autumn in the Fal.

Regression Analysis - Linear model: Y = a + b*X

Dependent variable: UEv axisautumn
Independent variable: UEx axis

Parameter	Estimate	Standard Error	T Statistic	P-Value
Intercept	6.78517	0.683228	9.93105	0.0000
Slope	-0.70018	0.106388	-6.58135	0.0002

Analysis of Variance

Source	Sum of Squares	Df	Mean Square	F-Ratio	P-Value
Model	67.7662	1	67.7662	43.31	0.0002
Residual	12.5162	8	1.56453		
Total (Corr.)	80.2824	9			

Correlation Coefficient = -0.918748
R-squared = 84.4098 percent
Standard Error of Est. = 1.25081

The equation of the fitted model is

UEv axisautumn = 6.78517 - 0.70018*UEx axis

Appendix 7.53 Normalised BBSS in the middle estuary site in summer in the Fal.

Regression Analysis - Linear model: Y = a + b*X

Dependent variable: MEv axissummer
Independent variable: MEx axis

Parameter	Estimate	Standard Error	T Statistic	P-Value
Intercept	6.27099	0.766554	8.18076	0.0000
Slope	-0.559929	0.125171	-4.47331	0.0015

Analysis of Variance

Source	Sum of Squares	Df	Mean Square	F-Ratio	P-Value
Model	52.2275	1	52.2275	20.01	0.0015
Residual	23.4901	9	2.61001		
Total (Corr.)	75.7176	10			

Correlation Coefficient = -0.830522
R-squared = 68.9767 percent
Standard Error of Est. = 1.61555

The equation of the fitted model is

MEv axissummer = 6.27099 - 0.559929*MEx axis

Appendix 7.54 Normalised BBSS in the middle estuary site in autumn in the Fal.

Regression Analysis - Linear model: Y = a + b*X

Dependent variable: MEv axisautumn
Independent variable: MEx axis

Parameter	Estimate	Standard Error	T Statistic	P-Value
Intercept	7.14628	0.31677	22.5598	0.0000
Slope	-0.323322	0.0517257	-6.25071	0.0001

Analysis of Variance

Source	Sum of Squares	Df	Mean Square	F-Ratio	P-Value
Model	17.4142	1	17.4142	39.07	0.0001
Residual	4.01133	9	0.445704		
Total (Corr.)	21.4256	10			

Correlation Coefficient = -0.901542
R-squared = 81.2778 percent
Standard Error of Est. = 0.66761

The equation of the fitted model is

MEv axisautumn = 7.14628 - 0.323322*MEx axis

Appendix 7.55 Normalised BBSS in the lower estuary site in summer in the Fal.

Regression Analysis - Linear model: Y = a + b*X

Dependent variable: LEv axissummer
Independent variable: LEx axis

Parameter	Estimate	Standard Error	T Statistic	P-Value
Intercept	8.92079	0.812619	10.9778	0.0000
Slope	-0.0675608	0.137171	-0.492532	0.6330

Analysis of Variance

Source	Sum of Squares	Df	Mean Square	F-Ratio	P-Value
Model	1.00599	1	1.00599	0.24	0.6330
Residual	41.4691	10	4.14691		
Total (Corr.)	42.4751	11			

Correlation Coefficient = -0.153897
R-squared = 2.36842 percent
Standard Error of Est. = 2.0364

The equation of the fitted model is

LEv axissummer = 8.92079 - 0.0675608*LEx axis

Appendix 7.56 Normalised BBSS in the lower estuary site in autumn in the Fal.

Regression Analysis - Linear model: Y = a + b*X

Dependent variable: LEv axisautumn
Independent variable: LEx axis

Parameter	Estimate	Standard Error	T Statistic	P-Value
Intercept	9.69589	0.871234	11.1289	0.0000
Slope	-0.00815912	0.147065	-0.0554798	0.9568

Analysis of Variance

Source	Sum of Squares	Df	Mean Square	F-Ratio	P-Value
Model	0.014672	1	0.014672	0.00	0.9568
Residual	47.6672	10	4.76672		
Total (Corr.)	47.6819	11			

Correlation Coefficient = -0.0175415
R-squared = 0.0307706 percent
Standard Error of Est. = 2.18328

The equation of the fitted model is

LEv axisautumn = 9.69589 - 0.00815912*LEx axis

REFERENCES

Ahn, I.-Y. and Choi, J.-W., 1998, Macrobenthic communities impacted by anthropogenic activities in an intertidal sand flat on the West Coast (Yellow Sea) of Korea.: Marine Pollution Bulletin, 36, 808-817.

Aledort, L. M., Weed, R. I., and Troup, S. B., 1966, Ionic effects on firefly bioluminescence assay of red blood cell ATP.: Analytical Biochemistry, 17, 268-277.

Aller, J. Y. and Stupakoff, I., 1996, The distribution and seasonal characteristics of benthic communities on the Amazon shelf as indicators of physical processes.: Continental Shelf Research, 16, 717-751.

Alongi, D. M., 1993, Extraction of protists in aquatic sediments via density gradient centrifugation, *in* Handbook of methods in aquatic microbial ecology (Kemp, P. F., Sherr, B. F., and Sherr, E. B. and Cole J. J., eds.): London, Lewis publishers, 109-114.

Aston, R. J. and Milner, A. G. P., 1980, A comparison of populations of the isopod *Asellus aquaticus* above and below power stations in organically polluted reaches of the River Trent.: Freshwater Biology, 10, 1-14.

Azam, F. and Holm-Hansen, O., 1973, Use of tritiated substrates in the study of heterotrophy in seawater.: Marine Biology, 23, 191-196.

Azam, F. and Hodson, R. E., 1977, Size distribution and activity of marine microheterotrophs: Limnology and Oceanography, 22, 492-501.

Bachelet, G., 1990, The choice of a sieving mesh size in the quantitative assessment of marine macrobenthos: a necessary compromise between aims and constraints.: Marine environmental Research, 30, 21-35.

Batterton, J. V. and Van Baalen, C., 1968, Phosphorus deficiency and phosphate uptake in the blue-green algae *Anacystis nidulans.*: Canadian Journal of Microbiology, 14, 341-348.

Begon, M., Harper, J. L., and Townsend, C. R., 1996, Interspecific Competition., *in* ECOLOGY individuals, populations and communities. (Blackwell Science Ltd., ed.): Oxford, Blackwell Science, 265-312.

Berman, T., Wynne, D., and Kaplan, B., 1990, Phosphatases revisited - Analysis of particle-associated enzyme-activities in aquatic systems.: Hydrobiologia, 207, 287-294.

Beukema, J. J., Essink, K., Michaelis, H., and Zwarts, L., 1993, Year-to-year variability in the biomass of macrobenthic animals on tidal flats of the Wadden Sea - How predictable is this food source for birds.: Netherlands journal of sea research, 31, 319-330.

Billen, G., Servais, P., and Becquevort, S., 1990, Dynamics of bacteriopplankton in oligotrophic and eutrophic aquatic environments: bottom-up or top-down control?: Hydrobiologia, 207, 37-42.

Blackburn, T. M., Harvey, P. H., and Pagel, M. D., 1990, Species number, population density and body size relationships in natural communities.: Journal of Animal Ecology, 59, 335-345.

Blackburn, T. M., Brown, V. K., Doube, B. M., Greenwood, J. J. D., Lawton, J. H., and Stork, N. E., 1993, The relationship between abundance and body size in natural animal assemblages.: Journal of Animal Ecology, 62, 519-528.

Borgmann, U., 1987, Models of the slope of, and biomass flow up, the biomass size spectrum.: Canadian Journal of Fisheries and Aquatic Sciences, 44, 136-140.

Bourassa, N. and Morin, A., 1995, Relationships between size structure of invertebrate assemblages and trophy and substrate composition in streams.: Journal of the North American Benthological Society, 14, 393-403.

Bowden, W. B., 1977, Comparison of Two Direct-count Techniques for Enumerating aquatic Bacteria.: Applied and Environmental Microbiology, 33, 1229-1232.

Brown, B. E., 1977, Uptake of copper and lead by a metal-tolerant isopod *Asellus meridianus* Rac.: Freshwater Biology, 7, 235-244.

Bryan, G. W. and Gibbs, P. E., 1983, Heavy metals in the Fal Estuary, Cornwall: a study of long-term contamination by mining waste and its effects on estuarine organisms.: Marine Biological Association, UK Occasional Publication, 1-111.

Bryan, G. W. and Langston, W. J., 1992, Bioavailability, accumulation and effects of heavy metals in sediments with special reference to UK estuaries.: Environmental Pollution, 76, 89-131.

Buchanan, J. B., 1984, Sediment analysis., *in* Methods for the study of marine benthos. (Holme, N. A. and McIntyre, A. D., eds.): London, U.K., Blackwell Scientific Publications, 41-65.

Bulleid, N. C., 1978, An improved method for the extraction of adenosine triphosphate from marine sediment and seawater.: Limnology and Oceanography, 23, 174-178.

Burgis, M. J., 1974, Revised estimates for the biomass and production of zooplankton in Lake George, Uganda.: Freshwater Biology, 4, 535-541.

Burns, C. W., 1969, Relation between filtering rate, temperature, and body size in four species of *Daphnia*.: Limnology and Oceanography, 14, 693-700.

Cattaneo, A., 1993, Size spectra of benthic communities in Laurentian streams.: Canadian Journal of Fisheries and Aquatic Sciences, 50, 2659-2666.

Chrzanowski, T. H. and Simek, K., 1990, Prey-size selection by freshwater flagellated protozoa.: Limnology and Oceanography, 35, 1429-1436.

Cole, J. J., Findlay, S., and Pace, M. L., 1988, Bacterial production in fresh and saltwater ecosystems: a cross-system overview.: Marine Ecology Progress Series, 43, 1-10.

Cole, J. J., Pace, M. L., Caraco, N. F., and Steinhart, G. S., 1993, Bacterial biomass and cell size distribution in lakes: More and larger cells in anoxic waters: Limnology and Oceanography, 38, 1627-1632.

Cotgreave, P., 1993, The relationship between body size and population abundance in animals.: Trends in Ecology and Evolution, 8, 244-248.

Cyr, H. and Peters, R. H., 1996, Biomass-size spectra and the prediction of fish biomass in lakes.: Canadian Journal of Fisheries and Aquatic Sciences, 53, 994-1006.

Damuth, J., 1981, Population density and body size in mammals.: Nature, 290, 699-700.

Damuth, J., 1987, Interspecific allometry of population density in mammals and other animals: the independence of body mass and population energy use.: Biological Journal of the Linnaean Society, 31, 193-246.

Damuth, J., 1991, Of size and abundance.: Nature, 351, 268-269.

Danovaro, R., Marrale, D., DellaCroce, N., DellAnno, A., and Fabiano, M., 1998, Heterotrophic nanoflagellates, bacteria, and labile organic compounds in continental shelf and deep-sea sediments of the Eastern Mediterranean.: Microbial Ecology, 35, 244-255.

DeBovee, F., Hall, P. O. J., Hulth, S., Hulthe, G., Landen, A., and Tengberg, A., 1996, Quantitative distribution of metazoan meiofauna in continental margin sediments of the Skagerrak (northeastern North Sea).: Journal of Sea Research, 35, 189-197.

delGiorgio, P. A. and Scarborough, G., 1995, Increase in the proportion of metabolically active bacteria along gradients of enrichment in fresh-water and marine plankton - implications for estimates of bacterial-growth and production-rates.: Journal of Plankton Research, 17, 1905-1924.

Dickie, L. M., Kerr, S. R., and Boudreau, P. R., 1987, Size-dependent processes underlying regularities in ecosystem structure.: Ecological monographs, 57, 233-250.

Doetsch, R. N. and Cook, T. M., 1973, Some General Structural Features of Bacteria., *in* Introduction to Bacteria and Their Ecobiology. (Doetsch, R. N. and Cook, T. M., eds.): Lancaster, England, Medical and Technical Publishing CO. LTD., 15-85.

Drake, L. A., Choi, K. H., Haskell, A. G. E., and Dobbs, F. C., 1998, Vertical profiles of virus-like particles and bacteria in the water column and sediments of Chesapeake Bay, USA.: Aquatic Microbial Ecology, 16, 17-25.

Drgas, A., Radziejewska, T., and Warzocha, J., 1998, Biomass size spectra of near-shore shallow-water benthic communities in the Gulf of Gdansk (Southern Baltic Sea): Marine Ecology, 19, 209-228.

Dugan, J. E., Hubbard, D. M., and Page, H. M., 1995, scaling population density to body size: Tests in two soft - sediment intertidal communities.: Journal of Coastal Research, 11, 849-857.

Dumont, H. J., DeVelde, I. V., and Dumont, S., 1975, The dry weight estimate of biomass in a selection of Cladocera, Copepoda and Rotifera from the plankton, periphyton and benthos of continental waters.: Oecologia, 19, 75-97.

Duplisea, D. E. and Hargrave, B. T., 1996, Response of meiobenthic size-structure, biomass and respiration to sediment organic enrichment.: Hydrobiologia, 339, 161-170.

Duplisea, D. E., 1998, Patterns of benthic organism biomass size-spectra in different basins of the Baltic sea and in relation to the sediment environment., *in* Structuring of Benthic Communities, with a Focus on Size-Spectra (Duplisea, D. E., ed.): Stockholm, Stockholm University, 1-28.

Duplisea, D. E. and Drgas, A., 1999, Sensitivity of a benthic, metazoan, biomass size spectrum to differences in sediment granulometry.: Marine Ecology Progress Series, 177, 73-81.

Echevarria, F., Carrillo, P., Jimenez, F., Sanchez-Castillo, P., Cruz-Pizarro, L., and Rodriguez, J., 1990, The size-abundance distribution and taxonomic composition of plankton in an oligotrophic, high mountain lake (La Caldera, Sierra Nevada, Spain).: Journal of Plankton Research, 12, 415-422.

Echevarria, F. and Rodriguez, J., 1994, The size structure of plankton during a deep bloom in a stratified reservoir.: Hydrobiologia, 284, 113-124.

Edgar, G. J., 1990, The use of the size structure of benthic macrofaunal communities to estimate faunal biomass and secondary production.: Journal of experimental marine biology and ecology, 137, 195-214.

Edgar, G. J., 1990, The influence of plant structure on the species richness, biomass and secondary production of macrofaunal assemblages associated with Western Australian seagrass beds.: Journal of experimental marine biology and ecology, 137, 215-240.

Elliott, J. M., 1977, Some methods for the statistical analysis of samples of benthic invertebrates.: Freshwater Biological Association Scientific Publication., 9-153.

Fabrikant, R., 1984, The effect of sewage effluent on the population density and size of the clam *Parvilucina tenuisculpta*.: Marine Pollution Bulletin, 15, 249-253.

Ferguson, R. L. and Rublee, P., 1976, Contribution of bacteria to the standing crop of coastal plankton.: Limnology and Oceanography, 21, 141-145.

Garcia, C. M., Echevarria, F., and Niell, F. X., 1995, Size structure of plankton in a temporary, saline inland lake.: Journal of Plankton Research, 17, 1803-1817.

Gasol, J. M., 1991, Seasonal variations in size structure and procaryotic dominance in sulfurous Lake Ciso.: Limnology and Oceanography, 36, 860-872.

Gasol, J. M., delGiorgio, P. A., Massana, R., and Duarte, C. M., 1995, Active versus inactive bacteria: size-dependence in a coastal marine plankton community.: Marine Ecology Progress Series, 128, 91-97.

Gee, J. M. and Warwick, R. M., 1996, A study of global biodiversity patterns in the marine motile fauna of hard substrata: Journal of marine biological Association UK, 76, 177-184.

Giere, O., 1993, The Distribution of Meiofauna., *in* Meiobenthology (Giere, O., ed.): Berlin Heidelberg, Springer-Verlag, 185-196.

Gilmour, C. C. and Henry, E. A., 1991, Mercury methylation in aquatic systems affected by acid deposition.: Environmental Pollution, 71, 131-169.

Goulder, R., 1991, Metabolic-activity of fresh-water bacteria.: Science progress, 75, 73-91.

Gower, A. M., Myers, G., Kent, M., and Foulkes, M. E., 1994, Relationships between macroinvertebrate communities and environmental variables in metal-contaminated streams in south-west England.: Freshwater Biology, 32, 199-221.

Grassle, J. F., Elmgren, R., and Grassle, J. P., 1980, Response of benthic communities in MERL experimental ecosystems to low level, chronic additions of No. 2 fuel oil.: Marine environmental Research, 4, 279-297.

Griffiths, D., 1992, Size, abundance, and energy use in communities.: Journal of Animal Ecology, 61, 307-315.

Hanson, J. M., Prepas, E. E., and Mackay, W. C., 1989, Size distribution of the macroinvertebrate community in a freshwater Lake.: Canadian Journal of Fisheries and Aquatic Sciences, 46, 1510-1519.

Hanson, J. M., 1990, Macroinvertebrate size-distributions of two contrasting freshwater macrophyte communities.: Freshwater Biology, 24, 481-491.

Havens, K. E., 1998, Size structure and energetics in a plankton food web.: Oikos, 81, 346-358.

Heldal, M., Norland, S., and Tumyr, O., 1985, X-ray microanalysis method for measurement of dry matter and elemental content of individual bacteria.: Applied and Environmental Microbiology, 50, 1251-1257.

Hendricks, A., Henley, D., Wyatt, J. T., Dickson, K. L., and Silvey, J. K. G., 1974, Utilization of diversity indices in evaluating the effect of a paper mill effluent on bottom fauna.: Hydrobiologia, 44, 463-474.

Hiscock, K. and Moore, J. Surveys of Harbours, rias and estuaries in southern Britain: Plymouth area including the Yealm. Hiscock, K. and Moore, J. FSC/OPRU/36/86, 1-143. 1986. Orielton, Pembroke, Dyfed, SA71 5EZ, Field Studies Council Oil Pollution Research Unit, Orielton, Pembroke.
Ref Type: Report

Hobbie, J. E., Daley, R. J., and Jasper, S., 1977, Use of nucleopore filters for counting bacteria by fluorescence microscopy.: Applied and Environmental Microbiology, 33, 1225-1228.

Hodda, M. and Nicholas, W. L., 1986, Nematode diversity and industrial pollution in the Hunter River Estuary, NSW, Australia.: Marine Pollution Bulletin, 17, 251-255.

Hutchinson, G. E., 1959, Homage to Santa Rosalia, or why are there so many kinds of animals?: American Naturalist, 93, 145-159.

Ishizaka, J., Harada, K., Ishikawa, K., Kiyosawa, H., Furusawa, H., Watanabe, Y., Ishida, H., Suzuki, K., Handa, N., and Takahashi, M., 1997, Size and taxonomic plankton community structure and carbon flow at the equator, 175°E during 1990-1994.: Deep-Sea Research II, 44, 1927-1949.

Josefson, A. B. and Widbom, B., 1988, Differential response of benthic macrofauna and meiofauna to hypoxia in the Gullmar Fjord basin.: Marine Biology, 100, 31-40.

Jurgens, K., Arndt, H., and Rothhaupt, K. O., 1994, Zooplankton-mediated changes of bacterial community structure.: Microbial Ecology, 27, 27-42.

Jurgens, K., Gasol, J. M., Massana, R., and Pedros-Alio, C., 1994, Control of heterotrophic bacteria and protozoans by *Daphnia pulex* in the epilimnion of Lake Ciso.: Archiv fur Hydrobiologie, 131, 55-78.

Jurgens, K., 1994, Impact of *Daphnia* on planktonic microbial food webs-A review.: Marine Microbial Food Webs, 8, 295-324.

Kajak, K., Bretschko, G., Schiemer, F., and Leveque, C., 1980, Zoobenthos., *in* The functioning of freshwater ecosystems. (Le Cren, E. D. and Lowe-McConnell, R. H., eds.): Cambridge, Cambridge University Press, 285-307.

Karl, D. M., 1993, Total microbial biomass estimation derived from the measurement of particulate Adenosine-5'-Triphosphate., *in* Handbook of methods in aquatic microbial ecology. (Kemp, P. F., Sherr, B. F., and Sherr, E. B. and Cole J. J., eds.): London, Lewis publishers, 359-368.

Kerr, S. R., 1974, Theory of size distribution in ecological communities.: Journal of the Fisheries Research Board of Canada, 31, 1859-1862.

Kleiber, M., 1961, Body size and metabolic rate, *in* The fire of life an introduction to animal energetics (Kleiber, M., ed.): New York, John Wiley & Sons, Inc., 177-216.

Lambshead, P. J. D., 1984, The nematode/copepod ratio.Some anomalous results from the Firth of Clyde.: Marine Pollution Bulletin, 15, 256-259.

Letarte, Y. and Pinel-Alloul, B., 1991, Relationships between bacterioplankton production and limnological variables: Necessity of bacterial size considerations.: Limnology and Oceanography, 36, 1208-1216.

Lind, O. T. and Davalos-Lind, L., 1991, Association of turbidity and organic carbon with bacterial abundance and cell size in a large, turbid, tropical lake.: Limnology and Oceanography, 36, 1200-1208.

Linley, E. A. S. and Koop, K., 1986, Significance of pelagic bacteria as a trophic resource in a coral reef lagoon, One Tree Island, Great Barrier Reef.: Marine Biology, 92, 457-464.

MacLean, M. H., Ang, K. J., Brown, J. H., Jauncey, K., and Fry, J. C., 1994, Aquatic and benthic bacteria responses to feed and fertiliser application in trials with the freshwater prawn, *Macrobrachium rosenbergii* (de Man): Aquaculture, 120, 81-93.

Mair, J. M., Matheson, I., and Appelbee, J. F., 1987, Offshore macrobenthic recovery in the Murchison field following the termination of Drill-cuttings discharges.: Marine Pollution Bulletin, 18, 628-634.

Marquet, P. A., Navarrete, S. A., and Castilla, J. C., 1995, Body size, population density, and the energetic equivalence rule.: Journal of Animal Ecology, 64, 325-332.

Martin, M. and Castle, W., 1984, Petrowatch: petroleum hydrocarbons, synthetic organic compounds, and heavy metals in Mussels from the Monterey Bay area of central California.: Marine Pollution Bulletin, 15, 259-266.

McIntyre, A. D. and Warwick, R. M., 1984, Meiofauna techniques., *in* Methods for the study of marine benthos. (Holme, N. A. and McIntyre, A. D., eds.): Oxford, Blackwell scientific publications, 217-244.

Meyer, E., 1989, The relatioship between body length parameters and dry mass in running water invertebrates.: Archiv fur Hydrobiologie, 117, 191-203.

Mills, E. L. and Schiavone, A., 1982, Evaluation of fish communities through assessment of zooplankton populations and measures of lake productivity.: North American Journal of Fisheries Management, 2, 14-27.

Mills, E. L., Green, D. M., and Schiavone, A., 1987, Use of zooplankton size to assess the community structure of fish populations in freshwater lakes.: North American Journal of Fisheries Management, 7, 369-378.

Moore, C. G. and Bett, B. J., 1989, The use of meiofauna in marine pollution impact assessment.: Zoological journal of the linnean society, 96, 263-280.

Morin, A. and Nadon, D., 1991, Size distribution of epilithic lotic invertebrates and implications for community metabolism: Journal of the North American Benthological Society, 10, 300-308.

Morin, A., Rodriguez, M. A., and Nadon, D., 1995, Temporal and environmental variation in the biomass spectrum of benthic invertebrates in streams: an application of thin-plate splines and relative warp analysis.: Canadian Journal of Fisheries and Aquatic Sciences, 52, 1881-1892.

Palmer, M. A. and Strayer, D. L., 1996, Meiofauna, *in* Methods in Stream Ecology. (Hauer, F. R. and Lamberti, G. A., eds.): London, Academic press, 315-337.

Pearre, S., Jr., 1980, The copepod width-weight relation and its utility in food chain research.: Canadian Journal of Zoology, 58, 1884-1891.

Perlmutter, D. G. and Meyer, J. L., 1991, The impact of a stream-dwelling harpacticoid copepod upon detritally associated bacteria.: Ecology, 72, 2170-2180.

Pernthaler, J., Sattler, B., Simek, K., Schwarzenbacher, A., and Psenner, R., 1996, Top-down effects on the size-biomass distribution of a freshwater bacterioplankton community.: Aquatic Microbial Ecology, 10, 255-263.

Peters, R. H. and Wassenberg, K., 1983, The effect of body size on animal abundance.: Oecologia, 60, 89-96.

Peters, R. H. and Raelson, J. V., 1984, Relations between individual size and mammalian population density.: American Naturalist, 124, 498-517.

Platt, T. and Denman, K., 1978, The structure of pelagic marine ecosystems.: Rapports et proces- verbaux des reunions conseil international pour l'exploration de la mer, 173, 60-65.

Poff, N. L., Palmer, M. A., Angermeier, P. L., Vadas, R. L. Jr., Hakenkamp, C. C., Bely, A., Arensburger, P., and Martin, A. P., 1993, Size structure of the metazoan community in a Piedmont stream.: Oecologia, 95, 202-209.

Posch, T, Pernthaler, J., Alfreider, A, and Psenner, R., 1997, Cell-Specific respiratory activity of aquatic bacteria studied with the Tetrazolium Reduction method, Cyto-Clear slides, and image analysis.: Applied and Environmental Microbiology, 63, 867-873.

Preston, F. W., 1948, The commonness, and rarity, of species.: Ecology, 29, 254-283.

Raffaelli, D. and Mason, C. F., 1981, Pollution monitoring with meiofauna, using the ratio of nematodes to copepods.: Marine Pollution Bulletin, 12, 158-163.

Raffaelli, D., 1982, An assessment of the potential of major meiofauna groups for monitoring organic pollution.: Marine environmental Research, 7, 151-164.

Raffaelli, D., 1987, The behaviour of the Nematode/Copepod Ratio in organic pollution studies.: Marine environmental Research, 23, 135-152.

Ramsay, P. M., Rundle, S. D., Attrill, M. J., Uttley, M. G., Williams, P. R, Elsmere, P. S., and Abada, A., 1997, A rapid method for estimating biomass size spectra of benthic metazoan communities.: Canadian Journal of Fisheries and Aquatic Sciences, 54, 1716-1724.

Rasmussen, J. B., 1993, Patterns in the size structure of littoral zone macroinvertebrate communities.: Canadian Journal of Fisheries and Aquatic Sciences, 50, 2192-2207.

Reise, K., Herre, E., and Sturm, M., 1994, Biomass and abundance of macrofauna in intertidal sediments of Konigshafen in the northern Wadden Sea.: Helgolander Meeresunters., 48, 201-215.

Ritterhoff, J. and Zauke, G. P., 1997, Influence of body length, life-history status and sex on trace metal concentrations in selected zooplankton collectives from the Greenland Sea.: Marine Pollution Bulletin, 34, 614-621.

Rodriguez, J., Jimenez, F., Bautista, B., and Rodriguez, V., 1987, Planktonic biomass spectra dynamics during a winter production pulse in Mediterranean coastal waters.: Journal of Plankton Research, 9, 1183-1194.

Rodriguez, M. A. and Magnan, P., 1993, Community structure of Lacustrine macrobenthos: Do taxon-based and size-based approaches yield similar insights?: Canadian Journal of Fisheries and Aquatic Sciences, 50, 800-815.

Rogers, L. E., Buschbom, R. L., and Watson, C. R., 1977, Length-Weight relationships of Shrub-Steppe invertebrates: Annals of the Entomological Society of America, 70, 51-53.

Saliot, A., Cauwet, G., Mazaudier, D., and Daumas, R., 1996, Microbial activities in the Lena River delta and Laptev Sea.: Marine Chemistry, 53, 247-254.

Schmidt-Nielsen, K., 1984, The size of living things., *in* Scaling why is animal size so important? (Schmidt-Nielsen, K., ed.): Cambridge., Press Syndicate of the University of Cambridge., 1-6.

Schoener, T. W., 1980, Length-Weight regression in tropical and temperate forest-understory insects.: Annals of the Entomological Society of america., 73, 106-109.

Schwinghamer, P., 1981, Characteristic size distributions of integral benthic communities.: Canadian Journal of Fisheries and Aquatic Sciences, 38, 1255-1263.

Schwinghamer, P., 1985, Observations on size-structure and pelagic coupling of some shelf and abyssal benthic communities., *in* Proceedings of the Nineteenth European Marine Biology Symposium (Gibbs, P. E., ed.): Cambridge, Cambridge University Press, 347-359.

Schwinghamer, P., 1988, Influence of pollution along a natural gradient and in a mesocosm experiment on biomass-size spectra of benthic communities.: Marine Ecology Progress Series, 46, 199-206.

Scullion, J. and Edwards, R. W., 1980, The effects of coal industry pollutants on the macroinvertebrate fauna of a small river in the South Wales coalfield.: Freshwater Biology, 10, 141-162.

Servais, P. and Garnier, J., 1993, Contribution of heterotrophic bacterial production to the cabon budget of the River Seine (France).: Microbial Ecology, 25, 19-33.

Sheldon, R. W., Prahash, A., and Sutcliffe, W. H., Jr., 1972, The size distribution of particles in the ocean.: Limnology and Oceanography, 17, 327-340.

Sherr, E. B., Caron, D. A., and Sherr, B. F., 1993, Staining of heterotrophic protists for visualization via epifluorescence microscopy., *in* Handbok of methods in aquatic microbial ecology. (Kemp, P. F. and others, eds.): London, Lewis, 213-227.

Shiells, G. M. and Anderson, K. J., 1985, pollution monitoring using the Nematode/Copepod Ratio a practical application.: Marine Pollution Bulletin, 16, 62-68.

Shirayama, Y. and Horikoshi, M., 1989, Comparison of the benthic size structure between sublittoral, upper-slope and deep-sea areas of the Western Pacific.: Internationale Revue Der Gesamten Hydrobiologie, 74, 1-13.

Silvert, W. and Platt, T., 1978, Energy flux in the pelagic ecosystem: A time-dependent equation.: Limnology and Oceanography, 23, 813-816.

Smock, L. A., 1980, Relatioships between body size and biomass of aquatic insects.: Freshwater Biology, 10, 375-383.

Soltwedel, T., Pfannkuche, O., and Thiel, H., 1996, The size structure of deep-sea meiobenthos in the North-Eastern Atlantic: nematode size spectra in relation to environmental variables.: Journal of marine biological Association UK, 76, 327-344.

Somerfield, P. J., Gee, J. M., and Warwick, R. M., 1994, Benthic community structure in relation to an instantaneous discharge of waste water from a Tin Mine.: Marine Pollution Bulletin, 28, 363-369.

Somerfield, P. J., Rees, H. L., and Warwick, R. M., 1995, Interrelationships in community structure between shallow-water marine meiofauna and macrofauna in relation to dredgings disposal.: Marine Ecology Progress Series, 127, 103-112.

Sprules, W. G. and Munawar, M., 1986, Plankton size spectra in relation to ecosystem productivity, Size, and perturbation.: Canadian Journal of Fisheries and Aquatic Sciences, 43, 1789-1794.

Stark, J. S., 1998, Heavy metal pollution and macrobenthic assemblages in soft sediments in two Sydney estuaries, Australia.: Marine and freshwater research, 49, 533-540.

Stark, J. S., 1998, Effects of copper on macrobenthic assemblages in soft sediments: a laboratory experimental study.: Ecotoxicology, 7, 161-173.

Steimle, F. W. Benthic Macrofauna and Habitat Monitoring on the Continental Shelf of the Northeastern United States 1. Biomass. Steimle, F. W. NOAA Technical Report NMFS 86, 1-28. 1990. U.S. Department of Commerce.
Ref Type: Report

Strayer, D., 1986, The size structure of a lacustrine zoobenthic community.: Oecologia, 69, 513-516.

Strayer, D., 1991, Perspectives on the size structure of lacustrine zoobenthos, its causes, and its consequences.: Journal of the North American Benthological Society, 10, 210-221.

Strayer, D. L., 1994, Body size and abundance of benthic animals in Mirror Lake, New Hampshire: Freshwater Biology, 32, 83-90.

Tittel, J., Zippel, B., and Geller, W., 1998, Relationships between plankton community structure and plankton size distribution in lakes of northern Germany.: Limnology and Oceanography, 43, 1119-1132.

Tokeshi, M., 1995, Polychaete abundance and dispersion patterns in Mussel beds - a nontrivial infaunal assemblage on a pacific South-American rocky shore.: Marine Ecology Progress Series, 125, 137-147.

Vanreusel, A., Vincx, M., and Rice, A. L., 1995, Nematode biomass spectra at 2 abyssal sites in the NE Atlantic with a contrasting food-supply.: Internationale Revue Der Gesamten Hydrobiologie, 80, 287-296.

Velji, M. I. and Albright, L. J., 1993, Improved sample preparation for enumeration of aggregated aquatic substrate bacteria., *in* Handbook of methods in aquatic microbial ecology (Kemp, P. F. and others, eds.): London, Lewis publishers, 139-142.

Viles, C. L. and Sieracki, M. E., 1992, Measurement of marine picoplankton cell size by using a cooled, charge-coupled device camera with image-analyzed fluorescence microscopy.: Applied and Environmental Microbiology, 58, 584-592.

Warwick, R. M., 1984, Species size distributions in marine benthic communities.: Oecologia (Berlin), 61, 32-41.

Warwick, R. M., 1986, A new method for detecting pollution effects on marine macrobenthic communities.: Marine Biology, 92, 557-562.

Warwick, R. M., Collins, N. R., Gee, J. M., and George, C. L., 1986, Species size distributions of benthic and pelagic metazoa: evidence for interaction?: Marine Ecology Progress Series, 34, 63-68.

Warwick, R. M. and Joint, I. R., 1987, The size distribution of organisms in the Celtic sea: from bacteria to metazoa.: Oecologia, 73, 185-191.

Warwick, R. M., Pearson, T. H., and Ruswahyuni., 1987, Detection of pollution effects on marine macrobenthos: further evaluation of the species abundance/biomass method.: Marine Biology, 95, 193-200.

Warwick, R. M., Carr, M. R., Clarke, K. R., Gee, J. M., and Green, R. H., 1988, A mesocosm experiment on the effects of hydrocarbon and copper pollution on a sublittoral soft-sediment meiobenthic community.: Marine Ecology Progress Series, 46, 181-191.

Warwick, R. M., 1993, Environmental impact studies on marine communities: Pragmatical considerations.: Australian journal of ecology, 18, 63-80.

Warwick, R. M. and Clarke, K. R., 1996, Relationships between body-size, species abundance and diversity in marine benthic assemblages: facts or artefacts?: Journal of experimental marine biology and ecology, 202, 63-71.

Watson, S. W., Novitsky, T. J., Quinby, H. L., and Valois, F. W., 1977, Determination of Bacterial Number and Biomass in the Marine Environment.: Applied and Environmental Microbiology, 33, 940-946.

Weinbauer, M. G. and Hofle, M. G., 1998, Size-specific mortality of lake bacterioplankton by natural virus communities: Aquatic Microbial Ecology, 15, 103-113.

Wen, Y. H., 1995, Hydrographic variations in size structure of plankton biomass in a Changjiang floodplain lake.: Archiv fur Hydrobiologie, 132, 427-435.

Widbom, B., 1984, Determination of average individual dry weights and ash-free dry weights in different sieve fractions of marine meiofauna.: Marine Biology, 84, 101-108.

Wiebe, W. J., 1984, Physiological and biochemical aspects of marine bacteria, *in* Heterotrophic activity in the sea. (Hobbie, J. E. and Williams, P. J. leB., eds.): New York, Plenum publishing corporation, 55-82.

Wiedenbrug, S., Nolte, U., and Wurdig, N. L., 1997, Macrozoobenthos of a coastal lake in southern Brazil.: Archiv fur Hydrobiologie, 140, 533-548.

Wieser, W., 1960, Benthic studies in Buzzards Bay II. The meiofauna.: Limnology and Oceanography, V, 121-137.

Williams, P. J., 1970, Heterotrophic utilization of dissolved organic compounds in the sea. 1. Size distribution of population and relatioship between respiration and incorporation of growth substrates.: Journal of marine biological Association UK, 50, 859-870.

Williams, P. R., Attrill, M. J., and Nimmo, M., 1998, Heavy metal concentrations and bioaccumulation within the Fal Estuary, UK: a reappraisal.: Marine Pollution Bulletin, 36, 643-645.

Winberg, G. G. and Duncan, A. Methods for the estimation of production of aquatic animals. 1971. London, Academic Press.
Ref Type: Report

Wright, R. T. and Coffin, R. B., 1984, Measuring microzooplankton grazing on planktonic marine bacteria by its impact on bacterial production.: Microbial Ecology, 10, 137-149.